Washington University in St. Louis
Washington University Open Scholarship

Spring 5-15-2019

Characterizing the Humoral Response to Flavivirus Infection

Estefania Fernandez
Washington University in St. Louis

Follow this and additional works at: https://openscholarship.wustl.edu/art_sci_etds

ᕫ Part of the Allergy and Immunology Commons, Immunology and Infectious Disease Commons, and the Medical Immunology Commons

WASHINGTON UNIVERSITY IN ST. LOUIS

Division of Biology and Biomedical Sciences
Immunology

Dissertation Examination Committee:
Michael Diamond, Chair
Daved Fremont
Robyn Klein
Gene Oltz
Haina Shin

Characterizing the Humoral Response to Flavivirus Infection
by
Estefanía Fernández

A dissertation presented to
The Graduate School
of Washington University in
partial fulfillment of the
requirements for the degree
of Doctor of Philosophy

May 2019
St. Louis, Missouri

Table of Contents

List of Figures

List of Tables

Acknowledgements

scientific curiosity in my future. Sharmila Nair, Rong Zhang, Arthur Kim, Jim White, Emma Winkler, Alex Wessel, James Earnest, Hongming Ma, Qing Tan, Vanessa Salazar, and Laura VanBlargan, you have been key members of my experiences during my time in lab and for that I will be eternally grateful! Thank you to Brett Jagger and Liz Caine for the willingness to listen to any of my thoughts, personal or otherwise. I do not think anyone else will be as intrigued by my weird dreams but you always engaged. The most special thank you to Julie Fox because my dad-to-day science was guided by the philosophy "what would Julie do?". I cannot imagine a better person to share all of antibody work with.

To my St. Louis family, you have made my time in St. Louis the best way to spend my twenties! I hope that the next stage of my life brings me friends as amazing as those that I have had the opportunity to meet here and am confident that I will continue to have the privilege of having you in my life.

Mencha y Papi. no seria la person que soy sin todo lo que me han enseñado. El apoyo constante me ha dado la fortaleza de seguir adelante en los momentos mas dificiles. Gracias por brindarme cariño y siempre estar interesados en todo lo que hago. To my seester, you have been a listening ear and a curious mind. I value your strength, wisdom, and insight more than I can ever express. To the biggest pieces of my heart- Oliver, Isabella, and Ingrid. I am so grateful for the opportunity to be a presence in your life, even if its long-distance. I hope I can provide the same amazing guidance that I have been fortunate to receive.

<div align="right">Estefania Fernandez</div>

Washington University in St. Louis

May 2019

ABSTRACT OF THE DISSERTATION

Characterizing the Humoral Response to Flavivirus Infection

by

Estefanía Fernández

Doctor of Philosophy in Biology and Biomedical Sciences

Immunology

Washington University in St. Louis, 2019

Professor Michael S. Diamond, Chairperson

Flaviviruses are positive (+) sense, single-stranded RNA viruses of the *Flaviviridae* family that are transmitted by mosquitoes. For our studies, we focused on Zika virus (ZIKV) and Japanese encephalitis virus (JEV). Most human infections with ZIKV historically resulted in a mild self-limiting febrile illness. However, since 2013, a worldwide spread and increase in ZIKV infections has been observed. Notably, ZIKV has been associated with autoimmune ascending paralysis (Guillain-Barré Syndrome) and ophthalmologic effects in adults and intrauterine growth restriction and microcephaly in developing fetuses. Current vaccine efforts utilize technologies implemented for related flaviviruses (yellow fever virus (YFV), Dengue virus (DENV), and JEV) including subunit-based, chemically inactivated, and live-attenuated vaccines. Furthermore, co-circulation of flaviviruses, such as DENV and ZIKV in regions of South America, make it desirable to generate a vaccine that protects against both.

JEV infections are usually clinically asymptomatic or result in a mild self-limiting febrile illness. However, disseminated infection and viral penetration of the blood-brain barrier into the central nervous system results in meningitis and encephalitis, which are associated with high

morbidity and mortality. Children are especially vulnerable to neuroinvasion due to lack of prior immunity and the relative immaturity of their immune responses. Although vaccination programs in endemic countries have decreased the incidence of disease, existing vaccines have limitations including multiple dose requirements and reactogenicity. Finally, a major issue in vaccine efficacy is the derivation from genotype III (GIII) strains, the concurrent diversity of JEV worldwide, and the scarcity of efficacy testing across multiple genotypes. Currently, there are five genotypes of JEV that encompass approximately 100 unique strains. In addition, the dominant genotypes vary by country and are not static over time.

We are interested in understanding the immunologic restriction of flavivirus infection by characterizing the interaction between viruses and the humoral response. We identified a panel of mouse and human derived anti-ZIKV monoclonal mAbs and found that ZIKV specific mAbs strongly neutralize multiple strains of ZIKV of Asian and African lineages compared to mAbs that recognize a cross-reactive determinant. Additionally, we identified a novel conformational inter-dimer epitope that when bound, results in significant reduction in *in vitro* infection and *in vivo* protection. We tested the prophylactic and therapeutic efficacy of the strongest neutralizing mAbs in adult male mice for lethality and pregnant female mice for transplacental protection of fetuses. We also tested a panel of anti-DENV mAbs derived from naturally infected patients. We confirmed that EDE1 mAbs, which have stronger virus binding in the absence of glycosylation compared to EDE2 mAbs, are more potent neutralizers of multiple ZIKV strains. We demonstrated that viral seeding of immune privileged sites, such as testis and fetus, occurs by the second day post-infection and mAb administration after this may reduce but not eliminate viral burden and effects in the acute and persistent stages of infection. For JEV, we generated a panel of mouse and human anti-JEV mAbs. We identified a subset of domain I and domain III specific mAbs that can

neutralize JEV strains representative of four different genotypes. Subsequent *in vivo* testing demonstrated a broad range of effective doses that protected prior to and following infection with highly virulent strains of JEV representative of multiple genotypes. We anticipate that further understanding of epitope specificity for neutralization and protection is essential for understanding the efficacy of current (for JEV) and future (for ZIKV) vaccines to multiple strains and genotypes. Moreover, this will improve our understanding of correlates of protection of flavivirus vaccines which remain poorly understood, apart from YFV.

Chapter 1:

Introduction to Flaviviruses

This chapter is partially adapted from a review published in Current Opinions in Virology:

1.1 Overview of Flaviviruses

Flaviviruses, which form a genus in the *Flaviviridae,* include mosquito and tick-transmitted arthropod-borne viruses. Flaviviruses with significant impact on human health and disease include dengue virus (DENV), Zika virus (ZIKV), West Nile virus (WNV), yellow fever virus (YFV), tick-borne encephalitis virus (TBEV), and Japanese encephalitis virus (JEV) [1–3]. Historically, Flaviviruses are categorized by different vector transmission or sequence relatedness [4,5]. By vector analysis, viruses are classified based on tick vectors, mosquito vectors, and those not transmitted by arthropod vectors [4]. Sequencing analysis of structural (envelope protein) and non-structural proteins (NS3 and NS5) have found the viruses distribute similarly between the clades distinguished (**Figure 1.1)** [5]. Additionally, the clades identified by sequencing analysis correspond to those observed by vector transmission [4].

1.2 Flavivirus virology and structure

Flavivirus genomes are organized as one open reading frame (ORF) encoding a single polyprotein that is co- and post-translationally cleaved into three structural (capsid (C), pre-membrane/membrane (prM/M), and envelope (E)) and seven non- structural (NS) proteins by host and viral proteases. The NS proteins are involved in viral replication and immune evasion, among other functions [6–10].

Multiple copies of C protein bind a single copy of viral RNA and forms the nucleocapsid (NC) that is contained within an endoplasmic reticulum (ER)-derived membrane [11,12]. PrM has two C-terminal transmembrane helices that anchor to the ER surface and assists in E protein processing in the ER, folding during maturation, and prevents premature activation that may otherwise occur at acidic pH [13,14].

Pulse-chase data of TBEV glycoproteins indicates that prM and E form a heterodimeric complex soon after synthesis, and that prM is necessary for proper E protein folding [15]. In the immature state, prM and E form 60 icosahedral spikes that protrude from the membrane surface and result in a slightly larger viral particle, ~600 Å [16]. The spikes are made up of trimers of prM-E where prM functions as a cap for the DII-FL at the tip of the E protein[16]. Maturation during transit through the trans-golgi network results in furin-mediated cleavage of prM to M [17] (**Figure 1.2**). Upon cleavage of the prM and release of pr at neutral pH in the extracellular space[18], the virion rearranges to a mature structure with 90 E protein homodimers in an anti-parallel orientation in rafts of three to form a herringbone array and a smooth virion surface [19]. The cleavage process is not completely efficient and may result in partially mature virions. The transitions undergone by viral particles expose different epitopes on the E protein that are essential for receptor-binding, entry, and fusion.

Potential N-linked glycosylation sites are found in structural and NS1 proteins [20–22], but the quantity and sites may differ between flaviviruses. N-linked glycosylation may alter overall protein structure and therefore impact host-range and cellular tropism. For example, DENV E protein is glycosylated at positions N67 and N153 whereas WNV and JEV E proteins are modified only at the analogous N154 in some but not all strains [23,24]. Cryo-EM studies have shown interactions between DC-SIGN on host cells and the N67 glycan on DV2 [25]; this interaction functions as an attachment factor to concentrate virus rather than as a *bona fide* entry receptor [26,27]. Mutations of N67, but not N153, of DV2 demonstrated a decrease in viral replication in mammalian cells although no difference was observed in mosquito cells [28]. In contrast, mutation of N154 in WNV showed reduced replication in mosquito cells [29] and mosquitoes [23] as well as decreased neuroinvasiveness [30]. Finally, the presence or absence of

glycosylation sites may alter antibody binding and neutralization. E-dimer epitope (EDE) mAbs (discussed in Chapter 4) are human-derived anti-DENV mAbs that have been subdivided in EDE1 and EDE2 based on their binding affinity for glycosylation site in the 150 loop. EDE1 mAbs bind better in the absence of the glycan versus EDE2 mAbs, which bind better in the presence of the glycan (discussed in Chapter 4) [2].

1.3 Flavivirus E protein

The E protein (~53 kDa) is the primary surface protein involved in cellular attachment, fusion, and entry [26,27,31,32]. A receptor-binding domain is implicated in both cellular tropism and host range [19,33–35]. The E protein also is the principal target for neutralizing antibodies. Discussed in this section are characteristics common to flaviviruses. Unique features will be discussed in the corresponding virus-specific sections below.

The E protein is subdivided into three domains: a central β-barrel domain (domain I, DI), an extended dimerization domain containing a hydrophobic fusion loop (FL) epitope at the distal end (domain II, DII), and an immunoglobulin-like segment implicated in receptor-binding and entry (domain III, DIII). Exposure to acidic pH in the endosome results in rearrangement of the E protein, trimerization, and exposure of DII-FL, which facilitates membrane fusion between the virus and the outer lipid layer of the host cell [36–39]. The fusion loop is highly conserved across flaviviruses and because of this, antibodies generated against DII-FL are cross-reactive therefore lack type specificity. These anti-DII-FL antibodies variably neutralize virions in part because of differential exposure of this epitope in the ensembles of flavivirus structural states [40–43]. I*n vivo* studies using murine models have shown a protective role for DII-FL specific antibodies, possibly through effector functions, but with limited efficacy[40,44].

DIII contains the putative receptor-binding domain and is also the region against which highly effective neutralizing antibodies are made [45]. DIII is a continuous ~100 amino acid residues that forms a beta (β)-barrel structure made up of six antiparallel strands resembling an immunoglobulin constant domain [46]. Single mutations generated by type-specific antibody selection to flaviviruses have been mapped to DIII and more specifically, to similar regions across multiple viruses [47]. The lateral ridge (DIII-LR) epitope includes the N-terminal linker region along with the BC, DE, and FG loops which, when folded, forms a single patch [46,48,49] and the A-strand epitope are primary sites for neutralizing epitopes by the humoral response. *In vivo* studies of anti-DIII mAb administration prior to and following infection have shown significant protection against flavivirus dissemination and subsequent lethality [43,48,50–53].

1.4 Flavivirus entry, replication, and assembly

Flaviviruses bind and enter target cells through clathrin-dependent receptor-mediated endocytosis facilitated by surface glycoproteins and cellular receptors, including heparin sulfate[34,35], DC-SIGN[27,54], and CLEC5A[55,56]. After low pH-dependent fusion between the virus and host membranes in the endosome, uncoating of the nucleocapsid, and finally release of the viral RNA genome into the host cytoplasm [57]. The positive-sense RNA of flaviviruses allows for immediate viral protein translation of the single open reading frame by host machinery, cleavage of the polypeptide into viral proteins by host and viral proteases, and subsequent viral replication mediated by NS5, the RNA-dependent RNA polymerase, [1,58,59].

Genome packaging occurs concurrently with RNA replication and immature viral particles are assembled in the lumen of the ER[60]. Viral particles then bud from the endoplasmic reticulum and once in the trans-Golgi, prM undergoes furin-mediated cleavage, and infectious virus is released by exocytosis (as discussed above). Flaviviruses do not exist in a single

homogeneous state and can also be found as subviral particles (SVPs), immature forms, and variants of the canonical mature form (partially mature virions). Subviral particles have an outer surface made of E and M proteins and a lipid membrane that is smaller than a mature viral particle and lacks genome content, and therefore is not subsequently infectious [18,61]. Recombinant SVPs can be generated using *in vitro* systems; as they retain immunogenic properties, they have been applied as vaccine platforms for inducing protective immunity. Immature viruses exist in a non-infectious spiky configuration. Mature virus exists as the smooth form often depicted but is also susceptible to variations in temperature and efficiency of furin-mediated cleavage. For DENV, an increase in temperature from 28°C to 35°C results in structural reorganization to generate a larger virion with a bumpier surface [62,63] which may impact virus stability, in the case of ZIKV.

1.5 Antibody-mediated protection against enveloped viruses

Neutralizing antibody titers are commonly used as correlates of protection following vaccination or natural infection [64]. Virus neutralization is defined as antibody binding via the Fab segment to the respective epitope on the virion and therefore inhibiting subsequent steps of infection or production of viral progeny[65].

Antibodies may also act through effector functions between the Fc segment and Fc receptors (FcR) or complement proteins to protect against viral infection. Antibody-dependent cellular cytotoxicity (ADCC) occurs when an antibody, for example HIV-1 mAb A32, detects a virus-infected cell by the Fab segment and simultaneously engages effector cells, such as natural killer cells, via the Fc region [66]. The complement system, particularly the classical complement pathway, is implicated as an antiviral response as well as detrimental to the host [67,68]. Antibody mediated protection *in vivo* is an interplay of mAb-antigen interaction and the

6

effector functions initiated via Fc-FcR interactions on effector cells. For example, studies on anti-influenza mAbs (anti-HA head) demonstrated a requirement of Fab-antigen binding to initiate mAb-FcR interaction [69]. The development and functional testing of mAbs may be limited by changes in the antigenic makeup of the virus over time, particularly for viruses with error-prone polymerases, and changes in antigenic availability based on environmental factors, such as temperature [62,63].

1.5.1 Antibody-defined epitopes in flaviviruses

The antibody response against flaviviruses is categorized by breadth of reactivity to viruses within and between related serologic groups. DENV is often used to exemplify the nomenclature as type-specific (a single DENV serotype), subcomplex-specific (more than one serotype), complex reactive (all serotypes), or reactive to multiple flaviviruses (cross-reactive). In many cases, type-specific mAbs most potently neutralize infection of a given virus and allow distinction between closely related viruses.

Domain I is the central domain within the E monomer and together with DIII, forms a hydrophobic pocket for the DII-FL from the opposing E monomer. Most antibodies generated against DI are type-specific with limited *in vitro* neutralization potential [42]. Within DI, the sites most commonly targeted are the DI-LR (e.g., bound by DV2-106 [70] and WNV mAb E121 [42]) and the DI-DII linker region (e.g., bound by WNV mAbs CR4353 and 7G5 [42,71]). *In vivo* therapeutic studies show 35% survival for animals treated with E121 compared with only 10% survival for those treated with 7G5 [42]. A chimpanzee-derived anti-DENV4 mAb, 5H2, mapped to DI by phage display library, neutralized three independent strains of DENV4, and was able to protect rhesus monkeys from infection-induced lethality[72,73]

One of the most immunodominant epitopes of the human humoral response to flaviviruses falls within the DII-FL, residues 98-110. As discussed above, DII-FL is highly conserved across flaviviruses, is transiently exposed during viral infection, and elicits a cross-reactive, limited neutralizing humoral response. A single mutation at W101 is sufficient to abolish binding of most DII-FL specific mAbs, although loss of binding is also observed at residues G104, G106, and G107 [42,74–78].

Studies on DENV, WNV, and YFV have mapped potent neutralizing mAbs to DIII, specifically, there are two epitopes that have been found to be critical for binding. The DIII A-strand is a short (~7 amino acid) segment made up of residues 305-313 on DENV that is bound by complex and subcomplex-specific mAbs. DENV mAb 1A1D-2 is potently neutralizing ($PRNT_{50}$ = 0.3 ug/ml) and cross-reacts with DENV-1, DENV-2, and DENV-3 [79]. Mapping studies showed binding of 1A1D-2 was sensitive to mutations at residues 305, 307, and 310 [52]. The DIII lateral ridge (DIII-LR) is a discontinuous epitope made up of residues of the BC (330-333), DE (365-368), FG (389-391) loops, and N-termini linker region. Antibodies that map to this region, such as WNV E16, are type-specific and neutralize at nanomolar concentration ($PRNT_{50}$= 4-18 ng/ml) [48,50].

Additional structural, quaternary epitopes have been identified that are comprised of residues in multiple domains within E protein dimers. The E-dimer epitope (EDE) was first identified through mapping of monoclonal mAbs generated from a DENV-infected patient [80]. The EDE is made up of DII-FL and additional DII residues along with DI and DIII amino acids found in the opposite E subunit of the dimer (discussed in Chapter 4). Additionally, CR4354 is a human mAb that binds a structural hinge region formed between E-DI and E-DII but is unable to bind a linear epitope [81].

1.6 Zika virus

1.6.1 Unique features of the E protein

Since the ZIKV epidemic began, research groups have sought to understand the cause of its emergence and its unique pathogenesis (i.e., congenital syndrome) that is not observed for related flaviviruses. Cryo-EM data demonstrates general similarities between the structures of mature ZIKV, DENV, and WNV. One difference is the protrusions of E protein glycan seen on ZIKV, not present on related viruses [82]. ZIKV only has a single glycosylation site (N154) compared to two glycosylation sites (N67 and the analogous N153) observed on DENV [82]. A second potential difference is the stability of ZIKV E protein on the virion, however, the data presented thus far has not demonstrated a conclusive effect of physiologic temperatures on ZIKV E protein stability [83,84]. These differences, along with differences in genetics (discussed below), have implications in the development of cross-reactive and cross-neutralizing mAbs.

1.6.2 Vaccination strategies against Zika virus

This section is adapted from a review published in Current Opinions in Virology [85]

Introduction Historically, Zika virus (ZIKV) infection caused a mild, self-limiting febrile illness that was associated with conjunctivitis, rash, headache, myalgia, and arthralgia [86]. However, during the recent epidemics in Asia and the Americas, more severe and unusual clinical consequences have been observed. Infection of fetuses during pregnancy, particularly during the first trimester, has been associated with placental insufficiency and congenital malformations including cerebral calcifications, microcephaly, and miscarriage [87–91]. In adults, ZIKV infection is linked to an increased incidence of Guillain-Barré syndrome (GBS), an autoimmune disease characterized by ascending paralysis and

polyneuropathy [92] that occurs during the acute phase of ZIKV infection or shortly afterward [93–95].

ZIKV was identified in 1947 from a sentinel Rhesus monkey in the Zika Forest of Uganda [96,97]. Prior to 2007, seroprevalence studies in Asia and Africa suggested ZIKV infections occurred periodically without evidence of severe disease [86,98]. Contemporary outbreaks of ZIKV arose in 2007 on Yap Island in the Federated States of Micronesia followed by an epidemic in French Polynesia in 2013 [99]; these events were associated with a high prevalence of infection, with greater than 11% of people on the islands presenting with ZIKV-associated symptoms [92,99]. A study in French Polynesia of patients diagnosed with GBS during the outbreak found that all had neutralizing antibodies against ZIKV compared to 56% of patients presenting to hospitals with non-febrile illnesses [92]. The next ZIKV outbreak began in late 2014 in northeastern Brazil, which was followed by a rapid spread to many other countries in the Americas in 2015 and 2016, including locally-transmitted infections in Florida and Texas in the United States [100–102]. Associated with the ZIKV epidemic were cases of GBS and congenital defects that correlated temporally with the growing number of infections [94]. *Aedes aegypti* and *Aedes albopictus* mosquitoes have tested positive for ZIKV and are believed to be primary agents of transmission [103,104]. In addition to mosquito vectors, sexual transmission of ZIKV was established from male-to-female [105,106] and subsequently from male-to-male and female-to-male [107,108]. Diagnostic studies have confirmed viral RNA in semen, sperm, and vaginal secretions of symptomatic patients up to 6 months following the onset of symptoms [109–111].

ZIKV belongs to the Flavivirus genus of the *Flaviviridae* family of positive-stranded, enveloped RNA viruses. ZIKV has an 11 kb RNA genome and one open reading

frame. Translation of infectious viral RNA in the cytoplasm generates a polyprotein that is cleaved into three structural proteins (capsid (C), pre-membrane/membrane (prM/M), and envelope (E)) and seven non-structural proteins (NS1, NS2A, NS2B, NS3, NS4A, NS4B, and NS5). ZIKV strains are classified into two genetic lineages, African and Asian/American. As the African lineage shows greater divergence [112], some studies have divided them into two African subtypes [113]. The existence of multiple lineages, however, does not impact antibody neutralization significantly and thus, ZIKV has been classified as a single serotype[114]. ZIKV is related genetically to several pathogens that cause disease globally including Dengue (DENV), yellow fever (YFV), West Nile (WNV), Japanese encephalitis (JEV), and tick-borne encephalitis (TBEV) viruses. Of these viruses, ZIKV is most closely related to the four serotypes of DENV and shares 54–59% amino acid identity across the viral E protein [115]. The sequence similarity between ZIKV and DENV poses unique issues for diagnosis and vaccination, and has implications for disease pathogenesis due to antibody cross-reactivity [115–118].

Studies on related flaviviruses have shown that antibody responses against the viral E protein can serve as correlates of protection in animals and humans [43,71,119–121]. The historical efficacy of the YFV, TBEV, and JEV vaccines in preventing infection and epidemics suggests that an effective vaccine targeting all strains of ZIKV should be feasible, especially given the limited (3–5%) amino acid variability between E proteins of the two lineages [112]. In terms of prioritization, pre-pubescent children and men and women of child-bearing age living within or traveling to endemic areas might be priority recipients in a ZIKV vaccination campaign **(Figure 1.3)** [122].

11

ZIKV vaccine epitope targets of humoral immunity The ZIKV E protein is composed

of three ectodomains (DI, DII, and DIII), which are displayed on the surface of the virion

and contribute to entry into susceptible cells. A large proportion of anti-ZIKV antibodies

generated during human infection target the fusion loop present in DII (DII-FL), which is

highly conserved across flaviviruses. Animal studies have shown some protective activity

of DII-FL antibodies in the context of flavivirus infection even though they generally have

poor neutralizing capacity *in vitro* [41,44]. Most DII-FL antibodies are not ideal from a

protection perspective because their epitope is partially inaccessible on the mature virion

[123] and they require Fc-dependent effector functions for *in vivo* activity, the latter of which

also is responsible for antibody dependent enhancement (ADE) of infection (see below)

[124]. DIII adopts an immunoglobulin-like fold and is believed to participate in viral

attachment and entry to host cells, which could influence cellular tropism and host range

[31,32,125]. The lateral ridge epitope within DIII (DIII-LR) is recognized by type-specific,

strongly neutralizing anti-ZIKV antibodies [117,126,127] (e.g., ZV-67 and Z004) that likely

block infection by preventing E protein rearrangements required for fusion [48,128]. A panel

of mAb generated from an infected individual against DII (SMZAb2) and DIII (SMZAb1

and SMZAb5) protected rhesus macaques against heterologous infection, however, the

exact epitopes were unindentified[129]. Additionally, several classes of conformational anti-

ZIKV antibodies that potently neutralize infection and recognize quaternary epitopes

formed by adjacent E proteins have been described. E-dimer-dependent (EDE) antibodies

(e.g., C10) bind to conserved sites along the E dimer interface to cross-link the E protein

in a prefusion state. Specifically, EDE antibodies bind to DII-FL and additional sites of DII

(b strand and ij loop) of one E subunit along with residues in DI and DIII of the opposite

E subunit of the dimer[2,130]. Although originally identified in the context of a humoral response to DENV [130], cross-reactive EDE antibodies neutralize ZIKV infection in cell culture and protect against lethal infection in mice [2,115,131–133]. Another conformational epitope is recognized by neutralizing antibodies (e.g., ZIKV-117) that bind across two adjacent ZIKV E protein dimers in DII. These inter-dimer binding antibodies can prevent fetal infection and disease in pregnancy models of ZIKV in mice [117]. A group of protective human antibodies with distinct binding activity was described recently [118]; Z3L1 and Z23 preferentially recognize ZIKV-specific epitopes in DI and DIII, respectively, whereas Z20 binds to an epitope in DII across the E dimer interface but in a distinct pattern from EDE antibodies [118]. Collectively, these studies define a suite of protective antibodies that bind distinct epitopes and suggest that vaccines capable of targeting accessible epitopes on the soluble E protein or conformational epitopes on the virion should elicit polyclonal antibody responses with broad protective activity against most, if not all, ZIKV strains.

ZIKV vaccine approaches Many approaches have been used for developing flavivirus vaccines against YFV, DENV, JEV, WNV, and TBEV including subunit-based (protein or DNA plasmid), chemically inactivated, and live-attenuated vaccines. Moreover, novel lipid-encapsulated modified mRNA vaccines [134,135] and viral vectored vaccines [136] have recently been adapted for ZIKV. Remarkably, in less than one year, several of these vaccines have progressed beyond pre-clinical studies in animals and are advancing into phase 1 human trials (**Table 1.1**). Additional platforms (e.g., live-attenuated vaccines) are in pre-clinical testing and expected to enter human trials in 2017 [137].

DNA and adenovirus-vectored vaccines Leading candidates for ZIKV immunization include DNA plasmid-based and adenovirus-vectored vaccines incorporating the prM and

E genes to produce a secreted E protein or subviral particle that elicits neutralizing antibody response. DNA plasmid-based vaccines have utility due to their ease of production, relative stability, and low reactogenicity [138]. Additionally, they lack risk of reversion, as can be observed with some live-attenuated virus vaccines. One limitation of DNA plasmid vaccines is that they must be introduced into cells (e.g., by electroporation) for optimal protein production [139]. Their low reactogenicity, however, makes this vaccine class a candidate for use in pregnant women [138,140]. Adenovirus-vectored vaccines share ease of production and stability with DNA plasmid vaccines; additionally, they have broad cellular tropism and can be manufactured to high titer, which allows for optimal delivery and immunogenicity. Limitations for adenovirus vaccines include their ability to induce toxic inflammatory responses at high doses, the potential for pre-existing immunity to naturally occurring human adenoviruses that results in accelerated clearance and dampened immunogenicity, and a size limit on the gene inserted [141]. Reactogenicity has been circumvented by deletion of genes required for replication, which also allows for larger inserts [141]. Identification of monkey adenoviruses as vaccine vectors can bypass pre-existing immunity to human adenoviruses [142].

Full-length prM-E (amino acids 93-794) DNA vaccines from a French Polynesian ZIKV strain (H/PF/2013) in a cytomegalovirus promoter-driven plasmid vector were constructed with mutations in the signal sequence or the E protein stem and transmembrane regions to improve expression [143]. Immunization of six rhesus macaques using a prime and boost scheme induced humoral immunity and protected against viremia independent of the challenge dose of a heterologous ZIKV strain (PRVABC59) when administered eight weeks after the boost [144]. Analysis of the pre- and post-challenge serum of immunized

animals demonstrated an inverse correlation between neutralizing antibody titer and viremia [144].

Engineering of the M-E genes (amino acids 216-794) of a Brazilian ZIKV isolate (BeH815744) into a mammalian expression plasmid yielded high levels of humoral and cellular immunity in BALB/c mice when assessed at three weeks following a single immunization [143]. Upon challenge of BALB/c mice with homologous or heterologous strains of ZIKV four weeks following immunization, the M-E plasmid vaccine abrogated ZIKV viremia. Antibody mediated responses were sufficient to confer protection, as CD4$^+$ or CD8$^+$ T cell depletion did not impact vaccine efficacy and passive transfer of vaccine-derived antibody to naïve mice protected against challenge [143]. Intramuscular immunization of four rhesus macaques with this ME plasmid induced protective humoral and cellular immune responses against a homologous strain of ZIKV, but only after boosting [136].

Full-length prM-E (amino acids 93-794) from a ZIKV consensus sequence was incorporated into a eukaryotic plasmid (pVax1) with the addition of an IgE leader sequence to improve expression [145]. Serial immunization of wild-type and immunodeficient mice induced humoral and cellular immunity that protected against challenge with a virulent American strain of ZIKV (ZIKV-PR209). Notably, vaccination also reduced disease severity in immunodeficient mice. Primary immunization of five rhesus macaques promoted a humoral response that was enhanced upon boosting [145].

A rhesus adenovirus serotype 52 (RhAd52) vaccine encoding the M-E genes from ZIKV BeH815744 induced broadly neutralizing humoral and cellular immunity after a single dose in four rhesus macaques [136]. The M-E sequence also was codon optimized and

inserted into a replication-defective adenovirus [146]. A single immunization of female C57BL/6 mice with RhAd52-M-E induced ZIKV-specific neutralizing IgG that was augmented upon boosting. Immunized female mice were mated with naïve sires, and neonatal mice were challenged with a heterologous ZIKV strain at day 7 after birth and followed for 21 days [146]. Maternally transmitted vaccine immunity protected suckling mice against ZIKV-induced weight loss and lethality.

Modified mRNA vaccines Although lipid encapsulated modified mRNA vaccines have been developed in the oncology field [147], more recently they have been adapted for viral vaccines, with two now described for ZIKV [134,135]. Many mRNA vaccines are non-amplifying and all platforms lack the capacity to integrate into the genome [147]. Modified mRNA vaccines contain a type I cap, a poly(A) tail, and untranslated regions that optimize translation efficiency and intracellular stability as well as nucleoside modifications (e.g., introduction of pseudouridine bases) to minimize the indiscriminate activation of innate immunity.

A lipid encapsulated mRNA vaccine encoding full-length prM-E of an Asian (Micronesia 2007) strain of ZIKV induced robust neutralizing antibody responses in mice against ZIKV [134]. Challenge studies with a heterologous African ZIKV strain (Dakar 41519) in immunodeficient (AG129) or immunocompetent (C57BL/6 and BALB/c) mice showed protection against weight loss and lethality when a prime and boost regimen was administered intramuscularly, and this effect was durable even 18-weeks after initial vaccination. A modified prM-E mRNA vaccine encoding mutations destroying the conserved fusion loop epitope in domain II of the E protein protected against ZIKV and diminished production of antibodies enhancing DENV infection in cells or mice [134].

A single intradermal dose of nucleoside-modified lipid encapsulated mRNA vaccine encoding prM-E of ZIKV H/PF/2013 (French Polynesia) induced a strong antibody response in C57BL/6 and BALB/c mice that persisted for 12- and 20-weeks, respectively [135]. Challenge with a heterologous Asian-American ZIKV (PRVABC59, Puerto Rico) at 2- and 20-weeks post vaccination yielded no detectable viremia. Furthermore, a single intradermal dose inoculation of rhesus macaques also induced high levels of neutralizing antibody [135]. Non-human primates challenged with the heterologous ZIKV strain (PRVABC59) at 5-weeks following mRNA vaccination were protected from developing viremia compared to placebo-immunized animals [135]. A single intramuscular dose of a lipid-encapsulated mRNA vaccine showed increased serum neutralization titers and decreased lethality in a lethal model of infection. The protective effect was particularly observed when a modified vaccine was generated with an abrogated fusion loop epitope (IgE$_{sig}$ prM-E FL) or substitution with the JEV signal sequence (JEV$_{sig}$ prM-E)[134].

Inactivated virus vaccines Purified, inactivated whole virus vaccines have been developed to circumvent issues associated with live-attenuated vaccines. This approach eliminates the possibility of viral replication yet retains, to varying degrees, the antigenicity of the structural proteins. Inactivated viral vaccines are considered desirable, especially for populations that are relatively immunocompromised (newborns, elderly, acquired or genetic immune deficiencies, or pregnant women) where live-attenuated virus vaccines may be contraindicated [148,149]. Inactivated whole virus vaccines have been used successfully for several flaviviruses including YFV, JEV, TBEV, and WNV (the latter for veterinary use only) [150].

An inactivated ZIKV vaccine (ZPIV) was developed based on a previous vaccine targeting JEV [151]. A Puerto Rican strain (PRVABC59) of ZIKV was cultured to high titer in Vero cells, purified, and inactivated with formalin treatment [143]. A single immunization of BALB/c mice with alum-adjuvant ZPIV yielded ZIKV specific IgG titers (1/100) that correlated with protection against challenge with a heterologous strain of ZIKV [143]. ZPIV testing in rhesus macaques also induced neutralizing antibodies and cellular immunity after two doses [136,152]. Subsequent challenge of nonhuman primates with homologous or heterologous strains of ZIKV resulted in complete protection against plasma viremia, or viral RNA in urine, cerebrospinal fluid, colorectal, and cervicovaginal secretions [136].

Live-attenuated vaccines. Arguably, the most successful flavivirus vaccine is YF-17D, a live-attenuated virus that was generated in the 1930s after 176 serial passages of the parent YFV Asibi strain in mouse and chicken tissues [153,154]. A single YF-17D dose induces high levels of neutralizing antibodies in most individuals and confers protection in 95% of recipients, which can last up to 40 years [154]. A chimeric vaccine against JEV was developed by substituting the prM-E genes of JEV into the backbone of the YF-17D capsid and non-structural protein genes. Immunization of subjects in endemic regions with ChimerVax JE™ resulted in responses that neutralized JEV strains of multiple genotypes [155,156] and is available in Australia, Malaysia, Philippines, Thailand, and Myanmar [157]. This chimeric vaccine platform also was adapted for DENV. Different industry groups have refined tetravalent formulations incorporating either chimeric DENV-YFV virus strains (approved as Dengvaxia1) or DENV-DENV chimera (phase 3 trials of TAK-003) to achieve an attenuated strains for vaccination [158,159]. Although a multi-dose regimen of Dengvaxia1

protected flavivirus-immune individuals from subsequent symptomatic DENV infection, it had less efficacy for naïve subjects[160,161].

Live-attenuated vaccines are a favored immunization strategy against flaviviruses because of their ability to induce durable and effective adaptive immunity at relatively low production cost[162]. However, they generally are avoided in immunocompromised populations (including pregnant women) due to possible reversion and pathogenicity. For YF-17D, there have been rare cases of vaccine associated neurotropic and viscerotropic disease following immunization, especially in the elderly [148,154]. Several groups have stated an intention of developing live-attenuated ZIKV vaccines although to date, no data showing immunogenicity or protection has yet been published [137]. Recently, a single dose of live-attenuated ZIKV vaccine lacking the 3'UTR (ZIKV-3'UTR-LAV) was administered to C57BL/6 female mice 35 days prior to mating and a week later were challenged with ZIKV. One week after challenge, dams and pups of vaccinated dams had enhanced antibody titer, reduced viral burden. Furthermore, A129 male mice demonstrated protection against viremia and testicular damage when challenged 30 days after immunization. Lastly, a rhesus macaque model showed that immunization with ZIKV-3'UTR-LAV was able to protect against challenge up to two months after infection[163]. These studies demonstrate that live-attenuated vaccines are highly immunogenic and are protective in multiple models of infection, including pregnancy but questions remain as to their relative safety when tested in pregnant women.

ZIKV vaccine challenges Beyond the generation of an immunogenic vaccine that elicits protective humoral and cell-mediated immunity, there are unique challenges to developing a ZIKV vaccine: *(a) Immune enhancement of heterologous DENV infection.* The DENV

complex is comprised of four genetically related serotypes. Whereas primary infection with DENV generates a protective antibody response that protects durably against the homologous serotype, secondary infection with a heterologous DENV serotype can result in a severe capillary permeability shock syndrome. This disease is attributed in part to ADE, whereby cross-reactive antibodies from the first DENV infection bind but fail to neutralize the second DENV serotype, and instead augment infection in myeloid cells expressing Fc-gamma receptors [124]. This phenomenon could be relevant to ZIKV vaccination because DENV and ZIKV are related closely to one another, the two viruses co-circulate, and their infections produce cross-reactive antibodies targeting the highly conserved DII-FL epitope of the E protein. Indeed, studies in cell culture have confirmed that ADE can occur reciprocally, with DENV and ZIKV antibodies augmenting infection of ZIKV and DENV, respectively [115,164–166]. Moreover, anti-ZIKV human monoclonal antibodies can enhance DENV infection and disease in mice [167] and reciprocally, anti-DENV and anti-WNV polyclonal antibodies enhanced ZIKV infection and disease in mice [168]. If ZIKV antibody responses are shown to augment DENV infection and disease in humans, vaccine strategies that minimize the generation of cross-reactive antibodies may be required to avoid sensitizing ZIKV vaccine recipients to severe DENV infections. In this case, soluble E protein or virus-like particle (prM-E) antigens that abrogate the DII-FL epitope but retain other protective epitopes may be useful [31,75,134,169]. *(b) Guillain–Barré syndrome.* Currently, there is an epidemiological association between ZIKV infection and GBS, although a causal link has not yet been established. The pathogenesis of GBS might be due to direct ZIKV infection of neurons and glial cells in the spinal cord or to autoimmune-mediated targeting, possibly due to antibodies or T cells that cross react

between viral and host antigens [95]. Prior to deployment of a ZIKV vaccine, it will be important to confirm that the elicited humoral or cellular anti-ZIKV responses in humans do not promote the development of GBS. *(c) Pregnancy.* Many vaccines are avoided during pregnancy due to the possible risks of infection or inflammation to the developing fetus. Indeed, vaccination prior to pregnancy remains the desired approach. Notwithstanding this, retrospective analysis of administered live-attenuated or inactivated vaccines have failed to establish conclusively adverse outcomes in fetuses of vaccinated mothers [170,171]. The current recommendation is to administer vaccines if the disease risk outweighs the potential of vaccine related effects [172]. Several recent studies suggest a relatively high frequency of adverse neurodevelopmental effects of fetuses of symptomatic and asymptomatic pregnant women following ZIKV infection [91,173–175]. With current information, it remains difficult to determine whether the risk of exposure to ZIKV in utero surpasses that associated with immunization with certain classes of vaccines.

Conclusions The consequences of the ZIKV epidemic highlight the need for rapid development and introduction of a vaccine. Decades of work on related flaviviruses have provided mature vaccine technologies and platforms, many of which can be adapted for use in immunocompromised and susceptible populations including children and pregnant women. Currently, DNA plasmid, modified mRNA, and purified, inactivated vaccines have demonstrated immunogenicity and protection in mice and nonhuman primates and now are entering Phase 1 clinical testing in humans. While optimism remains high for generating protective vaccines against ZIKV across multiple platforms, questions remain about their safety because of the unique clinical manifestations of ZIKV and its genetic

and serological relatedness to DENV. Parallel discovery and epidemiological efforts are needed to address these issues prior to widespread implementation of a ZIKV vaccine.

1.7 Japanese encephalitis virus

1.7.1 Virology

Genotypes of JEV are determined by sequence alignment and differences within prM-E [176]. There are 4 historically identified genotypes of JEV (genotype I, II, III, and IV) differing by a minimum nucleotide divergence of 7% [177–179] and amino acid divergence from 4.7-6.5% [180]. A fifth genotype (genotype V) has been identified, from a patient in Malaysia, which has approximately 20% nucleotide divergence from previously recognized isolates [178,181–183]. Sequence alignment with other members of the flavivirus family has shown an ~78% E protein amino acid alignment between JEV and WNV [184], the most closely related virus. The variation in sequence likely explains the differential mosquito vectors, pathogenicity, and immune system response against the two closely related members.

Structural studies of JEV E protein have identified features that may have a role in promoting viral stability. The JEV E dimer has less buried surface area compared to related flaviviruses and different residue interaction between dimers [185]. Furthermore, a cryo-EM structure of JEV reveals spaces present between the E monomers, which may confer virus stability and impact conformational changes during assembly and infection [186].

1.7.2 Epidemiology

Encephalitic epidemics attributable to JEV infection have been reported since 1871 and the first large outbreak described in 1924 [187] with more than 6,000 cases and 60% fatality. JEV was originally isolated in 1934 from the brain of a fatal human encephalitic

case in Tokyo [188] and in 1938 from *Culex tritaeniorhynchus* mosquitoes [188,189]. JEV, particularly genotypes (G) II and IV, are known to be endemic in tropical regions of Southeast Asia [190] where sporadic cases occur throughout the year, mainly affecting children younger than 15 years of age [191]. Epidemic outbreaks of GI and GIII occur in temperate and subtropical regions, such as Japan, following the rainy season [191].

Rural areas with open water sources serve as breeding grounds for JEV mosquito vectors. Pigs [190] and wading birds [192] are considered the major reservoir and amplification hosts as they develop high-titer viremia that can facilitate mosquito transmission. Wading birds are commonly referred to as carriers because of their mid-level titers and ability to travel larger distances and move between locations that have appropriate mosquito vectors as part of the environment.

Incidence of disease has been reduced substantially in countries that have implemented immunization and surveillance programs (see Current vaccines against JEV section below). However, there are still unprotected rural populations in South and Southeast Asia that are exposed and susceptible to JEV infection and disease due to their proximity to amplifying hosts and the difficulty in obtaining a full course of vaccination [193]. Even with the implementation of JEV vaccination, 81% of annual JEV infections occur in countries with vaccination programs [194].

1.7.3   Clinical presentation of disease

The annual incidence of clinical JEV infection worldwide is between <1 to >10 per 100,000, which is approximately 1% of those infected [195]. In endemic areas, symptomatic JEV infection is observed in children between the ages of 3 and 6-years old due to the absence of previous immunity [196,197]. However, people living in areas of epidemic

23

outbreaks or those traveling to endemic areas may be affected irrespective of age due to the absence of a previous immune response [197].

Initial infection manifests 5-15 days after infection as non-specific febrile illness accompanied by headache, malaise, and general discomfort. Patients with encephalitis experience behavioral abnormalities, seizures, or neurological deficits [198,199]. One group identified a poliomyelitis-like illness in 15% of children subsequent to JEV infection with pronounced viremia [200], however, upper limb paralysis is more commonly observed [201,202]. Alternatively, older children and adults may present with behavioral abnormalities [203]. Seizures occur especially among children, although still observed in adults, and when present, correlate with a negative outcome [204]. A combination of Parkinsonian effects and dystonia are more indicative of a long, protracted illness [199].

1.7.4   Humoral immune response to JEV infection

Epidermal tissue-resident dendritic cell (DC) are among the first cells in humans to detect JEV following arthropod-mediated transmission [205]. DCs are myeloid-derived antigen presenting cells (APCs) that serve as a link between the innate and adaptive immune systems. Skin-resident DCs internalize JEV, migrate to draining lymph nodes (DLN) where they present antigen to T cells for clonal expansion and activation of effector functions [206]. The internalization of JEV leads to the maturation and migration of DCs to the DLN and presents the opportunity for viral dissemination and pathogenesis.

The humoral immune response to flaviviruses is classified into primary, if first exposure, or secondary, following an unspecified infection with an alternate flavivirus. Primary infection results in early high levels of anti-JEV IgM in the serum and if symptomatic, they are also present in the cerebrospinal fluid (CSF). The inability to mount

a robust IgM response during primary infection is associated with a poor outcome for JEV and also WNV [207,208]. The antibody response restricts viral replication and in its absence, infectious virus can be isolated from blood of patients for prolonged periods [207]. Alternatively, secondary infection with JEV following primary infection with a heterologous flavivirus can result in high levels of cross-reactive anti-flavivirus IgG early after infection [199,207].

1.7.5 Anti-JEV monoclonal antibodies

Kimuro-Kuroda *et al.* generated a panel of mAbs against JEV-JaGAr- 01 (GIII) in BALB/c mice and found that JEV-specific mAbs against the E protein were better able to neutralize JEV *in vitro* and protect *in vivo* [119,207,209]. Studies in mice with non-neutralizing mAbs found partial prophylactic protection though the mechanism was not further studied. Distinct panels of mAbs from BALB/c mice immunized and boosted with JEV-Nakayama (GIII) again showed that JEV-specific mAbs were better able to neutralize JEV *in vitro* compared to cross-reactive mAbs; however, not all type-specific mAbs had strong neutralization activity [120,210]. One key finding was the identification of the E protein as the antigenic determinant and specifically a 95 amino acid stretch, residues 303-398, required for binding of highly neutralizing mAbs. However, administration of the fragment was unable to confer prophylactic protection in mice infected with a heterologous strain, JEV-Beijing (GIII). Specifically, E-DIII was identified as the target of strongly neutralizing mAbs against JEV. such as E3.3, as has been observed with related flaviviruses[46]. NMR spectrometry and alanine scan mutagenesis identified the top of the ß-barrel, and specifically S331 and N332 to be important for mAb binding[46,47]. Computer modeling of E3.3 bound with DIII shows S331 is closely contact with R94 and N332 was closely

associated with Y27, Y32, and R94[47]. Distinct but spatially related epitopes are also targeted by neutralizing mAbs, as judged by competition binding assays [120,211].

The shift in genotypes over time from GIII to GI has prompted investigators to generate mAbs against GI strains. A group of mAbs were generated with *in vitro* cross-neutralization to multiple genotypes and members of the serocomplex, including WNV and DENV [212]. The use of humanized mAbs derived from immunized chimpanzees has also provided a panel of cross-neutralizing mAbs that provide *in vivo* prophylactic protection against a heterologous strain of the same genotype [213]. To date, 8 panels of mAbs against JEV have been published (**Table 1.2**).

1.7.6 Vaccines against JEV

There are currently 4 classes of licensed JEV vaccines used worldwide, depending on the country. Vaccine trials have been limited to testing efficacy against GIII strains, from which vaccines are derived due to the high prevalence of GIII strains. The first vaccine, JE-VAX®, was licensed in Japan and was derived by inoculating young mice intracranially with Nakayama or Beijing-1, infectious strains of JEV. The brains are harvested, purified, and formalin inactivated. The recommended regimen is a three-dose series with subsequent boost doses. The presence of animal products and development of cell-based vaccine technologies have led to the discontinuation of this vaccine strategy. Inactivated, cell-based vaccines, such as IXIARO®, are derived by culturing live virus in immortalized animal cell lines and inactivating using formalin. A two-dose regiment is required and an adjuvant may be included to further boost the immune response. This class of vaccines is licensed for infants between 2-6 months old in contrast with remaining vaccine platforms that may only be used in infants older than 8 months of age. A live-

attenuated, cell-based vaccine, SA14-14-2, was formulated by passaging a wild-type virulent strain of JEV, SA-14, in chick embryo cells. A single dose is required, an advantage over previously described platforms particularly in remote areas where JEV is endemic. Most recently, a chimeric JEV vaccine (ChimeriVax-JE) was developed based on the YFV vaccine by replacing the structural genes for those of JEV. ChimeriVax-JEV is a live, attenuated vaccine that is protective in mouse and non-human primate models over a range of doses by assessing viremia and clinical signs [156,214,215] and when is protective as a single dose without a further protection seen with a booster dose [216]. Recent work shows limited efficacy of current GIII-derived vaccine platforms against GV disease in mouse model of infection [217], indicating a need to reassess and potentially update the available vaccines.

1.7.7 Conclusions

Current studies of anti-JEV mAbs are beginning to address the shift in genotype and the impact of this on efficacy of current vaccine platforms. A key gap in our understanding is how neutralizing epitopes differ across genotypes [212,213]. Additionally, although mechanisms of neutralization have been hypothesized, it is important to characterize the critical steps for infection and determine whether these are unique from the steps inhibited by mAb binding and neutralization.

1.8 References

1. Chambers, T. J., Hahn, C. S., Galler, R. & Rice, C. M. Flavivirus genome organization, expression, and replication. *Annu. Rev. Microbiol.* **44,** 649–88 (1990).
2. Barba-Spaeth, G. *et al.* Structural basis of potent Zika–dengue virus antibody cross-neutralization. *Nature* **536,** 48–53 (2016).
3. Seo, H. J. *et al.* Molecular Detection and Genotyping of Japanese Encephalitis Virus in Mosquitoes during a 2010 Outbreak in the Republic of Korea. *PLoS One* **8,** 1–11 (2013).
4. Kuno, G. *et al.* Phylogeny of the Genus Flavivirus Phylogeny of the Genus Flavivirus. **72,** 72–83 (1998).
5. Grard, G. *et al.* Genetic characterization of tick-borne flaviviruses: New insights into evolution, pathogenetic determinants and taxonomy. *Virology* **361,** 80–92 (2007).
6. Lindenbach, B. D. & Rice, C. M. Genetic Interaction of Flavivirus Nonstructural Proteins NS1 and NS4A as a Determinant of Replicase Function. *J. Virol.* **73,** 4611–4621 (1999).
7. Lindenbach, B. D. & Rice, C. M. trans-Complementation of yellow fever virus NS1 reveals a role in early RNA replication. *J. Virol.* **71,** 9608–9617 (1997).
8. Khromykh, A. A., Sedlak, P. L. & Westaway, E. G. trans-Complementation Analysis of the Flavivirus Kunjin ns5 Gene Reveals an Essential Role for Translation of Its N-Terminal Half in RNA Replication. *J. Virol.* **73,** 9247–9255 (1999).
9. Wilson, J. R., de Sessions, P. F., Leon, M. A. & Scholle, F. West Nile Virus Nonstructural Protein 1 Inhibits TLR3 Signal Transduction. *J. Virol.* **82,** 8262–8271 (2008).
10. Leung, J. Y. *et al.* Role of Nonstructural Protein NS2A in Flavivirus Assembly. *J. Virol.* **82,** 4731–4741 (2008).
11. Khromykh, A. A. & Westaway, E. G. RNA binding properties of core protein of the flavivirus Kunjin. *Arch Virol* **141,** 685–699 (1996).
12. Jones, C. T. *et al.* Flavivirus capsid is a dimeric alpha-helical protein. *J. Virol.* **77,** 7143–9 (2003).
13. Guirakhoo, F., Heinz, F. X., Mandl, C. W., Holzmann, H. & Kunz, C. Fusion activity of flaviviruses: comparison of mature and immature (prM-containing) tick-borne encephalitis virions. *J. Gen. Virol.* **72,** 1323–1329 (1991).
14. Guirakhoo, F., Bolin, R. A. & Roehrig, J. T. The Murray Valley encephalitis virus prM protein confers acid resistance to virus particles and alters the expression of epitopes within the R2 domain of E glycoprotein. *Virology* **191,** 921–31 (1992).
15. Lorenz, I. C., Allison, S. L., Heinz, F. X. & Helenius, A. Folding and dimerization of tick-borne encephalitis virus envelope proteins prM and E in the endoplasmic reticulum. *J. Virol.* **76,** 5480–91 (2002).
16. Zhang, Y. Structures of immature flavivirus particles. *EMBO J.* **22,** 2604–2613 (2003).
17. Stadler, K., Allison, S. L., Schalich, J. & Heinz, F. X. Proteolytic activation of tick-borne encephalitis virus by furin. *J. Virol.* **71,** 8475–81 (1997).
18. Mukhopadhyay, S., Kuhn, R. J. & Rossmann, M. G. A structural perspective of the flavivirus life cycle. *Nat. Rev. Microbiol.* **3,** 13–22 (2005).
19. Rey, F. a, Heinz, F. X., Mandl, C., Kunz, C. & Harrison, S. C. The envelope glycoprotein from tick-borne encephalitis virus at 2 A resolution. *Nature* **375,** 291–298 (1995).
20. Naik, N. G. & Wu, H.-N. Mutation of Putative N-Glycosylation Sites on Dengue Virus NS4B Decreases RNA Replication. *J. Virol.* **89,** 6746–6760 (2015).
21. Kim, J.-M. *et al.* A Single N-Linked Glycosylation Site in the Japanese Encephalitis Virus

prM Protein Is Critical for Cell Type-Specific prM Protein Biogenesis, Virus Particle Release, and Pathogenicity in Mice. *J. Virol.* **82,** 7846–7862 (2008).

22. Yap, S. S. L., Nguyen-Khuong, T., Rudd, P. M. & Alonso, S. Dengue virus glycosylation: What do we know? *Front. Microbiol.* **8,** 1–16 (2017).

23. Moudy, R. M., Zhang, B., Shi, P.-Y. & Kramer, L. D. West Nile virus envelope protein glycosylation is required for efficient viral transmission by Culex vectors. *Virology* **387,** 222–8 (2009).

24. Zhang, Y., Chen, P., Cao, R. & Gu, J. Mutation of putative N-Linked Glycosylation Sites in Japanese encephalitis Virus Premembrane and Envelope proteins enhances humoral immunity in BALB/C mice after DNA vaccination. *Virol. J.* **8,** 138 (2011).

25. Pokidysheva, E. *et al.* Cryo-EM Reconstruction of Dengue Virus in Complex with the Carbohydrate Recognition Domain of DC-SIGN. *Cell* **124,** 485–493 (2006).

26. Navarro-Sanchez, E. *et al.* Dendritic-cell-specific ICAM3-grabbing non-integrin is essential for the productive infection of human dendritic cells by mosquito-cell-derived dengue viruses. *EMBO Rep.* **4,** 723–728 (2003).

27. Tassaneetrithep, B. *et al.* DC-SIGN (CD209) Mediates Dengue Virus Infection of Human Dendritic Cells. *J. Exp. Med.* **197,** 823–829 (2003).

28. Mondotte, J. A., Lozach, P.-Y., Amara, A. & Gamarnik, A. V. Essential Role of Dengue Virus Envelope Protein N Glycosylation at Asparagine-67 during Viral Propagation. *J. Virol.* **81,** 7136–7148 (2007).

29. Hanna, S. L. *et al.* N-Linked Glycosylation of West Nile Virus Envelope Proteins Influences Particle Assembly and Infectivity N-Linked Glycosylation of West Nile Virus Envelope Proteins Influences Particle Assembly and Infectivity. *J. Virol.* **79,** 13262–13274 (2005).

30. Beasley, D. W. C. *et al.* Envelope Protein Glycosylation Status Influences Mouse Neuroinvasion Phenotype of Genetic Lineage 1 West Nile Virus Strains. *J. Virol.* **79,** 8339–8347 (2005).

31. Crill, W. D. & Roehrig, J. T. Monoclonal antibodies that bind to domain III of dengue virus E glycoprotein are the most efficient blockers of virus adsorption to Vero cells. *J. Virol.* **75,** 7769–73 (2001).

32. Lee, E. & Lobigs, M. Substitutions at the putative receptor-binding site of an encephalitic flavivirus alter virulence and host cell tropism and reveal a role for glycosaminoglycans in entry. *J. Virol.* **74,** 8867–8875 (2000).

33. Lee, E. & Lobigs, M. Mechanism of virulence attenuation of glycosaminoglycan-binding variants of Japanese encephalitis virus and Murray Valley encephalitis virus. *J. Virol.* **76,** 4901–11 (2002).

34. Hung, S. L. *et al.* Analysis of the steps involved in Dengue virus entry into host cells. *Virology* **257,** 156–167 (1999).

35. Chen, Y. *et al.* Dengue virus infectivity depends on envelope protein binding to target cell heparan sulfate. *Nat. Med.* **3,** 866–871 (1997).

36. Yu, I. *et al.* Structure of the Immature Dengue Virus at Low pH Primes Proteolytic Maturation. *Science (80-.).* **319,** 1834–1837 (2008).

37. Wengler, G. & Wengler, G. Cell-associated West Nile flavivirus is covered with E+pre-M protein heterodimers which are destroyed and reorganized by proteolytic cleavage during virus release. *J. Virol.* **63,** 2521–2526 (1989).

38. Modis, Y., Ogata, S., Clements, D. & Harrison, S. C. A ligand-binding pocket in the

dengue virus envelope glycoprotein. *Proc. Natl. Acad. Sci. U. S. A.* **100,** 6986–91 (2003).

39. Bressanelli, S. *et al.* Structure of a flavivirus envelope glycoprotein in its low-pH-induced membrane fusion conformation. *EMBO J.* **23,** 728–738 (2004).

40. Deng, Y.-Q. Q. *et al.* A broadly flavivirus cross-neutralizing monoclonal antibody that recognizes a novel epitope within the fusion loop of e protein. *PLoS One* **6,** (2011).

41. Dai, L. *et al.* Structures of the Zika Virus Envelope Protein and Its Complex with a Flavivirus Broadly Protective Antibody. *Cell Host Microbe* **19,** 696–704 (2016).

42. Oliphant, T. *et al.* Antibody Recognition and Neutralization Determinants on Domains I and II of West Nile Virus Envelope Protein. *J. Virol.* **80,** 12149–12159 (2006).

43. Vogt, M. R. *et al.* Human Monoclonal Antibodies against West Nile Virus Induced by Natural Infection Neutralize at a Postattachment Step. *J. Virol.* **83,** 6494–6507 (2009).

44. Vogt, M. R. *et al.* Poorly Neutralizing Cross-Reactive Antibodies against the Fusion Loop of West Nile Virus Envelope Protein Protect In Vivo via Fc Receptor and Complement-Dependent Effector Mechanisms. *J. Virol.* **85,** 11567–11580 (2011).

45. Beasley, D. W. C. & Barrett, A. D. T. Identification of Neutralizing Epitopes within Structural Domain III of the West Nile Virus Envelope Protein. *J. Virol.* **76,** 13097–13100 (2002).

46. Wu, K.-P. *et al.* Structural Basis of a Flavivirus Recognized by Its Neutralizing Antibody. *J. Biol. Chem.* **278,** 46007–46013 (2003).

47. Lin, C.-W. & Wu, S.-C. A functional epitope determinant on domain III of the Japanese encephalitis virus envelope protein interacted with neutralizing-antibody combining sites. *J. Virol.* **77,** 2600–6 (2003).

48. Nybakken, G. E. *et al.* Structural basis of West Nile virus neutralization by a therapeutic antibody. *Nature* **437,** 764–769 (2005).

49. Sánchez, M. D. *et al.* Characterization of neutralizing antibodies to West Nile virus. *Virology* **336,** 70–82 (2005).

50. Oliphant, T. *et al.* Development of a humanized monoclonal antibody with therapeutic potential against West Nile Virus. *Nat. Med.* **11,** 522–530 (2005).

51. Edeling, M. A. *et al.* Potent Dengue Virus Neutralization by a Therapeutic Antibody with Low Monovalent Affinity Requires Bivalent Engagement. *PLoS Pathog.* **10,** (2014).

52. Sukupolvi-Petty, S. *et al.* Type- and subcomplex-specific neutralizing antibodies against domain III of dengue virus type 2 envelope protein recognize adjacent epitopes. *J. Virol.* **81,** 12816–26 (2007).

53. Martina, B. E. *et al.* Immunization with West Nile virus envelope domain III protects mice against lethal infection with homologous and heterologous virus. *Vaccine* **26,** (2008).

54. Wang, P. *et al.* DC-SIGN as an attachment factor mediates Japanese encephalitis virus infection of human dendritic cells via interaction with a single high-mannose residue of viral E glycoprotein. *Virology* **488,** 108–119 (2016).

55. Wu, M. F. *et al.* CLEC5A is critical for dengue virus-induced inflammasome activation in human macrophages. *Blood* **121,** 95–106 (2013).

56. Chen, S.-T. *et al.* CLEC5A is critical for dengue-virus-induced lethal disease. *Nature* **453,** 672–676 (2008).

57. Heinz, F. X. & Allison, S. L. Structures and mechanisms in flavivirus fusion. in *ADVANCES IN VIRUS RESEARCH* 231–269 (2000). doi:10.1016/S0065-3527(00)55005-2

58. Tan, B.-H. *et al.* Recombinant Dengue Type 1 Virus NS5 Protein Expressed in

Escherichia coli Exhibits RNA-Dependent RNA Polymerase Activity. *Virology* **216,** 317–325 (1996).

59. Rice, C. *et al.* Nucleotide sequence of yellow fever virus: implications for flavivirus gene expression and evolution. *Science (80-.).* **229,** 726–733 (1985).

60. Khromykh, A. A., Varnavski, A. N., Sedlak, P. L. & Westaway, E. G. Coupling between Replication and Packaging of Flavivirus RNA: Evidence Derived from the Use of DNA-Based Full-Length cDNA Clones of Kunjin Virus. *J. Virol.* **75,** 4633–4640 (2001).

61. Ferlenghi, I. *et al.* Molecular organization of a recombinant subviral particle from tick-borne encephalitis virus. *Mol. Cell* **7,** 593–602 (2001).

62. Fibriansah, G. *et al.* Structural Changes in Dengue Virus When Exposed to a Temperature of 37 C. *J. Virol.* **87,** 7585–7592 (2013).

63. Zhang, X. *et al.* Dengue structure differs at the temperatures of its human and mosquito hosts. *Proc. Natl. Acad. Sci.* **110,** 6795–6799 (2013).

64. Plotkin, S. A. Correlates of protection induced by vaccination. *Clinical and Vaccine Immunology* **17,** 1055–1065 (2010).

65. Klasse, P. J. Neutralization of Virus Infectivity by Antibodies: Old Problems in New Perspectives. *Adv. Biol.* **2014,** 1–24 (2014).

66. Ferrari, G. *et al.* An HIV-1 gp120 Envelope Human Monoclonal Antibody That Recognizes a C1 Conformational Epitope Mediates Potent Antibody-Dependent Cellular Cytotoxicity (ADCC) Activity and Defines a Common ADCC Epitope in Human HIV-1 Serum. *J. Virol.* **85,** 7029–7036 (2011).

67. Shresta, S. Role of Complement in Dengue Virus Infection: Protection or Pathogenesis? *MBio* **3,** e00003-12-e00003-12 (2012).

68. Vasek, M. J. J. *et al.* A complement–microglial axis drives synapse loss during virus-induced memory impairment. *Nature* **534,** 538–543 (2016).

69. DiLillo, D. J., Tan, G. S., Palese, P. & Ravetch, J. V. Broadly neutralizing hemagglutinin stalk–specific antibodies require FcγR interactions for protection against influenza virus in vivo. *Nat. Med.* **20,** 143–151 (2014).

70. Sukupolvi-Petty, S. *et al.* Structure and function analysis of therapeutic monoclonal antibodies against dengue virus type 2. *J. Virol.* **84,** 9227–9239 (2010).

71. Throsby, M. *et al.* Isolation and characterization of human monoclonal antibodies from individuals infected with West Nile Virus. *J. Virol.* **80,** 6982–92 (2006).

72. Lai, C.-J. C.-J. *et al.* Epitope Determinants of a Chimpanzee Dengue Virus Type 4 (DENV-4)-Neutralizing Antibody and Protection against DENV-4 Challenge in Mice and Rhesus Monkeys by Passively Transferred Humanized Antibody. *J. Virol.* **81,** 12766–12774 (2007).

73. Men, R. *et al.* Identification of chimpanzee Fab fragments by repertoire cloning and production of a full-length humanized immunoglobulin G1 antibody that is highly efficient for neutralization of dengue type 4 virus. *J. Virol.* **78,** 4665–74 (2004).

74. Crill, W. D. & Chang, G.-J. J. Localization and Characterization of Flavivirus Envelope Glycoprotein Cross-Reactive Epitopes. *J. Virol.* **78,** 13975–13986 (2004).

75. Hughes, H. R., Crill, W. D. & Chang, G.-J. J. Manipulation of immunodominant dengue virus E protein epitopes reduces potential antibody-dependent enhancement. *Virol. J.* **9,** 115 (2012).

76. Chiou, S.-S., Fan, Y.-C., Crill, W. D., Chang, R.-Y. & Chang, G.-J. J. Mutation analysis of the cross-reactive epitopes of Japanese encephalitis virus envelope glycoprotein. *J.*

Gen. Virol. **93,** 1185–1192 (2012).

77. Roberson, J. A., Crill, W. D. & Chang, G. J. J. Differentiation of West Nile and St. Louis encephalitis virus infections by use of noninfectious virus-like particles with reduced cross-reactivity. *J. Clin. Microbiol.* **45,** 3167–3174 (2007).

78. Crill, W. D., Trainor, N. B. & Chang, G. J. J. A detailed mutagenesis study of flavivirus cross-reactive epitopes using west Nile virus-like particles. *J. Gen. Virol.* **88,** 1169–1174 (2007).

79. Roehrig, J. T., Bolin, R. A. & Kelly, R. G. Monoclonal antibody mapping of the envelope glycoprotein of the dengue 2 virus, Jamaica. *Virology* **246,** 317–328 (1998).

80. Dejnirattisai, W. *et al.* A new class of highly potent, broadly neutralizing antibodies isolated from viremic patients infected with dengue virus. *Nat. Immunol.* **16,** 170–177 (2014).

81. Kaufmann, B. *et al.* Neutralization of West Nile virus by cross-linking of its surface proteins with Fab fragments of the human monoclonal antibody CR4354. *Proc. Natl. Acad. Sci. U. S. A.* **107,** 18950–5 (2010).

82. Sirohi, D. *et al.* The 3.8 A resolution cryo-EM structure of Zika virus. *Science (80-.).* **352,** 467–470 (2016).

83. Goo, L. *et al.* Zika virus is not uniquely stable at physiological temperatures compared to other flaviviruses. *MBio* **110,** 6795–6799 (2013).

84. Kostyuchenko, V. A. *et al.* Structure of the thermally stable Zika virus. *Nature* (2016). doi:10.1038/nature17994

85. Fernandez, E. & Diamond, M. S. Vaccination strategies against Zika virus. *Curr. Opin. Virol.* **23,** 59–67 (2017).

86. Weaver, S. C. *et al.* Zika virus: History, emergence, biology, and prospects for control. *Antiviral Res.* **130,** 69–80 (2016).

87. Brasil, P. P. *et al.* Zika Virus Infection in Pregnant Women in Rio de Janeiro. *N. Engl. J. Med.* **375,** 2321–2334 (2016).

88. Rasmussen, S. A., Jamieson, D. J., Honein, M. A. & Petersen, L. R. Zika Virus and Birth Defects — Reviewing the Evidence for Causality. *N. Engl. J. Med.* **374,** 1981–1987 (2016).

89. van der Eijk, A. A. *et al.* Miscarriage Associated with Zika Virus Infection. *N. Engl. J. Med.* **375,** 1002–1004 (2016).

90. Schaub, B. *et al.* Analysis of blood from Zika virus-infected fetuses: a prospective case series. *Lancet Infect. Dis.* **17,** 520–527 (2017).

91. Honein, M. A. *et al.* Birth Defects Among Fetuses and Infants of US Women With Evidence of Possible Zika Virus Infection During Pregnancy. *JAMA* **317,** 59 (2017).

92. Cao-Lormeau, V.-M. *et al.* Guillain-Barré Syndrome outbreak associated with Zika virus infection in French Polynesia: a case-control study. *Lancet* **387,** 1531–1539 (2016).

93. dos Santos, T. *et al.* Zika Virus and the Guillain–Barré Syndrome — Case Series from Seven Countries. *N. Engl. J. Med.* **375,** 1598–1601 (2016).

94. Santana do Rosario, M. *et al.* Case Report : Guillain – Barré Syndrome after Zika Virus Infection in Brazil. *Am. J. Trop. Med. Hyg.* **95,** 1157–1160 (2016).

95. Parra, B. *et al.* Guillain- Barre Syndrome Associated with Zika Virus Infection in Colombia. *N. Engl. J. Med.* **373,** 1513–1523 (2016).

96. Dick, G. W. ., Kitchen, S. . & Haddow, A. . Zika Virus (I). Isolations and serological specificity. *Trans. R. Soc. Trop. Med. Hyg.* **46,** 509–520 (1952).

97.   Dick, G. W. A. Zika Virus (II). Pathogenicity and Physical Properties. *Trans. R. Soc. Trop. Med. Hyg.* **46,** 521–534 (1952).

98.   Zanluca, C. & dos Santos, C. N. D. Zika virus – an overview. *Microbes Infect.* **18,** 295–301 (2016).

99.   Musso, D., Nilles, E. J. J. & Cao-Lormeau, V.-M. M. Rapid spread of emerging Zika virus in the Pacific area. *Clin. Microbiol. Infect.* **20,** O595–O596 (2014).

100. Campos, G., Bandeira, A. & Sardi, S. Zika Virus Outbreak, Bahia Brazil. *Emerg. Infect. Dis.* **21,** 1885–6 (2015).

101. Frieden, T. R., Schuchat, A. & Petersen, L. Zika Virus 6 Months Later. *J. Am. Med. Assoc.* **316,** 1443 (2016).

102. Castro, L. A. *et al.* Real-time Zika risk assessment in the United States. *bioRxiv* 56648 (2016). doi:10.1101/056648

103. Grard, G. *et al.* Zika Virus in Gabon (Central Africa) - 2007: A New Threat from Aedes albopictus? *PLoS Negl. Trop. Dis.* **8,** 1–6 (2014).

104. Smith-Bindman, R. Is Computed Tomography Safe? *N. Engl. J. Med.* **363,** 1–4 (2010).

105. Foy, B. D. *et al.* Probable Non-Vector-borne Transmission of Zika Virus, Colorado, USA. *Emerg. Infect. Dis.* **17,** 880–882 (2011).

106. Russell, K. *et al.* Male-to-Female Sexual Transmission of Zika Virus — United States, January–April 2016. *Clin. Infect. Dis.* **64,** ciw692 (2016).

107. Davidson, A., Slavinski, S., Komoto, K., Rakeman, J. & Weiss, D. Suspected Female-to-Male Sexual Transmission of Zika Virus — New York City, 2016. *MMWR. Morb. Mortal. Wkly. Rep.* **65,** 716–717 (2016).

108. Deckard, D. T. *et al.* Male-to-Male Sexual Transmission of Zika Virus — Texas, January 2016. *MMWR. Morb. Mortal. Wkly. Rep.* **65,** 372–374 (2016).

109. Gornet, M., Bracero, N. & Segars, J. Zika Virus in Semen: What We Know and What We Need to Know. *Semin. Reprod. Med.* **34,** 285–292 (2016).

110. Mansuy, J. M. *et al.* Zika virus: High infectious viral load in semen, a new sexually transmitted pathogen? *Lancet Infect. Dis.* **16,** 405 (2016).

111. Murray, K. O. *et al.* Prolonged Detection of Zika Virus in Vaginal Secretions and Whole Blood. *Emerg. Infect. Dis.* **23,** 99–101 (2017).

112. Haddow, A. D. *et al.* Genetic Characterization of Zika Virus Strains: Geographic Expansion of the Asian Lineage. *PLoS Negl. Trop. Dis.* **6,** e1477 (2012).

113. Shen, S. *et al.* Phylogenetic analysis revealed the central roles of two African countries in the evolution and worldwide spread of Zika virus. *Virol. Sin.* **31,** 118–130 (2016).

114. Dowd, K. A. *et al.* Broadly Neutralizing Activity of Zika Virus-Immune Sera Identifies a Single Viral Serotype. *Cell Rep.* **16,** 1485–1491 (2016).

115. Dejnirattisai, W. *et al.* Dengue virus sero-cross-reactivity drives antibody-dependent enhancement of infection with zika virus. *Nat. Immunol.* **17,** 1102–1108 (2016).

116. Priyamvada, L. *et al.* Human antibody responses after dengue virus infection are highly cross-reactive to Zika virus. *Proc. Natl. Acad. Sci. U. S. A.* **113,** 7852–7 (2016).

117. Sapparapu, G. *et al.* Neutralizing human antibodies prevent Zika virus replication and fetal disease in mice. *Nature* **540,** 443–447 (2016).

118. Wang, Q. *et al.* Molecular determinants of human neutralizing antibodies isolated from a patient infected with Zika virus. *Sci. Transl. Med.* **8,** 369ra179-369ra179 (2016).

119. Kimura-Kuroda, J. & Yasui, K. Protection of mice against Japanese encephalitis virus by passive administration with monoclonal antibodies. *J. Immunol.* **141,** 3606–10 (1988).

120. Mason, P. W. *et al.* Molecular characterization of a neutralizing domain of the Japanese encephalitis virus structural glycoprotein. *J. Gen. Virol.* **70,** 2037–2049 (1989).

121. Gotuzzo, E., Yactayo, S. & Córdova, E. Review article: Efficacy and duration of immunity after yellow fever vaccination: Systematic review on the need for a booster every 10 years. *Am. J. Trop. Med. Hyg.* **89,** 434–444 (2013).

122. Marston, H. D., Lurie, N., Borio, L. L. & Fauci, A. S. Considerations for Developing a Zika Virus Vaccine. *N. Engl. J. Med.* **375,** 1209–1212 (2016).

123. Nelson, S. *et al.* Maturation of West Nile Virus Modulates Sensitivity to Antibody-Mediated Neutralization. *PLoS Pathog.* **4,** e1000060 (2008).

124. Halstead, S. B., Mahalingam, S., Marovich, M. A., Ubol, S. & Mosser, D. M. Intrinsic antibody-dependent enhancement of microbial infection in macrophages: disease regulation by immune complexes. *Lancet Infect. Dis.* **10,** 712–722 (2010).

125. Mandl, C. W., Allison, S. L., Holzmann, H., Meixner, T. & Heinz, F. X. Attenuation of tick-borne encephalitis virus by structure-based site-specific mutagenesis of a putative flavivirus receptor binding site. *J. Virol.* **74,** 9601–9 (2000).

126. Zhao, H. *et al.* Structural Basis of Zika Virus-Specific Antibody Protection. *Cell* **166,** 1016–1027 (2016).

127. Robbiani, D. F. *et al.* Recurrent Potent Human Neutralizing Antibodies to Zika Virus in Brazil and Mexico. *Cell* **169,** 597–609.e11 (2017).

128. Dai, L. *et al.* Molecular basis of antibody-mediated neutralization and protection against flavivirus. *IUBMB Life* **68,** 783–791 (2016).

129. Magnani, D. M. *et al.* Neutralizing human monoclonal antibodies prevent Zika virus infection in macaques. *Sci. Transl. Med.* **9,** eaan8184 (2017).

130. Rouvinski, A. *et al.* Recognition determinants of broadly neutralizing human antibodies against dengue viruses. *Nature* **520,** 109–113 (2015).

131. Swanstrom, J. A. *et al.* Dengue Virus Envelope Dimer Epitope Monoclonal Antibodies Isolated from Dengue Patients Are Protective against Zika Virus. *MBio* **7,** e01123-16 (2016).

132. Zhang, S. *et al.* Neutralization mechanism of a highly potent antibody against Zika virus. *Nat. Commun.* **7,** 13679 (2016).

133. Fernandez, E. *et al.* Human antibodies to the dengue virus E-dimer epitope have therapeutic activity against Zika virus infection. *Nat. Immunol.* **18,** 1261–1269 (2017).

134. Richner, J. M. *et al.* Modified mRNA Vaccines Protect against Zika Virus Infection. *Cell* 1–12 (2017). doi:10.1016/j.cell.2017.02.017

135. Pardi, N. *et al.* Zika virus protection by a single low-dose nucleoside-modified mRNA vaccination. *Nature* 1–16 (2017). doi:10.1038/nature21428

136. Abbink, P. *et al.* Protective efficacy of multiple vaccine platforms against Zika virus challenge in rhesus monkeys. *Science (80-.).* **353,** 1129–1132 (2016).

137. Durbin, A. Vaccine Development for Zika Virus—Timelines and Strategies. *Semin. Reprod. Med.* **34,** 299–304 (2016).

138. Beckett, C. G. *et al.* Evaluation of a prototype dengue-1 DNA vaccine in a Phase 1 clinical trial. *Vaccine* **29,** 960–968 (2011).

139. Ferraro, B. *et al.* Clinical applications of DNA vaccines: Current progress. *Clin. Infect. Dis.* **53,** 296–302 (2011).

140. Martin, J. E. *et al.* A West Nile Virus DNA Vaccine Induces Neutralizing Antibody in Healthy Adults during a Phase 1 Clinical Trial. *J. Infect. Dis.* **196,** 1732–1740 (2007).

141. Tatsis, N. & Ertl, H. C. Adenoviruses as vaccine vectors. *Mol. Ther.* **10,** 616–629 (2004).
142. Abbink, P. *et al.* Construction and evaluation of novel rhesus monkey adenovirus vaccine vectors. *J. Virol.* **89,** 1512–22 (2015).
143. Larocca, R. A. *et al.* Vaccine protection against Zika virus from Brazil. *Nature* **536,** 474–478 (2016).
144. Dowd, K. A. *et al.* Rapid development of a DNA vaccine for Zika virus. *Science (80-.).* **354,** 237–240 (2016).
145. Muthumani, K. *et al.* In vivo protection against ZIKV infection and pathogenesis through passive antibody transfer and active immunisation with a prMEnv DNA vaccine. *npj Vaccines* **1,** 16021 (2016).
146. Kim, E. *et al.* Preventative Vaccines for Zika Virus Outbreak: Preliminary Evaluation. *EBioMedicine* **13,** 315–320 (2016).
147. Schlake, T., Thess, A., Fotin-Mleczek, M. & Kallen, K.-J. Developing mRNA-vaccine technologies. *RNA Biol.* **9,** 1319–1330 (2012).
148. Monath, T. P. *et al.* Inactivated yellow fever 17D vaccine: Development and nonclinical safety, immunogenicity and protective activity. *Vaccine* **28,** 3827–3840 (2010).
149. Monath, T. P. *et al.* An inactivated cell-culture vaccine against yellow fever. *N. Engl. J. Med.* **364,** 1326–1333 (2011).
150. Heinz, F. X. & Stiasny, K. Flaviviruses and flavivirus vaccines. *Vaccine* **30,** 4301–4306 (2012).
151. Tauber, E. *et al.* Safety and immunogenicity of a Vero-cell-derived, inactivated Japanese encephalitis vaccine: a non-inferiority, phase III, randomised controlled trial. *Lancet* **370,** 1847–1853 (2007).
152. Routh, J. Testing of Investigational Inactivated Zika Vaccine in Human Beings. (2016). Available at: https://www.nih.gov/news-events/news-releases/testing-investigational-inactivated-zika-vaccine-humans-begins. (Accessed: 12th June 2016)
153. Beck, A. S. & Barrett, A. D. T. Current status and future prospects of yellow fever vaccines. *Expert Rev. Vaccines* **14,** 1479–92 (2015).
154. Barrett, A. D. & Teuwen, D. E. Yellow fever vaccine - how does it work and why do rare cases of serious adverse events take place? *Curr. Opin. Immunol.* **21,** 308–313 (2009).
155. Bonaparte, M. *et al.* Immune response to live-attenuated Japanese encephalitis vaccine (JE-CV) neutralizes Japanese encephalitis virus isolates from south-east Asia and India. *BMC Infect. Dis.* **14,** 156 (2014).
156. Monath, T. P. *et al.* Clinical proof of principle for ChimeriVax™: Recombinant live, attenuated vaccines against flavivirus infections. *Vaccine* **20,** 1004–1018 (2002).
157. Barrett, A. D. *Vaccines Available against JE.* (2014).
158. Guy, B. & Jackson, N. Dengue vaccine: hypotheses to understand CYD-TDV-induced protection. *Nat. Rev. Microbiol.* **14,** 45–54 (2015).
159. Kirkpatrick, B. D. *et al.* The live attenuated dengue vaccine TV003 elicits complete protection against dengue in a human challenge model. *Sci. Transl. Med.* **8,** 330ra36-330ra36 (2016).
160. Capeding, M. R. *et al.* Clinical efficacy and safety of a novel tetravalent dengue vaccine in healthy children in Asia: A phase 3, randomised, observer-masked, placebo-controlled trial. *Lancet* **384,** 1358–1365 (2014).
161. Villar, L. *et al.* Efficacy of a Tetravalent Dengue Vaccine in Children in Latin America. *N. Engl. J. Med.* **372,** 113–123 (2015).

162. Durbin, A. P. *et al.* A 12-Month–Interval Dosing Study in Adults Indicates That a Single Dose of the National Institute of Allergy and Infectious Diseases Tetravalent Dengue Vaccine Induces a Robust Neutralizing Antibody Response. *J. Infect. Dis.* **214,** 832–835 (2016).

163. Shan, C. *et al.* A single-dose live-attenuated vaccine prevents Zika virus pregnancy transmission and testis damage. *Nat. Commun.* **8,** 676 (2017).

164. Charles, A. S. & Christofferson, R. C. Utility of a Dengue-Derived Monoclonal Antibody to Enhance Zika Infection In Vitro. *PLoS Curr.* **8,** 1–31 (2016).

165. Kawiecki, A. B. & Christofferson, R. C. Zika Virus–Induced Antibody Response Enhances Dengue Virus Serotype 2 Replication In Vitro. *J. Infect. Dis.* **214,** 1357–1360 (2016).

166. Paul, L. M. *et al.* Dengue virus antibodies enhance Zika virus infection. *Clin. Transl. Immunol.* **5,** e117 (2016).

167. Stettler, K. *et al.* Specificity, cross-reactivity, and function of antibodies elicited by Zika virus infection. *Science (80-.).* **353,** 823–826 (2016).

168. Bardina, S. V. *et al.* Enhancement of Zika virus pathogenesis by preexisting antiflavivirus immunity. *Science (80-.).* **356,** 175–180 (2017).

169. Chabierski, S. *et al.* Distinguishing West Nile virus infection using a recombinant envelope protein with mutations in the conserved fusion-loop. *BMC Infect. Dis.* **14,** 1–8 (2014).

170. Sur, D. K., Wallis, D. H. & O'Connell, T. X. Vaccinations in pregnancy. *Am. Fam. Physician* **68,** 299–304 (2003).

171. Munoz, F. M. Infant Protection Against Influenza Through Maternal Immunization. *JAMA Pediatr.* **170,** 832 (2016).

172. Kroger, A. T., Sumaya, C. V, Pickering, L. K. & Atkinso, W. L. General Recommendations on immunization: recommendations of the Advisory Committee on Immunization Practices. *MMWR* **60,** 1–60 (2016).

173. Soares de Oliveira-Szejnfeld, P. *et al.* Congenital Brain Abnormalities and Zika Virus: What the Radiologist Can Expect to See Prenatally and Postnatally. *Radiology* **281,** 203–218 (2016).

174. Cuevas, E. L. *et al.* Preliminary Report of Microcephaly Potentially Associated with Zika Virus Infection During Pregnancy — Colombia, January–November 2016. *MMWR. Morb. Mortal. Wkly. Rep.* **65,** 1409–1413 (2016).

175. van der Linden, V. *et al.* Description of 13 Infants Born During October 2015–January 2016 With Congenital Zika Virus Infection Without Microcephaly at Birth — Brazil. *MMWR. Morb. Mortal. Wkly. Rep.* **65,** 1343–1348 (2016).

176. Han, N. *et al.* Comparison of Genotypes I and III in Japanese encephalitis virus reveal distinct differences in their genetic and host diversity. *J. Virol.* **88,** 11469–11479 (2014).

177. Uchil, P. D. & Satchidanandam, V. Phylogenetic analysis of Japanese encephalitis virus: Envelope gene based analysis reveals a fifth genotype, geographic clustering, and multiple introductions of the virus into the Indian subcontinent. *Am. J. Trop. Med. Hyg.* **65,** 242–251 (2001).

178. Unni, S. K. *et al.* Japanese encephalitis virus: From genome to infectome. *Microbes Infect.* **13,** 312–321 (2011).

179. Sumiyoshi, H. *et al.* Complete nucleotide sequence of the Japanese encephalitis virus genome RNA. *Virology* **161,** 497–510 (1987).

180. Solomon, T. *et al.* Origin and Evolution of Japanese Encephalitis Virus in Southeast Asia. *J. Virol.* **77,** 3091–3098 (2003).
181. Chen, W. R., Rico-Hesse, R. & Tesh, R. B. A new genotype of Japanese encephalitis virus from Indonesia. *Am. J. Trop. Med. Hyg.* **47,** 61–69 (1992).
182. Mohammed, M. A. F. F. *et al.* Molecular phylogenetic and evolutionary analyses of Muar strain of Japanese encephalitis virus reveal it is the missing fifth genotype. *Infect. Genet. Evol.* **11,** 855–862 (2011).
183. Li, M.-H. *et al.* Genotype V Japanese Encephalitis Virus Is Emerging. *PLoS Negl. Trop. Dis.* **5,** e1231 (2011).
184. Hanna, S. L. *et al.* N-Linked Glycosylation of West Nile Virus Envelope Proteins Influences Particle Assembly and Infectivity. *J. Virol.* **79,** 13262–13274 (2005).
185. Luca, V. C., AbiMansour, J., Nelson, C. a. & Fremont, D. H. Crystal Structure of the Japanese Encephalitis Virus Envelope Protein. *J. Virol.* **86,** 2337–2346 (2012).
186. Wang, X. *et al.* Near-atomic structure of Japanese encephalitis virus reveals critical determinants of virulence and stability. *Nat. Commun.* **8,** 14 (2017).
187. Mackenzie, J. S., Williams, D. T. & Smith, D. W. Japanese Encephalitis Virus: The Geographic Distribution, Incidence, and Spread of a Virus with a Propensity to Emerge in New Areas. *Perspectives in Medical Virology* **16,** 201–268 (2006).
188. van den Hurk, A. F., Ritchie, S. A. & Mackenzie, J. S. Ecology and Geographical Expansion of Japanese Encephalitis Virus. *Annu. Rev. Entomol.* **54,** 17–35 (2009).
189. Hammon, W. M. & Tigertt, W. D. Isolations of Japanese B encephalitis virus from naturally infected Culex tritaeniorhynchus collected in Japan. *Am. J. Hyg.* **50,** 51–6 (1949).
190. Burke, D. S., Tingpalapong, M., Ward, G. S., Andre, R. & Leake, C. J. Intense transmission of Japanese encephalitis virus to pigs in a region free of epidemic encephalitis. *Southeast Asian J. Trop. Med. Public Health* **16,** 199–206 (1985).
191. Mackenzie, J. S., Gubler, D. J. & Petersen, L. R. Emerging flaviviruses: the spread and resurgence of Japanese encephalitis, West Nile and dengue viruses. *Nat. Med.* **10,** S98–S109 (2004).
192. Buescher, E. L. *et al.* Ecologic studies of Japanese encephalitis virus in Japan. IV. Avian infection. *Am. J. Trop. Med. Hyg.* **8,** 678–88 (1959).
193. Erlanger, T. E., Weiss, S., Keiser, J., Utzinger, J. & Wiedenmayer, K. Past, present, and future of Japanese encephalitis. *Emerg. Infect. Dis.* **15,** 1–7 (2009).
194. Campbell, G. *et al.* Estimated global incidence of Japanese encephalitis: *Bull. World Health Organ.* **89,** 766–774 (2011).
195. WHO | Japanese encephalitis. *WHO* (2017).
196. Borah, J., Dutta, P., Khan, S. A. A. & Mahanta, J. A comparison of clinical features of Japanese encephalitis virus infection in the adult and pediatric age group with Acute Encephalitis Syndrome. *J. Clin. Virol.* **52,** 45–49 (2011).
197. Vaughn, D. W. & Hoke, C. H. The epidemiology of Japanese encephalitis: prospects for prevention. *Epidemiol. Rev.* **14,** 197–221 (1992).
198. Halstead, S. B. & Solomon, T. Japanese Encephalitis. in *Vaccines: A Biography* 317–333 (Springer New York, 2010). doi:10.1007/978-1-4419-1108-7_18
199. Solomon, T. Japanese encephalitis. *J. Neurol. Neurosurg. Psychiatry* **68,** 405–415 (2000).
200. Solomon, T. *et al.* Poliomyelitis-like illness due to Japanese encephalitis virus. *Lancet* **351,** 1094–7 (1998).

201. Chen, K. M. *et al.* Clinical manifestations of Japanese encephalitis in southern Taiwan. *J. Microbiol. Immunol. Infect.* **42,** 296–302 (2009).
202. Chung, C.-C. *et al.* Acute Flaccid Paralysis as an Unusual Presenting Symptom of Japanese Encephalitis: A Case Report and Review of the Literature. *Infection* **35,** 30–32 (2007).
203. Lincoln, A. F. F. & Sivertson, S. E. ACUTE PHASE OF JAPANESE B ENCEPHALITIS. *J. Am. Med. Assoc.* **150,** 268 (1952).
204. Solomon, T. *et al.* Seizures and raised intracranial pressure in Vietnamese patients with Japanese encephalitis. *Brain* **125,** 1084–93 (2002).
205. Mackenzie, J. Wrapping Things up about Virus RNA Replication. *Traffic* **6,** 967–977 (2005).
206. Thongtan, T. *et al.* Highly permissive infection of microglial cells by Japanese encephalitis virus: a possible role as a viral reservoir. *Microbes Infect.* **12,** 37–45 (2010).
207. Kimura-Kuroda, J. & Yasui, K. Antigenic Comparison of Envelope Protein E between Japanese Encephalitis Virus and Some Other Flaviviruses Using Monoclonal Antibodies. *J. Gen. Virol.* **67,** 2663–2672 (1986).
208. Diamond, M. S. *et al.* A critical role for induced IgM in the protection against West Nile virus infection. *J. Exp. Med.* **198,** 1853–1862 (2003).
209. Kimura-Kuroda, J. & Yasui, K. Topographical analysis of antigenic determinants on envelope glycoprotein V3 (E) of Japanese encephalitis virus, using monoclonal antibodies. *J. Virol.* **45,** 124–132 (1983).
210. Kobayashi, Y. & Hasegawa, H. Antigenic relationships among strains of Japanese encephalitis virus by using monoclonal antibodies. *Kansenshogaku Zasshi.* **59,** 237–44 (1985).
211. Cecilia, B. D., A Gadkari, I. D., Kedarnath, N. & Ghosh, S. N. Epitope Mapping of Japanese Encephalitis Virus Envelope Protein Using Monoclonal Antibodies against an Indian Strain. *J. gen. Virol* **69,** 2741–2747 (1988).
212. Shimoda, H. *et al. Production and characterization of monoclonal antibodies to Japanese encephalitis virus. Journal of Veterinary Medicine* **75,** 1077–1080 (2013).
213. Goncalvez, A. P. *et al.* Humanized monoclonal antibodies derived from chimpanzee Fabs protect against Japanese encephalitis virus in vitro and in vivo. *J. Virol.* **82,** 7009–21 (2008).
214. Guirakhoo, F. *et al.* Immunogenicity, Genetic Stability, and Protective Efficacy of a Recombinant, Chimeric Yellow Fever-Japanese Encephalitis Virus (ChimeriVax-JE) as a Live, Attenuated Vaccine Candidate against Japanese Encephalitis. *Virology* **257,** 363–372 (1999).
215. Monath, T. P. P. *et al.* Chimeric Yellow Fever Virus 17D-Japanese Encephalitis Virus Vaccine: Dose-Response Effectiveness and Extended Safety Testing in Rhesus Monkeys. *J. Virol.* **74,** 1742–1751 (2000).
216. Monath, T. P. *et al.* Chimeric Live, Attenuated Vaccine against Japanese Encephalitis (ChimeriVax-JE): Phase 2 Clinical Trials for Safety and Immunogenicity, Effect of Vaccine Dose and Schedule, and Memory Response to Challenge with Inactivated Japanese Encephalitis Antigen. *J. Infect. Dis.* **188,** 1213–1230 (2003).
217. Cao, L. *et al.* Low Protective Efficacy of the Current Japanese Encephalitis Vaccine against the Emerging Genotype 5 Japanese Encephalitis Virus. *PLoS Negl. Trop. Dis.* **10,** (2016).

218. Deng, W. L. *et al.* Fine mapping of a linear epitope on EDIII of Japanese encephalitis virus using a novel neutralizing monoclonal antibody. *Virus Res* **179,** 133–139 (2014).

219. Kulkarni, R., Sapkal, G., Mahishi, L., Shil, P. & Gore, M. M. Design and characterization of polytope construct with multiple B and T H epitopes of Japanese encephalitis virus. *Virus Res.* **166,** 77–86 (2012).

220. Gupta, A. K., Lad, V. J. & Koshy, A. A. Protection of mice against experimental Japanese encephalitis virus infections by neutralizing anti-glycoprotein E monoclonal antibodies. *Acta Virol.* **47,** 141–5 (2003).

221. Cecilia, D. *et al.* Epitope mapping of Japanese encephalitis virus envelope protein using monoclonal antibodies against an Indian strain. *J Gen Virol* **69 (Pt 11,** 2741–2747 (1988).

222. Butrapet, S., Kimura-Kuroda, J., Zhou, D. S. & Yasui, K. Neutralizing mechanism of a monoclonal antibody against Japanese encephalitis virus glycoprotein E. *Am. J. Trop. Med. Hyg.* **58,** 389–398 (1998).
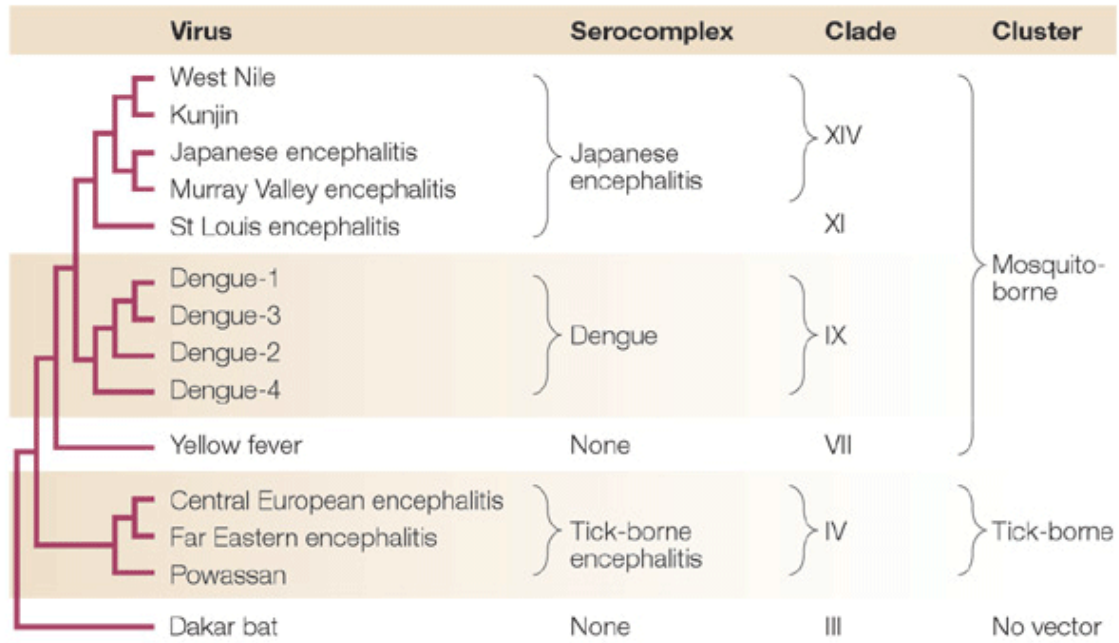
Figure 1.1: Phylogenetic tree of the Flavivirus genus

The distribution of Flaviviruses depending on the proteins utilized for sequence alignment, the structural envelope (E) amino acid sequence. The serocomplex is shown in the second column. The fourth column denotes the grouping based on vector for transmission (adapted from Mukopadhyay *et al.,* 2005).
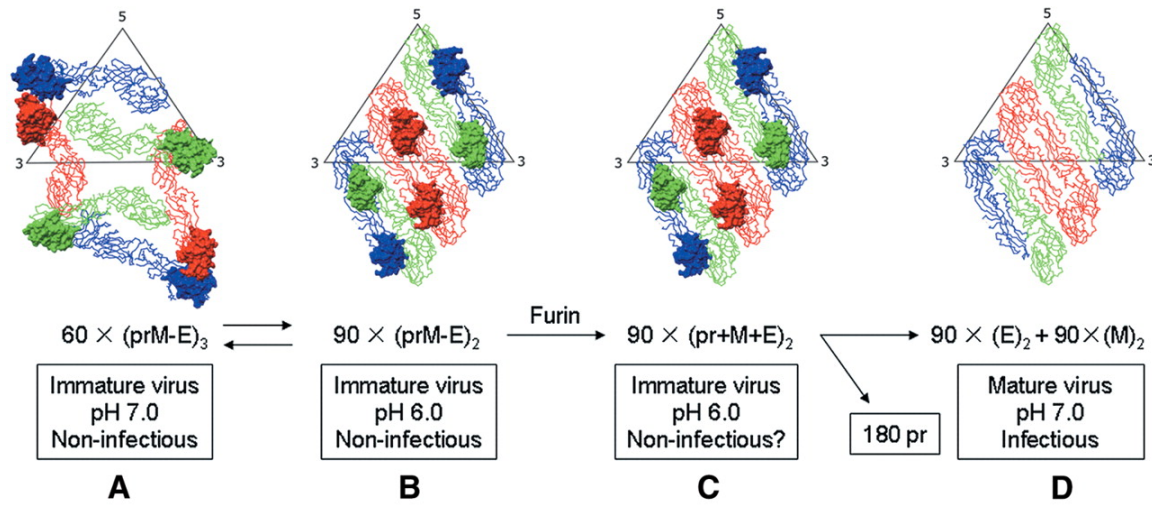
Figure 1.2: Conformational changes of JEV during maturation

During virus maturation, the E protein rearranges oligomeric conformation. The transition from immature to mature virion exposes different epitopes that may impact viral binding and entry as well as humoral immune response (adapted from Li *et al.,* 2008).
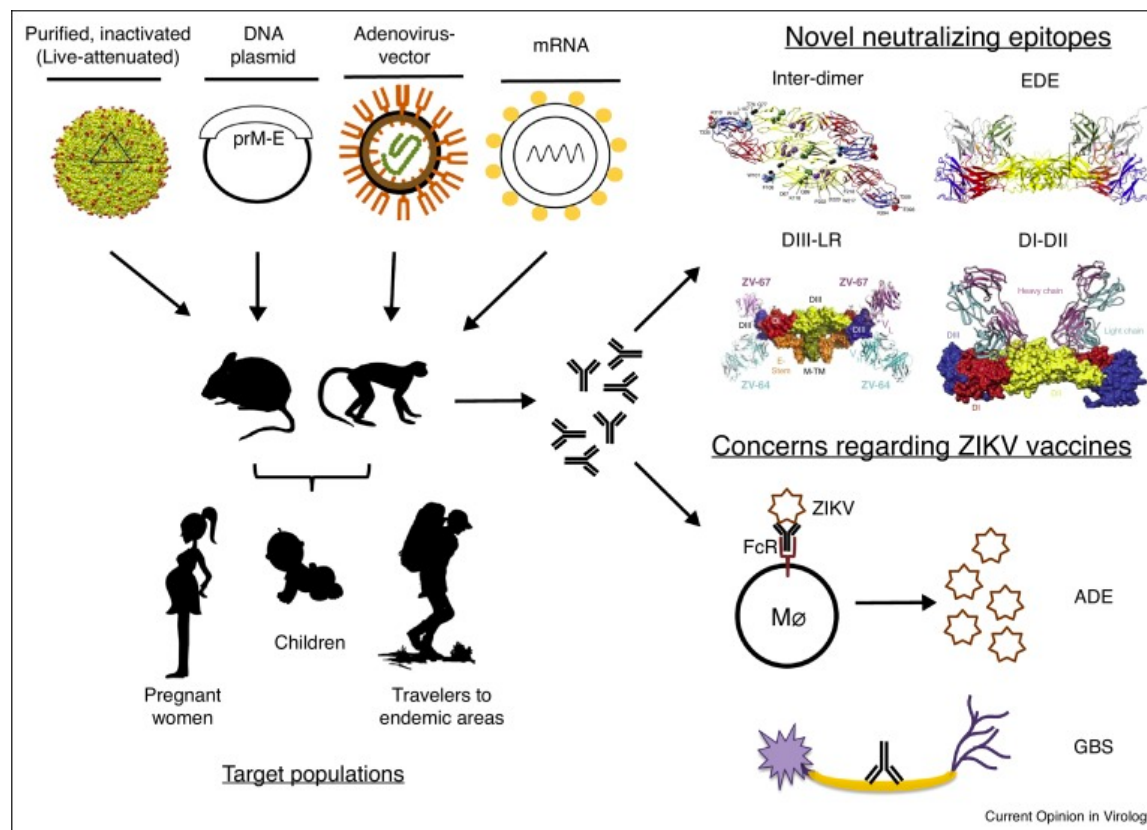
Figure 1.3: ZIKV vaccine candidates, targets, and challenges.

(*Left*) Current platforms entering Phase 1 clinical trials in humans include purified, inactivated virus (adapted from Sirohi *et al.,* 2016), DNA plasmid, adenovirus-vectored, and modified mRNA vaccines, all of which have demonstrated pre-clinical efficacy in mice and non-human primates. The primary target populations are indicated. (*Right*, *top*) Structural analysis of monoclonal antibodies derived from infected mice and human subjects identified protective epitopes for vaccine targeting: Inter-dimer (adapted from Sapparapu *et al.,* 2016), Intra-dimer (EDE) (adapted from Barba-Spaeth *et al.,* 2016), DIII-LR (adapted from Ref. [47]), and DI-DII (adapted from Wang *et al.,* 2016). (*Right*, *bottom*) Concerns for ZIKV vaccine development and deployment include immune-mediated enhancement (ADE) of DENV infection and Guillain–Barré syndrome (GBS) due to the possible induction of autoreactive antibodies and/or T cells (latter not shown).

Table 1.1: ZIKV vaccine candidates entering humans in 2016-2017

Table 1

ZIKV vaccine candidates entering humans in 2016–2017

Vaccine name	Technology	Target	Strain	Sponsor	Clinical trial identifier	Phase	Citation
VRC-ZKADNA085-00-VP	DNA vaccine	prM-E	H/PF/2013	NIH Vaccine Research Center	NCT02840487	1	[56,58]
GLS-5700	DNA vaccine	prM-E	ZIKV consensus	GeneOne Life Science	NCT02887482 NCT02809443	1	[59]
VRC-ZKADNA090-00-VP	DNA vaccine	prM-E	H/PF/2013	NIH Vaccine Research Center	NCT02996461	1	
ZPIV	Inactivated virus vaccine	Whole virion	PRVABC59	WRAIR/NIAID	NCT02937233 NCT02952833 NCT02963909 NCT03008122	1	[56,58,60]
MV-ZIKA	Viral vector (measles)	E		Themis Bioscience	NCT02996890	1	
mRNA-1325	mRNA vaccine	prM-E	Micronesia 2007	Moderna Therapeutics	NCT03014089	1/2	[54]

Table 1.2: Summary of mAbs to JEV

mAb	Source	Immunization	Epitope	EC_{50}	Citation
2B4	BALB/c	JEV E, E-DIII	394-397	500 ng/ml	[218]
7E5	BALB/c	JEV/sw/Chiba/88/2002	52, 276	1:102,400	[212]
3-3H8			52	1:102,400	[212]
P-JEV	Plasmid		B cell, T_H	1:10	[219]
Hs-1 to Hs-4	Swiss	JEV-733913	E protein	>1:890	[220,221]
NHA		JEV-733913		1:100	[211]
A3, B2, E3	Chimpanzee	JEVAX		2.55-7.91 nM	[213]
503	BALB/c	JEV-JaGAr-01	E protein	1:32,000	[207,209,222]
J2	BALB/c	JEV-Nakayama	E-DIII	>1:640	[120]
J3			E-DIII	>1:5120	[120]

Chapter 2:

Structural Basis of Zika Virus-Specific Antibody Protection

This chapter is adapted from a manuscript published in Cell:

Zhao H*, **Fernandez E*,** Dowd KA, Speer SD, Platt DJ, Gorman MJ, Govero J, Nelson CA, Pierson TC, Diamond MS, Fremont DH. 2016. Structural basis of Zika virus- specific antibody protection. *Cell.* 2016 Aug 11; 166(4): 1016- 27.

H.Z., E.F., K.A.D., S.D.S., T.C.P., M.S.D., and D.H.F. designed the experiments. H.Z. generated Fabs and performed the ELISA experiments. H.Z. and C.A.N. purified the recombinant proteins and performed the BLI experiments. H.Z. and D.H.F. performed the crystallography experiments. E.F. and D.J.P. generated the mAbs. E.F., D.J.P., S.D.S., and K.A.D. performed the neutralization and enhancement assays and tested binding to SVPs. M.J.G. generated the ZIKV. J.G. and E.F. performed infection studies. H.Z., C.A.N., E.F., K.A.D., T.C.P., and M.S.D. analyzed the data. M.S.D., T.C.P., and D.H.F. wrote the manuscript with all authors providing editorial comments.

2.1   Summary

Zika virus (ZIKV) infection during pregnancy has emerged as a global public health problem because of its ability to cause severe congenital disease. Here, we developed six mouse monoclonal antibodies (mAbs) against ZIKV including four (ZV-48, ZV-54, ZV-64, and ZV-67) that were ZIKV specific and neutralized infection of African, Asian, and American strains to varying degrees. X-ray crystallographic and competition binding analyses of Fab fragments and scFvs defined three spatially distinct epitopes in DIII of the envelope protein corresponding to the lateral ridge (ZV-54 and ZV-67), C-C' loop (ZV-48 and ZV-64), and ABDE sheet (ZV-2) regions. *In vivo* passive transfer studies revealed protective activity of DIII-lateral ridge specific neutralizing mAbs in a mouse model of ZIKV infection. Our results suggest that DIII is targeted by multiple type-specific antibodies with distinct neutralizing activity, which provides a path for developing prophylactic antibodies for use in pregnancy or designing epitope-specific vaccines against ZIKV.

2.2   Introduction

Zika virus (ZIKV), a flavivirus transmitted by Aedes species mosquitoes, was originally identified in 1947 from a sentinel rhesus monkey in the Zika forest of Uganda[1,2]. It is closely related to the four serotypes of dengue (DENV) as well as other globally relevant viruses including yellow fever (YFV), West Nile (WNV), and Japanese encephalitis (JEV) viruses[3]. Since its identification almost 70 years ago, there were few studies of ZIKV until this past year, when large epidemics in the Americas were accompanied by unexpectedly severe clinical manifestations. Although in most instances ZIKV infection results in a mild febrile illness associated with rash and conjunctivitis, severe neurological phenotypes have been described including Guillain-Barré syndrome and meningoencephalitis[4,5]. Infection in pregnant women[6] and mice[7–9] is now linked causally to fetal abnormalities including microcephaly, spontaneous abortion, and intrauterine growth restriction due to placental insufficiency. Like other flaviviruses, ZIKV is a positive-sense RNA virus with an ~11-kilobase open reading frame flanked by 5' and 3' non-coding regions. The genome encodes a single polyprotein that is post-translationally cleaved by host and viral proteases into three structural proteins (capsid [C], pre-membrane [prM], and envelope [E]) and seven non-structural proteins. C forms a nucleocapsid when bound to viral RNA; prM complexes with E shortly after synthesis to facilitate folding and prevent premature fusion to host membranes; and E mediates viral assembly, attachment, entry, and fusion. The ZIKV E protein is divided into three domains: a central β-barrel domain (domain I [DI]), an extended dimerization domain (DII), and an immunoglobulin-like segment (DIII)[10]. The distal end of DII contains the fusion loop (FL), a hydrophobic sequence that inserts into the host cell endosomal membrane during pH-dependent

47

conformational changes that drive fusion. Two high-resolution cryoelectron microscopic structures show that, like other flaviviruses, mature ZIKV virions are smooth particles that incorporate 180 copies each of the E and cleaved M proteins[11,12]. As in DENV[13], the E proteins of ZIKV pack as antiparallel dimers in a herringbone pattern that lie relatively flat against the lipid envelope. Neutralizing antibodies have important roles in the protection against infection by many flaviviruses and are considered correlates of protection for licensed YFV and tick-borne encephalitis virus (TBEV) vaccines[14,15]. The E protein is a primary antigenic target of neutralizing antibodies, which bind epitopes in all three structural domains, with many type-specific protective antibodies recognizing determinants in DIII[16–19]. Potently neutralizing anti-flavivirus antibodies also recognize complex quaternary epitopes composed of more than one domain or E protein[20–22]. In comparison, antibodies that recognize the fusion loop in DII are more cross-reactive and neutralize flaviviruses less efficiently, although they may still have protective activity *in vivo*[10,23,24]. In this study, we developed six mouse monoclonal antibodies (mAbs) against ZIKV after immunizing with live virus and boosting with infectious virus or recombinant E proteins. Four of the mAbs (ZV-48, ZV-54, ZV-64, and ZV-67) neutralized infection of African, Asian, and American strains of ZIKV to varying degrees, whereas two (ZV-2 and ZV-13) inhibited infection poorly. High-resolution crystal structures were determined for three Fabs and one single-chain variable fragment (scFv) bound to DIII, defining three non-overlapping conformational epitopes: the lateral ridge (LR) (ZV-54 and ZV-67), the C-C' loop (ZV-48 and ZV-64), and the ABDE sheet (ZV-2). *In vivo* passive transfer studies in a lethal mouse model of ZIKV infection revealed protective activity of neutralizing DIII LR

mAbs. Overall, our results suggest that DIII is targeted by several different type-specific antibodies with distinct neutralizing activities.

2.3   Results

Generation of mAbs against ZIKV E Protein. To generate a panel of antibodies against ZIKV, we serially infected *Irf3*^{-/-} mice 30 days apart with ZIKV MR-766 (Uganda, 1947) and ZIKV H/PF/2013 (French Polynesia, 2013). *Irf3*^{-/-} mice were used instead of wild-type (WT) mice, because ZIKV strains are deficient in evading type I interferon-mediated immunity[25,26]. 3 days before myeloma-splenocyte fusion, mice were boosted intravenously with ZIKV H/PF/2013 or recombinant DIII (amino acids 299 to 407 of the ZIKV E protein). After screening ~2,000 hybridomas, we isolated six mAbs that recognized ZIKV E protein by ELISA **(Table 2.1)**.

We tested the mAbs for their specificity by evaluating reactivity with cells infected by ZIKV, DENV (all four serotypes), or JEV. Five of the mAbs (ZV-2, ZV-48, ZV-54, ZV-64, and ZV-67) were ZIKV specific and did not recognize DENV- or JEV-infected cells by flow cytometry **(Figure 2.1A**; data not shown); these mAbs all bound to recombinant ZIKV DIII in a direct ELISA **(Figure 2.1B)**. In contrast, ZV-13 was cross-reactive and bound to cells infected with all serotypes of DENV **(Figure 2.1A)**. Consistent with these data, only ZV- 13 bound to WNV E protein, as detected by ELISA **(Figure 2.1B)**. ZV- 13 recognized the conserved FL in DII, as binding was lost to a ZIKV E protein with mutations in highly conserved residues within and immediately proximal to the FL **(Figure 2.1B)**.

Neutralizing Activity against ZIKV *In Vitro*. We evaluated the mAbs for their ability to inhibit ZIKV H/PF/2013 infection. Four (ZV-48, ZV-54, ZV-64, and ZV-67) of the six

mAbs had neutralizing activity, whereas two (ZV-2 and ZV-13) did not inhibit infection appreciably **(Figure 2.1C)**. To determine the breadth of their activity, the mAbs were evaluated for inhibition of infection by three other ZIKV isolates including two African (MR-766, Uganda, 1947 and Dakar 41519, Senegal, 1982) and an American (Paraiba, Brazil, 2015) strain. Whereas ZV-54 and ZV-67 neutralized all four ZIKV strains, ZV-48 and ZV-64 had reduced inhibitory activity against the other tested strains **(Figure 2.1C; Table 2.1)**.

Binding Characteristics of Anti-ZIKV mAbs. We next assessed whether the variation in neutralizing activity among our antibodies could be explained by differences in binding to the ZIKV E protein derived from H/PF/2013. Based on the ELISA data **(Figure 2.1B)**, we tested the mAbs for binding to a recombinant DIII produced in E. coli using biolayer interferometry (BLI) **(Figure 2.2A; Table 2.1)** or, for the fusion-loop epitope binding ZV-13, the monomeric form of the ectodomain of E expressed in mammalian cells **(Figure 2.3; Table 2.1)**. These biophysical analyses showed that mAbs with stronger neutralizing capacity had greater binding affinities for recombinant proteins. The best neutralizing antibodies, ZV-54 and ZV-67, had the highest affinities with KD equilibrium values less than 10 nM. These two mAbs also showed the slowest dissociation rates, with half-lives of 33 and 13.8 min, respectively. The mAbs with intermediate neutralizing capacity, ZV-64 and ZV-48, had lower affinities, with KD equilibrium values around 35 nM, and more rapid off rates, having half-lives of 1 and 3.2 min, respectively. ZV-2 and ZV-13, which do not inhibit infection appreciably, showed weaker binding, with KD equilibrium values >250 nM.

Based on the interactions of individual mAbs with purified ZIKV proteins, we speculated that differences in the stoichiometry of binding to the viral particle, which also is a function of epitope accessibility[27], might correlate with our neutralization data. To test this idea, we captured purified ZIKV subviral particles (SVPs, prM-E) on 96-well plates and analyzed binding of biotinylated detection mAbs over a range of concentrations. There was an association between the functional avidity of binding and the ability to neutralize infection: ZV-67 and ZV-54 bound more avidly than did ZV-2 and ZV-13 **(Figure 2.2B)**. These data also showed that even at the highest concentrations tested, ZV-2 and ZV-13 failed to saturate binding to the SVPs.

We confirmed these results with pseudo-infectious reporter virus particles (RVPs) in a functional assay. Antibody-mediated neutralization requires engagement of the virions by antibody with a stoichiometry sufficient for neutralization. Antibody-dependent enhancement of infection (ADE) occurs following engagement of the virion by fewer antibody molecules and thus represents a sensitive functional probe for antibody binding to an infectious virion. We evaluated the antibody concentration dependence and magnitude of ADE of ZIKV and DENV by our anti-ZIKV mAbs using an established assay (Pierson et al., 2007) in Fcγ receptor II (FcγRII, CD32A) expressing human K562 cells. While all ZIKV mAbs enhanced infection to varying degrees, those which bound SVPs weakly (e.g., ZV-2) only supported FcgRII-mediated infection at high concentrations **(Figure 2.2C)**. Reciprocally, as described previously for WNV antibodies (Pierson et al., 2007), the most inhibitory anti-ZIKV mAbs (ZV-54 and ZV-67) exhibited ADE, but this occurred only at sub-neutralizing concentrations. These experiments also corroborated the type-specificity of the mAbs, as only ZV-13 supported ADE of DENV. This latter

observation suggests that at least some ZIKV-specific antibodies generated during natural infection can enhance DENV infection *in vitro*.

Structures of ZIKV Antibodies in Complex with DIII. To gain insight into the basis for differential binding and neutralization of the ZIKV mAbs, we generated Fab fragments or scFvs and undertook crystal screening using DIII of ZIKV H/PF/2013. X-ray crystal structures were obtained for four antibody complexes with DIII: ZV-2 Fab to 1.7-A˚ resolution, ZV-48 scFv to 1.7-A˚ resolution, ZV-64 Fab to 1.4-A˚ resolution, and ZV-67 Fab to 1.4-A˚ resolution (**Figure 2.4A**; data collection and refinement statistics in **Table 2.2** and antibody-antigen structural analysis in **Tables 2.3, 2.4, and 2.5**). In all four complexes, ZIKV DIII adopts a conserved structure nearly identical to that observed in soluble E dimers[10] as well as mature virions[11,12] with variation observed primarily at the N- and C-terminal regions of the domain. Analysis of antibody contact residues indicates that ZV-2 and ZV-67 binding is dominated by heavy chain complementarity determining region (CDR) usage, whereas ZV-48 and ZV-64, which appear to be siblings and engage DIII in a similar manner, primarily use light-chain CDRs **(Tables 2.3, 2.4, and 2.5; Figure 2.5)**. Notably, 10 of 12 light chain CDR contact residues are identical in ZV-48 and ZV-64, whereas only 2 of 11 heavy-chain CDR residues are the same, with the most significant difference in the short CDRH3 of ZV-48 that makes more contact with DIII than the long CDR-H3 found in ZV-64 **(Figures 2.4A and 2.5)**. Comparison of the sequences of ZV-67 with ZV-54, for the latter of which we lack structural data, suggests that they bind DIII very similarly, as only two contact residues differ, CDR-L3 Tyr/Phe^{L96} and CDR-H1 Ser/Thr^{H31}.

ZIKV mAbs Bind Three Spatially Distinct Epitopes on DIII. Analysis of the docking of our mAbs onto DIII indicates that ZV-2 and ZV-67 binding should not compete with ZV-48 or ZV-64 binding, whereas ZV-48 and ZV-64 should compete with each other **(Figure 2.4B)**. To evaluate this prediction experimentally, we set up a competitive BLI assay **(Figure 2.4C)**. When ZV-67 was immobilized, we observed that both ZV-64 and ZV-2 could bind in a DIII-dependent manner. In contrast, ZV-54 binding was excluded, supporting the idea that ZV-67 and ZV-54 recognize the same DIII determinants. Analogously, immobilized ZV-48 allowed for the binding of ZV-67 and ZV-2 after DIII capture, but ZV-64 was blocked competitively. This analysis strongly supports our structural observations and defines three distinct ZIKV type-specific epitopes on DIII.

ZIKV DIII Epitope Mapping. We examined the precise footprints of our mAbs on ZIKV DIII **(Figure 2.6A and 2.6B)**. ZV-2 binds to a large, fairly flat surface on the exposed face of the ABDE b sheet of DIII **(Table 2.3)**. The ABDE sheet epitope is highly conserved among ZIKV sequences but many of the primary contacts diverge in other flaviviruses. Previous structural studies of the DENV cross-reactive mAb 2H12 revealed that it contacts six of the same residue positions, especially near the A-B loop[28]. ZV-48 and ZV- 64 both engage the C- and C'-β strands and connecting loop, which project away from the b sandwich core of DIII. The C-C' loop epitope recognized by ZV-48 and ZV-64 is remarkably similar to that engaged by the DENV-1 type-specific antibody E111[29], with 9 structurally related positions contacted **(Figure 2.6A)**.

The epitope recognized by ZV-67 is created by four discrete secondary structure elements: the A-strand, B-C loop, D-E loop, and F-G loop. A total of 21 residues are contacted by ZV-67, with only one difference between the two ZIKV immunizing strains

(E^{E393} in H/PF/2013, D^{E393} in MR-766). This epitope region has been termed the LR and was described in relation to the binding of the potently neutralizing E16 mAb to WNV DIII[30]. Notably, 13 contact positions of E16 and WNV DIII are shared by ZV-67 **(Figure 2.6A)**. DV1-E106 is another mAb recognizing the LR-epitope[31], and it shares 10 contact positions with ZV-67, four of which are conserved in the B-C loops of WNV and ZIKV. Another related DIII epitope (termed the A-strand) has been described for two DENV-complex-specific mAbs, 1A1D-2[32] and 4E11[33] **(Figure 2.6A)**. These A-strand epitope binding mAbs do not make significant contact with the B-C or F-G loop residues engaged by LR-epitope mAbs. Collectively, the three distinct ABDE sheet, C-C' loop, and LR epitopes recognized by our mAbs represent nearly one half of the total ZIKV DIII surface area with no overlap in the contact residues.

Exposed and Cryptic ZIKV Epitopes. We docked our mAb-DIII structures onto the cryoelectron microscopy (cryo-EM)-derived model of the mature ZIKV virion[11,12]. Whereas the LR epitope for ZV-67 was accessible on the mature virion **(Figure 2.7A)**, the C-C' loop and ABDE sheet epitopes were occluded almost completely in all three symmetry environments. We next examined the exposure of the ABDE sheet epitope on the E ectodomain crystal structure[10] and found that Fab binding is blocked sterically due to the adjacent positioning of DI **(Figure 2.7B)**. Furthermore, dimerization of E would preclude ZV-2 mAb binding as its CDR loops contact several of the same DIII residues that are contacted by DII residues in the dimer. Examination of the binding of ZV-64 reveals that it likely engages the cryptic C-C' loop epitope in a manner similar to the DENV-1 specific mAb DV1-E111[29] **(Figures 2.7C and 2.7D)**. Residues on the C-C' loop are intimately involved in lateral E protein contacts on the mature virion, so their exposure

would require substantial reorganization of the particle, which perhaps could occur locally rather than globally. Our most potent mAbs, ZV-67 and ZV-54, recognize the LR epitope in a manner similar to WNV-E16, which can bind up to 120 of the 180 copies of DIII on the mature virion[30,34] **(Figures 2.7C and 2.7E)**. This is the same stoichiometry observed for the binding of the A-strand-specific mAb 1A1D-2[32], which like 4E11[33], can broadly neutralize multiple DENV serotypes **(Figure 2.7F)**. The clustering of DIII LR epitopes around the 5-fold axis of symmetry appears to preclude binding at this site **(Figure 2.7A)**, although minor repacking of the interface could lead to possible binding[31].

***In Vivo* Protection Studies**. Recently, we and others have generated *in vivo* models of ZIKV pathogenesis in mice deficient in type I IFN signaling[25,26]. To evaluate whether neutralizing mAbs protected against ZIKV infection *in vivo*, we treated 4- to 5-week-old WT C57BL/6 mice at day 1 with anti-Ifnar (2 mg) and anti-ZIKV or isotype control mAbs (250 mg) and then infected animals at day 0 with an African ZIKV strain that is more pathogenic in mice than isolates from Asia or the Americas[25]. Treatment of mice with anti-Ifnar mAb and a non-binding isotype control mAb (CHIKV-166) resulted in high levels of ZIKV RNA in serum at day 3 **(Figure 2.8A)** and significant weight loss and mortality **(Figures 2.8B and 2.8C)**. In comparison, treatment with anti-Ifnar mAb and the DIII LR mAbs ZIKV-54 or ZIKV-67 resulted in reduced viremia and complete clinical protection. Consistent with a recent vaccine study that showed antibody-mediated protection against ZIKV viremia in BALB/c mice[35], our neutralizing anti-ZIKV mAbs can protect against lethal ZIKV infection in IFN-deficient C57BL/6 mice. This model is a stringent test of protection, since in humans, the overwhelming majority of infections does not result in lethality.

2.4   Discussion

We set out to develop a panel of mAbs against ZIKV that could provide insight into epitopes that are recognized by neutralizing antibodies. After inoculating mice with infectious ZIKV, we generated and characterized a panel of ZIKV-specific mAbs at both the functional and structural level. Four of the mAbs were ZIKV specific, bound to sites within DIII, and neutralized infection of a contemporary Asian strain of ZIKV. Whereas ZV-54 and ZV- 67 neutralized other ZIKV strains efficiently, ZV-48 and ZV-64 showed reduced inhibitory activity against American and African ZIKV strains. Sequence analysis of the V_L region of ZV-48 and ZV-64 suggest they are sibling clones, although the V_H domains of the IgG heavy chains are distinct and make little contact with DIII. In comparison, the functionally related ZV-54 and ZV-67 mAbs have highly similar V_L and V_H sequences **(Figure 2.5)**. From these analyses, we defined three spatially distinct type-specific epitopes on ZIKV DIII (LR, C-C' loop, and ABDE sheet) with functionally different properties. Finally, *in vivo* passive transfer studies revealed protective activity of ZV-54 and ZV- 67 against an African ZIKV strain in a lethal challenge model in mice.

Type-specific protective and neutralizing mAbs in DIII have been observed in studies with other flaviviruses. As no other ZIKV-specific mAbs have been described to date, it remains uncertain whether the DIII epitopes reported here are immunodominant in humans. However, antibodies to DIII, which is prominently displayed on the surface of flaviviruses (Pierson and Diamond, 2013), appear less dominant in the human response against other flaviviruses[36–38]. The structures of three other antibodies with reactivity against ZIKV have been published recently. Dai et al. (2016) described the 3.0-A° structure of ZIKV E protein in complex with a cross-reactive murine antibody, 2A10G6. This

antibody bound the highly conserved FL in DII and was poorly neutralizing (PRNT50 of 249 mg/mL) yet still protected mice against lethal ZIKV infection. ZV-13 had a similar neutralizing profile *in vitro* and also bound to a DII-FL epitope. Barba-Spaeth et al. (2016) reported 2.4-A˚ and 2.6-A˚ structures of ZIKV E protein complexed with Fab fragments of C8 or A11 antibodies, both of which recognize EDE dimer epitopes[22]. Although these cross-reactive anti-DENV antibodies inhibited ZIKV infection efficiently ($FRNT_{50}$ of ~14 and 135 ng/mL, respectively, against H/PF/2013), no protection experiments with C8 or A11 and ZIKV were undertaken in animals.

Three of our mAbs recognized cryptic epitopes in the ABDE sheet (ZV-2) and C-C' loop (ZV-48 and ZV-64) on DIII, which are not predicted to be accessible on the mature virion[11,12]. So how were these antibodies generated *in vivo*? ZV-48 and ZV-64 were the product of serial infections with two different strains of ZIKV (MR-766 and H/PF/2013) and a final 3-day boost with purified DIII prior to fusion and hybridoma generation. While it is possible that ZV-48 and ZV-64 were selected against the recombinant protein during the last boost, given the extensive somatic hypermutation seen in the sequences **(Figure 2.5)**, it seems more likely that viral breathing (Dowd et al., 2011) allows exposure of the C-C' loop, as observed previously for a neutralizing DENV-1 mAb[29]. For ZV-2, it is more difficult to comprehend, as this mAb was a product only of prime-boosts with infectious ZIKV MR-766 and H/PF/2013. Other possible ways to generate antibodies against cryptic epitopes include exposure of the epitope on partially mature viruses, SVPs, ''broken'' viral particles, or cleaved soluble envelope proteins.

The two mAbs (ZV-48 and ZV-64) that bound to the C-C' loop showed reduced neutralizing activity against the American and African strains. Sequence alignment of the

C-C' loop contact residues in DIII of all four tested strains failed to reveal an explanation for the loss of inhibitory activity relative to the Asian H/PF/ 2013 ZIKV strain. Only a single amino acid change (A343V) in the crystallographic footprint was identified in MR-766 and Dakar 41671, and this substitution was not present in the Paraiba, 2015 sequence. This phenotype is similar to a neutralizing mAb (DV1-E111) that bound the C-C' loop of DENV-1 DIII, in which we observed a genotype-dependent pattern of neutralization[29] that mapped to a single conservative amino acid substitution in DII remote from the footprint of the epitope[39].

We observed protection *in vivo* by DIII LR neutralizing mAbs (ZV-54 and ZV-67). This result is similar to that observed for other DIII LR mAbs against flaviviruses that protected against lethal infection by WNV[17], DENV-1[18], or DENV-2[19]. Although mechanistic studies with ZV-54 and ZV-67 remain to be performed, protective mAbs against WNV and DENV that bound the DIII LR epitope inhibited infection at a post-attachment stage including blocking viral fusion from the endosome[40].

A key question remains whether neutralizing antibodies will protect pregnant women and their developing fetuses from ZIKV infection and congenital malformations, including microcephaly. Although we and others have developed models of infection of pregnant mice with resultant injury to the fetus[7,9], we chose not to perform such protection studies because mice, in contrast to many other mammalian species, lack expression of the neonatal Fc receptor (FcRn) on their trophoblasts in the chorioallantoic placenta[41]. Rather, FcRn is expressed in the mouse yolk sac endoderm, and thus, the transfer of IgG in mice is believed to be predominantly postnatal[42]. As reduced levels of transport of maternal or exogenous IgG into the fetus occur in mice, protection by a given antibody may be

underestimated. Passive antibody transfer studies during pregnancy may require experiments in mammals with more similar placental anatomy that are susceptible to ZIKV infection (e.g., nonhuman primates).

Our studies identify ZIKV DIII as a potential target of neutralizing antibodies and thus a possible immunogen for vaccines. DIII has been used previously in the context of different flavivirus vaccines[43,44]. Although neutralizing antibodies are generated in several animal species in response to soluble DIII immunogens, the titers have been lower than expected, possibly because of immunodominance of regions of DIII that normally are inaccessible on the viral particle. Alternatively, the mouse V_H-CDR3 regions are shorter and vary in amino acid composition compared to other species (Shi et al., 2014), which could impact immunodominance against DIII epitopes in a species-specific manner. Our structural analysis provides a hierarchy of neutralization efficacy associated with distinct epitopes on DIII. Masking of epitopes that fail to elicit neutralizing antibodies could be combined with epitope-focused vaccine design approaches[45] to generate DIII variants that induce more protective responses.

In summary, we identified a panel of type-specific ZIKV mAbs, several of which bind to distinct regions on DIII and have disparate functional activities. Type-specific anti-ZIKV mAbs could be useful for diagnostic assays that distinguish ZIKV antigens from closely related flaviviruses, including DENV. Alternatively, their characterization may provide a path forward for developing prophylactic antibodies for use in pregnancy, for therapeutic antibodies to potentially prevent viral persistence, or for the design of domain and minimal epitope-specific vaccines against ZIKV infection.

2.5   Experimental Procedures

Ethics Statement. This study was carried out in accordance with the recommendations in the Guide for the Care and Use of Laboratory Animals of the NIH. The protocols were approved by the Institutional Animal Care and Use Committee at the Washington University School of Medicine.

Viruses. ZIKV strain H/PF/2013 (French Polynesia, 2013) was obtained from X. de Lamballerie (Aix Marseille Université). ZIKV Brazil Paraiba 2015 was provided by S. Whitehead (Bethesda) and originally obtained from P.F.C. Vasconcelos (Instituto Evandro Chagas). ZIKV MR-766 (Uganda, 1947) and Dakar 41519 (Senegal, 1982) were provided by the World Reference Center for Emerging Viruses and Arboviruses (R. Tesh, University of Texas Medical Branch). Nicaraguan DENV strains (DENV-1 1254-4, DENV-2 172-08, DENV-3 N2845-09, and DENV-4 N703-99) were generously provided by E. Harris (University of California, Berkeley). Virus stocks were propagated in C6/36 *Aedes albopictus* cells[25]. ZIKV Dakar 41519 was passaged *in vivo* in *Rag1*$^{-/-}$ mice (M.J.G. and M.S.D., unpublished data) and a brain homogenate was used. Virus stocks were titrated by focus-forming assay (FFA) on Vero cells as described[46].

mAb Generation. *Irf3*$^{-/-}$ mice were infected and boosted with 103 FFU of ZIKV (MR-766 and H/ PF/2013, respectively) and given a final intravenous boost with infectious 10^6 FFU of ZIKV (H/PF/2013) or purified DIII 3 days prior to fusion with P3X63.Ag.6.5.3 myeloma cells. Hybridomas secreting antibodies that reacted with ZIKV-infected Vero cells were cloned by limiting dilution. All mAbs were purified by protein A affinity chromatography. The V_H and V_L sequences of mAbs were amplified from hybridoma cell RNA by a 5' RACE procedure.

ZIKV mAb Domain Mapping by ELISA. A MAXISORP 96-well plate (Nunc) was coated with 50 µL of 2 µg/mL of recombinant ZIKV E, ZIKV E-FL (fusion-loop mutant), ZIKV DIII, WNV-E, or DV4-E overnight at 4°C. Plates were washed three times with PBS with 0.02% Tween 20 followed by incubation with PBS, 2% BSA, and 0.02% Tween 20 for 1 hr at 37°C. MAbs (0.5 µg/mL) were added for 1 hr at room temperature. Plates were washed again and then sequentially incubated with 2 mg/mL of HRP-conjugated anti-mouse IgG and tetramethylbenzidine substrate. The reaction was stopped by the addition of 1 N H_2SO_4 to the medium, and emission (450 nm) was read using an iMark microplate reader (Bio-Rad).

Neutralization Assays. Serial dilutions of mAbs were incubated with 100 FFU of different ZIKV for 1 hour at 37°C. mAb-virus complexes were added to Vero cell monolayers in 96-well plates. After 90 min, cells were overlaid with 1% (w/v) methylcellulose in MEM supplemented with 4% FBS. Plates were harvested 40 hr later and fixed with 1% PFA in PBS. The plates were incubated sequentially with 500 ng/mL of ZV-16 (E.F., unpublished data) and HRP-conjugated goat anti-mouse IgG in PBS supplemented with 0.1% saponin and 0.1% BSA. ZIKV-infected foci were visualized using TrueBlue peroxidase substrate (KPL) and quantitated on an ImmunoSpot 5.0.37 macroanalyzer (Cellular Technologies).

mAb Binding to Flavivirus-Infected Cells. Vero or C6/36 cells were inoculated with different flaviviruses in DMEM supplemented with 10 mM HEPES, penicillin and streptomycin, and 10% FBS. At different time points after infection (ZIKV H/PF/2013, MOI of 5, 24 hr, Vero cells; DENV strains, MOI of 0.01, 120 hr, C6/36 cells), cells were fixed with 4% PFA diluted in PBS for 20 min at room temperature and permeabilized with HBSS, 10 mM HEPES, 0.1% saponin (Sigma), and 0.025% NaN3 for 10 min at room

temperature. Fifty-thousand cells were transferred to a U-bottom plate and incubated for 1 hr at 4°C with 5 μg/mL of anti-ZIKV mAbs or isotype controls (negative, CHK-166[47]; positive, WNV E53 [Oliphant et al., 2006]). After washing, cells were incubated with an Alexa Fluor 647-conjugated goat anti-mouse IgG (Invitrogen), fixed in 1% PFA in PBS, processed on a FACS Array (BD Biosciences), and analyzed using FlowJo software (Tree Star).

Biolayer Interferometry Binding Assays. The binding affinity of purified ZIKV E or ZIKV DIII protein with ZIKV mAbs was monitored by BLI using an Octet-Red96 device (Pall ForteBio). Briefly, 100 μg of each antibody was mixed with biotin (EZ-Link-NHS-PEG4-Biotin, Thermo Fisher) at a molar ratio of 20:1 biotin:protein and incubated at room temperature for 30 min. The unreacted biotin was removed by passage through a desalting column (5 mL Zeba Spin 7K MWCO, Thermo Fisher). The antibodies were loaded onto streptavidin biosensors (ForteBio) until saturation, typically 2 mg/mL for 3 min, in 10 mM HEPES (pH 7.4), 150 mM NaCl, 3 mM EDTA, and 0.005% P20 surfactant with 3% BSA. Association and dissociation were measured at 25°C for all mAbs. The real-time data were analyzed using Biaevaluation 4.1 (GE Healthcare). Association and dissociation profiles, as well as steady-state equilibrium concentration curves, were fitted using a 1:1 binding model.

SVP Production and Binding Assay. ZIKV SVPs were generated as described previously for WNV (Hanna et al., 2005). Briefly, a plasmid encoding the prM-E gene of ZIKV H/PF/2013 was transfected into HEK293T cells. SVPs were harvested every 24 hr and stored aliquoted at 80°C. 96-well high-binding plates (Immulon 4HBX; Thermo Scientific) were coated with 1 mg/mL of ZV-67 in coating buffer (15 mM sodium carbonate, 35 mM

sodium bicarbonate [pH 9.6]) overnight at 4°C. Plates were blocked with PBS-T + 1.5%

BSA, followed by capture of SVPs diluted in blocking buffer for 1 hr at 37°C. Plates were

incubated with the indicated concentrations of biotin-conjugated mAbs for 30 min at 37°C,

followed by incubation with 30 ng/mL streptavidin-HRP for 30 min at 37°C. The plates

were developed with SureBlue TMB substrate (KPL) and stopped with 1 M HCl. Plates

were analyzed at 450 nm, with a 570 nm correction (BioTek).

ADE Studies. RVP production and ADE assays were performed using approaches detailed

in prior studies with WNV and DENV RVPs[27,48] using plasmids expressing the C-prM-E

genes of ZIKV H/PF/2013 or DENV-2 16681 and a plasmid encoding a WNV replicon

expressing GFP. Infection of human K562 cells were carried out at 37°C and GFP-positive

infected cells were detected by flow cytometry 48 hr later.

Mouse Protection Experiments. C57BL/6 mice (4- to 5-week-old, Jackson Laboratories)

were inoculated with ZIKV by subcutaneous (footpad) route with 105 FFU of mouse-

adapted ZIKV Dakar in a volume of 50 mL. One day prior, mice were treated with 2 mg

of an Ifnar-blocking mAb (MAR1-5A3) by intraperitoneal injection[25]. ZIKV mAbs were

administered as a single 250 ug dose 1 day before infection via an intraperitoneal route.

Serum samples were obtained at day 3 after ZIKV infection and extracted with the Viral

RNA Mini Kit (QIAGEN). ZIKV RNA levels were determined by TaqMan one-step qRT-

PCR on an ABI 7500 Fast Instrument using published primers and conditions[49].

Statistical Analysis. All virological data were analyzed with GraphPad Prism software.

Kaplan-Meier survival curves were analyzed by the log rank test, and weight losses and

viremia were compared using an ANOVA with a multiple comparisons test. A p value of

<0.05 indicated statistically significant differences. SVP ELISA data were analyzed by non-linear regression analysis using a one-site binding model.

2.6   Acknowledgements

2.7   References

1.   Dick, G. W. ., Kitchen, S. . & Haddow, A. . Zika Virus (I). Isolations and serological specificity. *Trans. R. Soc. Trop. Med. Hyg.* **46,** 509–520 (1952).
2.   Dick, G. W. A. Zika Virus (II). Pathogenicity and Physical Properties. *Trans. R. Soc. Trop. Med. Hyg.* **46,** 521–534 (1952).
3.   Lazear, H. M. & Diamond, M. S. Zika Virus: New Clinical Syndromes and its Emergence in the Western Hemisphere. *J. Virol.* JVI.00252-16 (2016). doi:10.1128/JVI.00252-16
4.   Carteaux, G. *et al.* Zika Virus Associated with Meningoencephalitis. *N. Engl. J. Med.* **374,** 1595–1596 (2016).
5.   Oehler, E. *et al.* Zika virus infection complicated by Guillain-Barre syndrome--case report, French Polynesia, December 2013. *Euro Surveill.* **19,** (2014).
6.   Brasil, P. P. *et al.* Zika Virus Infection in Pregnant Women in Rio de Janeiro. *N. Engl. J. Med.* **375,** 2321–2334 (2016).
7.   Cugola, F. R. *et al.* The Brazilian Zika virus strain causes birth defects in experimental models. *Nature* **534,** (2016).
8.   Li, C. *et al.* Zika Virus Disrupts Neural Progenitor Development and Leads to Microcephaly in Mice. *Cell Stem Cell* **19,** 120–126 (2016).
9.   Miner, J. J. *et al.* Zika virus infection during pregnancy in mice causes placental damage and fetal demise. *Cell* **165,** 1081–1091 (2016).
10.   Dai, L. *et al.* Structures of the Zika Virus Envelope Protein and Its Complex with a Flavivirus Broadly Protective Antibody. *Cell Host Microbe* **19,** 696–704 (2016).
11.   Kostyuchenko, V. A. *et al.* Structure of the thermally stable Zika virus. *Nature* (2016). doi:10.1038/nature17994
12.   Sirohi, D. *et al.* The 3.8 A resolution cryo-EM structure of Zika virus. *Science (80-.).* **352,** 467–470 (2016).
13.   Kuhn, R. J. *et al.* Structure of dengue virus: Implications for flavivirus organization, maturation, and fusion. *Cell* **108,** 717–725 (2002).
14.   Belmusto-Worn, V. E. *et al.* Randomized, double-blind, phase III. Pivotal field trial of the comparative immunogenicity, safety, and tolerability of two yellow fever 17D vaccines (ARILVAX^{TM} and YF-VAX®) in healthy infants and children in Peru. *Am. J. Trop. Med. Hyg.* **72,** 189–197 (2005).
15.   Heinz, F. X., Holzmann, H., Essl, A. & Kundi, M. Field effectiveness of vaccination against tick-borne encephalitis. *Vaccine* **25,** 7559–7567 (2007).
16.   Beasley, D. W. C. & Barrett, A. D. T. Identification of Neutralizing Epitopes within Structural Domain III of the West Nile Virus Envelope Protein. *J. Virol.* **76,** 13097–13100 (2002).
17.   Oliphant, T. *et al.* Development of a humanized monoclonal antibody with therapeutic potential against West Nile Virus. *Nat. Med.* **11,** 522–530 (2005).
18.   Shrestha, B. *et al.* The development of therapeutic antibodies that neutralize homologous

and heterologous genotypes of dengue virus type 1. *PLoS Pathog.* **6,** e1000823 (2010).

19. Sukupolvi-Petty, S. *et al.* Structure and function analysis of therapeutic monoclonal antibodies against dengue virus type 2. *J. Virol.* **84,** 9227–9239 (2010).

20. de Alwis, R. *et al.* Identification of human neutralizing antibodies that bind to complex epitopes on dengue virions. *Proc. Natl. Acad. Sci.* **109,** 7439–7444 (2012).

21. Kaufmann, B. *et al.* Neutralization of West Nile virus by cross-linking of its surface proteins with Fab fragments of the human monoclonal antibody CR4354. *Proc. Natl. Acad. Sci. U. S. A.* **107,** 18950–5 (2010).

22. Rouvinski, A. *et al.* Recognition determinants of broadly neutralizing human antibodies against dengue viruses. *Nature* **520,** 109–113 (2015).

23. Cherrier, M. V *et al.* Structural basis for the preferential recognition of immature flaviviruses by a fusion-loop antibody. *EMBO J.* **28,** 3269–3276 (2009).

24. Vogt, M. R. *et al.* Poorly Neutralizing Cross-Reactive Antibodies against the Fusion Loop of West Nile Virus Envelope Protein Protect In Vivo via Fc Receptor and Complement-Dependent Effector Mechanisms. *J. Virol.* **85,** 11567–11580 (2011).

25. Lazear, H. M. *et al.* A Mouse Model of Zika Virus Pathogenesis. *Cell Host Microbe* **in press,** (2016).

26. Rossi, S. L. *et al.* Characterization of a Novel Murine Model to Study Zika Virus. *Am. J. Trop. Med. Hyg.* **94,** 1362–1369 (2016).

27. Pierson, T. C. *et al.* The Stoichiometry of Antibody-Mediated Neutralization and Enhancement of West Nile Virus Infection. *Cell Host Microbe* **1,** 135–145 (2007).

28. Midgley, C. M. *et al.* Structural Analysis of a Dengue Cross-Reactive Antibody Complexed with Envelope Domain III Reveals the Molecular Basis of Cross-Reactivity. *J. Immunol.* **188,** 4971–4979 (2012).

29. Austin, S. K. *et al.* Structural Basis of Differential Neutralization of DENV-1 Genotypes by an Antibody that Recognizes a Cryptic Epitope. *PLoS Pathog.* **8,** (2012).

30. Nybakken, G. E. *et al.* Structural basis of West Nile virus neutralization by a therapeutic antibody. *Nature* **437,** 764–769 (2005).

31. Edeling, M. A. *et al.* Potent Dengue Virus Neutralization by a Therapeutic Antibody with Low Monovalent Affinity Requires Bivalent Engagement. *PLoS Pathog.* **10,** (2014).

32. Lok, S.-M. *et al.* Binding of a neutralizing antibody to dengue virus alters the arrangement of surface glycoproteins. *Nat. Struct. Mol. Biol.* **15,** 312–317 (2008).

33. Cockburn, J. J. B. *et al.* Mechanism of dengue virus broad cross-neutralization by a monoclonal antibody. *Structure* **20,** 303–314 (2012).

34. Kaufmann, B. *et al.* West Nile virus in complex with the Fab fragment of a neutralizing monoclonal antibody. *Proc. Natl. Acad. Sci. U. S. A.* **103,** 12400–4 (2006).

35. Larocca, R. A. *et al.* Vaccine protection against Zika virus from Brazil. *Nature* **536,** 474–478 (2016).

36. Beltramello, M. *et al.* The Human Immune Response to Dengue Virus is Dominated by Highly Cross- Reactive Antibodies Endowed with Neutralizing and Enhancing Activity.

Cell Host Microbe **8,** (2010).

37. Jarmer, J. *et al.* Variation of the Specificity of the Human Antibody Responses after Tick-Borne Encephalitis Virus Infection and Vaccination. *J. Virol.* **88,** 13845–13857 (2014).

38. Smith, S. A. *et al.* The Potent and Broadly Neutralizing Human Dengue Virus-Specific Monoclonal Antibody 1C19 Reveals a Unique Cross-Reactive Epitope on the bc Loop of Domain II of the Envelope Protein. *MBio* **4,** e00873-13-e00873-13 (2013).

39. Dowd, K. A., DeMaso, C. R. & Pierson, T. C. Genotypic Differences in Dengue Virus Neutralization Are Explained by a Single Amino Acid Mutation That Modulates Virus Breathing. *MBio* **6,** e01559-15 (2015).

40. Thompson, B. S. *et al.* A Therapeutic Antibody against West Nile Virus Neutralizes Infection by Blocking Fusion within Endosomes. *PLoS Pathog.* **5,** e1000453 (2009).

41. Kim, J. *et al.* FcRn in the Yolk Sac Endoderm of Mouse Is Required for IgG Transport to Fetus. *J. Immunol.* **182,** 2583–2589 (2009).

42. Pentšuk, N. & van der Laan, J. W. An interspecies comparison of placental antibody transfer: new insights into developmental toxicity testing of monoclonal antibodies. *Birth Defects Res. B Dev. Reprod. Toxicol.* **86,** 328–344 (2009).

43. Martina, B. E. *et al.* Immunization with West Nile virus envelope domain III protects mice against lethal infection with homologous and heterologous virus. *Vaccine* **26,** (2008).

44. Schneeweiss, A. *et al.* A DNA vaccine encoding the E protein of West Nile Virus is protective and can be boosted by recombinant domain DIII. *Vaccine* **29,** 6352–6357 (2011).

45. Correia, B. E. *et al.* Proof of principle for epitope-focused vaccine design. *Nature* **507,** 201–206 (2014).

46. Brien, J. D., Lazear, H. M. & Diamond, M. S. Propagation, Quantification, Detection, and Storage of West Nile Virus. in *Current Protocols in Microbiology* 15D.3.1-15D.3.18 (John Wiley & Sons, Inc., 2013). doi:10.1002/9780471729259.mc15d03s31

47. Pal, P. *et al.* Development of a highly protective combination monoclonal antibody therapy against Chikungunya virus. *PLoS Pathog.* **9,** e1003312 (2013).

48. Dowd, K. A., Jost, C. A., Durbin, A. P., Whitehead, S. S. & Pierson, T. C. A dynamic landscape for antibody binding modulates antibody-mediated neutralization of West Nile virus. *PLoS Pathog.* **7,** (2011).

49. Lanciotti, R. S. Genetic and serologic properties of Zika virus associated with an epidemic, Yap State, Micronesia, 2007. *Emerg. Infect. Dis.* **14,** 1232–1239 (2008).

Table 2.1: Characteristic of Anti-ZIKV mAbs

mAb	Priming[a]	Isotype[b]	Domain Localization and Epitope[c]	Cross-reactivity[d]	Affinity for DIII or ZIKV E K_D (nM)[e]	$t_{1/2}$[f] (min)	H/PF/2013[g] FRNT$_{50}$ (ng/mL)	Paraiba 2015 FRNT$_{50}$ (ng/mL)	Dakar 41519 FRNT$_{50}$ (ng/mL)	MR-766 FRNT$_{50}$ (ng/mL)
ZV-2	Virus	IgG2c	DIII (ABDE sheet)	none	266 ± 42	0.3	>10,000	>10,000	>10,000	>10,000
ZV-13	Virus	IgG2c	DI-II (fusion loop)	WNV, JEV, DENV-1,-2, -3, -4	254 ± 10	3.3	>10,000	>10,000	>10,000	>10,000
ZV-48	Virus + DIII	IgG2c	DIII (C-C' loop)	none	35 ± 0.8	3.2	485	>10,000	>10,000	>10,000
ZV-54	Virus + DIII	IgG2c	DIII (LR)	none	7.9 ± 0.2	33.0	87	312	192	582
ZV-64	Virus + DIII	IgG2c	DIII (C-C' loop)	none	32 ± 13	1.0	1,000	>10,000	>10,000	>10,000
ZV-67	Virus + DIII	IgG2c	DIII (LR)	none	8.8 ± 1.7	13.8	143	511	145	282

[a]To generate mAbs, mice were infected and boosted with 10^3 FFU of ZIKV (MR-766 and H/PF/2013, respectively) and given a final intravenous boost with live ZIKV (H/PF/2013) or purified DIII.

[b]mAb isotype was determined using a commercial ELISA kit.

[c]Domain localization and epitope was determined by binding to WT or mutant recombinant proteins or X-ray crystallography (Figures 1 and 3).

[d]Cross-reactivity was determined by flow cytometric analysis of flavivirus-infected cells.

[e]K_D (equilibrium) were determined by BLI with ZIKV E (ZV-13) or DIII (ZV-2, ZV-48, ZV-54, ZV-64, ZV-67) as described in Figure 2 and Figure S1.

[f]Calculated from the dissociation constant, k_d kinetic.

[g]Purified mAb was incubated with 10^2 FFU of indicated ZIKV strains for 1 hour at 37°C. FRNT$_{50}$ values were determined by non-linear regression and are shown as ng/mL Results are the average of at least three independent experiments.
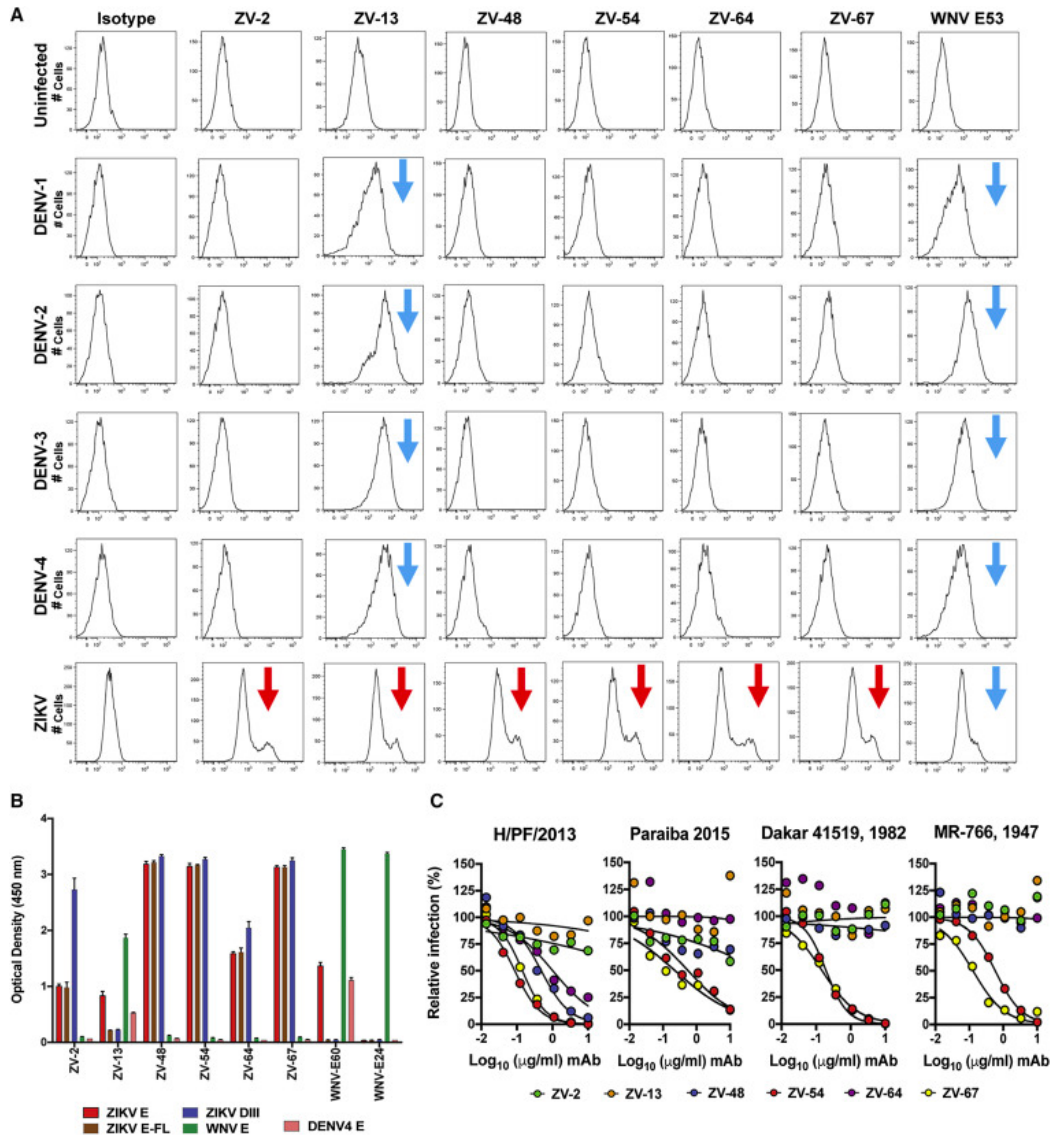
Figure 2.1: Profile of Neutralizing mAbs Against ZIKV

(A) Cells were infected with DENV-1, DENV-2, DENV-3, DENV-4, or ZIKV (H/PF/2013), and stained with indicated anti-ZIKV mAbs or isotype controls and processed by flow cytometry. The data are representative of several independent experiments. Blue arrows indicate binding of cross-reactive mAbs (ZV-13 or WNV E53) to DENV and ZIKV-infected cells. Red arrows indicate binding of ZIKV mAbs to ZIKV-infected cells. (B) The indicated flavivirus proteins (ZIKV E, ZIKV E-FL [fusion loop mutant], ZIKV DIII, WNV E, and DENV-4 E) were incubated with the indicated anti-ZIKV mAbs or controls (WNV E60 [flavivirus cross-reactive] and WNV E24 [WNV type-specific]). Binding was determined by ELISA and the results are representative of two independent experiments performed in triplicate. (C) Focus reduction neutralization tests (FRNT). Different ZIKV strains (H/PF/2013, Paraiba, 2015, Dakar 41519, and MR-766) were incubated with increasing concentrations of mAbs for 1 hr at 37°C prior to infection of Vero cells. Subsequently, an FRNT assay was performed (Experimental Procedures). The results reflect pooled data from two or more independent experiments performed in triplicate.

69
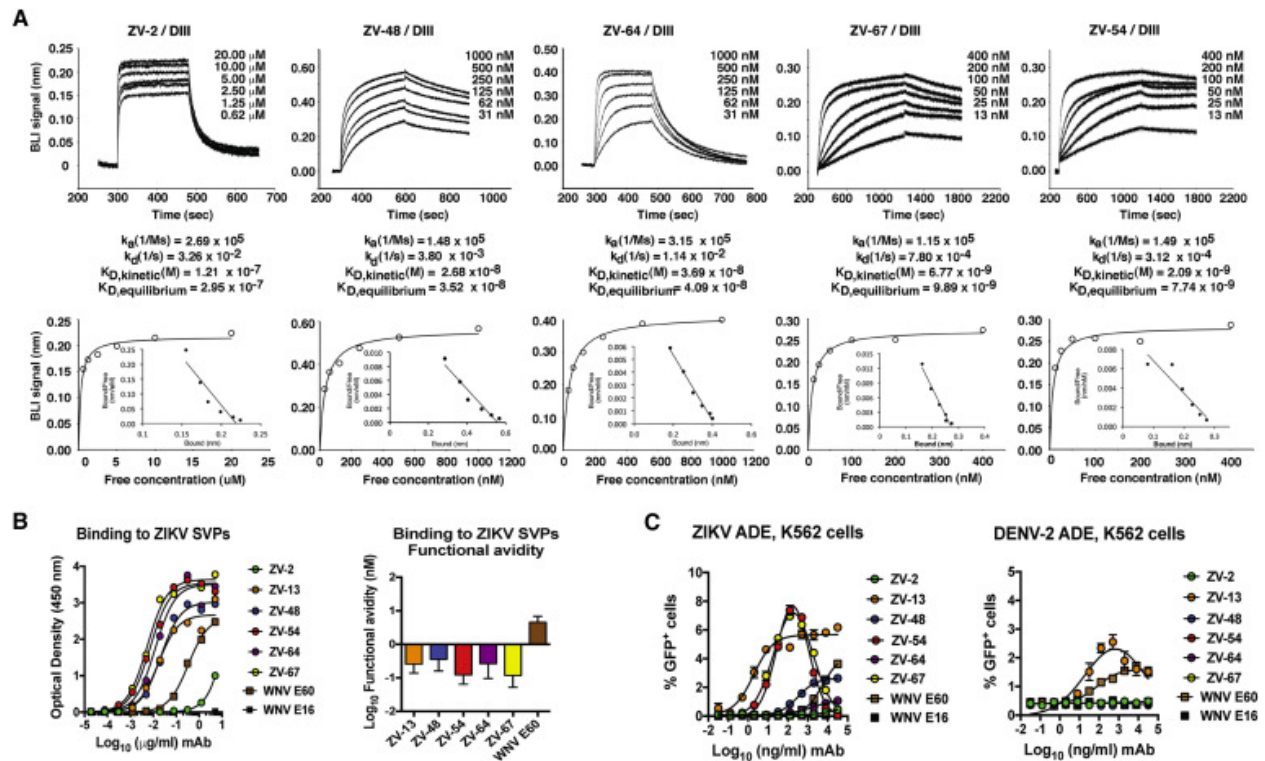
Figure 2.2: Differential Binding and ADE Activity of Different Anti-ZIKV mAbs

(A) Quantitative analysis of DIII binding to anti-ZIKV mAbs by BLI. Shown in the top panel are binding curves obtained by passing different concentrations of DIII over biotinylated anti-ZIKV antibody immobilized on a biosensor surface. The kinetic values were obtained by simultaneously fitting the association and dissociation responses to a 1:1 Langmuir binding model (K_D, kinetic). The lower panels show the steady-state analysis results (K_D, equilibrium). Plotted in the bottom panels (open circles) is the binding response (nm) versus concentration of DIII offered. In each case, the binding was saturable. Bottom insets, Scatchard plots suggest a single binding affinity for each interaction. The data are representative of two independent experiments per mAb. (B) Left: ZIKV SVPs were adsorbed to 96-well plates and detected with the indicated biotinylated anti-ZIKV or control (WNV E60 [flavivirus cross-reactive] and WNV E16 [WNV type-specific]) mAbs by ELISA. Right: the relative avidity of binding was calculated. Data are representative of five independent experiments, and the avidity values reflect the mean of the five experiments. Error bars indicate SDs. (C) ADE studies. Serial dilutions of anti-ZIKV or control (WNV E60 [flavivirus cross-reactive] and WNV E16 [WNV type-specific]) mAbs were mixed with (left) ZIKV H/PF/2013 or (right) DENV-2 RVPs (which encode for GFP) prior to infection of FcγRIIa+ human K562 cells and processing by flow cytometry. One representative experiment of two is shown. Error bars indicate the range of duplicate technical replicates.

70
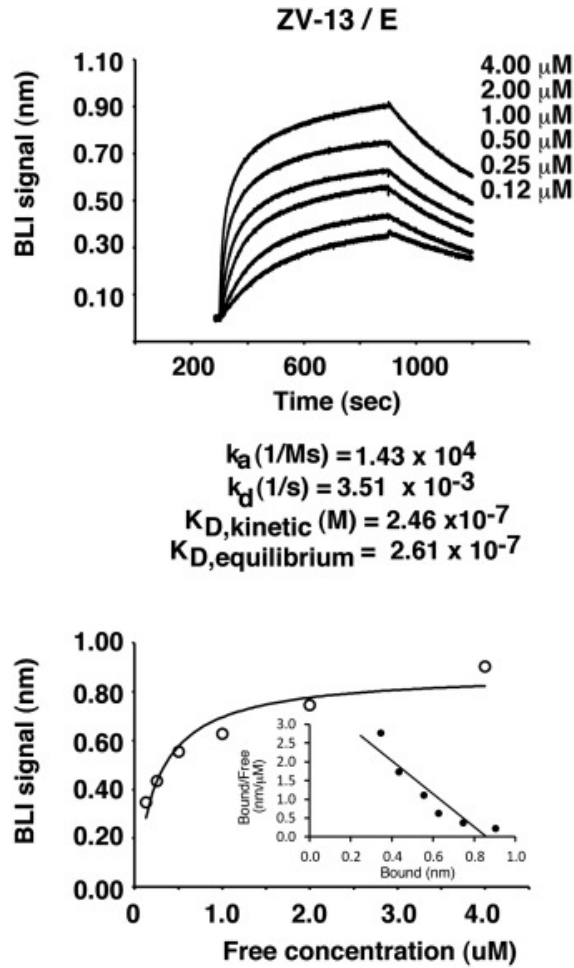
Figure 2.3: BLI Binding Data

ZV-13 mAb binding to recombinant soluble ZIKV E protein was assayed by BLI. Randomly biotinylated ZV-13 mAb was coated onto Streptavidin biosensor pins. The pins were equilibrated in binding buffer alone (HBS-EP +1% BSA) before being plunged into wells containing various concentrations of recombinant ZIKV E ectodomain protein. The association lasted ten minutes before the pins were placed back in binding buffer to allow for dissociation. The real-time data were analyzed using Biaevaluation 4.1 (GE Healthcare). Association and dissociation profiles, as well as steady-state equilibrium concentration curves, were fitted assuming a 1:1 binding model.
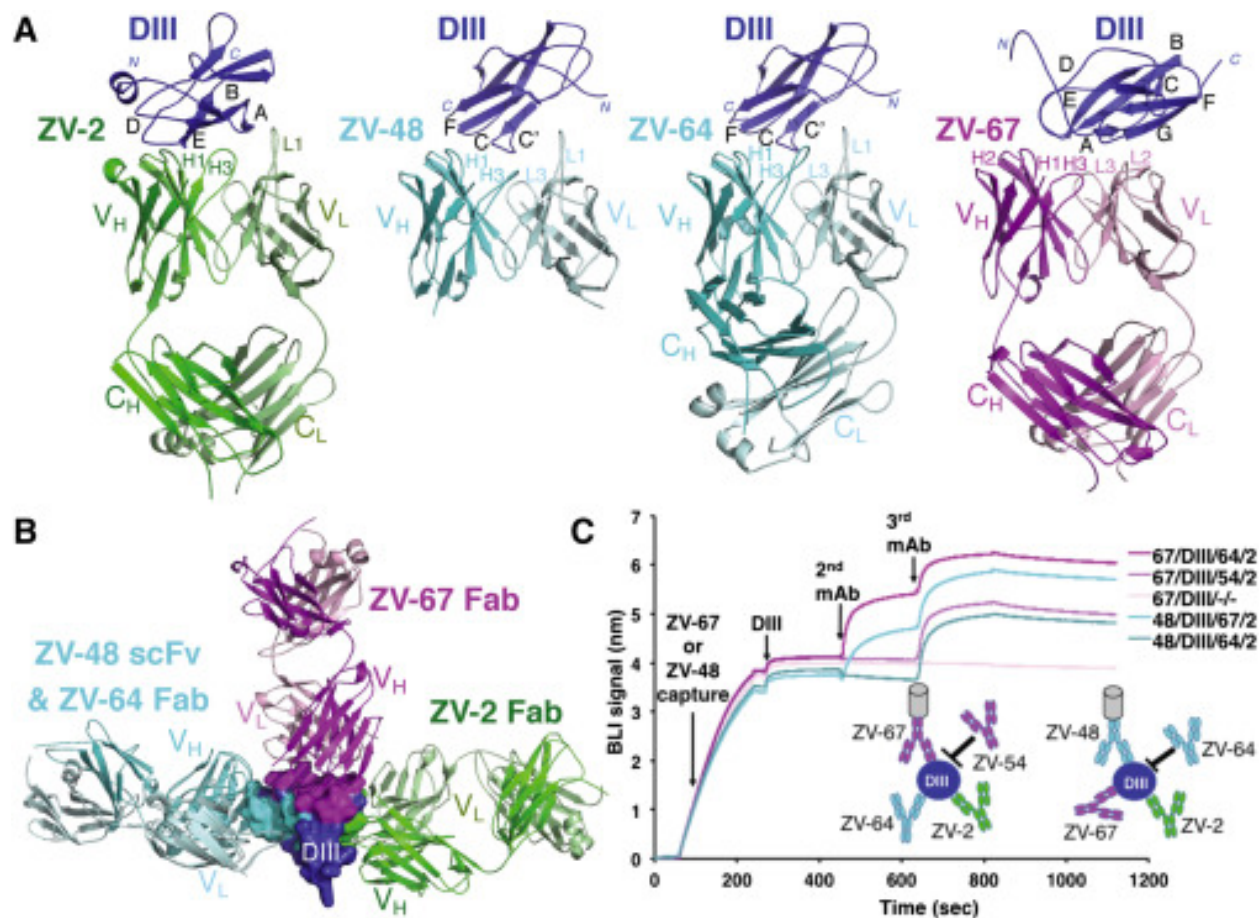
Figure 2.4: Structures of Anti-ZIKV Fabs and scFv Complexed with DIII

(A) Ribbon diagrams of four ZIKV DIII (H/PF/2013) complexes with antibody fragments. The crystal structure of ZV-2 Fab (outer left, green), ZV-48 scFv (inner left, cyan), ZV-64 Fab (inner right, cyan), and ZV-67 Fab (outer right, magenta) are shown with light chains rendered in paler colors. DIII is colored dark blue with contact segments labeled. (B) Docking of the ZV-2, ZV-48, and ZV-64 complexes onto ZV-67-DIII. DIII is rendered as a molecular surface with each mAb contact surface color coded. Simultaneous docking of ZV-2 and ZV-67 with either ZV-48 or ZV-64 buries nearly half of the solvent surface of DIII and creates no van der Waal contacts between adjacent mAbs. (C) Five mAbs were probed for competitive and non-competitive binding against the DIII antigen by BLI. In one experiment, biotin-labeled ZV-67 was captured on the streptavidinsensor, the antibody was then loaded with ZIKV DIII followed by either ZV-54 or ZV-64, and finally, ZV-2 was added. In another experiment, ZV-48 was immobilized and ZV-64 or ZV-67 was added after DIII followed by ZV-2. Additional BLI signal indicates an unoccupied epitope (non-competitor), whereas no binding indicates epitope blocking (competition). In this experiment, ZV-48 competed with ZIKV-64 as expected given that they both bind nearly identical epitopes, while ZV-67 competed with its presumed sibling clone ZV-54. A dash (-) represents that no 2nd or 3rd antibody was offered.

72

Figure 2.5: mAb Sequence Alignments and Antigen Contacts

Amino acid sequence alignment of the variable heavy chain (V_H) and light chain (V_L) of the mAbs ZV-2 (A), ZV-48 and ZV-64 (B), and ZV-54 and ZV-67 (C) against the C57BL/6 germline. Nucleotide and amino acid sequences were analyzed using NCBI/IgBlast and IMGT/V-Quest to identify the germline V, D and J gene members with the highest sequence identity. The top sequence in each alignment is the presumptive germline IgV, D, and J genes. Red stars indicate positions of somatic hypermutation. Red triangles mark insertions at the junctions of rearrangement. The mAb-DIII contact residues are boxed in the color of the epitope they bind: green for the ABDE epitope, cyan for the C-C' loop epitope, and magenta for the LR epitope. Absent residues are denoted with (.). Consensus variable domain numbering is given above the aligned sequences, with insertions as described (Al-Lazikani et al., 1997). Complementarity determining regions (CDR 1-3) are marked at the top of the alignment. The secondary structure elements are indicated in blue (arrows for β sheet and coil for α helices). A table of the number of somatic mutations for each antibody is provided at the bottom.
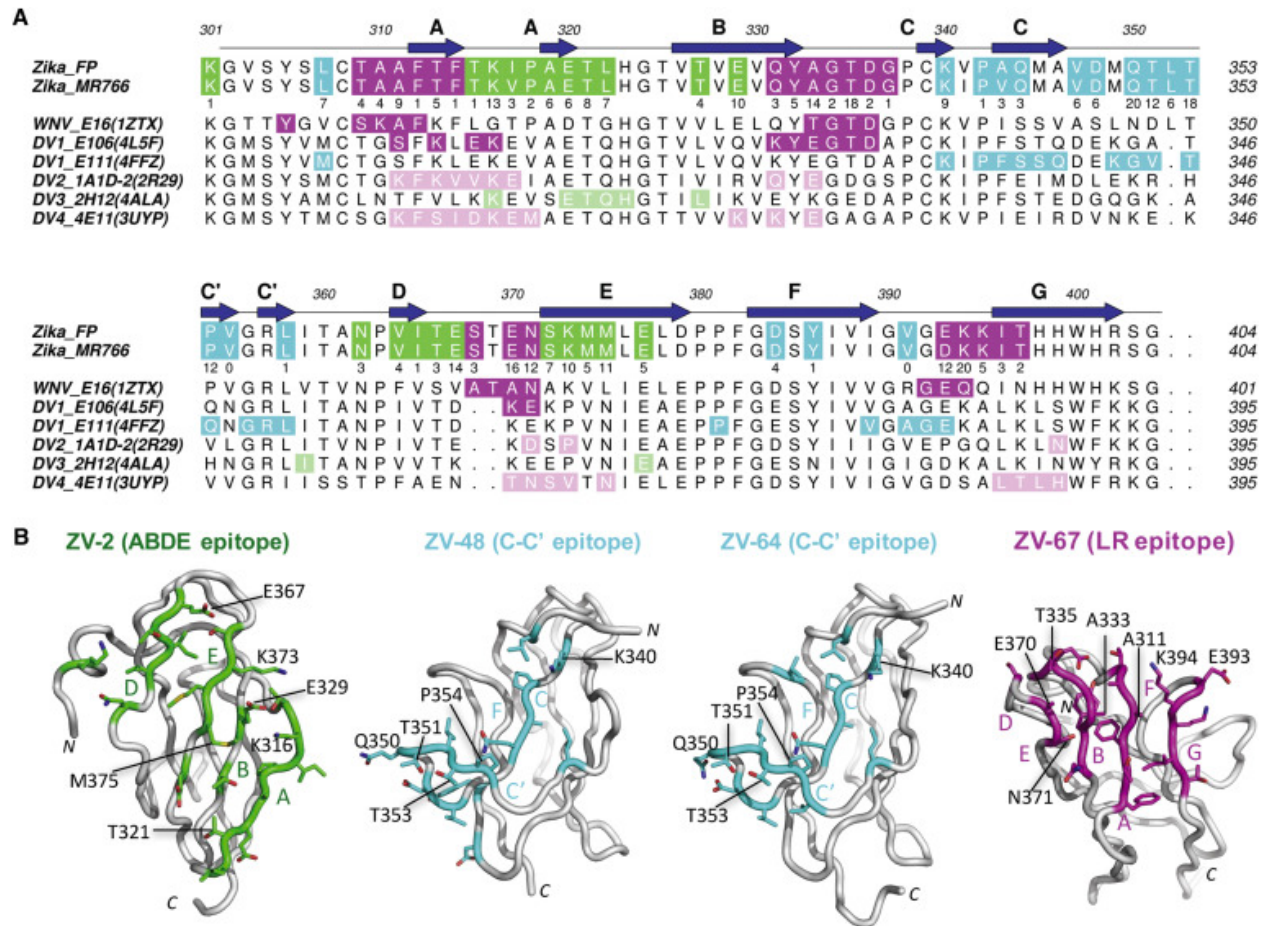
Figure 2.6: Structural Definition of ZIKV-Specific DIII Epitopes

(A) Sequence alignment of DIII from our ZIKV immunizing stains (H/PF/2013 and MR-766), WNV, DENV-1, DENV-2, DENV-3, and DENV-4 and highlighting of structurally defined DIII epitopes. The ABDE sheet epitope of ZV-2 is shown in green, the C-C′ loop epitope of ZV-48 and ZV-64 is shown in cyan, and the LR epitope of ZV-67 is shown in magenta. DIII residues are colored if they make van der Waals contact of ≤3.90-Å distance, and the total number of contacts for each epitope residue are shown below the ZIKV sequences. For comparison, the same structurally defined DIII epitopes of WNV E16 (magenta, LR), DV1-E106 (magenta, LR), DV1-E111 (cyan, C-C′ loop), DV2 1A1D-2 (pink, A-strand), DV3 2H12 (light-green, A-B-loop), and DV4 4E11 (pink, A-strand) are displayed. The ZIKV β strands are labeled and shown in dark blue above the sequences. (B) Delineation of the epitope contact regions on the ZIKV DIII structures of ZV-2 (ABDE sheet), ZV-48 (C-C′ loop), ZV-64 (C-C′ loop) and ZV-67 (LR). DIII epitope residues are colored as in (A), with side chains drawn as sticks and labeled if they make eight or more van der Waals contacts.

74
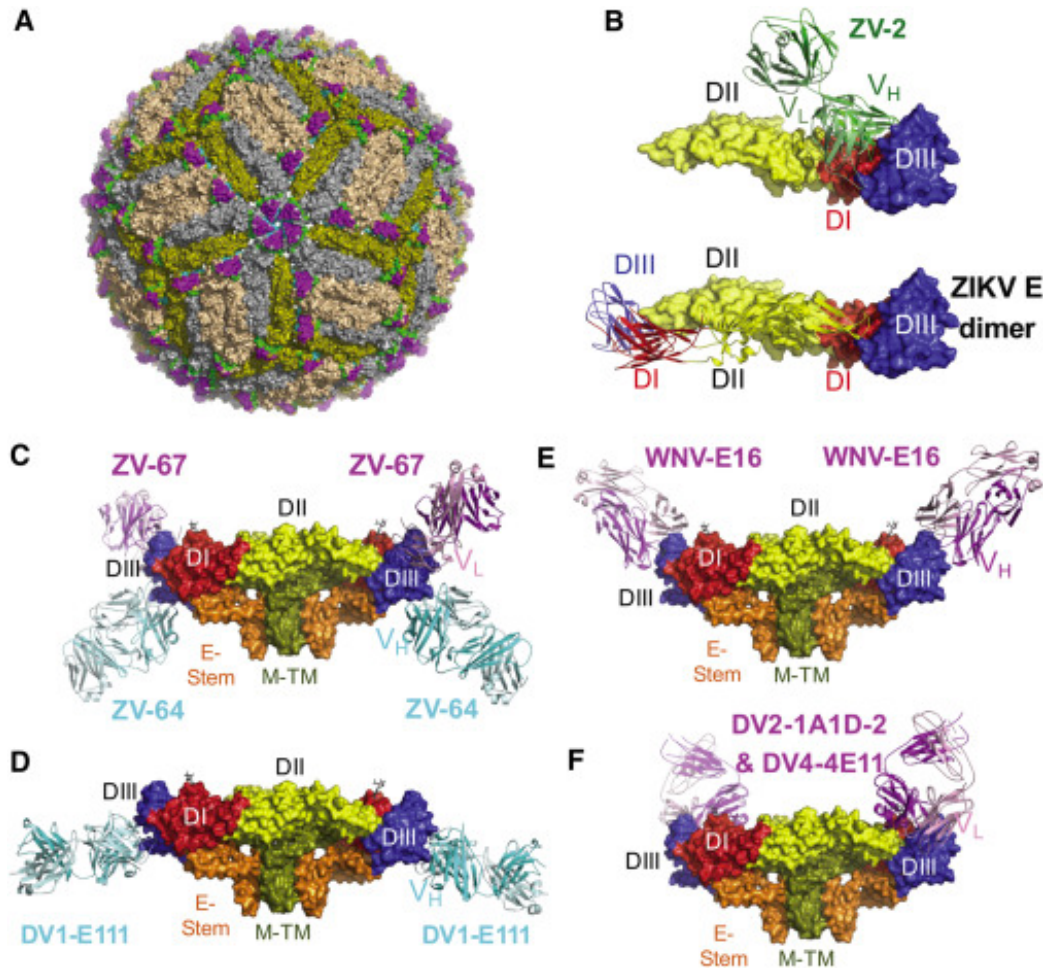
Figure 2.7: Accessibility of ZIKV DIII Epitopes

(A) Mapping of the three distinct ZIKV DIII epitopes onto the mature virion (5IRE) (Sirohi et al., 2016). The surface distribution of the ABDE sheet (green), C-C′ loop (cyan), and LR (magenta) epitopes are rendered on the three symmetrically unique E proteins colored olive, wheat, and gray. While the ABDE sheet and C-C′ loop epitopes are dominantly buried in all three symmetry environments, the LR epitope is solvent accessible on the mature virion. (B) Docking of the ZV-2-DIII complex onto the crystal structure of dimeric ZIKV (5JHM) (Dai et al., 2016). Shown above is the ZV-2 Fab docked to a soluble E monomer, which indicates that the ABDE sheet epitope is occluded by DI with clashes by the V_H domain. Below, the ZIKV dimer is depicted, showing how it would sterically clash with the ZV-2 V_L domain. ZV-2 CDR loops contact several of the same DIII residues that are contacted by the DII fusion loop in the dimer. (C) Docking of the ZV-64-DIII and ZV-67-DIII complexes onto the cryoelectron microscopymodel of the M-E dimer that forms the mature virion. ZV-67 binding to the LR epitope allows for the projection of the Fab away from the viral membrane whereas ZV-64 binding to the C-C′ loop epitope positions the Fab in the plane of the viral envelope and membrane. (D) Comparative docking of the DV1-E111 Fab-DIII complex (Austin et al., 2012) onto the cryptic C-C′ loop epitope suggests similar steric clashes as predicted for ZV-64. (E) Comparative docking of the WNV-E16 Fab-DIII complex (Nybakken et al., 2005) onto the exposed LR epitope. (F) Comparative docking of the DV2-1A1D-2 Fab-DIII complex (Lok et al., 2008) and DV4-4E11 scFv-DIII complex (Cockburn et al., 2012) onto the exposed A-strand epitope.
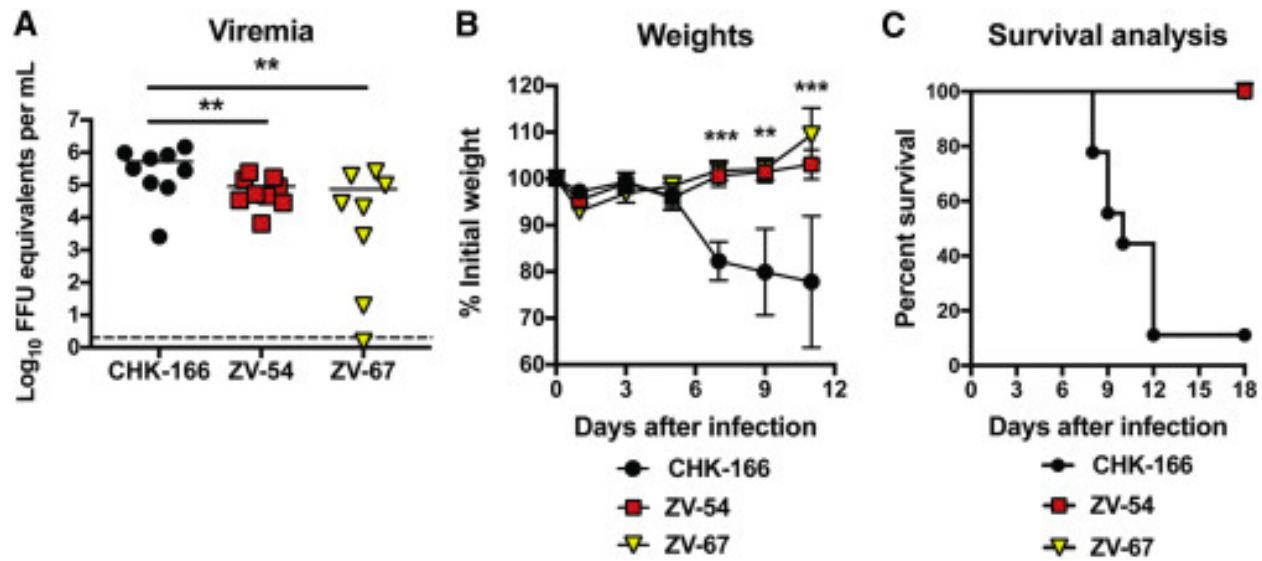
Figure 2.8: *In Vivo* Protection of Anti-ZIKV mAbs

4- to 5-week-old C57BL/6 mice were passively transferred 2 mg of anti-Ifnar1 mAb and 250 µg of the indicated mAbs (CHK-166, ZV-54, or ZV-67) via an intraperitoneal injection1 day before subcutaneous inoculation with 10^5 FFU of ZIKV Dakar 41519. (A and B) (A) On day 3 after infection, serum was collected for analysis of viral RNA by qRT-PCR. (B) Daily weights were measured. For (A) and (B), statistical significance was analyzed by a one-way ANOVA with a Dunnett's multiple comparisons test ($^{**}p < 0.01$; $^{***}p < 0.001$). (C) ZV-54 and ZV-67 protected against ZIKV infection compared to the control CHK-166 mAb ($^{***}p < 0.001$, log rank test). The results are pooled from two independent experiments with n = 8–9 mice for each treatment condition.

Chapter 3:

Neutralizing human antibodies prevent Zika virus replication and fetal disease in mice

This chapter is adapted from a manuscript published in Nature:

3.1   Summary

Zika virus (ZIKV) is an emerging mosquito-transmitted flavivirus that can cause severe disease, including congenital birth defects during pregnancy[1]. To develop candidate therapeutic agents against ZIKV, we isolated a panel of human monoclonal antibodies from subjects that were previously infected with ZIKV. We show that a subset of antibodies recognize diverse epitopes on the envelope (E) protein and exhibit potent neutralizing activity. One of the most inhibitory antibodies, ZIKV-117, broadly neutralized infection of ZIKV strains corresponding to African and Asian-American lineages. Epitope mapping studies revealed that ZIKV-117 recognized a unique quaternary epitope on the E protein dimer–dimer interface. We evaluated the therapeutic efficacy of ZIKV-117 in pregnant and non-pregnant mice. Monoclonal antibody treatment markedly reduced tissue pathology, placental and fetal infection, and mortality in mice. Thus, neutralizing human antibodies can protect against maternal–fetal transmission, infection and disease, and reveal important determinants for structure-based rational vaccine design efforts.

3.2   Main

Recent ZIKV epidemics are linked to Guillain–Barré syndrome in adults and microcephaly in fetuses and newborn infants[2–5]. Although ZIKV infection can potentially cause severe disease, specific treatments and vaccines for ZIKV are not currently available. We sought to isolate neutralizing human monoclonal antibodies (mAbs) with broad specificity against all ZIKV strains and protective activity *in vivo*. We tested the serological response of subjects who had previously been infected with ZIKV in diverse geographic locations. Serum from each subject contained antibodies that were shown by ELISA assays to react with ZIKV E protein and to neutralize infection of a contemporary Asian isolate (H/PF/2013) from French Polynesia (**Figures 3.1A and 3.1B**). We studied the B cells of subject 1001 in greater detail. Based on the results of replicate assays, the frequency of B cells that secrete antibodies against ZIKV E protein in the peripheral blood was between 0.36% and 0.61% (**Figures 3.1C and 3.1D**). We next tested the reactivity of antibodies with domain III (DIII) of the E protein from ZIKV or the related dengue (DENV) and West Nile (WNV) viruses. Only a subset (6%) of the ZIKV-E-reactive antibodies bound to DIII, and most were specific for ZIKV (**Figure 3.1C**). Comparative binding to a wild-type or mutant ZIKV E protein lacking the conserved fusion loop epitope in DII (mutant denoted hereafter as E-FLM) established immunodominance (binding around 70% of mAbs) of the fusion loop.

We obtained 29 cloned hybridomas secreting mAbs that bound to ZIKV E protein from the cells of three donors (mAb ZIKV-195 from subject 1011, mAb ZIKV-204 from subject 973, and the remaining 27 mAbs from subject 1001). All of the mAbs except for one belonged to the IgG1 isotype (two could not be determined), with an equal distribution

79

of κ and λ light chains (**Table 3.1**); sequence analysis of cDNA of the antibody variable gene regions revealed that each mAb represented an independent clone (**Table 3.1**). We determined the half-maximal effective concentrations for binding to ZIKV E protein (EC_{50}) and neutralization (IC_{50}) of infection (**Figure 3.2A and 3.3**); most of the mAbs bound to E protein at low concentrations ($EC_{50} < 100$ ng ml^{-1}), whereas only four of the 29 mAbs exhibited strong neutralizing activity ($IC_{50} = 5–420$ ng ml^{-1}). We next determined how many antigenic sites on ZIKV E were recognized using quantitative competition binding. We identified four major competition groups (designated A, B, C or D). Group A mAbs had 23 members that were directed against the fusion loop in DII, as determined by differential binding to E and E-FLM (**Figure 3.3**), and had only one clone (ZIKV-88) with moderate neutralizing potency. The group B mAb ZIKV-116 neutralized ZIKV infection and bound to E, DIII and E-FLM. Group C mAbs (ZIKV-19 and ZIKV-190) bound to E and E-FLM weakly, but did not potently neutralize infection. The group D mAb ZIKV-195 neutralized with moderate potency and was similar in binding to both E and E-FLM. The most inhibitory group D mAb, ZIKV-117, bound to both E and E-FLM weakly.

We mapped the epitopes of representative mAbs using a shotgun alanine-scanning mutagenesis library[6] of ZIKV prM and E protein variants (**Figure 3.2B and 3.4**). Loss-of-binding analysis confirmed that group A mAbs bound to the fusion loop in DII, whereas the group B mAb bound to DIII. Group B mAb ZIKV-116 bound to an epitope involving residues T309, E393 and K394 along the lateral ridge of DIII (DIII-LR), which was confirmed in an ELISA that showed reduced binding to DIII with mutations A310E and T335K in DIII-LR[7]. The epitope mapping studies suggest that the group D mAb ZIKV-117 binds specifically to DII across two adjacent dimers at the 'dimer–dimer' interface

(**Figure 3.2C**). We were unable to isolate virus neutralization escape mutant viruses for ZIKV-117, despite six passages in cell culture under mAb selection pressure.

Because of their potency, we assessed whether group B mAb ZIKV-116 and group D mAb ZIKV-117 could inhibit diverse ZIKV strains encompassing the African and Asian-American lineages. ZIKV-117 neutralized all of the ZIKV strains tested, including two African (MR 766 and Dakar 41519), two Asian (Malaysia P6740 and H/PF/2013), and an American (Brazil Paraiba 2015) strain with IC_{50} values of 5 to 25 ng ml^{-1} (**Figures 3.2D and 3.2E**). ZIKV-116 inhibited four of the five strains efficiently, but was inactive against MR 766, the original African strain (**Figures 3.2D and 3.2E**). Alignment of the sequences of ZIKV H/PF/2013 and MR 766, with respect to residues in DIII-LR[7] that ZIKV-116 binds, revealed only one difference (a conservative E393D change). Given these data, we hypothesize that the DIII-LR epitope of ZIKV-116 is displayed differently on MR 766 owing to allosteric effects of changes in other parts of the E protein, which could regulate epitope accessibility[8,9].

As recent studies have suggested that cross-reactive ZIKV-specific human mAbs can enhance DENV infection *in vivo*[10], we tested whether these two ZIKV-neutralizing mAbs could bind to DENV-infected cells. ZIKV-117 showed a restricted type-specific binding pattern as it failed to stain cells infected with DENV-1, DENV-2, DENV-3 or DENV-4, or bind to purified WNV E protein (**Figure 3.5** and data not shown). In comparison, ZIKV-116 bound to cells infected with DENV-1, DENV-2 or DENV-4, but did not bind to DENV-2 DIII or WNV DIII in ELISA.

In vivo models of ZIKV pathogenesis and antibody prophylaxis have been reported[7,10,11] in mice deficient in type-I interferon signaling. To determine whether ZIKV-

117 had therapeutic activity, we treated 4–5-week-old wild-type male C57BL/6 mice at day −1 with anti-Ifnar1 mAbs, and then inoculated animals with 10^3 focus-forming units (FFU) of a mouse-adapted African strain of ZIKV-Dakar[7]. Animals were treated with a single dose of ZIKV-117 or non-binding isotype control (human (h)CHK-152)[12], on day +1 (100 μg; 6.7 mg kg^{-1}) or day +5 (250 μg; 16.7 mg kg^{-1}). Animals treated with hCHK-152 sustained significant lethality compared to those receiving ZIKV-117 (**Figure 3.6A**), which were protected even when administered only a single dose 5 days after virus inoculation.

We and others have demonstrated placental injury and fetal demise following ZIKV infection of pregnant mice with deficiencies in type-I interferon signalling[13–15]. To assess the protective ability of ZIKV-117 during fetal development, we treated *Ifnar1*$^{-/-}$ pregnant dams mated to wild-type male mice with a single 250 μg dose of ZIKV-117 or isotype control mAb (hCHK-152) on embryo day 5.5 (E5.5), the day before ZIKV inoculation. Whereas inoculation with ZIKV-Brazil at E6.5 following administration with hCHK-152 resulted in high levels of maternal infection and almost uniform fetal demise by E13.5, treatment with ZIKV-117 improved fetal outcome (**Figure 3.6B and 3.6C**).

Because of the extent of demise at E13.5 after ZIKV infection of *Ifnar1*$^{-/-}$ dams, we could not recover adequate numbers of fetuses to measure viral titerss. Accordingly, we switched to a wild-type mouse model with an acquired type-I interferon deficiency using the mouse-adapted African ZIKV-Dakar strain. Wild-type pregnant dams were treated at day −1 (E5.5) with an anti-Ifnar1 mAbs. At the same time, these animals were administered vehicle control (PBS), 250 μg isotype control hCHK-152, or 250 μg ZIKV-117. One day later, dams were inoculated subcutaneously with 10^3 FFU of ZIKV-Dakar.

Fetuses from dams treated with anti-Ifnar1 mAbs and given PBS or hCHK-152 showed high levels (for example, around 10^5 to 10^7 FFU equivalents per gram) of viral RNA in the placenta and fetal brain (**Figure 3.6D**). In comparison, mice treated with anti-Ifnar1 and ZIKV-117 had reduced virus levels in the placenta and fetal brain (for example, around $10°$ to 10^3FFU equivalents per gram). This phenotype was associated with transport of human ZIKV E-specific IgG across the maternal–fetal placental barrier (816 ± 53 ng ml^{-1} for the placenta and $1,675 \pm 203$ ng ml^{-1} for the fetal head; **Figure 3.7**). As levels of neonatal Fc receptor in the mouse placenta are lower than other mammalian species[16], reduced levels of transport of maternal or exogenous IgG into the fetus is expected[17]. Although this factor could underestimate the therapeutic effect of exogenous anti-ZIKV IgG or maternal antibodies, we nonetheless achieved levels in the placenta and fetal head that were orders of magnitude above the IC$_{50}$ neutralization value for ZIKV-117. Dams treated with ZIKV-117 also had substantially lower levels of viral RNA in the maternal brain and serum **(Figure 3.6E)**.

Antibody-dependent enhancement of flavivirus infection occurs when type-specific or cross-reactive antibodies fail to reach a stoichiometric threshold for neutralization and instead facilitate infection of FcγR-expressing myeloid cells[18]. Because antibodies can promote antibody-dependent enhancement of ZIKV in cell culture[19,20], we evaluated the protective efficacy of a recombinant form of ZIKV-117 IgG containing a leucine (L) to alanine (A) substitution at positions 234 and 235 (LALA)[21], which lacked efficient binding to FcγR, retained interactions with FcRn[22], and neutralized ZIKV *in vitro* equivalently compared to the parent mAb (**Figure 3.8**). The LALA variant of ZIKV-117 showed similar protective activity against infection of the placenta and fetus relative to the parent mAb

(**Figure 3.6F**). As the protection conferred by ZIKV-117 in the pregnancy model is probably due to neutralization and not Fc effector functions, LALA variants could be used without a risk of antibody-dependent enhancement.

We next assessed the post-exposure efficacy of ZIKV-117 during pregnancy. Mice treated with anti-Ifnar1 mAbs at E5.5 were inoculated with 10^3 FFU of ZIKV-Dakar at E6.5 and then administered a single dose of PBS, 250 μg of hCHK-152, or 250 μg of ZIKV-117 at E7.5. Compared to PBS or isotype control mAb treatment, administration of ZIKV-117 markedly reduced the viral burden in the dams, the placenta and fetus when measured at E13.5 (**Figures 3.6G and 3.6H**).

The reduction in viral load mediated by ZIKV-117 was associated with decreased damage of the placenta (as judged by labyrinth layer and overall placenta area), less trophoblast cell death, and increased body size of the fetus (**Figure 3.9A- 3.9C**) compared to fetuses of PBS- or hCHK-152-treated dams. ZIKV-117 protected against ZIKV-induced placental insufficiency, as the placental area and fetal size from infected dams treated with anti-ZIKV mAbs were similar to that of uninfected placentas[14]. *In situ* hybridization revealed an almost complete absence of viral RNA in the junctional zone and decidua of the placenta in animals treated with ZIKV-117 compared to staining observed in PBS- or hCHK-152-treated controls (**Figures 3.9D and 3.10**). We also observed vascular damage associated with ZIKV infection of the placenta[14], characterized as diminished vimentin staining of fetal endothelial cells, which was rescued by ZIKV-117 to levels seen in uninfected placentas (**Figure 3.9E**). The histopathological data suggests that ZIKV-117 treatment can reduce the ability of ZIKV to cross the fetal endothelial cell barrier, and thereby prevent vertical transmission and improve fetal outcome.

Our most potent neutralizing antibodies exhibited a breadth of inhibitory activity against strains from Africa, Asia, and the Americas. Even a single ZIKV-117 dose given 5 days after infection protected mice against lethal infection, a timeline similar to the most protective antibodies against other flaviviruses[23]. Prophylaxis or post-exposure therapy of pregnant mice with ZIKV-117 reduced infection in mothers, and in placental and fetal tissues. As the extent to which these observations in mice translate to humans remains unclear, protection studies in non-human primates, which share a placental architecture similar to humans, seem warranted. If the results were consistent, ZIKV-117 or human antibodies with similar profiles[10,19] could be developed as a treatment measure during pregnancy for at-risk humans. By defining key epitopes on the E protein associated with antibody-mediated protection, our studies also inform vaccine efforts to design new immunogens that elicit highly protective antibody responses against ZIKV.

3.3 Methods

Research subjects. We studied eight subjects in the United States with previous or recent ZIKV infection (**Table 3.2**). The studies were approved by the Institutional Review Board of Vanderbilt University Medical Center; samples were obtained after informed consent was obtained by the Vanderbilt Clinical Trials Center. Two subjects (972 and 973) were infected with an African lineage strain in 2008 (one subject while working in Senegal, the second acquired the infection by sexual transmission from the first, as previously reported[24]). The other six subjects were infected during the current outbreak of an Asian lineage strain, following exposure in Brazil, Mexico or Haiti.

Generation and quantification of human B-cell lines secreting ZIKV E protein specific antibodies. Peripheral blood mononuclear cells (PBMCs) from heparinized blood

were isolated with Ficoll-Histopaque by density gradient centrifugation. The cells were used immediately or cryopreserved in the vapour phase of liquid nitrogen until use. Ten million PBMCs were cultured in 384-well plates (Nunc) using culture medium (ClonaCell-HY Medium A, StemCell Technologies) supplemented with 8 μg ml^{-1} of the TLR agonist CpG (phosphorothioate-modified oligodeoxynucleotide ZOEZOEZZZZZOEEZOEZZZT, Invitrogen), 3 μg ml^{-1} of Chk2 inhibitor (Sigma), 1 μg ml^{-1} of cyclosporine A (Sigma), and clarified supernatants from cultures of B95.8 cells (ATCC) containing Epstein–Barr virus. After 7 days, cells from each 384-well culture plate were expanded into four 96-well culture plates (Falcon) using ClonaCell-HY Medium A containing 8 μg ml^{-1} of CpG, 3 μg ml^{-1} of Chk2 inhibitor, and 10^7 irradiated heterologous human PBMCs (Nashville Red Cross) and cultured for an additional 4 days. Supernatants were screened in ELISA (described below) for reactivity with various ZIKV E proteins, which are described below. The minimal frequency of ZIKV E-reactive B cells was estimated based on the number of wells with E protein-reactive supernatants compared with the total number of lymphoblastoid cell line colonies in the transformation plates (calculation: E-reactive B-cell frequency = (number of wells with E-reactive supernatants) divided by (number of LCL colonies in the plate) × 100).

Protein expression and purification. The ectodomains of ZIKV E (H/PF/2013; GenBank Accession KJ776791) and the fusion-loop mutant E-FLM (containing four mutations: T76A, Q77G, W101R, L107R) were expressed transiently in Expi293F cells and purified as described previously[7]. ZIKV DIII (residues 299–407 of strain H/PF/2013), WNV DIII (residues 296–405 of strain New York 1999) and DENV-2 DIII (residues 299-410 of strain 16681) were expressed in BL21 (DE3) as inclusion bodies and refolded *in vitro*[25]. Briefly,

inclusion bodies were denatured and refolded by gradual dilution into a refolding buffer (400 mM L-arginine, 100 mM Tris (pH 8.3), 2 mM EDTA, 5 and 0.5 mM reduced and oxidized glutathione) at 4 °C. Refolded proteins were purified by size-exclusion chromatography using a Superdex 75, 16/60 (GE Healthcare).

Generation of human hybridomas. Cells from wells with transformed B cells containing supernatants that exhibited reactivity to ZIKV E protein were fused with HMMA2.5 myeloma cells (gift from L. Cavacini) using an established electrofusion technique[26]. After fusion, hybridomas were suspended in a selection medium containing 100 μM hypoxanthine, 0.4 μM aminopterin, 16 μM thymidine (HAT Media Supplement, Sigma), and 7 μg ml^{-1} ouabain (Sigma) and cultured in 384-well plates for 18 days before screening hybridomas for antibody production by ELISA. After fusion with HMMA2.5 myeloma cells, hybridomas producing ZIKV E-specific antibodies were cloned biologically by single-cell fluorescence-activated cell sorting. Hybridomas were expanded in post-fusion medium (ClonaCell-HY Medium E, STEMCELL Technologies) until 50% confluent in 75-cm^2 flasks (Corning).

For antibody production, cells from one 75-cm^2 flask were collected with a cell scraper and expanded to four 225-cm^2 flasks (Corning) in serum-free medium (Hybridoma-SFM, Life Technologies). After 21 days, supernatants were clarified by centrifugation and filtered using 0.45-μm pore size filter devices. HiTrap Protein G or HiTrap MAbSelectSure columns (GE Healthcare Life Sciences) were used to purify antibodies from filtered supernatants.

Sequence analysis of antibody variable region genes. Total cellular RNA was extracted from pelleted cells from hybridoma clones, and an RT–PCR reaction was performed using

mixtures of primers designed to amplify all heavy-chain or light-chain antibody variable regions[27]. The generated PCR products were purified using AMPure XP magnetic beads (Beckman Coulter) and sequenced directly using an ABI3700 automated DNA sequencer. The variable region sequences of the heavy and light chains were analysed using the IMGT/V-Quest program[28,29].

ELISA and EC$_{50}$ binding analysis. Wells of microtitre plates were coated with purified, recombinant ectodomain of ZIKV E, DIII, DIII-LR mutants (DIII containing A310E and T335K mutations) or DIII of related flaviviruses DENV-2 or WNV and incubated at 4 °C overnight. In ELISA studies with purified mAbs, we used recombinant ZIKV E protein ectodomain with His$_6$ tag produced in Sf9 insect cells (Meridian Life Sciences R01635). Plates were blocked with 5% skimmed milk in PBS-T for 1 h. B-cell culture supernatants or purified antibodies were added to the wells and incubated for 1 h at ambient temperature. The bound antibodies were detected using goat anti-human IgG (γ-specific) conjugated with alkaline phosphatase (Southern Biotech) and pNPP disodium salt hexahydrate substrate (Sigma). In ELISAs that assessed binding of mAbs to DIII and DIII LR mutants, we used previously described murine mAbs ZV-2 and ZV-54 (ref. **7**) as controls. A goat anti-mouse IgG conjugated with alkaline phosphatase (Southern Biotech) was used for detection of these antibodies. Colour development was monitored at 405 nm in a spectrophotometer (Biotek). For determining EC$_{50}$, microtitre plates were coated with ZIKV E or E-FLM that eliminated interaction of fusion-loop specific antibodies. Purified antibodies were diluted serially and applied to the plates. Bound antibodies were detected as above. A nonlinear regression analysis was performed on the resulting curves using Prism (GraphPad) to calculate EC$_{50}$ values.

ELISA for detection of human antibodies in murine tissues. Fetal head and placental tissues were collected at E13.5 from groups treated with ZIKV-117 or PBS (as a negative control), homogenized in PBS (250 μl) and stored at −20 °C. ELISA plates were coated with ZIKV E protein, and thawed, clarified tissue homogenates were applied undiluted in triplicate. Bound antibodies were detected using goat anti-human IgG (Fc-specific) antibody conjugated with alkaline phosphatase. The quantity of antibody was determined by comparison with a standard curve constructed using purified ZIKV-117 in a dilution series.

Biolayer interferometry competition binding assay. His$_6$-tagged ZIKV E protein was immobilized on anti-His coated biosensor tips (Pall) for 2 min on an Octet Red biosensor instrument. After measuring the baseline signal in kinetics buffer (PBS, 0.01% BSA, and 0.002% Tween 20) for 1 min, biosensor tips were immersed into the wells containing first antibody at a concentration of 10 μg ml^{-1} for 7 min. Biosensors then were immersed into wells containing a second mAb at a concentration of 10 μg ml^{-1} for 7 min. The signal obtained for binding of the second antibody in the presence of the first antibody was expressed as a percentage of the uncompeted binding of the second antibody that was derived independently. The antibodies were considered competing if the presence of first antibody reduced the signal of the second antibody to less than 30% of its maximal binding and non-competing if the signal was greater than 70%. A level of 30–70% was considered intermediate competition.

Shotgun mutagenesis epitope mapping. Epitope mapping was performed by shotgun mutagenesis essentially as described previously[6]. A ZIKV prM/E protein expression construct (based on ZIKV strain SPH2015) was subjected to high-throughput alanine

scanning mutagenesis to generate a comprehensive mutation library. Each residue within prM/E was changed to alanine, with alanine codons mutated to serine. In total, 672 ZIKV prM/E mutants were generated (100% coverage), sequence confirmed, and arrayed into 384-well plates. Each ZIKV prM/E mutant was transfected into HEK-293T cells and allowed to express for 22 h. Cells were fixed in 4% (v/v) paraformaldehyde (Electron Microscopy Sciences), and permeabilized with 0.1% (w/v) saponin (Sigma-Aldrich) in PBS plus calcium and magnesium (PBS++). Cells were incubated with purified mAbs diluted in PBS++, 10% normal goat serum (Sigma), and 0.1% saponin. Primary antibody screening concentrations were determined using an independent immunofluorescence titration curve against wild-type ZIKV prM/E to ensure that signals were within the linear range of detection. Antibodies were detected using $3.75\,\mu\text{g}\,\text{ml}^{-1}$ of AlexaFluor488-conjugated secondary antibody (Jackson ImmunoResearch Laboratories) in 10% NGS/0.1% saponin. Cells were washed three times with PBS++/0.1% saponin followed by two washes in PBS. Mean cellular fluorescence was detected using a high-throughput flow cytometer (HTFC, Intellicyt). Antibody reactivity against each mutant prM/E clone was calculated relative to wild-type prM/E protein reactivity by subtracting the signal from mock-transfected controls and normalizing to the signal from wild-type prM/E-transfected controls. Mutations within clones were identified as critical to the mAb epitope if they did not support reactivity of the test MAb, but supported reactivity of other ZIKV antibodies. This counter-screen strategy facilitates the exclusion of prM/E mutants that are locally misfolded or have an expression defect.

Vertebrate animal studies ethics statement. This study was carried out in accordance with the recommendations in the Guide for the Care and Use of Laboratory Animals of the

National Institutes of Health. The protocols were approved by the Institutional Animal Care and Use Committee at the Washington University School of Medicine (Assurance number A3381-01). Inoculations were performed under anaesthesia induced and maintained with ketamine hydrochloride and xylazine, and all efforts were made to minimize animal suffering. No statistical methods were used to predetermine sample size. The experiments were not randomized and the investigators were not blinded to allocation during experiments and outcome assessment.

Viruses and cells. ZIKV strain H/PF/2013 (French Polynesia, 2013) was obtained from X. de Lamballerie (Aix Marseille Université). ZIKV Brazil Paraiba 2015 was provided by S. Whitehead (Bethesda) and originally obtained from P. F. C. Vasconcelos (Instituto Evandro Cargas). ZIKV MR 766 (Uganda, 1947), Malaysia P6740 (1966), and Dakar 41519 (Senegal, 1982) were provided by the World Reference Center or Emerging Viruses and Arboviruses (R. Tesh, University of Texas Medical Branch). Nicaraguan DENV strains (DENV-1 1254-4, DENV-2 172-08, DENV-3 N2845-09, and DENV-4 N703-99) were provided generously by E. Harris (University of California, Berkeley). Virus stocks were propagated in C6/36 *Aedes albopictus* cells (DENV) or Vero cells (ZIKV). ZIKV Dakar 41519 (ZIKV-Dakar) was passaged twice *in vivo* in $Rag1^{-/-}$ mice (M. Gorman and M. Diamond, unpublished data) to create a mouse-adapted strain. Virus stocks were titrated by focus-forming assay (FFA) on Vero cells. All cell lines were checked regularly for mycoplasma contamination and were negative. Cell lines were authenticated at acquisition with short tandem repeat method profiling; Vero cells, though commonly misidentified in the field, were used as they are the standard cell line for flavivirus titration.

Neutralization assays. Serial dilutions of mAbs were incubated with 10^2 FFU of different ZIKV strains (MR 766, Dakar 41519, Malaysia P6740, H/PF/2013, or Brazil Paraiba 2015) for 1 h at 37 °C. The mAb–virus complexes were added to Vero cell monolayers in 96-well plates for 90 min at 37 °C. Subsequently, cells were overlaid with 1% (w/v) methylcellulose in MEM supplemented with 4% heat-inactivated FBS. Plates were fixed 40 h later with 1% PFA in PBS for 1 h at room temperature. The plates were incubated sequentially with 500 ng ml^{-1} mouse anti-ZIKV (ZV-16, E.F. and M.S.D., unpublished data) and horseradish-peroxidase-conjugated goat anti-mouse IgG in PBS supplemented with 0.1% (w/v) saponin (Sigma) and 0.1% BSA. ZIKV-infected cell foci were visualized using TrueBlue peroxidase substrate (KPL) and quantitated on an ImmunoSpot 5.0.37 macroanalyzer (Cellular Technologies).

mAb binding to ZIKV- or DENV-infected cells. C6/36 *Aedes albopictus* cells were inoculated with a MOI 0.01 of ZIKV (H/PF/2013) or different DENV serotypes (Nicaraguan strains DENV-1 1254-4, DENV-2 172-08, DENV-3 N2845-09, DENV-4 N703-99). At 120 h post infection, cells were fixed with 4% PFA diluted in PBS for 20 min at room temperature and permeabilized with HBSS supplemented with 10 mM HEPES, 0.1% saponin and 0.025% NaN_3 for 10 min at room temperature. 50,000 cells were transferred to U-bottom plates and incubated for 30 min at 4 °C with 5 μg ml^{-1} of anti-ZIKV human mAbs or negative (hCHK-152)[12], or positive (hE60)[30] isotype controls. After washing, cells were incubated with Alexa-Fluor-647-conjugated goat anti-human IgG (Invitrogen) at 1:500, fixed in 1% PFA in PBS, processed on MACSQuant Analyzed (Miltenyi Biotec), and analysed using FlowJo software (Tree Star).

Recombinant antibody expression and purification. Total RNA was extracted from hybridoma cells and genes encoding the VH and VL domains were amplified in RT–PCR using IgExp primers[31]. The PCR products were directly cloned into antibody expression vectors containing the constant domains of wild-type γ1 chain, LALA mutant (leucine (L) to alanine (A) substitution at positions 234 and 235) γ1 chain for the VH domains, and wild-type κ chain for the VL domain in an isothermal amplification reaction (Gibson reaction)[32]. Plasmids encoding the heavy and light chain were transfected into 293F cells and full-length recombinant IgG was secreted into transfected cell supernatants. Supernatants were collected and IgG purified using Protein G chromatography and eluted into PBS. The functional abrogation of the binding of the LALA variant IgG was confirmed in an ELISA binding assay with recombinant human FcγRI. The binding of wild-type ZIKV-117 or LALA antibody to FcγRI was evaluated, in comparison with the binding pattern of control antibodies (human mAb CKV063[33] LALA mutated IgG).

Adult mouse lethal protection experiments. C57BL/6 male mice (4–5-week-old, Jackson Laboratories) were inoculated with 10^3 FFU of mouse-adapted ZIKV-Dakar by subcutaneous route in the footpad. One-day before infection, mice were treated with 2 mg anti-Ifnar1 mAb (MAR1-5A3, Leinco Technologies) by intraperitoneal injection. ZIKV-specific human mAb (ZIKV-117) or an isotype control (hCHK-152) was administered as a single dose at day +1 (100 μg) or day +5 (250 μg) after infection through an intraperitoneal route. Animals were monitored for 21 days.

Pregnant mouse protection experiments. Wild-type C57BL/6 mice were bred in a specific pathogen-free facility at Washington University School of Medicine. (1) *Ifnar1*$^{-/-}$ dams, prophylaxis studies: *Ifnar1*$^{-/-}$ female and wild-type male mice were

mated; at E5.5, dams were treated with a single 250 μg dose of ZIKV mAb or isotype control by intraperitoneal injection. At E6.5, mice were inoculated with 10^3 FFU of ZIKV Brazil Paraiba 2015 by subcutaneous injection in the footpad. (2) Wild-type dams, prophylaxis studies: wild-type female and male mice were mated; at embryonic days E5.5, dams were treated with a single 250 μg dose of ZIKV mAb or isotype control by intraperitoneal injection as well as a 1 mg injection of anti-Ifnar1 (MAR1-5A3). At E6.5, mice were inoculated with 10^3 FFU of mouse-adapted ZIKV-Dakar by subcutaneous injection in the footpad. At E7.5, dams received a second 1 mg dose of anti-Ifnar1 through an intraperitoneal route. (3) Wild-type dams, therapy studies: wild-type female and male mice were mated; at embryonic days E5.5, dams were treated with a 1 mg injection of anti-Ifnar1 (MAR1-5A3). At E6.5, mice were inoculated with mouse-adapted 10^3 FFU of ZIKV-Dakar by subcutaneous injection in the footpad. At E7.5, dams received a second 1 mg dose of anti-Ifnar1 as well as a single 250 μg dose of ZIKV mAb or isotype control through an intraperitoneal route. All animals were euthanized at E13.5, and placentas, fetuses and maternal tissues were collected. Fetus size was measured as the crown-rump length × occipitofrontal diameter of the head.

Measurement of viral burden. ZIKV-infected tissues were weighed and homogenized with stainless steel beads in a Bullet Blender instrument (Next Advance) in 200 μl of PBS. Samples were clarified by centrifugation (2,000g for 10 min). All homogenized tissues from infected animals were stored at −20 °C. Tissue samples and serum from ZIKV-infected mice were extracted with RNeasy 96 Kit (tissues) or Viral RNA Mini Kit (serum) (Qiagen). ZIKV RNA levels were determined by TaqMan one-step quantitative reverse transcriptase PCR (qRT–PCR) on an ABI7500 Fast Instrument using published primers

94

and conditions[34]. Viral burden was expressed on a $\log_{10}$ scale as viral RNA equivalents per g or ml after comparison with a standard curve produced using serial tenfold dilutions of ZIKV RNA.

Viral RNA *in situ* hybridization. RNA *in situ* hybridization was performed with RNAscope 2.5 (Advanced Cell Diagnostics) according to the manufacturer's instructions. PFA-fixed paraffin embedded placental sections were deparaffinized by incubation for 60 min at 60 °C. Endogenous peroxidases were quenched with H_2O_2 for 10 min at room temperature. Slides were boiled for 15 min in RNAscope Target Retrieval Reagents and incubated for 30 min in RNAscope Protease Plus before probe hybridization. The probe targeting ZIKV RNA was designed and synthesized by Advanced Cell Diagnostics (catalogue number 467771). Negative (targeting bacterial gene *dapB*) control probes were also obtained from Advanced Cell Diagnostics (catalogue number 310043). Tissues were counterstained with Gill's haematoxylin and visualized with standard bright-field microscopy.

Histology and immunohistochemistry. Collected placentas were fixed in 10% neutral buffered formalin at room temperature and embedded in paraffin. At least three placentas from different litters with the indicated treatments were sectioned and stained with haematoxylin and eosin to assess morphology. Surface area and thickness of placenta and different layers were measured using Image J software. For immunofluorescence staining on mouse placentas, deparaffinized tissues were blocked in blocking buffer (1% BSA, 0.3% Triton, PBS) for 2 h and incubated with anti-vimentin antibody (1:500, rabbit, Abcam ab92547). Secondary antibody conjugated with Alexa 488 (1:500 in PBS) was applied for

1 h at room temperature. Samples were counterstained with DAPI (4′6′-diamidino-2-phenilindole, 1:1,000 dilution).

Statistical analysis. All virological data were analysed with GraphPad Prism software. Kaplan–Meier survival curves were analysed by the log rank test, and viraemia was compared using an ANOVA with a multiple comparisons test. $P < 0.05$ indicated statistically significant differences.

3.4 Acknowledgements

3.5   References

1.   Coyne, C. B. & Lazear, H. M. Zika virus — reigniting the TORCH. *Nat. Rev. Microbiol.* **14,** 707–715 (2016).
2.   Oehler, E. *et al.* Zika virus infection complicated by Guillain-Barre syndrome--case report, French Polynesia, December 2013. *Euro Surveill.* **19,** (2014).
3.   Musso, D. & Gubler, D. J. Zika Virus. *Clin. Microbiol. Rev.* **29,** 487–524 (2016).
4.   Araujo, A. Q. C., Silva, M. T. T. & Araujo, A. P. Q. C. Zika virus-associated neurological disorders: a review. *Brain* **139,** 2122–2130 (2016).
5.   Gatherer, D. & Kohl, A. Zika virus: a previously slow pandemic spreads rapidly through the Americas. *J. Gen. Virol.* **97,** 269–273 (2016).
6.   Davidson, E. & Doranz, B. J. A high-throughput shotgun mutagenesis approach to mapping B-cell antibody epitopes. *Immunology* **143,** 13–20 (2014).
7.   Zhao, H. *et al.* Structural Basis of Zika Virus-Specific Antibody Protection. *Cell* **166,** 1016–1027 (2016).
8.   Dowd, K. A., DeMaso, C. R. & Pierson, T. C. Genotypic Differences in Dengue Virus Neutralization Are Explained by a Single Amino Acid Mutation That Modulates Virus Breathing. *MBio* **6,** e01559-15 (2015).
9.   Dowd, K. A., Mukherjee, S., Kuhn, R. J. & Pierson, T. C. Combined Effects of the Structural Heterogeneity and Dynamics of Flaviviruses on Antibody Recognition. *J. Virol.* **88,** 11726–11737 (2014).
10.   Stettler, K. *et al.* Specificity, cross-reactivity, and function of antibodies elicited by Zika virus infection. *Science (80-.).* **353,** 823–826 (2016).
11.   Swanstrom, J. A. *et al.* Dengue Virus Envelope Dimer Epitope Monoclonal Antibodies Isolated from Dengue Patients Are Protective against Zika Virus. *MBio* **7,** e01123-16 (2016).
12.   Pal, P. *et al.* Development of a highly protective combination monoclonal antibody therapy against Chikungunya virus. *PLoS Pathog.* **9,** e1003312 (2013).
13.   Mysorekar, I. U. & Diamond, M. S. Modeling Zika Virus Infection in Pregnancy. *N. Engl. J. Med.* **375,** 481–484 (2016).
14.   Miner, J. J. *et al.* Zika virus infection during pregnancy in mice causes placental damage and fetal demise. *Cell* **165,** 1081–1091 (2016).
15.   Yockey, L. J. *et al.* Vaginal exposure to Zika virus during pregnancy leads to fetal brain infection. *Cell* **166,** 1247–1256.e4 (2016).
16.   Kim, J. *et al.* FcRn in the Yolk Sac Endoderm of Mouse Is Required for IgG Transport to Fetus. *J. Immunol.* **182,** 2583–2589 (2009).
17.   Pentšuk, N. & van der Laan, J. W. An interspecies comparison of placental antibody transfer: new insights into developmental toxicity testing of monoclonal antibodies. *Birth Defects Res. B Dev. Reprod. Toxicol.* **86,** 328–344 (2009).
18.   Pierson, T. C. *et al.* The Stoichiometry of Antibody-Mediated Neutralization and Enhancement of West Nile Virus Infection. *Cell Host Microbe* **1,** 135–145 (2007).

19. Dejnirattisai, W. *et al.* Dengue virus sero-cross-reactivity drives antibody-dependent enhancement of infection with zika virus. *Nat. Immunol.* **17,** 1102–1108 (2016).

20. Charles, A. S. & Christofferson, R. C. Utility of a Dengue-Derived Monoclonal Antibody to Enhance Zika Infection In Vitro. *PLoS Curr.* **8,** 1–31 (2016).

21. Hessell, A. J. *et al.* Fc receptor but not complement binding is important in antibody protection against HIV. *Nature* **449,** 101–104 (2007).

22. Oliphant, T. *et al.* Development of a humanized monoclonal antibody with therapeutic potential against West Nile Virus. *Nat. Med.* **11,** 522–530 (2005).

23. Foy, B. D. *et al.* Probable Non-Vector-borne Transmission of Zika Virus, Colorado, USA. *Emerg. Infect. Dis.* **17,** 880–882 (2011).

24. Nelson, C. A., Lee, C. A. & Fremont, D. H. Oxidative Refolding from Inclusion Bodies. in *Methods in molecular biology* **1140,** 145–157 (2014).

25. Yu, X., McGraw, P. A., House, F. S. & Crowe, J. E. An optimized electrofusion-based protocol for generating virus-specific human monoclonal antibodies. *J. Immunol. Methods* **336,** 142–151 (2008).

26. Thornburg, N. J. *et al.* Human antibodies that neutralize respiratory droplet transmissible H5N1 influenza viruses. *J. Clin. Invest.* **123,** 4405–4409 (2013).

27. Brochet, X., Lefranc, M.-P. & Giudicelli, V. IMGT/V-QUEST: the highly customized and integrated system for IG and TR standardized V-J and V-D-J sequence analysis. *Nucleic Acids Res.* **36,** W503–W508 (2008).

28. Giudicelli, V. & Lefranc, M. P. IMGT/junctionanalysis: IMGT standardized analysis of the V-J and V-D-J junctions of the rearranged immunoglobulins (Ig) and T cell receptors (TR)2011. *Cold Spring Harb. Protoc.* 716–725 (2011).

29. Williams, K. L. *et al.* Therapeutic Efficacy of Antibodies Lacking FcγR against Lethal Dengue Virus Infection Is Due to Neutralizing Potency and Blocking of Enhancing Antibodies. *PLoS Pathog.* **9,** e1003157 (2013).

30. Thornburg, N. J. *et al.* H7N9 influenza virus neutralizing antibodies that possess few somatic mutations. *J. Clin. Invest.* **126,** 1482–1494 (2016).

31. Gibson, D. G. *et al.* Enzymatic assembly of DNA molecules up to several hundred kilobases. *Nat. Methods* **6,** 343–345 (2009).

32. Fong, R. H. *et al.* Exposure of Epitope Residues on the Outer Face of the Chikungunya Virus Envelope Trimer Determines Antibody Neutralizing Efficacy. *J. Virol.* **88,** 14364–14379 (2014).

33. Lanciotti, R. S. Genetic and serologic properties of Zika virus associated with an epidemic, Yap State, Micronesia, 2007. *Emerg. Infect. Dis.* **14,** 1232–1239 (2008).
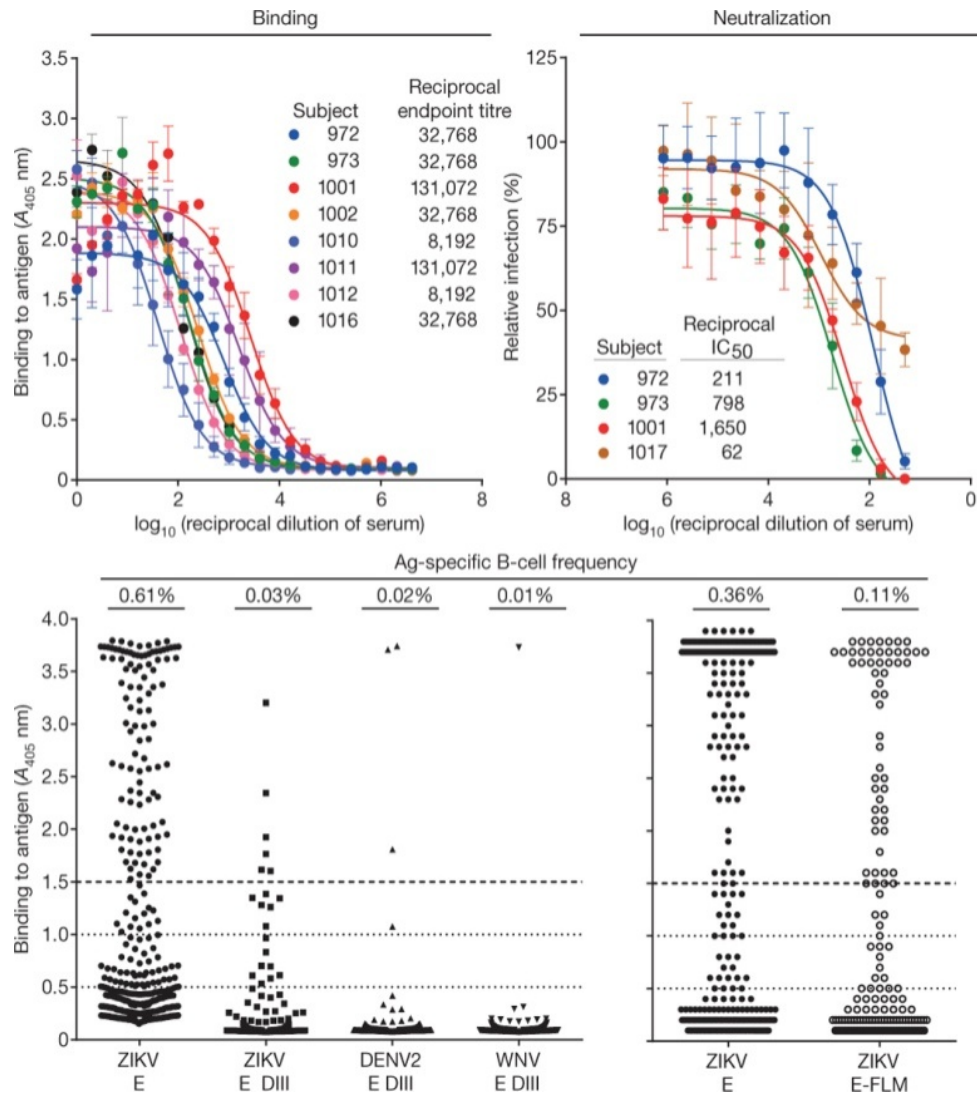
Figure 3.1: Human antibody and B-cell response to ZIKV infection

A, **B**, Serum samples from humans with a previous ZIKV infection were tested for binding to ZIKV E protein in ELISA (**A**) (with two technical replicates) and neutralization of ZIKV (**B**) (at least two independent repeats in triplicate). Subject 1001 had the highest endpoint titre in the binding assay and displayed potent neutralizing activity. Subject 657 was a control without history of exposure to ZIKV. **c**, Supernatants of Epstein–Barr virus (EBV)-transformed B-cell cultures from subject 1001 were tested for binding to ZIKV E or DIII of ZIKV E or related flavivirus E proteins; the WNV-reactive clone and all but one DENV-reactive B-cell line also reacted with ZIKV E protein. The frequency of antigen-specific cells against each viral protein was determined with a threshold absorbance value at 405 nm ($A_{405\ nm}$) of 1.5 as indicated. **d**, In four additional separate B-cell transformation experiments, the frequency of B cells reactive with intact ZIKV E or E-FLM was determined.

99
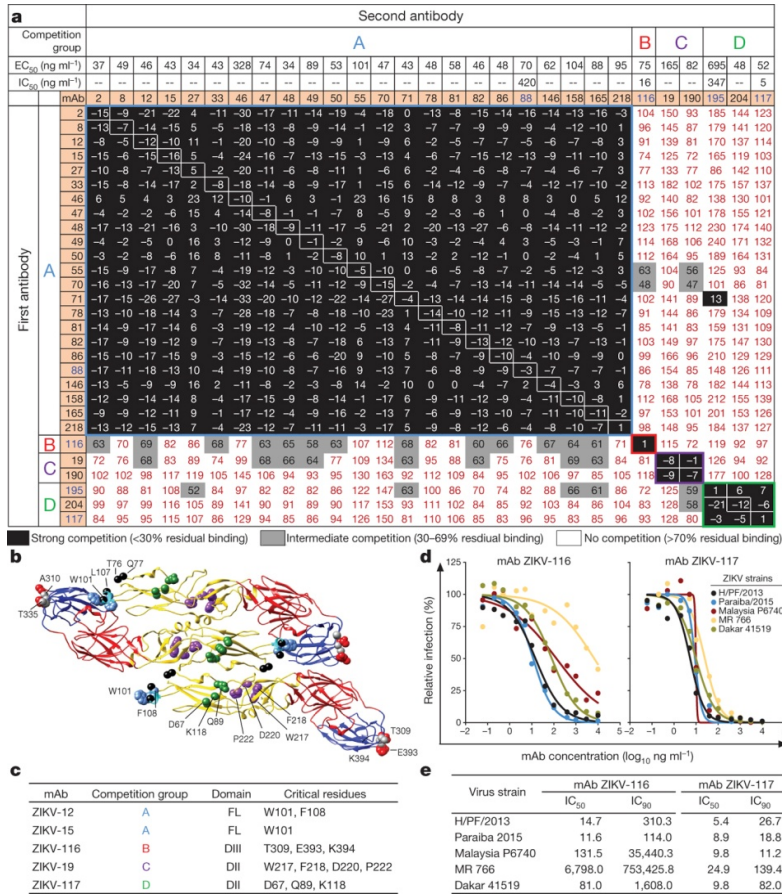
Figure 3.2: Characterization of anti-ZIKV mAbs

A) We tested 29 mAbs in binding, neutralization, and competition binding assays. The EC_{50} against ZIKV E and the IC_{50} (by focus reduction neutralization test) against H/PF/2013 strain for neutralizing antibodies (highlighted in blue) are shown. The mAbs are displayed in four groups (A, B, C or D) based on a competition binding assay. The values are the percentage of binding that occurred during competition compared to non-competed binding, which was normalized to 100% and the range of competition is indicated by the box colours. Black filled boxes indicate strongly competing pairs (residual binding <30%), grey filled boxes indicate intermediate competition (residual binding 30–69%), and white filled boxes indicate non-competing pairs (residual binding ≥ 70%). The IC_{50} against H/PF/2013 strain for neutralizing antibodies is shown with neutralizing clones highlighted in blue. **B**, A ribbon diagram of three protomers of ZIKV E (DI in red, DII in yellow and DIII in blue) is shown with critical residues highlighted as spheres from epitope mapping experiments for representative antibodies in each of the competition binding groups. The colours of the critical residues correspond to the competition group designation as in **A**. The mutations in the E-FLM and DIII-LR mutants are indicated by black and silver spheres, respectively. **C**, Representative mAbs from each competition binding group are listed with the domains and residues critical for binding. FL, fusion loop. **D**, Two mAbs were tested for neutralization of five strains of ZIKV. The concentrations (ng ml^{-1}) at which 50% or 90% neutralization occurred are listed in **E**. The neutralization data are pooled from at least three independent experiments performed in triplicate.
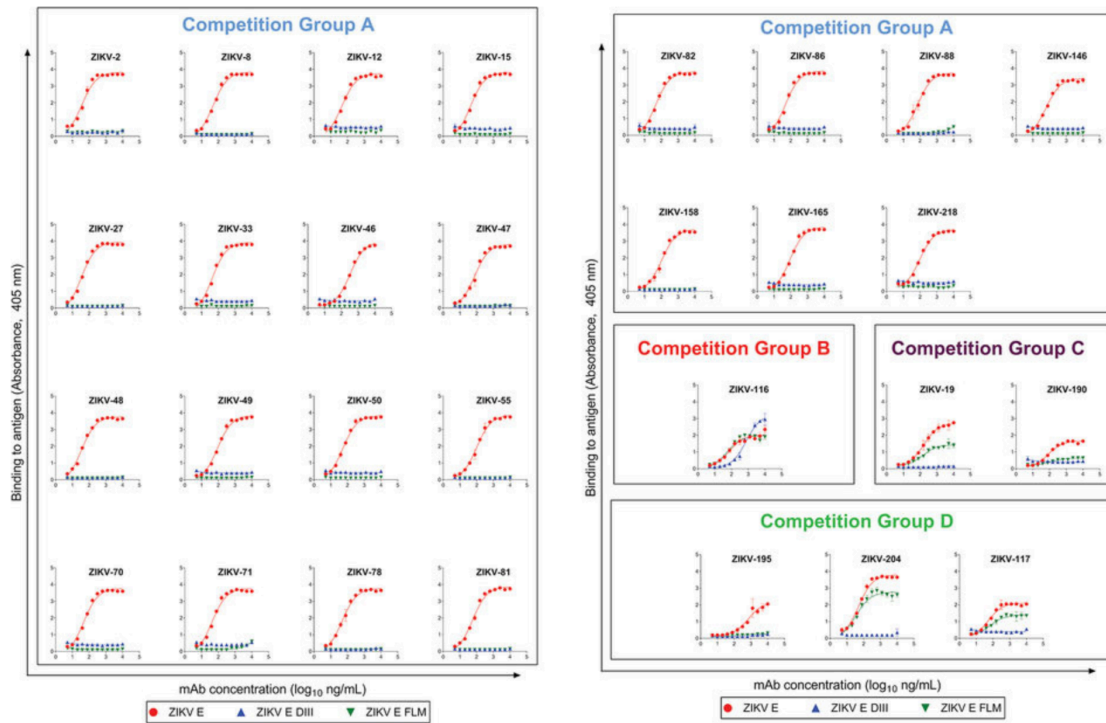
Figure 3.3: Binding of human mAbs to Zika E protein, E-DIII or E-FLM

mAbs are organized by competition binding groups A to D. Purified mAbs were tested for binding to different antigens as indicated in ELISA as described in Methods. Non-linear regression analysis of the data was performed, and the data plotted are the mean and s.d.
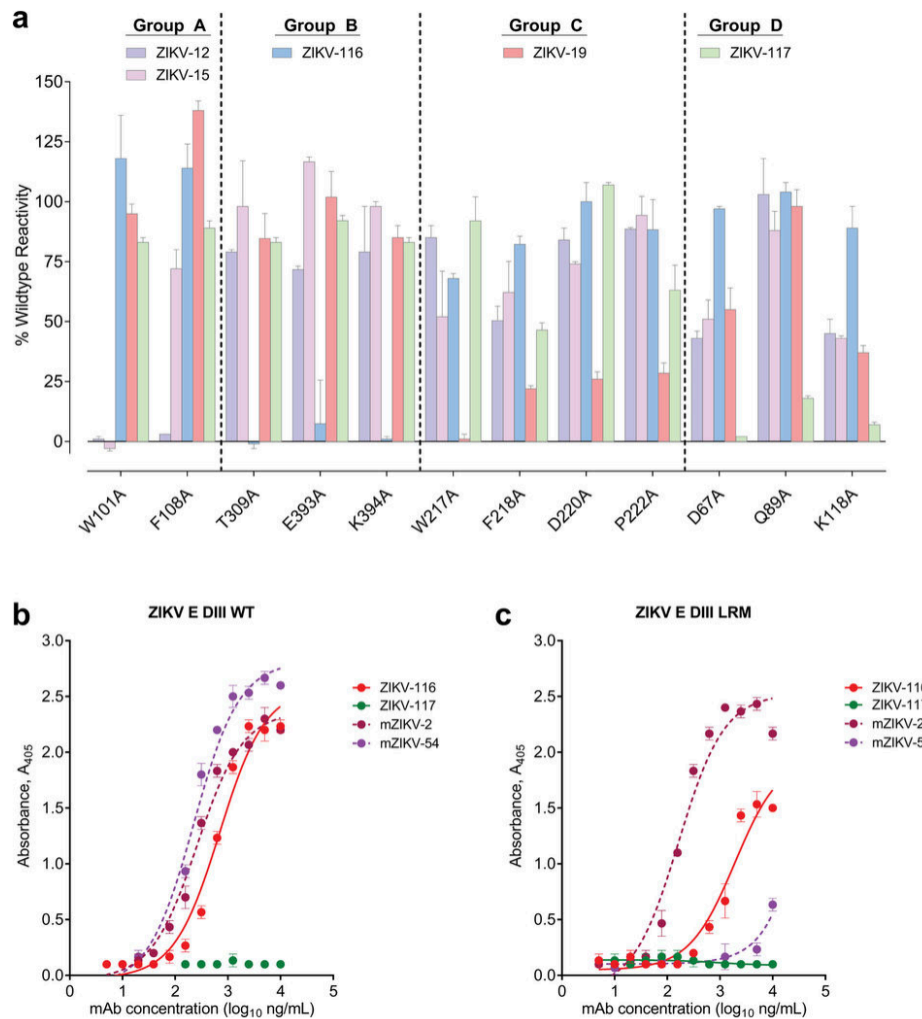
Figure 3.4: High resolution epitope mapping of ZIKV mAbs

a, An alanine scanning mutation library for ZIKV envelope protein was constructed, in which each amino acid of prM/E was mutated individually to alanine (and alanine to serine) and expression constructs arrayed into 384-well plates, one mutation per well. Each clone in the ZIKV prM/E mutation library, expressed in HEK-293T cells, was tested for immunoreactivity with five mAbs from competition groups A–D, measured using an Intellicyt high-throughput flow cytometer. Shown here for each of the five mAbs is the reactivity with the ZIKV E protein mutants that identified the epitope residues for these mAbs. mAb reactivity for each alanine mutant are expressed as percent of the reactivity of mAb with wild-type ZIKV prM/E. Clones with reactivity <30% relative to wild-type ZIKV prM/E were identified as critical for mAb binding. Bars represent the mean and range of at least two replicate data points. Binding of group B mAbs, ZIKV-116 to wild-type ZIKV E DIII (**b**) or DIII LR mutant (**c**) was compared with mouse mAbs ZV-2 and ZV-54. Binding of ZIKV-116 was decreased by mutations in DIII-LR. Data plotted are mean ± s.d.

102
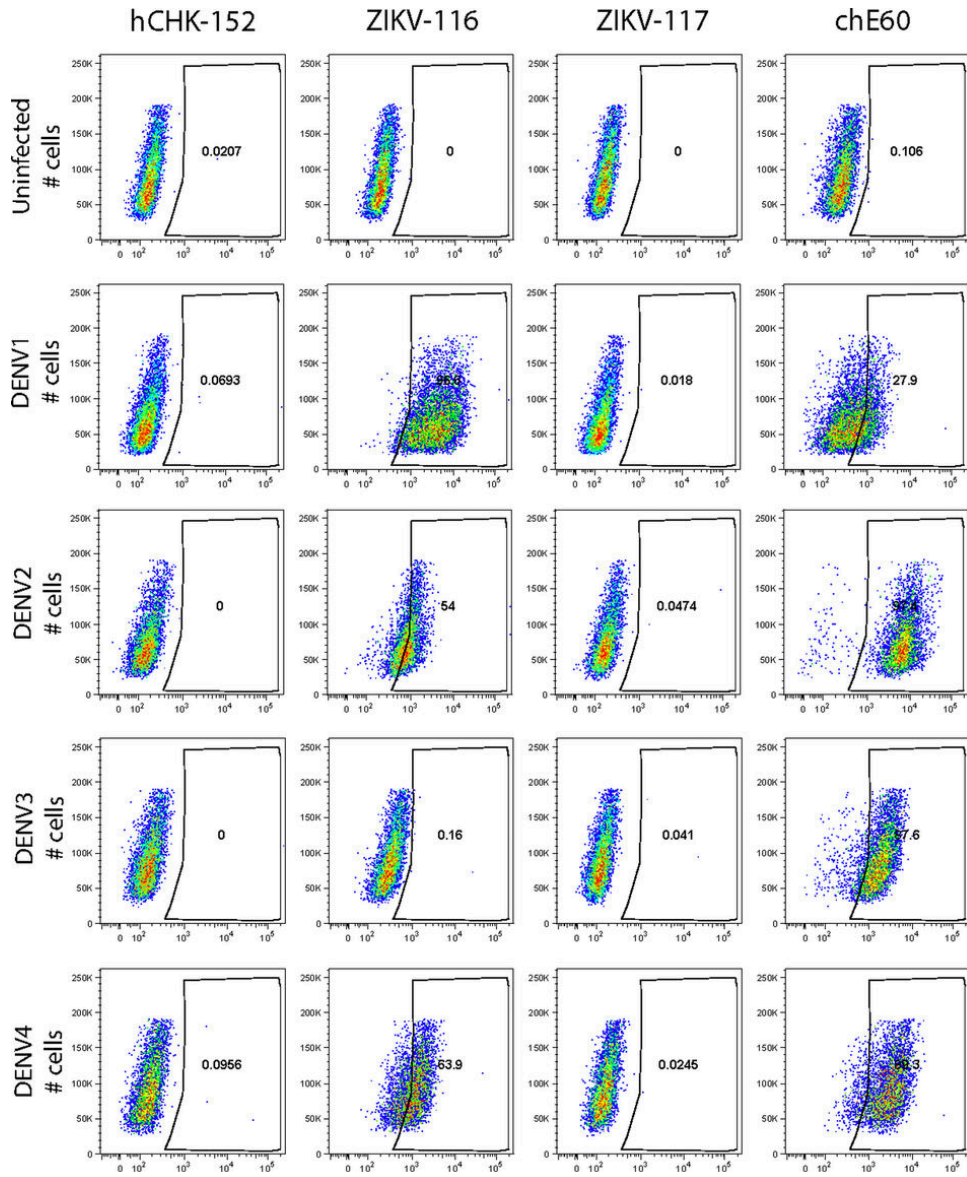
Figure 3.5: Binding of human mAbs to permeabilized DENV-infected C6/36 cells

C6/36 cells were infected with DENV-1, DENV-2, DENV-3, DENV-4 or mock infected. Cells were stained with the indicated anti-ZIKV mAbs, an isotype negative control (hCHK-152), or a positive control (a cross-reactive antibody to DENV; chimeric human E60 (chE60)) and processed by flow cytometry. The data are representative of two independent experiments. The numbers in the box indicate the fraction of cells that stained positively.
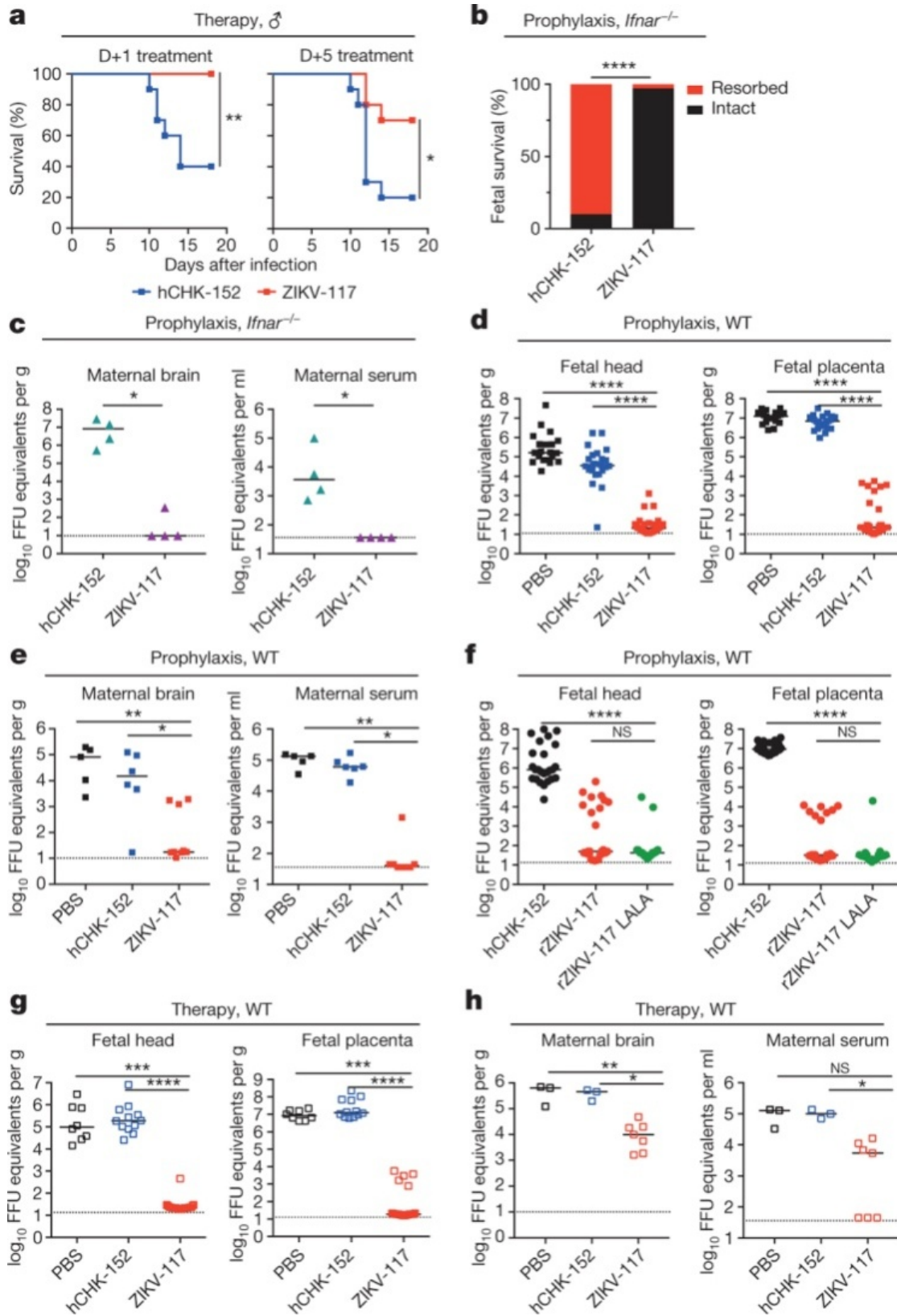
Figure 3.6: Protective activity of ZIKV-117 in adult male and pregnant female mice

A, We treated 4–5-week-old wild-type male mice with 2 mg of anti-Ifnar1 mAb followed by subcutaneous inoculation with 10^3 FFU of mouse-adapted ZIKV-Dakar. Mice were treated with a single 100 µg or 250 µg dose of isotype control mAb (hCHK-152) or ZIKV-117 on D+1 or D+5 ($n = 10$ per group from two independent experiments), respectively. Significance was analysed by the log-rank test (*$P < 0.05$; **$P < 0.01$). **B**,**C**, *Ifnar1*$^{-/-}$ female mice were mated with wild-type sires. At E5.5, dams were treated with 250 µg of either hCHK-152 isotype control mAb or ZIKV-117. Bars indicate the median values and reflect data pooled from four independent experiments. Significance for fetal survival and viral RNA was analysed by chi-square (**B**; ****$P < 0.0001$) and Mann–Whitney (**C**; *$P < 0.05$) tests, respectively. **D-F**, Wild-type female mice were mated with wild-type sires. At E5.5, dams were treated with anti-Ifnar1 mAb and one of the following: PBS (**D,E**), 250 µg (**D-F**) of hCHK-152 isotype control mAb, 250 µg of ZIKV-117 (**D-F**) or 250 µg of ZIKV-117 LALA (**f**). At E6.5, dams were inoculated with 10^3 FFU of ZIKV-Dakar. **D-F**, Fetuses and placentas (**D,F**) and maternal brain and serum (**e**) were collected on E13.5 and viral RNA was measured by qRT–PCR. Bars indicate the median values of samples collected from three biological replicates (**D**, $n = 20$–36; **E**, $n = 5$–9; **F**, $n = 23$–28). Significance was analysed by ANOVA with a Dunn's multiple comparison test (*$P < 0.05$, **$P < 0.01$, ***$P < 0.001$, ****$P < 0.0001$). **G,H**, Wild-type female mice were mated with wild-type sires. At E5.5, dams were treated with anti-Ifnar1 mAb. At E6.5, dams were inoculated with 10^3 FFU of ZIKV-Dakar. At E7.5 (day +1 after infection), dams were treated with PBS, 250 µg of hCHK-152 isotype control mAb, or 250 µg of ZIKV-117. **G**, **H**, Fetuses and placentas (**G**) and maternal brain and serum (**H**) were collected on E13.5 and viral RNA was measured by qRT–PCR. Bars indicate the median values of samples collected from three biological replicates (**G**, $n = 8$–20; **H**, $n = 3$–7). Significance was analysed by ANOVA with Dunn's (**G**) or Tukey's (**H**) multiple comparisons test (*$P < 0.05$, ***$P < 0.001$, ****$P < 0.0001$). Dashed lines indicate the limit of detection of the assay.

Concentration of human IgG in fetal tissues
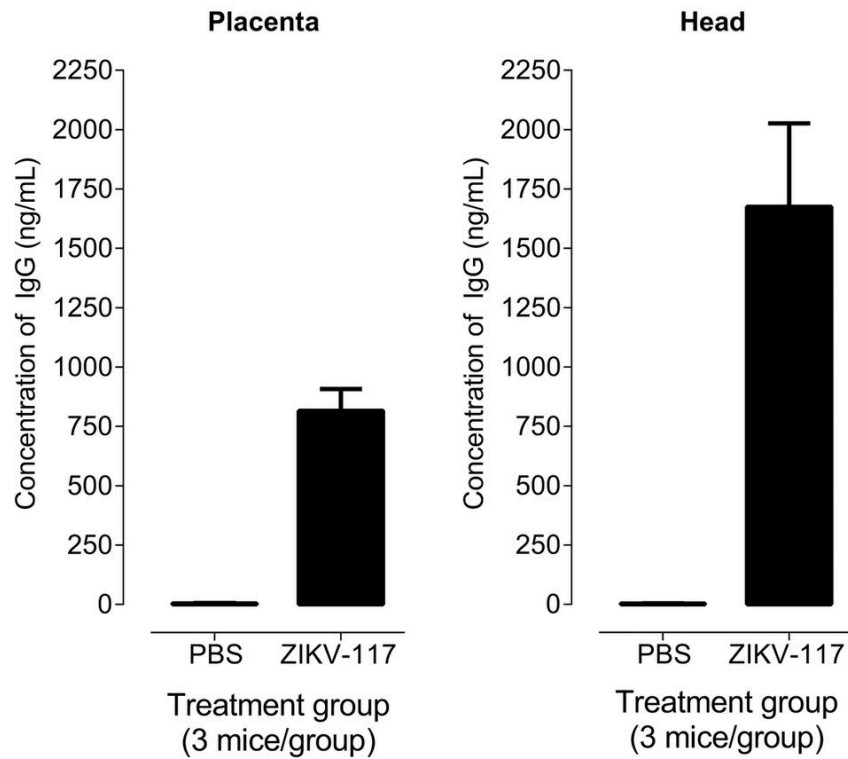
Figure 3.7: Detection of human IgG in placenta or fetal head tissues in ZIKV-117- or PBS-treated pregnant mice

As described in **Figure 3.6**, wild-type female mice were mated with wild-type sires and monitored for pregnancy. At E5.5, dams were treated with anti-Ifnar1 mAb and PBS or 250 μg of ZIKV-117. One day later (E6.5), dams were inoculated with 10^3 FFU of ZIKV-Dakar. Fetuses and placentas ($n = 4$ each) were collected on E13.5, homogenized, and tested for human IgG by ELISA. Human antibody in tissues was captured on ELISA plates coated with ZIKV E protein and detected using goat anti-human IgG (Fc-specific) antibody. The quantity of antibody was determined by comparison with a standard curve constructed using purified ZIKV-117 in a dilution series. Four replicate measurements were performed for each mouse tissue and the results were averaged. The graphs represent the mean + s.e.m. from 3 mice per group.
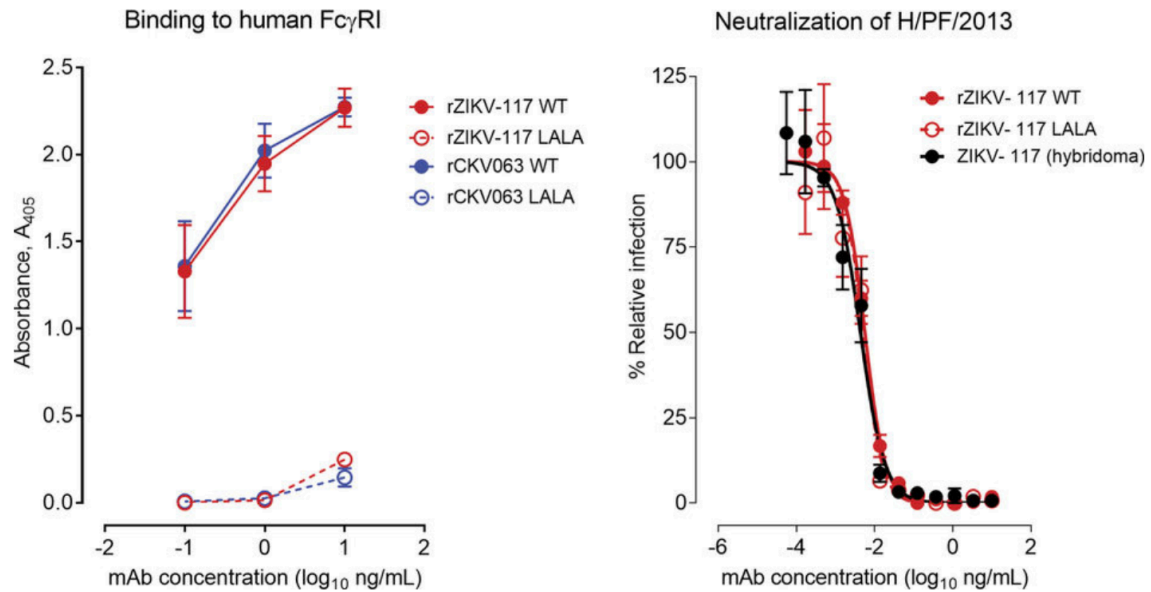
Figure 3.8: Comparison of wild-type and LALA-mutated antibodies

A, Binding to recombinant human FcγR1. The functional abrogation of the binding of the LALA variant IgG was confirmed in an ELISA binding assay with recombinant human FcγRI. ZIKV-117 wild-type bound to FcγRI, whereas the ZIKV-117 LALA antibody did not. Wild-type and LALA versions of another human mAb, CKV063, were used as controls. Binding to human FcγRI is one representative experiment of two, and error bars indicate s.e.m. of triplicate technical replicates. **B**, Neutralization assays. Wild-type ZIKV-117 and LALA antibodies exhibited equivalent neutralizing activity *in vitro* to each other and to the hybridoma-derived antibody. Neutralization assays are representative of two independent experiments completed in triplicate.
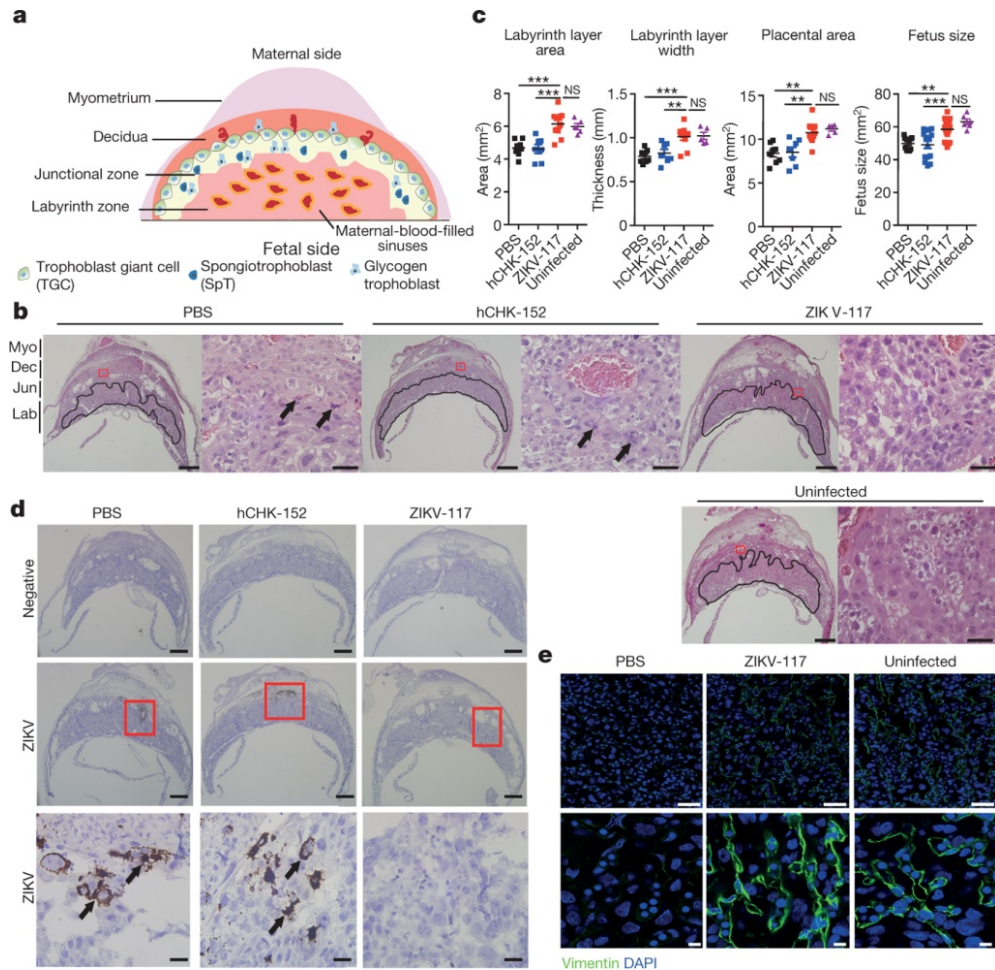
Figure 3.9: Effect of ZIKV-117 treatment on the placenta and the fetus

A, Cartoon depicting murine placental structures and zones. **B-E**, Pregnant dams were treated with PBS, hCHK-152, or ZIKV-117 as described in Fig. 3d–f before infection with ZIKV-Dakar or mock-infected. **B**, Haematoxylin and eosin staining of placenta at E13.5. Placental labyrinth zone is marked with a solid line. Low power (scale bar, 1 mm) and high power (scale bar, 50 μm) images are presented in sequence. Black arrows indicate apoptotic trophoblasts in areas corresponding to regions of ZIKV infectivity (see panel **D**, below). **C**, Measurements of thickness and indicated areas of placenta and fetus body size. Each symbol represents data from an individual placenta or fetus. Significance was analysed by ANOVA with a Dunn's multiple comparison test (*$P < 0.05$, **$P < 0.01$, ***$P < 0.001$, ****$P < 0.0001$, $P > 0.05$, NS, not significant). **D**, *In situ* hybridization. Low (scale bar, 500 μm) and high (scale bar, 50 μm) power images are presented in sequence. Black arrows indicate cells positive for ZIKV RNA in the junctional zone of the placenta. The images in panels are representative of several placentas from independent dams. **E**, Low (scale bar, 50 μm) and high (scale bar, 10 μm) power magnified images of immunofluorescence staining of placentas for vimentin (in green, which marks fetal capillary endothelium) from ZIKV-infected dams treated with PBS or ZIKV-117 or from uninfected pregnant animals. Nuclei are counter-stained blue with DAPI.
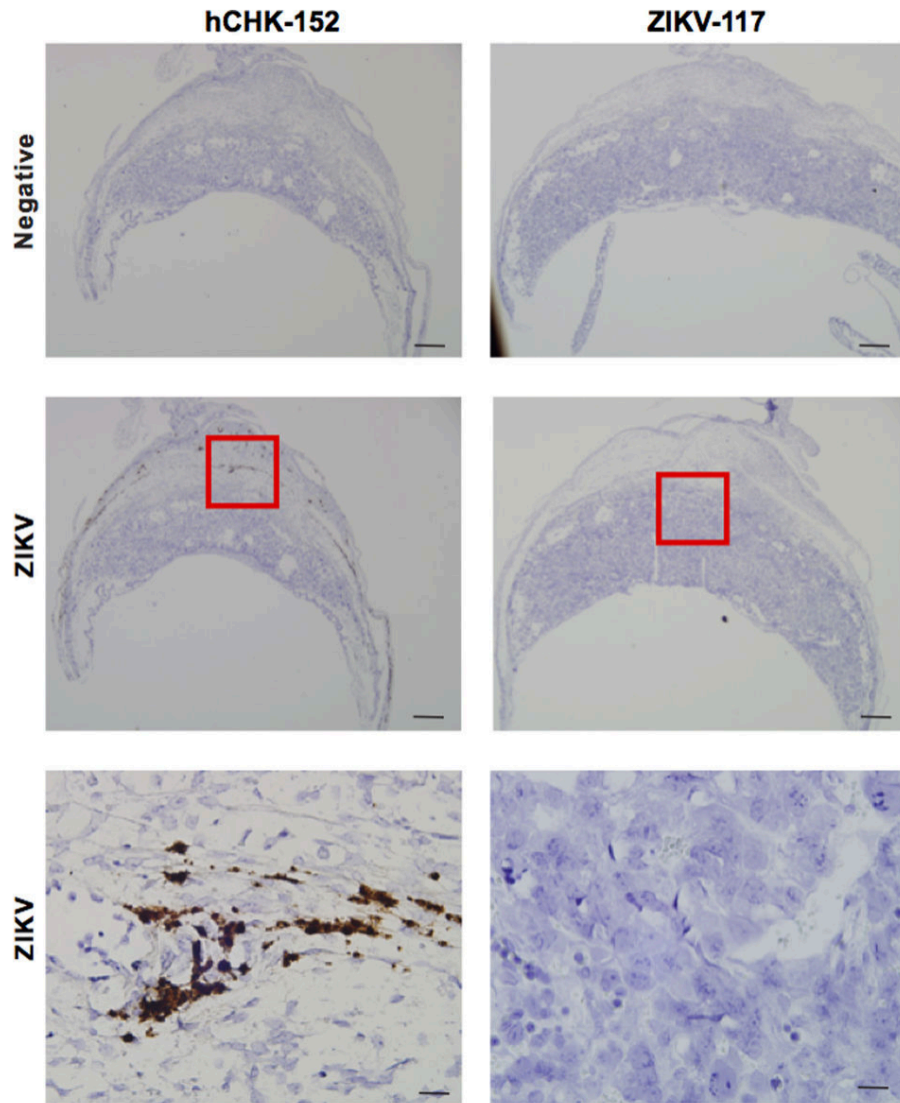
Figure 3.10: *In situ* hybridization of *Ifnar1*$^{+/-}$ placenta after inoculation with ZIKV-Brazil and treatment with ZIKV-117

As described in **Figure 3.6Bs**, *Ifnar1*$^{-/-}$ female mice were mated with wild-type sires and monitored for pregnancy. At E5.5, dams were treated with 250 μg of either hCHK-152 isotype control or ZIKV-117. At E6.5, dams were inoculated with 10^3 FFU of ZIKV-Brazil. Collected placentas were fixed in 10% neutral buffered formalin at ambient temperature and embedded in paraffin. At least three placentas from different litters with the indicated treatments were sectioned for *in situ* hybridization staining using negative or ZIKV-specific RNA probes. Low (scale bar, 500 μm) and high (scale bar, 50 μm) power images are presented in sequence.

Chapter 4:

Human antibodies to the dengue virus E-dimer epitope have therapeutic activity against Zika virus infection

This chapter is adapted from a manuscript published in Nature Immunology:

Fernandez E, Dejnirattisai W, Cao B, Scheaffer SM, Supasa P, Wongwiwat W, Esakky P, Drury A, Mongkolsapaya J, Moley KH, Mysorekar IU, Screaton GR, Diamond MS. 2017. Human antibodies to the dengue virus E-dimer epitope have therapeutic activity against Zika virus infection. *Nat Immnol.* 2017 Sep 25; 18: 1261-1269.

4.1   Summary

The Zika virus (ZIKV) epidemic has resulted in congenital abnormalities in fetuses and neonates. Although some cross-reactive dengue virus (DENV)-specific antibodies can enhance ZIKV infection in mice, those recognizing the DENV E-dimer epitope (EDE) can neutralize ZIKV infection in cell culture. We evaluated the therapeutic activity of human monoclonal antibodies to DENV EDE for their ability to control ZIKV infection in the brains, testes, placentas, and fetuses of mice. A single dose of the EDE1-B10 antibody given 3 d after ZIKV infection protected against lethality, reduced ZIKV levels in brains and testes, and preserved sperm counts. In pregnant mice, wild-type or engineered LALA variants of EDE1-B10, which cannot engage Fcg receptors, diminished ZIKV burden in maternal and fetal tissues, and protected against fetal demise. Because neutralizing antibodies to EDE have therapeutic potential against ZIKV, in addition to their established inhibitory effects against DENV, it may be possible to develop therapies that control disease caused by both viruses.

4.2 Introduction

Zika virus (ZIKV) is an arthropod-transmitted, positive-sense RNA virus that is closely related to viruses causing human disease, such as dengue (DENV), yellow fever (YFV), West Nile (WNV), and Japanese encephalitis (JEV) viruses. Historically, ZIKV infection in humans has been associated with a self-limiting mild, febrile illness[1]. Since its epidemic emergence in 2007, ZIKV infection has become linked to more severe clinical syndromes. For example, infection of pregnant women, particularly during the first trimester, can result in congenital Zika syndrome, which includes microcephaly, neurodevelopmental abnormalities, and fetal demise[2–4]. In adults, ZIKV infection is associated with Guillain–Barré syndrome (GBS), an autoimmune disease characterized by ascending paralysis and polyneuropathy[5,6].

The ZIKV genome is organized as a single open reading frame that has genes encoding three structural (capsid (C), pre-membrane/membrane (prM/M), and envelope (E)) and seven nonstructural (NS) proteins. The ZIKV E protein is composed of three domains: a central β-barrel domain (domain I; DI), an extended dimerization domain containing a hydrophobic fusion loop (FL) epitope at the distal end (domain II; DII), and an immunoglobulin-like segment implicated in receptor-binding and entry (domain III; DIII)[7]. In the immature state of the virion, the prM and E proteins form 60 spiky heterotrimers that protrude from the viral membrane surface[8]. Maturation during transit through the *trans*-Golgi network results in furin-mediated cleavage of prM to M. After this cleavage event, the E protein homodimers re-arrange in an anti-parallel orientation to form a herringbone array and a smooth virion surface. The transitions undergone by the viral particles expose different epitopes on the E protein that are essential for receptor-binding,

entry, and fusion. The E protein is also the primary target for neutralizing antibody responses.

ZIKV strains are classified into two genetic lineages, the African and the Asian–American lineages. Because their neutralization by serum and monoclonal antibodies (mAbs) is quite similar, ZIKV is categorized as a single serotype[9]. Genetic clustering places ZIKV in close relationship to DENV, with the E proteins showing 54–59% amino acid identity[10,11].

The humoral response to ZIKV infection has been studied by several groups, with advances made in our understanding of the epitopes engaged by protective mAbs[12]. MAbs that target the conserved DII-FL epitope generally are poorly neutralizing against ZIKV; despite this, passive transfer studies in mice have suggested that these mAbs can offer some degree of protection against ZIKV infection, possibly because of 'virus breathing' and further exposure of this epitope[7,13,14]. DII-FL-specific mAbs generated against DENV or ZIKV also have the potential to induce reciprocal antibody-dependent enhancement (ADE) of ZIKV or DENV infection in myeloid cells bearing transmembrane Fcγ receptors (FcγRs)[15,16] and in mice[17]. In comparison, strongly neutralizing and protective mouse and human mAbs to ZIKV have been described that bind epitopes in DIII (lateral ridge or A-strand[18–20]), across adjacent dimers in DII[19], or to sites in DI[21]. A distinct class of cross-reactive mAbs that engage DII-FL are the EDE-specific mAbs. These mAbs were isolated from DENV-infected patients, bind to an inter-dimer quaternary epitope with contact residues in DI, DII, and DIII, and cross-react with ZIKV[10,11,16,22]. EDE-specific mAbs are classified by their binding in the context of *N*-linked glycosylation at position Asn154 of

113

the E protein. EDE1 mAbs, which bind in the absence of the *N*-linked glycan, inhibit ZIKV more potently than do EDE2 mAbs[10,16].

Studies in mice, nonhuman primates, and humans have shown that ZIKV can infect and persist in several immune-privileged sites including the eye[4,23,24], brain[23,25,26], testis[27,28], and placenta[25,29]. Here we evaluated the therapeutic activity of EDE1 mAbs in ZIKV infection. Although EDE1-B10 showed protective activity when administered within 5 d of infection, it was less effective at clearing infection from immune-privileged tissues after ZIKV disseminated to these sites. In the context of pregnancy, leucine and alanine (LALA) variants of EDE1, which cannot bind FcγR, protected against ZIKV infection, as did recombinant wild-type (WT) mAbs. Our studies suggest that it may be possible to develop EDE1 LALA mAb therapeutics that prevent both ZIKV and DENV infection without the possibility for pathological antibody-dependent immune enhancement.

4.3   Results

Human mAbs to DENV inhibit ZIKV infection. Previous studies have established that the EDE1-C8 and EDE1-C10 mAbs bind to and neutralize ZIKV with half-maximal effective concentration (EC_{50}) values ranging from 9 to 14 ng/ml[10,30]. We compared the ability of another EDE1 mAb, EDE1-B10, to neutralize the four serotypes of DENV and the two lineages of ZIKV. EDE1-B10 strongly neutralized virions of the DENV-1, DENV-2, and DENV-3 serotypes (EC_{50} ~28–138 ng/ml) and showed weaker activity against virions of the more distantly related DENV-4 serotype (**Figure 4.1A**). We tested EDE1-B10 for its ability to inhibit virus strains that represented the African (HD78788) and Asian–American (Brazil PE243) lineages of ZIKV and found that it had a stronger

neutralization profile (EC_{50} ~2–4 ng/ml) than that of EDE1-C8 and other published EDE-specific mAbs[10,16] (**Figure 4.1B**). As with other EDE-specific mAbs, EDE1-B10 engages a quaternary epitope on the virion and does not bind monomeric E protein although the epitope is restored on covalently linked E-dimers[30,31]. Like many other flavivirus-specific antibodies, subneutralizing concentrations of EDE-specific mAbs can trigger ADE of FcγR-expressing myeloid cells. To prevent possible ADE, we engineered LALA substitutions into the Fc region of EDE1-B10 and EDE1-C8, which disrupted engagement of the mAbs with Fc receptors and prevented ADE, but did not change neutralizing activity against ZIKV (**Figures 4.1C** and **4.1D**)[32]. Thus, mAbs to DENV EDE strongly neutralize ZIKV infection, and LALA variants that do not promote ADE can be generated without a loss of inhibitory activity in cell culture.

EDE1 mAb therapy controls ZIKV infection. We tested EDE-specific human mAbs for their ability to protect mice against ZIKV-induced lethality when administered as a post-exposure therapy. To create a lethal challenge model in 4- to 5 week-old C57BL/6 mice, we passively transferred a blocking antibody specific for the type I interferon receptor Ifnar1 1 d before infection with 10^3 focus-forming units (FFUs) of a mouse-adapted African strain of ZIKV (ZIKV-Dakar)[18,19]. The mice were then treated with a single dose of EDE1-B10, EDE1-C8 (EC_{50} = 2–15 ng/ml), EDE2-A11 (EC_{50} = 69–125 ng/ml)[10], or an isotype control mAb (Flu 28C) 1 d (day +1; 100 μg), 3 d (day +3; 250 μg), or 5 d (day +5; 250 μg) after infection and the weight and survival of the mice were monitored for 21 d (**Figures 4.2A and 4.3**). The mice that were administered EDE1-B10, EDE1-C8, or EDE2-A11 were protected against lethality when they were treated at 1 or 3 d after infection. Furthermore, treatment with EDE1-B10 at 5 d after infection resulted in partial protection

against lethality and weight loss (**Figures 4.2A and 4.3**). Given the greater neutralization activity of EDE1-B10 *in vitro*, relative to that with the other EDE-specific mAbs, and its ability to robustly protect against lethality, most of the subsequent *in vivo* studies were performed with only EDE1-B10.

As a first step toward determining how EDE1 mAbs protect against disease, we defined the kinetics of viral dissemination for the tissues of interest. Within 2 d of infection, ZIKV RNA was readily detectable in the serum (1.7×10^5 FFU equivalents per ml; **Figure 4.2B**), brain (3.5×10^3 FFU equivalents per g tissue; **Figure 4.2C**), testis (4.8×10^3 FFU equivalents per g tissue; **Figure 4.2D**), epididymis (5.0×10^2 FFU equivalents per g tissue; **Figure 4.2E**), and eye (8.8×10^2 FFU equivalents per g tissue; **Figure 4.2F**). At the last time point assessed (day +5), viral titers were still increasing in these organs.

We then evaluated the efficacy of EDE1-B10 therapy on the control of ZIKV infection at different immune-privileged sites during the acute and persistent phases of infection. Adult C57BL/6 male mice were pretreated with an Ifnar1-specific blocking antibody and inoculated with 10^5 FFUs of mouse-adapted ZIKV-Dakar. The mice were then administered a single dose of EDE1-B10 or an isotype control mAb at day +1 (100 μg), day +3 (250 μg), or day +5 (250 μg) after infection, and viral RNA levels were assessed at day +5 (acute phase) or at day +21 (persistent phase) after infection. Treatment at day +1 decreased the levels of ZIKV RNA in serum at day +5 (52-fold; $P < 0.001$; **Figure 4.2G**). Similarly, EDE1-B10 therapy at day +1 reduced viral RNA levels in the following tissues at day +5 (**Figures 4.2H-4.2J**) and day +21 (**Figures 4.2L-4.2N**), relative to that observed in mice treated with the isotype control mAb: brain (1,760-fold and 42-fold, respectively; $P < 0.001$), testis (1,650-fold and 312-fold, respectively; $P < 0.001$), and

epididymis (4,780- fold and 206-fold, respectively; $P < 0.001$). Whereas reduced levels were observed in the eye at day +5 after EDE1-B10 therapy at day +1 (1,550-fold; $P < 0.001$; **Figure 4.2K**), ZIKV RNA levels were low at day +21 in EDE1-B10 and isotype control mAb groups suggesting clearance occurred independently of mAb treatment (**Figure 4.2O**).

In another set of experiments, we treated mice with EDE1-B10 at day +3 after infection and evaluated viral burden in tissues at day +5 and day +21 after infection. Treatment with EDE1-B10 at day +3 after infection had less of an effect on viral RNA levels at day +5 than treatment with EDE1-B10 at day +1, with smaller reductions observed in serum (fourfold; $P < 0.05$), brain (ninefold; $P < 0.001$), testis (threefold; $P > 0.05$), epididymis (116-fold, $P < 0.001$), and eye (threefold; $P < 0.05$) (**Figures 4.2G-4.2K**). In comparison, EDE1-B10 treatment at day +3 after infection resulted in decreased ZIKV RNA levels in the testis (62-fold; $P < 0.05$) and epididymis (1,800-fold; $P < 0.05$) at day +21 after infection, although levels in the brain were not affected, as compared to the treatment with the isotype control mAb (**Figures 4.2L-4.2N**).

Finally, we evaluated EDE1-B10 therapy at day +5 after infection for its effect on viral burden at day +21. However, treatment with EDE1-B10 beginning at day +5 after infection failed to decrease ZIKV RNA levels at day +21 in any of the sites tested, as compared to that after treatment with the isotype control mAb (**Figures 4.2L-4.2O**). To begin to define why EDE1-B10 was protective at some sites but not others, we measured mAb levels in tissues at day +5 after therapy was initiated at day +1 or day +3 after infection (**Figure 4.4**). Although the levels of EDE1-B10 in serum at day +5 were relatively equivalent, levels of the mAb in the brain and testis were lower ($P < 0.01$) when therapy

117

was started at day +1 after infection than at day +3 after infection. This may reflect the dimished systemic viral burden associated with treatment at day +1 after infection, which we speculate limits pro-inflammatory immune responses that compromise the function of the blood–brain barrier and the blood–testis barrier and allows EDE1-B10 access. Notably, lower amounts of EDE1-B10 penetrated into the eye at day +5 after treatment regardless of when the treatment was initiated, which may be due to a less permeable blood–retinal barrier[33]. Because treatment at day +5 failed to reduce viral RNA levels at day +21, this suggested that once immune-privileged sites were seeded, it may be difficult to accumulate sufficient amounts of the EDE1-B10 mAb to control or clear the infection. In summary, these experiments show that there is a narrow window of time after infection during which treatment with the EDE1-B10 mAb is able to reduce ZIKV RNA levels in some, but not other, immune-privileged sites once viral seeding had occurred.

To corroborate the protective effects observed with EDE1-B10 therapy, we evaluated ZIKV infection in the male reproductive tract at day +21 using RNA *in situ* hybridization (ISH). RNA ISH confirmed the absence of ZIKV RNA in the testis and epididymis of mice treated with EDE1-B10 at day +1 after infection and showed reduced viral RNA levels when treatment was initiated at day +3 after infection (**Figures 4.5A** and **4.6**). By comparison, mice treated with the isotype control mAb had high viral RNA levels, similar to those reported for untreated, infected mice[27]. Treatment with EDE1-B10 at day +1 or day +3 after infection also protected against ZIKV-induced inflammation and damage to the seminiferous tubules that was observed in mice treated with the isotype control mAb (**Figures 4.5B** and **4.6**) and described previously[27,28]. In contrast, treatment that was initiated at day +5 after infection minimally protected against ZIKV infection or

injury. We also evaluated the functional effect of EDE1-B10 treatment in the testis by computer-assisted sperm analysis. Whereas ZIKV-infected mice treated with the isotype control mAb showed low numbers of motile sperm, treatment with EDE1-B10 at day +1 or day +3 after infection but not at day +5 after infection resulted in higher numbers of motile sperm (16-fold and 100-fold, respectively; $P < 0.001$) at day +21 after infection (**Figure 4.5C**), which were similar to those observed in age-matched, uninfected male mice (**Figure 4.5C**). These data suggest that EDE1-B10 treatment can reduce viral persistence in select immune-privileged sites (for example, brain and testis) and protect against tissue injury when administered within a few days of infection.

EDE1-B10 therapy in maternal and fetal tissues. In pregnant mice that are deficient in type I interferon signaling, placental damage, and fetal infection and injury, occur after ZIKV infection[24,29,34,35]. To assess the protective ability of EDE1-B10 treatment during pregnancy, we mated *Ifnar1*$^{-/-}$ dams with WT C57BL/6 sires, and on embryonic day 6.5 (E6.5), we inoculated the dams subcutaneously with a Brazilian ZIKV strain (Paraiba 2015)[19,34]. One day after infection (at E7.5), we administered a single 250-µg dose of EDE1-B10 or an isotype control mAb and monitored the effects on the *Ifnar1*$^{-/-}$ dam and the *Ifnar1*$^{+/-}$ placenta and fetus. Seven days after ZIKV inoculation (at E13.5), we observed a 90% rate of fetal demise in the group that was treated with the isotype control mAb versus a 10% rate of fetal demise in the group that was treated with EDE1-B10 ($P < 0.0001$) (**Figure 4.7A, left**). Histological analysis confirmed that the fetal demise caused by ZIKV infection was prevented by the EDE1-B10 therapy (**Figure 4.7A, right**). Consistent with these data, EDE1-B10 treatment at day +1 after infection reduced viral RNA burden in the maternal serum (~71-fold; $P < 0.01$) and brain (~39,000-fold; $P < 0.05$) at day +7 after

119

infection, as compared to that after treatment with the isotype control mAb (**Figure 4.7B and 4.7C**). Analysis of the placentas by ISH showed ZIKV RNA in the maternal decidua and the junctional layer of the placenta in the mice that were treated with the isotype control mAb; in contrast, viral RNA staining was not observed in the dams that were treated with EDE1-B10 (**Figure 4.7D**). Histological analysis after ZIKV infection showed reductions in the size of the labyrinth layer of the placenta in the control-mAb-treated dams, but this was not seen for the dams that were treated with EDE1-B10 at day +1 after infection (**Figure 4.7E**).

The extent of fetal demise after ZIKV infection of $Ifnar1^{-/-}$ dams precluded virological assessment of EDE1-B10 protection in the fetus. To obtain such data, we used a second model of ZIKV infection in pregnancy with an acquired deficiency of type I interferon signaling[19,34]. WT females that were mated with WT males were treated with an Ifnar1-specific blocking mAb at E5.5. One day later (at E6.5), the dams were inoculated subcutaneously with mouse-adapted ZIKV-Dakar, and 1 d (at E7.5) or 3 d (at E9.5) later they were treated with EDE1-B10 or an isotype control mAb. Treatment of pregnant dams with EDE1-B10 at day +1 after infection resulted in reduced levels of viral RNA in the maternal serum (~240-fold; $P < 0.001$) and brain (~3,000-fold; $P < 0.05$), as compared to that in the serum and brain of dams that were treated with the isotype control mAb (**Figures 4.8A** and **4.8B**). When treatment was initiated at day +1 after infection, we observed markedly less ZIKV RNA levels in the placenta and fetal head (660,000-fold and 4,900-fold, respectively; $P < 0.0001$) of EDE1-B10-treated dams than in those of the control-mAb-treated dams (**Figures 4.8C** and **4.8D**). Treatment of dams with EDE1-B10 at day +3 after infection also reduced ZIKV RNA levels in the maternal serum (22-fold; $P < 0.05$)

and brain (114-fold; $P < 0.001$), as compared to that in the dams that were treated with the isotype control mAb (**Figures 4.8A and 4.8B**). Although ZIKV levels in the placenta (23-fold; $P < 0.0001$) and fetal head (19-fold; $P < 0.0001$) were lower in the EDE1-B10-treated group than in the control-mAb-treated group, therapy administered at this time point did not prevent virus seeding (**Figures 4.8C and 4.8D**).

We next evaluated whether antibody effector functions were required for EDE1-B10-mediated protection. We generated a mutant version of the EDE1-B10 mAb (LALA variant)[32] that was unable to bind to FcγR and promote ADE (**Figure 4.1C**), and we tested its efficacy *in vivo* during pregnancy. Like therapy with the recombinant WT EDE1-B10 mAb, treatment of dams with EDE1-B10 LALA at day +1 after infection resulted in reduced viral RNA levels in the maternal serum (240-fold; $P < 0.01$), maternal brain (3,000-fold; $P < 0.05$), placenta (633,000-fold; $P < 0.0001$), and fetal head (4,600-fold; $P < 0.0001$) (**Figures 4.8A and 4.8B**). Analogous experiments with paired recombinant WT EDE1-C8 and EDE1-C8 LALA yielded similar results (**Figure 4.9**). Thus, *in utero* protection mediated by EDE1 mAbs occurs independently of Fc effector functions and is probably mediated by direct virus neutralization. The mutant mAbs that are unable to bind FcγR could be safer immunotherapies, as they lack the potential to mediate ADE and immunopathogenesis.

To corroborate the protective effects the EDE-B10 mAb in the placenta, we analyzed tissue sections for virus infection and tissue injury. RNA ISH of placentas from dams that were treated at day +1 after infection showed a virtual absence of ZIKV-infected cells in the decidua and placenta, and mice that were treated at day +3 after infection also showed reduced viral RNA staining in these tissues, as compared to that in the tissues of

control-mAb-treated dams (**Figure 4.8E**). Histological measurements of the placental layers showed that treatment at day +1 after infection, but not at day +3 after infection, with EDE1-B10 restored the area and width of the junctional area, the total placental area, and the overall fetal size (**Figures 4.8F-4.8I**), as compared to treatment with the isotype control mAb. These data confirm a narrow therapeutic window for EDE1-B10 in preventing ZIKV infection and injury to the developing placenta and fetus.

Sexual transmission is an established route of ZIKV infection[36–41]. Male-to-female transmission of ZIKV has been modeled in pregnant mice through direct intravaginal inoculation of virus[29]. Although recent vaccine studies indicate that adaptive immune responses can protect against *in utero* transmission for ZIKV inoculated subcutaneously[42], no study has shown this in the context of vaginal transmission. We assessed whether administration of EDE1-B10 through a peripheral route could prevent *in utero* transmission following intravaginal inoculation of ZIKV (**Figure 4.10**). WT dams that were mated with WT sires were then treated with the Ifnar1-specific blocking mAb and a single 250-µg dose of EDE1-B10 or isotype control mAb at E5.5. At E6.5, the dams were inoculated with mouse-adapted ZIKV-Dakar via the intravaginal route. At E7.5, the dams were given a second dose of anti-Ifnar1. At E13.5, we determined the viral RNA burden in maternal and fetal tissues, including those of the female reproductive tract. Treatment with EDE1-B10 reduced ZIKV RNA levels in the maternal serum (427-fold; $P < 0.05$) and brain (45,490-fold; $P < 0.01$) (**Figures 4.10A** and **4.10B**), as compared to those in the control-mAb-treated mice. In EDE1-B10-treated dams, ZIKV RNA levels were diminished, relative to those in the control-mAb-treated mice, in all female reproductive-tract tissues, including the vagina (106,840-fold; $P < 0.01$), cervix (12,450-fold; $P < 0.01$), and ovaries (341,300-

fold; $P < 0.01$) (**Figures 4.10C-4.10E**). Because EDE1-B10 treatment also reduced ZIKV RNA levels in the placenta (1,725,600-fold; $P < 0.0001$) and fetal head (3,020-fold; $P < 0.0001$) (**Figures 4.10F** and **4.10G**), this indicated that circulating neutralizing antibodies can prevent transvaginal transmission of ZIKV to the placenta and fetus. Consistent with these data, staining by ISH showed a virtual absence of ZIKV RNA in the placenta and decidua of EDE1-B10-treated dams, as compared to that in control-mAb-treated dams (**Figure 4.10H**). Overall, these experiments establish that EDE1-B10 therapy can protect against ZIKV infection and transmission to the fetus after subcutaneous or intravaginal inoculation.

4.4   Discussion

A primary goal of this study was to identify human mAbs that could potently neutralize ZIKV and provide post-exposure protection *in vivo*, including reduction of infection in key immune-privileged sites. Prior studies had shown that EDE-specific mAbs that had been isolated from DENV-infected subjects could neutralize DENV and ZIKV *in vitro*[10,11] and protect against ZIKV lethality *in vivo* when administered as prophylaxis[22]. Studies with more ZIKV-specific human mAbs that do not cross-react with DENV also have demonstrated post-exposure therapeutic activity in lethality models in mice[17,19–21]. On the basis of *in vitro* neutralization studies, we defined EDE1-B10 as a candidate immunotherapeutic because of its strong inhibitory activity against three virus strains that encompass the genetic diversity of ZIKV, as well as its neutralizing activity against DENV-1, DENV-2, and DENV-3. Of interest, EDE1-B10 failed to bind or neutralize DENV-4 efficiently; this phenotype was similar to that described for cross-reactive mouse mAbs to DENV that react with the DII-FL epitope[43].

We compared EDE1-B10 with the previously published EDE-specific mAbs[10,11] EDE1-C8 and EDE2-A11 for their post-exposure therapeutic activity against lethal ZIKV challenge. Although all three EDE-specific mAbs completely protected when given 3 d after ZIKV inoculation, EDE1-B10 also reduced lethality when administered 5 d after infection. The combination of increased neutralizing and protective activity led us to select EDE1-B10 for subsequent studies. We assessed how EDE1-B10 functioned at immune-privileged sites, which were seeded within 2 d of virus inoculation. ZIKV replication in immune sanctuary sites may contribute to its persistence in human and animal body fluids, including semen, urine, and saliva[27,28,44,45]. During the acute phase of infection, EDE1-B10 treatment markedly reduced viral RNA in multiple immune-privileged sites when administered at day +1 after infection. However, the reductions were lower in magnitude when EDE1-B10 treatment was initiated at day +3 after infection. Correspondingly, persistence of ZIKV RNA at day 21 after inoculation was markedly diminished at most immune-privileged sites when therapy was initiated at day +1 after infection. However, when therapy was started at day +3 after infection, viral RNA persisted at day +21 after infection at several immune-privileged sites (eye, brain, and testis). Thus, the likely protective role of the EDE1 mAbs is to limit ZIKV dissemination, with antibody-mediated clearance of already infected sites being substantially less efficient. Consistent with this observation, protection of the placenta and fetuses by the WT and LALA variants of EDE1-B10 and EDE1-C8 was equivalent in the dam model of infection and was not dependent on Fc-dependent interactions. These results contrast with those in HIV[32], Ebola virus[46], influenza A virus[47], and respiratory syncytial virus[48] studies in which antibody effector functions enhanced protection. Fc effector functions may contribute to antibody-

mediated protection of these viruses because, unlike ZIKV, they bud from the plasma membrane and express structural proteins on the cell surface, which can serve as targets for antibody-dependent cellular cytotoxicity and phagocytosis.

Sexual transmission is an established route of ZIKV spread and of concern to individuals within and traveling to endemic regions, particularly for those of child-bearing age. Our study shows that systemic mAb administration can protect against intravaginal transmission of ZIKV infection in the context of pregnancy. This observation is relevant, as studies in macaques suggest that ZIKV replication in the female reproductive tract precedes infection of peripheral organ tissues that contribute to viremia[49]. Our passive antibody-transfer experiments in mice suggest that ZIKV vaccines that induce robust neutralizing antibody responses and protect against *in utero* transmission after subcutaneous virus challenge[42] may also prevent sexual transmission.

ZIKV epidemics in the Americas now occur in DENV-endemic regions. Cross-reactive antibodies against ZIKV and DENV could protect or mediate pathogenesis[50] depending on the stoichiometry of binding and mechanism of action[31]. Our preclinical studies with LALA variants of EDE1-B10 and EDE1-C8 provide a first step toward developing a safe and effective therapeutic antibody against both ZIKV and DENV, without the possibility for pathogenic immune enhancement. Nonetheless, as the extent to which these findings in mice translate to humans remains unclear, protection studies with EDE1 mAbs in nonhuman primate models of ZIKV infection in pregnancy are warranted. If these data are promising, then human clinical trials will be required to show efficacy. The design of such trials will be challenging given the ephemeral nature of mosquito-

transmitted virus epidemics in a given locale and the absolute need for safety in the context of transmission studies with pregnant women.

4.5   Methods

Viruses. ZIKV-Brazil (Paraiba, 2015) was provided by S. Whitehead (US National Institutes of Health) and was originally obtained from P.F.C. Vasconcuelos (Instituto Evandro Chagas). Mouse-adapted ZIKV-Dakar 41519 was passaged twice *in vivo* in immunodeficient $Rag1^{-/-}$ mice (M.S.D., unpublished data) and grown in Vero cells. The DENV-2 strain D2S20 was a gift from S. Shresta) and was grown in the C6/36 *Aedes albopictus* cell line. Primary isolates of DENV-1 (02-0435; GenBank accession number JQ740878), DENV-3 (2-1969; GenBank accession number JQ740881), and DENV-4 (1-0093; GenBank accession number JQ740883) were obtained from DENV-infected patients in Thailand (provided by P. Malasit and S. Noisakran). DENV-2 strain DF-699 (GenBank accession number FM210221) was isolated from a patient in Vietnam (provided by C. Simmons). DENV-2 strain 16681 was a gift from the Armed Forces Research Institute of Medical Sciences (AFRIMS), Thailand. Additional ZIKV strains from Brazil (PE243, provided by A. Kohl, R.F. de Oliveira Freitas, and L.J. Pena) and Africa (HD78788, provided by A. Sakuntabhai) were used for neutralization assays. Virus stocks were titered by the focus-forming assay (FFA) on Vero cells, as previously described[51].

Antibody generation. Activated antibody-secreting cells (CD19^{+}, CD3^{−}, CD20^{lo} or CD20^{−}, CD27^{hi} and CD138^{hi}) were sorted by flow cytometry. To amplify the VH- and VL-encoding genes, one-step RT–PCR (Qiagen) and nested PCR (Qiagen) were performed. The nested PCR products were cloned into expression vectors encoding the human IgG1

constant region or the LALA-variant IgG1 (leucine-to-alanine substitutions at positions 116 and 117) for the VH gene and the human Igκ constant region for the VL gene. Plasmids encoding the heavy and light chains were co-transfected into HEK 293T cells by the polyethylenimine method (Sigma). WT and LALA-variant IgG1 were purified by Protein G plus/Protein A agarose (Merck).

Neutralization assays. Serial dilutions of mAbs were incubated with 10^2 FFU of the different DENV serotypes or ZIKV strains for 1 h at 37 °C. The mAb–virus complexes were added to Vero cell monolayers in 96-well plates for 2 h at 37 °C. Subsequently, the cells were overlaid with 1.5% (wt/vol) carboxymethyl cellulose in modified Eagle's medium (MEM) supplemented with 3% heat-inactivated FBS. Plates were fixed 72h later for DENV and 48 h later for ZIKV with 4% paraformaldehyde (PFA) in PBS for 10 min and then permeabilized with 2% Triton X-100 in PBS for 10 min at room temperature. Plates were stained with mAb 4G2 (cross-reactive mouse mAb to the FL epitope of flaviviruses) at 37 °C for 1 h followed by incubation with peroxidase-conjugated goat anti-mouse-immunoglobulin (Sigma) at a dilution of 1:1,000 in 0.05% Tween–PBS for 1 h at 37 °C. Foci were visualized by adding DAB substrate (Sigma) at a concentration of 0.6 mg/ml.

ADE assay. Serial dilutions of mAbs were incubated with virus at a multiplicity of infection (MOI) of 5 at 37 °C for 1 h before adding them to U937 myelomonocytic leukemia cells. After 24 h of incubation at 37 °C, cells were harvested and washed with FACS buffer (2% FBS, 0.5% BSA, and 0.1% NaN$_3$ in PBS). Cells were fixed and permeabilized for 10 min at room temperature with 4% PFA in PBS and 0.5% (wt/vol)

saponin in FACS buffer, respectively. Finally, the cells were stained with Alexa-Fluor-647-conjugated 4G2 mAb and analyzed using a BD LSRFORTESSA X-20 flow cytometer.

Mouse experiments. Mouse studies were performed in accordance with the recommendations of the Guide for the Care and Use of Laboratory Animals of the National Institutes of Health and were approved by the Institutional Animal Care and Use Committee at the Washington University School of Medicine (assurance number A3381-01). Mice were inoculated with ZIKV after anesthetizing them with ketamine hydrochloride and xylazine, and all efforts were made to minimize pain and suffering. Antibody-protection studies were performed in the following models: a lethal challenge model in which WT C57BL/6 mice (4–5 weeks old; Jackson Laboratories) were administered 2 mg anti-Ifnar1 mAb (MAR1-5A3, Leinco Technologies) by an intraperitoneal (i.p.) injection 1 d before inoculation with 10^3 FFU of mouse-adapted ZIKV-Dakar by the s.c. route in the footpad. Cross-reactive EDE mAbs (EDE1-C8, EDE1-B10, or EDE2-A11) or isotype control (Flu 28C) human mAbs were administered by the i.p. route as a single dose at day +1 (100 μg, 5 mg per kg body weight (mg/kg)), day +3 (250 μg, 12.5 mg/kg), or day +5 (250 μg, 12.5 mg/kg) after infection. All of the mice were monitored for lethality for 21 d. Time course studies in which WT C57BL/6 mice (8–9 weeks old; Jackson Laboratories) were treated with 0.5 mg of anti-Ifnar1 mAb by intraperitoneal injection 1 d before inoculation with 10^5 FFU of mouse-adapted ZIKV-Dakar by the subcutaneous route. Mice were euthanized at day +1, day +2, day +3, day +4, or day +5 after infection. Acute-phase mAb protection studies in which WT C57BL/6 mice (8–9 weeks old; Jackson Laboratories) were treated with 0.5 mg anti-Ifnar1 mAb by intraperitoneal injection 1 d before inoculation with 10^5 FFU of mouse-adapted ZIKV-

Dakar by the subcutaneous route. Cross-reactive EDE1-B10 or an isotype control mAb (Flu 28C) was administered by the administered route as a single dose at day +1 or day +3 after infection as described above. All of the mice were euthanized at day +5 after infection, and tissues were harvested following extensive perfusion with PBS. Persistence-phase mAb protection studies in which WT C57BL/6 mice (8–9 weeks old; Jackson Laboratories) were treated with 0.5 mg anti-Ifnar1 mAb by intraperitoneal injection 1 d before inoculation with 10^5 FFU of mouse-adapted ZIKV-Dakar by the subcutaneous route. Cross-reactive EDE1-B10 or an isotype control mAb (Flu 28C) was administered by the intraperitoneal route as a single dose at day +1, day +3, or day +5 after infection as described above. All animals were euthanized at day +21 after infection, and tissues were harvested.

Pregnancy studies were done in WT C57BL/6 mice that were bred in a specific-pathogen-free facility at Washington University School of Medicine. In some experiments, *Ifnar1*$^{-/-}$ females and WT males were mated. At embryonic day E6.5, dams were inoculated with 10^3 FFU of ZIKV-Brazil (Paraiba 2015) by the s.c. route. At E7.5, dams were treated by the intraperitoneal. route with a single 250-μg dose of EDE1-B10 or an isotype control mAb. In another series of experiments, WT female and male mice were mated. At E5.5, dams were treated with 1 mg of anti-Ifnar1 by the intraperitoneal route. At E6.5, the mice were inoculated with 10^3 FFU mouse-adapted ZIKV-Dakar by the subcutaneous route. At E7.5, all of the mice received a second 1-mg dose of anti-Ifnar1 mAb through an intraperitoneal route. For treatment, mice received a single 250-μg dose of EDE1-B10, EDE1-B10 LALA, EDE1-C8, EDE1-C8 LALA, or isotype control mAb by the intraperitoneal route on E7.5 (day +1 after infection) or E9.5 (day +3 after infection,

excluding the LALA mutants). All of the mice were euthanized at E13.5, and placentas, fetuses, and maternal tissues were collected. Finally, in another series of studies, WT female and male mice were mated. At E5.5, dams were treated via an intraperitoneal route with 1.5 mg of anti-Ifnar1 mAb and a single 250-μg dose of EDE1-B10 or isotype control mAb. At E6.5, mice were inoculated with 10^5 FFU mouse-adapted ZIKV-Dakar in 10 μl by the intravaginal route. At E7.5, all of the mice received a second 1-mg dose of anti-Ifnar1. At E13.5, the mice were euthanized, and placentas, fetuses, and maternal tissues were collected.

Measurement of viral burden. Tissues from ZIKV-infected mice were weighed and homogenized with stainless steel beads in a Bullet Blender instrument (Next Advance) in 600 μl (brain) or 200 μl (testis, epididymis, eye, vagina, cervix, and ovaries) of PBS. Samples were clarified by centrifugation (2,000g for 10 min). All of the homogenized tissues from the infected mice were stored at −80 °C. Tissue samples and serum from ZIKV-infected mice were extracted with the RNeasy 96 Kit (for tissues) or Viral RNA Mini kit (for serum) (Qiagen). ZIKV RNA levels were determined by Taqman one-step qRT–PCR on an ABI7500 Fast Instrument using published primers and conditions[52]. Viral burden was expressed on a $\log_{10}$ scale as viral RNA equivalents per g or ml after comparison with a standard curve produced using serial tenfold dilutions of ZIKV RNA.

Measurement of EDE1-B10 in tissues. Tissues of ZIKV-infected mice that were perfused were weighed and homogenized with stainless steel beads in a Bullet Blender instrument (Next Advance) in 600 μl (brain) or 300 μl (testis, epididymis, and eye) of PBS. Samples were clarified by centrifugation (2,000g for 10 min). All of the homogenized tissues from infected animals were stored at −80 °C. Flat-bottom 96-well MaxiSorp (ThermoFisher)

plates were coated with goat anti–human (IgG H+L chain) antibody (KPL) and then blocked with PBS + 2% BSA (Sigma) for 1 h at 37 °C. Tissue homogenates were diluted in PBS + 2% BSA and incubated for 1 h at 4 °C. Plates were washed six times and then incubated with AffiniPure horseradish peroxidase (HRP)-conjugated goat-antihuman-IgG (Jackson Immuno) for 1 h at 4 °C and developed with TMB substrate. The reaction was stopped by addition of 2N H_2SO_4, and emission (450 nm) was read using a TriStar LB 941 reader (Berthold Technologies). EDE1-B10 levels are shown in 'µg/ml' after comparison with a standard curve and logistical regression produced using serial threefold dilutions of EDE1-B10 in corresponding homogenates of tissues from naive mice.

Viral RNA *in situ* hybridization (ISH). RNA ISH was performed with RNAscope 2.5 (Advanced Cell Diagnostics) according to the manufacturer's instructions. PFA-fixed paraffin-embedded placental sections were deparaffinized by incubation for 60 min at 60 °C. Endogenous peroxidases were quenched by treatment with H_2O_2 for 10 min at room temperature. Slides were boiled for 15 min in RNAscope Target Retrieval Reagent and incubated for 30 min in RNAscope Protease Plus before probe hybridization. The probe targeting ZIKV RNA was designed and synthesized by Advanced Cell Diagnostics (catalog number 467771). A negative control probe (targeting bacterial gene *dapB*) was also obtained from Advanced Cell Diagnostics (catalog number 310043). Tissues were counterstained with Gill's haematoxylin and visualized with standard bright-field microscopy.

Histology. Testis and epididymis were collected and fixed overnight in 4% PFA in PBS. Subsequently, 5-µm-thick sections from EDE1-B10-treated or isotype-control-mAb-treated mice were processed for histology by H&E staining. Collected placentas were fixed

in 10% neutral-buffered formalin at room temperature and embedded in paraffin. Placentas were sectioned and stained with H&E to assess morphology. Surface area and thickness of the placenta and of the different layers were measured using ImageJ software.

Computer-assisted sperm analysis. Mature sperm from the cauda epididymis of EDE1-B10-treated or isotype-control-mAb-treated mice at day +21 after infection were collected immediately after euthanasia as reported[53]. The sperm suspension, *in vitro* fert medium (Cook Medical), was analyzed using the HTM-IVOS Vs12 integrated visual optical system motility analyzer (Hamilton-Thorne Research) as described previously[54]. All measurements of motile sperm were made within 60 min of dissection of the cauda epididymis.

Statistical analysis. All data were analyzed with GraphPad Prism software. Kaplan–Meier survival curves were analyzed by the log-rank test. Viral burden and viremia were analyzed by the Mann–Whitney test. Motile sperm and placental and fetal measurements were analyzed by ANOVA using either a Kruskal–Wallis or Holm–Sidak test with a multiple-comparisons correction. Fetal outcome was assessed by Fisher's exact test.

4.6   Acknowledgments

4.7   References

1.   Weaver, S. C. *et al.* Zika virus: History, emergence, biology, and prospects for control. *Antiviral Res.* **130,** 69–80 (2016).
2.   Brasil, P. P. *et al.* Zika Virus Infection in Pregnant Women in Rio de Janeiro. *N. Engl. J. Med.* **375,** 2321–2334 (2016).
3.   Schaub, B. *et al.* Analysis of blood from Zika virus-infected fetuses: a prospective case series. *Lancet Infect. Dis.* **17,** 520–527 (2017).
4.   Honein, M. A. *et al.* Birth Defects Among Fetuses and Infants of US Women With Evidence of Possible Zika Virus Infection During Pregnancy. *JAMA* **317,** 59 (2017).
5.   Cao-Lormeau, V.-M. *et al.* Guillain-Barré Syndrome outbreak associated with Zika virus infection in French Polynesia: a case-control study. *Lancet* **387,** 1531–1539 (2016).
6.   Parra, B. *et al.* Guillain- Barre Syndrome Associated with Zika Virus Infection in Colombia. *N. Engl. J. Med.* **373,** 1513–1523 (2016).
7.   Dai, L. *et al.* Structures of the Zika Virus Envelope Protein and Its Complex with a Flavivirus Broadly Protective Antibody. *Cell Host Microbe* **19,** 696–704 (2016).
8.   Kuhn, R. J. *et al.* Structure of dengue virus: Implications for flavivirus organization, maturation, and fusion. *Cell* **108,** 717–725 (2002).
9.   Dowd, K. A. *et al.* Broadly Neutralizing Activity of Zika Virus-Immune Sera Identifies a Single Viral Serotype. *Cell Rep.* **16,** 1485–1491 (2016).
10.   Barba-Spaeth, G. *et al.* Structural basis of potent Zika–dengue virus antibody cross-neutralization. *Nature* **536,** 48–53 (2016).
11.   Dejnirattisai, W. *et al.* A new class of highly potent, broadly neutralizing antibodies isolated from viremic patients infected with dengue virus. *Nat. Immunol.* **16,** 170–177 (2014).
12.   Fernandez, E. & Diamond, M. S. Vaccination strategies against Zika virus. *Curr. Opin. Virol.* **23,** 59–67 (2017).
13.   Nelson, S. *et al.* Maturation of West Nile Virus Modulates Sensitivity to Antibody-Mediated Neutralization. *PLoS Pathog.* **4,** e1000060 (2008).
14.   Kam, Y.-W. *et al.* Cross-reactive dengue human monoclonal antibody prevents severe pathologies and death from Zika virus infections. *JCI Insight* **2,** (2017).
15.   Halstead, S. B., Mahalingam, S., Marovich, M. A., Ubol, S. & Mosser, D. M. Intrinsic antibody-dependent enhancement of microbial infection in macrophages: disease regulation by immune complexes. *Lancet Infect. Dis.* **10,** 712–722 (2010).
16.   Dejnirattisai, W. *et al.* Dengue virus sero-cross-reactivity drives antibody-dependent enhancement of infection with zika virus. *Nat. Immunol.* **17,** 1102–1108 (2016).
17.   Stettler, K. *et al.* Specificity, cross-reactivity, and function of antibodies elicited by Zika virus infection. *Science (80-.).* **353,** 823–826 (2016).
18.   Zhao, H. *et al.* Structural Basis of Zika Virus-Specific Antibody Protection. *Cell* **166,** 1016–1027 (2016).
19.   Sapparapu, G. *et al.* Neutralizing human antibodies prevent Zika virus replication and fetal disease in mice. *Nature* **540,** 443–447 (2016).
20.   Robbiani, D. F. *et al.* Recurrent Potent Human Neutralizing Antibodies to Zika Virus in Brazil and Mexico. *Cell* **169,** 597–609.e11 (2017).
21.   Wang, Q. *et al.* Molecular determinants of human neutralizing antibodies isolated from a patient infected with Zika virus. *Sci. Transl. Med.* **8,** 369ra179-369ra179 (2016).

22.   Swanstrom, J. A. *et al.* Dengue Virus Envelope Dimer Epitope Monoclonal Antibodies Isolated from Dengue Patients Are Protective against Zika Virus. *MBio* **7,** e01123-16 (2016).

23.   Hirsch, A. J. *et al.* Zika Virus infection of rhesus macaques leads to viral persistence in multiple tissues. *PLoS Pathog.* **13,** (2017).

24.   Miner, J. J. *et al.* Zika Virus Infection in Mice Causes Panuveitis with Shedding of Virus in Tears. *Cell Rep.* **16,** 3208–3218 (2016).

25.   Bhatnagar, J. *et al.* Zika virus RNA replication and persistence in brain and placental tissue. *Emerg. Infect. Dis.* **23,** 405–414 (2017).

26.   Aid, M. *et al.* Zika Virus Persistence in the Central Nervous System and Lymph Nodes of Rhesus Monkeys. *Cell* **169,** 610–620.e14 (2017).

27.   Govero, J. *et al.* Zika virus infection damages the testes in mice. *Nature* **540,** 438–442 (2016).

28.   Ma, W. *et al.* Zika Virus Causes Testis Damage and Leads to Male Infertility in Mice. *Cell* **167,** 1511–1524.e10 (2016).

29.   Yockey, L. J. *et al.* Vaginal exposure to Zika virus during pregnancy leads to fetal brain infection. *Cell* **166,** 1247–1256.e4 (2016).

30.   Rouvinski, A. *et al.* Covalently linked dengue virus envelope glycoprotein dimers reduce exposure of the immunodominant fusion loop epitope. *Nat. Commun.* **8,** 15411 (2017).

31.   Pierson, T. C. & Diamond, M. S. A game of numbers: The stoichiometry of antibody-mediated neutralization of flavivirus infection. *Progress in Molecular Biology and Translational Science* **129,** 141–166 (2015).

32.   Hessell, A. J. *et al.* Fc receptor but not complement binding is important in antibody protection against HIV. *Nature* **449,** 101–104 (2007).

33.   Magdelaine-Beuzelin, C., Pinault, C., Paintaud, G. & Watier, H. Therapeutic antibodies in ophthalmology: Old is new again. *MAbs* **2,** 176–180 (2010).

34.   Miner, J. J. *et al.* Zika virus infection during pregnancy in mice causes placental damage and fetal demise. *Cell* **165,** 1081–1091 (2016).

35.   Cugola, F. R. *et al.* The Brazilian Zika virus strain causes birth defects in experimental models. *Nature* **534,** (2016).

36.   Foy, B. D. *et al.* Probable Non-Vector-borne Transmission of Zika Virus, Colorado, USA. *Emerg. Infect. Dis.* **17,** 880–882 (2011).

37.   Musso, D. *et al.* Potential sexual transmission of zika virus. *Emerg. Infect. Dis.* **21,** 359–361 (2015).

38.   Russell, K. *et al.* Male-to-Female Sexual Transmission of Zika Virus — United States, January–April 2016. *Clin. Infect. Dis.* **64,** ciw692 (2016).

39.   Davidson, A., Slavinski, S., Komoto, K., Rakeman, J. & Weiss, D. Suspected Female-to-Male Sexual Transmission of Zika Virus — New York City, 2016. *MMWR. Morb. Mortal. Wkly. Rep.* **65,** 716–717 (2016).

40.   Deckard, D. T. *et al.* Male-to-Male Sexual Transmission of Zika Virus — Texas, January 2016. *MMWR. Morb. Mortal. Wkly. Rep.* **65,** 372–374 (2016).

41.   Barzon, L. *et al.* Infection dynamics in a traveller with persistent shedding of Zika virus RNA in semen for six months after returning from Haiti to Italy, January 2016. *Euro Surveill.* **21,** (2016).

42.   Richner, J. M. *et al.* Vaccine Mediated Protection Against Zika Virus-Induced Congenital Disease. *Cell* **170,** 273–283.e12 (2017).

43.   Sukupolvi-Petty, S. *et al.* Functional Analysis of Antibodies against Dengue Virus Type 4 Reveals Strain-Dependent Epitope Exposure That Impacts Neutralization and Protection. *J. Virol.* **87,** 8826–8842 (2013).

44.   Mansuy, J. M. *et al.* Zika virus: High infectious viral load in semen, a new sexually transmitted pathogen? *Lancet Infect. Dis.* **16,** 405 (2016).

45.   Murray, K. O. *et al.* Prolonged Detection of Zika Virus in Vaginal Secretions and Whole Blood. *Emerg. Infect. Dis.* **23,** 99–101 (2017).

46.   Zeitlin, L. *et al.* Enhanced potency of a fucose-free monoclonal antibody being developed as an Ebola virus immunoprotectant. *Proc. Natl. Acad. Sci.* **108,** 20690–20694 (2011).

47.   DiLillo, D. J., Palese, P., Wilson, P. C. & Ravetch, J. V. Broadly neutralizing anti-influenza antibodies require Fc receptor engagement for in vivo protection. *Journal of Clinical Investigation* **126,** 605–610 (2016).

48.   Hiatt, A. *et al.* Glycan variants of a respiratory syncytial virus antibody with enhanced effector function and in vivo efficacy. *Proc. Natl. Acad. Sci. U. S. A.* **111,** 5992–7 (2014).

49.   Carroll, T. *et al.* Zika virus preferentially replicates in the female reproductive tract after vaginal inoculation of rhesus macaques. *PLoS Pathog.* **13,** e1006537 (2017).

50.   Halstead, S. B. Biologic evidence required for zika disease enhancement by dengue antibodies. *Emerg. Infect. Dis.* **23,** 569–573 (2017).

51.   Brien, J. D., Lazear, H. M. & Diamond, M. S. Propagation, Quantification, Detection, and Storage of West Nile Virus. in *Current Protocols in Microbiology* 15D.3.1-15D.3.18 (John Wiley & Sons, Inc., 2013). doi:10.1002/9780471729259.mc15d03s31

52.   Lanciotti, R. S. Genetic and serologic properties of Zika virus associated with an epidemic, Yap State, Micronesia, 2007. *Emerg. Infect. Dis.* **14,** 1232–1239 (2008).

53.   Hansen, D. A., Esakky, P., Drury, A., Lamb, L. & Moley, K. H. The Aryl Hydrocarbon Receptor Is Important for Proper Seminiferous Tubule Architecture and Sperm Development in Mice. *Biol. Reprod.* **908,** 1–12 (2014).

54.   Goodson, S. G., Zhang, Z., Tsuruta, J. K., Wang, W. & O'Brien, D. A. Classification of Mouse Sperm Motility Patterns Using an Automated Multiclass Support Vector Machines Model1. *Biol. Reprod.* **84,** 1207–1215 (2011).
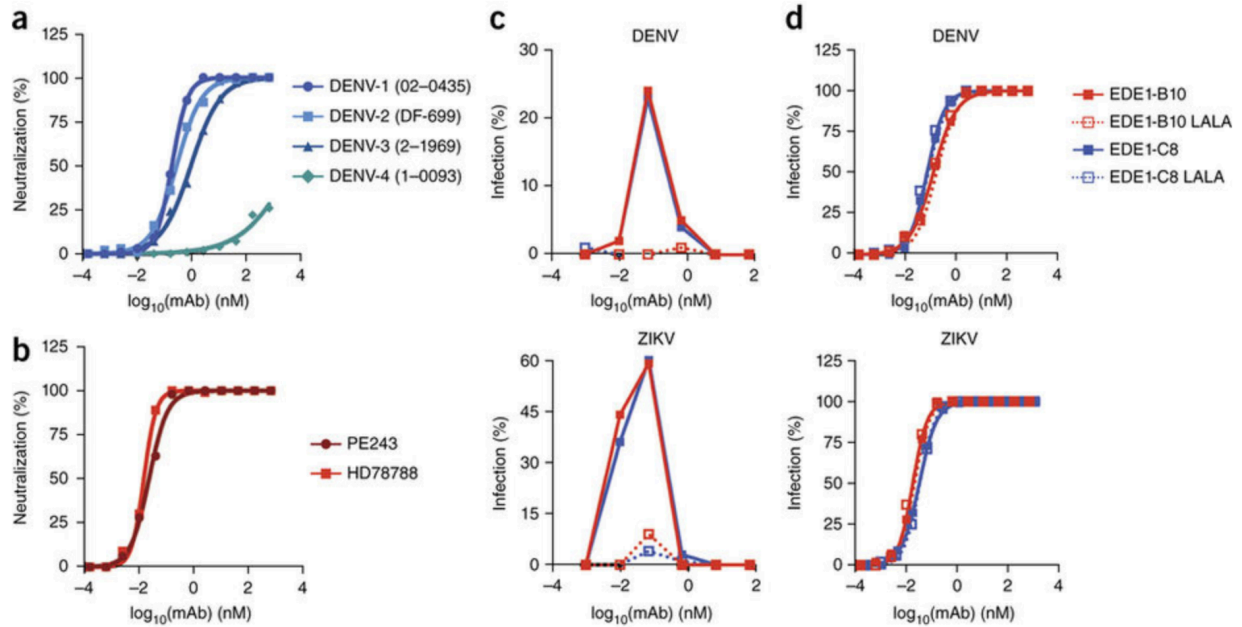
Figure 4.1: EDE1-B10 is a human mAb to DENV that cross-neutralizes ZIKV infection

(**a**) Serial dilutions of EDE1-B10 were tested for neutralization of DENV-1, DENV-2, DENV-3, and DENV-4 serotypes using a focus-reduction neutralization test. (**b**) EDE1-B10 was tested for neutralization of ZIKV strains from Africa (HD78788) and Brazil (PE243). The data in **a**,**b** are expressed as the percentage of neutralized virus. (**c**,**d**) ADE (**c**) and neutralization (**d**) studies with WT and LALA recombinant variants of EDE1-B10 and EDE1-C8 with DENV-2 (16681) and ZIKV (HD78788). Infection of U937 cells (**c**) in the presence of mAbs EDE1-B10, EDE1-C8, or their LALA mutants is presented as the percentage of infection. Data are representative of three independent experiments (**a**–**d**).
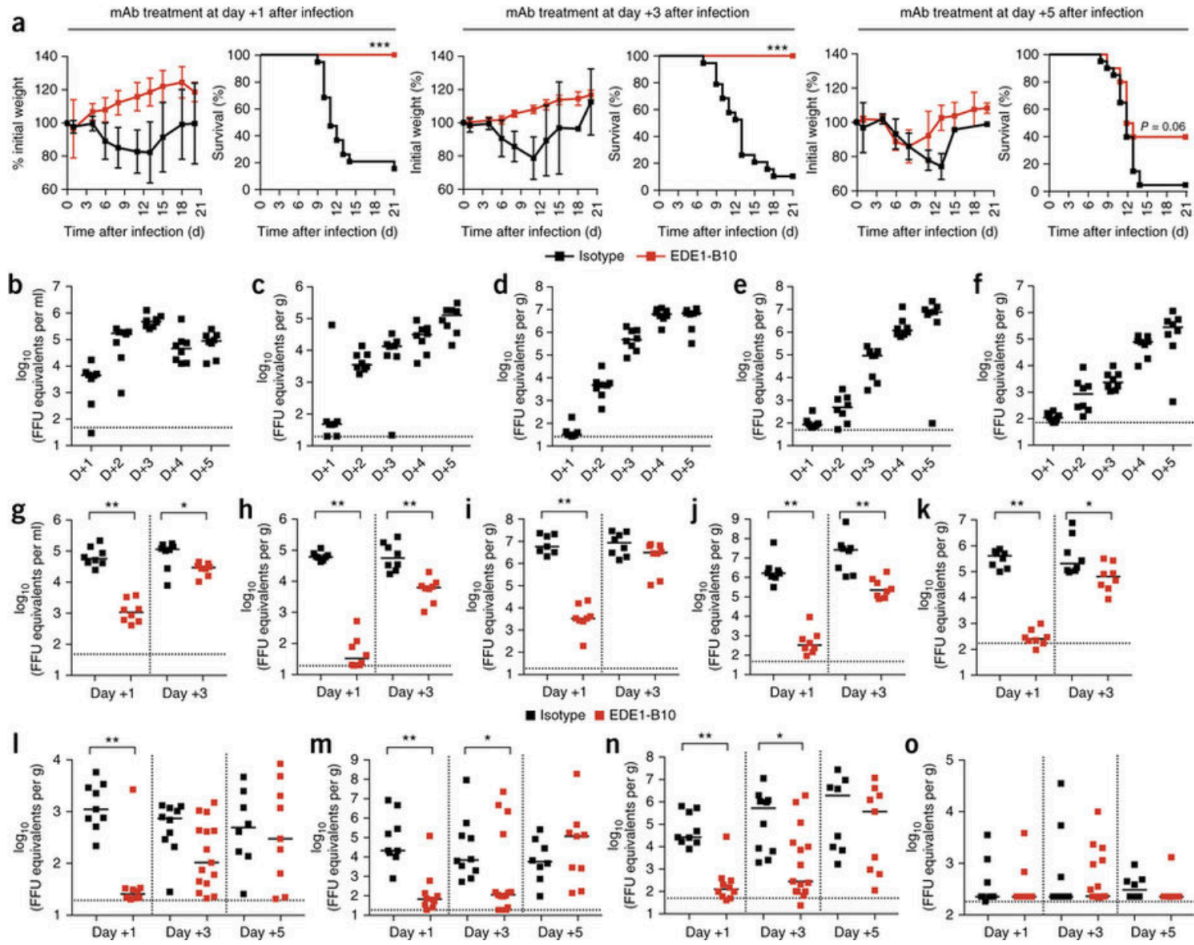
Figure 4.2: EDE1-B10 protects against ZIKV-induced lethality and viral burden

(**a**) Four- to five-week-old male WT mice were treated with anti-Ifnar1 followed by s.c. infection with mouse-adapted ZIKV-Dakar. Mice were then treated with isotype control mAb or EDE1-B10 at day +1 (100 μg, left), day +3 (250 μg, middle), or day +5 (250 μg, right) after infection. Weight and survival data were pooled from two (EDE1-B10) or three (isotype) independent experiments (isotype-mAb-treated, n = 19 mice per group; EDE1-B10-treated, n = 10 mice per group). (**b–f**) Eight- to nine-week-old male WT mice were treated with anti-Ifnar1 followed by s.c. inoculation with mouse-adapted ZIKV-Dakar. Viral RNA was measured in serum (**b**), brain (**c**), testis (**d**), epididymis (**e**), and eye (**f**) by qRT–PCR at 1 d (D+1), 3 d (D+3), or 5 d (D+5) after infection. Bars indicate median values from two experimental replicates (n = 8 mice per group). (**g–k**) Eight- to nine-week-old male WT mice were treated with anti-Ifnar1 followed by subcutaneous inoculation with mouse-adapted ZIKV-Dakar. Mice were treated with isotype control mAb or EDE1-B10 at day +1 (100 μg) or day +3 (250 μg) after infection. At day +5 after infection, viral RNA was measured in serum (**g**), brain (**h**), testis (**i**), epididymis (**j**), and eye (**k**). Bars indicate median values collected from two experimental replicates (n = 8 mice per group). (**l–o**) Eight- to nine-week-old male WT mice were treated with anti-Ifnar1 followed by s.c. inoculation with mouse-adapted ZIKV-Dakar. Mice were treated with isotype control mAb or

EDE1-B10 at day +1 (100 µg; isotype, $n = 9$; EDE1-B10, $n = 10$), day +3 (250 µg; isotype, $n = 10$; EDE1-B10, $n = 15$), or day +5 (250 µg; isotype, $n = 8$; EDE1-B10, $n = 9$) after infection. At day +21 after infection, viral RNA was measured in the brain (**l**), testis (**m**), epididymis (**n**), and eye (**o**). Bars indicate median values collected from three experimental replicates. Throughout, the dashed lines indicate the limit of detection of the assay. $*P < 0.05$, $**P < 0.001$, and $***P < 0.0001$ (log-rank (**a**) or Mann–Whitney (**g–n**) test). Data from two (**a**, **b–k**) or three (**a**, **l–o**) independent experiments (**a**: mean ± s.d.).
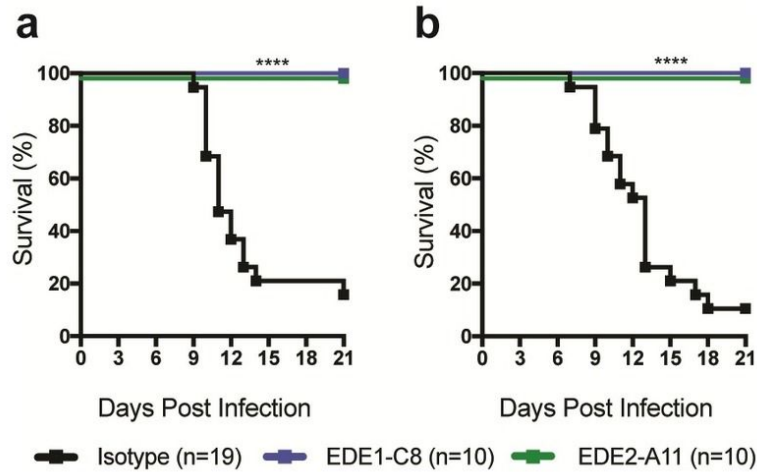
Figure 4.3: EDE-specific mAbs protect against ZIKV-induced lethality

Four to five week-old WT male mice were treated with anti-Ifnar1 mAb followed by subcutaneous infection with 10^3 FFU of mouse-adapted ZIKV-Dakar. Mice then were treated with isotype-control, EDE1-C8, or EDE2-A11 mAbs at day +1 (100 μg, left) or day +3 (250 μg, right). Data were pooled from two (isotype-control mAb) or three (EDE1-C8 and EDE2-A11) independent experiments (isotype-control mAb, n = 19; EDE1-C8, n = 10; EDE2-A11, n = 10). Statistical significance was analyzed (log-rank test: ****, P < 0.0001).
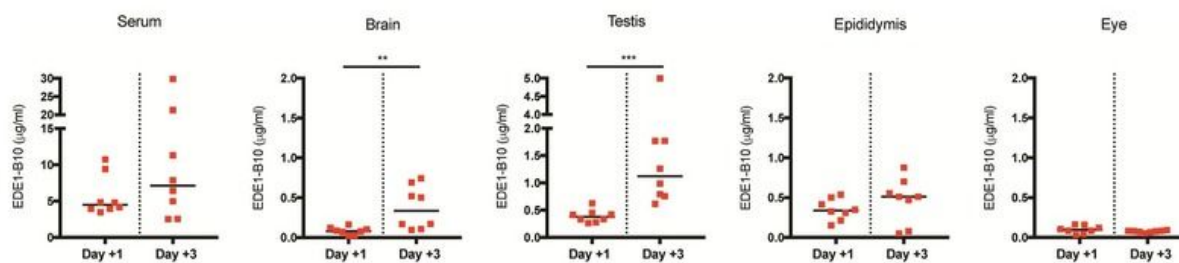
Figure 4.4: Levels of EDE1-B10 mAb in tissues at day +5 after infection.

Eight to nine week old WT male mice were treated with a single dose of EDE1-B10 mAb at day +1 or +3 as described in **Figure 4.2. a**. At D+5, tissues were harvested and EDE1-B10 levels were assessed by ELISA using a standard curve. Bars indicate median values. Data were pooled from two independent experiments, and symbols correspond to individual mice (*n* = 8 per group). Statistical analysis was determined (Mann-Whitney test: **, *P* < 0.01; ***, *P* < 0.001).

Figure 4.5: EDE1-B10 protects against testis infection and injury.

Eight- to nine-week old male WT mice were treated with isotype control or EDE1-B10 mAb at day +1 (n = 6 mice per group), day +3 (n = 4 mice per group), or day +5 (n = 8 mice per group) after infection, as described in **Figure 4.2**. (**a**) Low-magnification (top) and high-magnification (bottom) images after RNA ISH staining of testis at day +21 after infection using ZIKV-specific RNA probes. (**b**) Low-magnification (top) and high-magnification (bottom) images of hematoxylin and eosin (H&E)-stained samples of testis from mice that were treated with isotype control or EDE1-B10 mAbs at day +1 (n = 4 mice per group), day +3 (n = 4 mice per group), or day +5 (n = 7 mice per group). (**c**) The number of motile sperm from each mouse, as determined by computer-assisted sperm analysis (uninfected: n = 10; day +1: isotype, n = 8; EDE-B10, n = 10; day +3: isotype, n = 10; EDE-B10, n = 15; day +5: isotype, n = 9 per group). Bars indicate median values. In **a**,**b**, scale bars, 500 μm (top) and 20 μm (bottom). *P < 0.01; n.s., not significant (ANOVA with a Dunn's multiple-comparison test). Data are representative of two (**a**,**b**) or three (**c**) independent experiments.

142

Figure 4.6: ISH and histological analysis of epididymis from mice treated with EDE1-B10.

Eight- to nine- week old male WT mice were treated with isotype control or EDE1-B10 mAb at day +1 (n=6 mice), day +3 (n=4 mice), day +5 (n=8 mice) after infection, as described in **Figure 4.2**. **a**. RNA *in situ* hybridization (ISH) staining of epididymis at day +21 using ZIKV-specific RNA probes. Low power (scale bar = 500 μm) and high power (scale bar = 20 μm) images are presented in sequence. The images in the panels are representative of sections from 4 to 6 mice. **b**. H & E staining of epididymis. Low power (scale bar = 500 μm) and high power (scale bar = 20 μm) images are shown in sequence. The images are representative of sections from 3 to 5 mice.
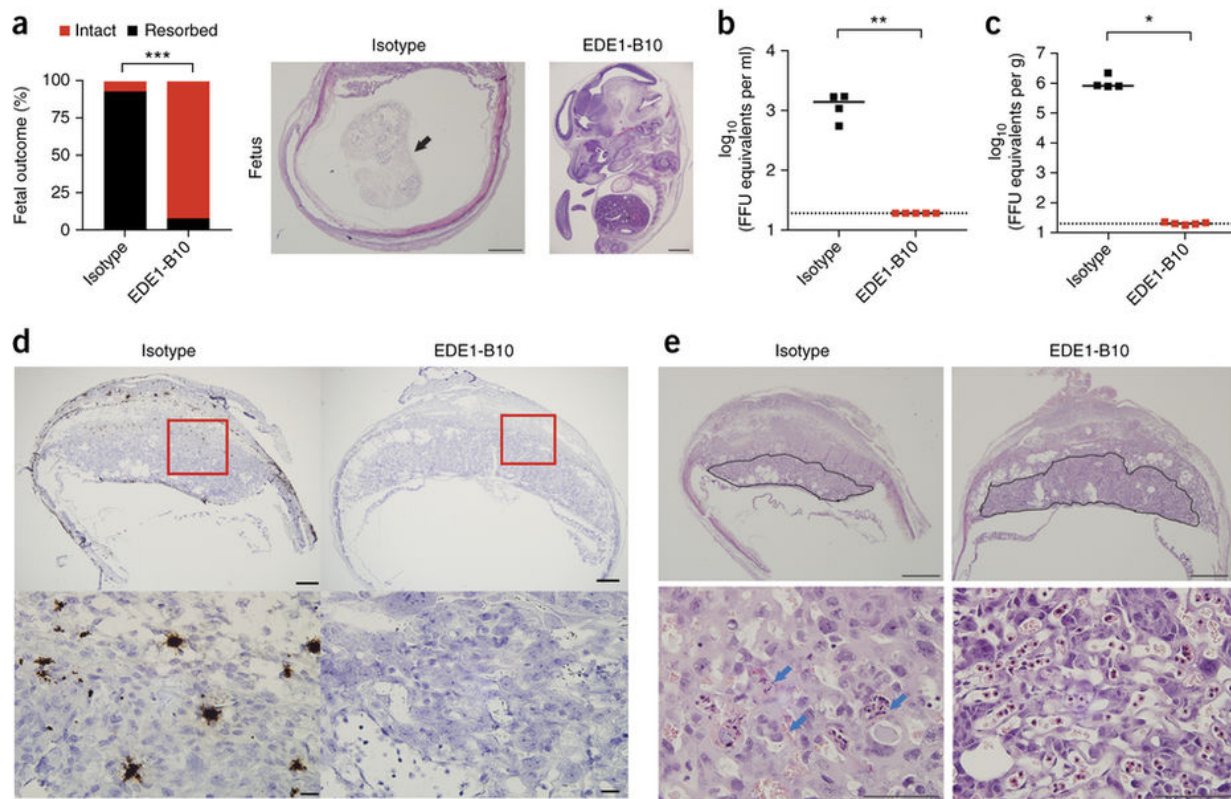
Figure 4.7: EDE1-B10 protects *Ifnar1*$^{-/-}$ pregnant dams.

Ifnar1$^{-/-}$ female mice were mated with WT sires. At E6.5, dams were infected with ZIKV-Brazil and treated on E7.5 with 250 μg of an isotype control mAb or EDE1-B10. Dams were harvested on E13.5 to assess fetal survival and maternal viral burden. (**a**) Left, fetal outcome, presented as intact versus resorbed fetuses at the time of harvest. Middle and right, images of fetal histology; black arrow indicates a partially resorbed fetus in the uterus. Scale bars, 1 mm. (**b**,**c**) Viral burden in the maternal brain (**b**) and serum (**c**). Horizontal bars indicates median values, and dashed lines indicate limit of detection for the assay. (**d**) Low-magnification (top) and high-magnification (bottom) images after RNA ISH staining of placentas at E13.5. Scale bars, 500 μm (top) and 20 μm (bottom). The images are representative of placenta from one (isotype control mAb) or three (EBE-B10) dams. (**e**) Low-magnification (top) and high-magnification (bottom) H&E-stained images of a placenta at E13.5. Placental labyrinth zone is marked with a solid line. The images are representative of placenta from one (isotype control mAb) or three (EDE1-B10) dams. Scale bars, 1 mm (top) and 100 μm (bottom). Blue arrows indicate apoptotic trophoblasts in the labyrinth zone. *$P < 0.05$, **$P < 0.01$, and ***$P < 0.0001$ (Fisher's exact test (**a**) or Mann–Whitney test (**b**,**c**)). Data were pooled from two independent experiments (**a**–**c**) or are representative of one (**d**,**e**), two (**a**), and three (**d**,**e**) experiments.
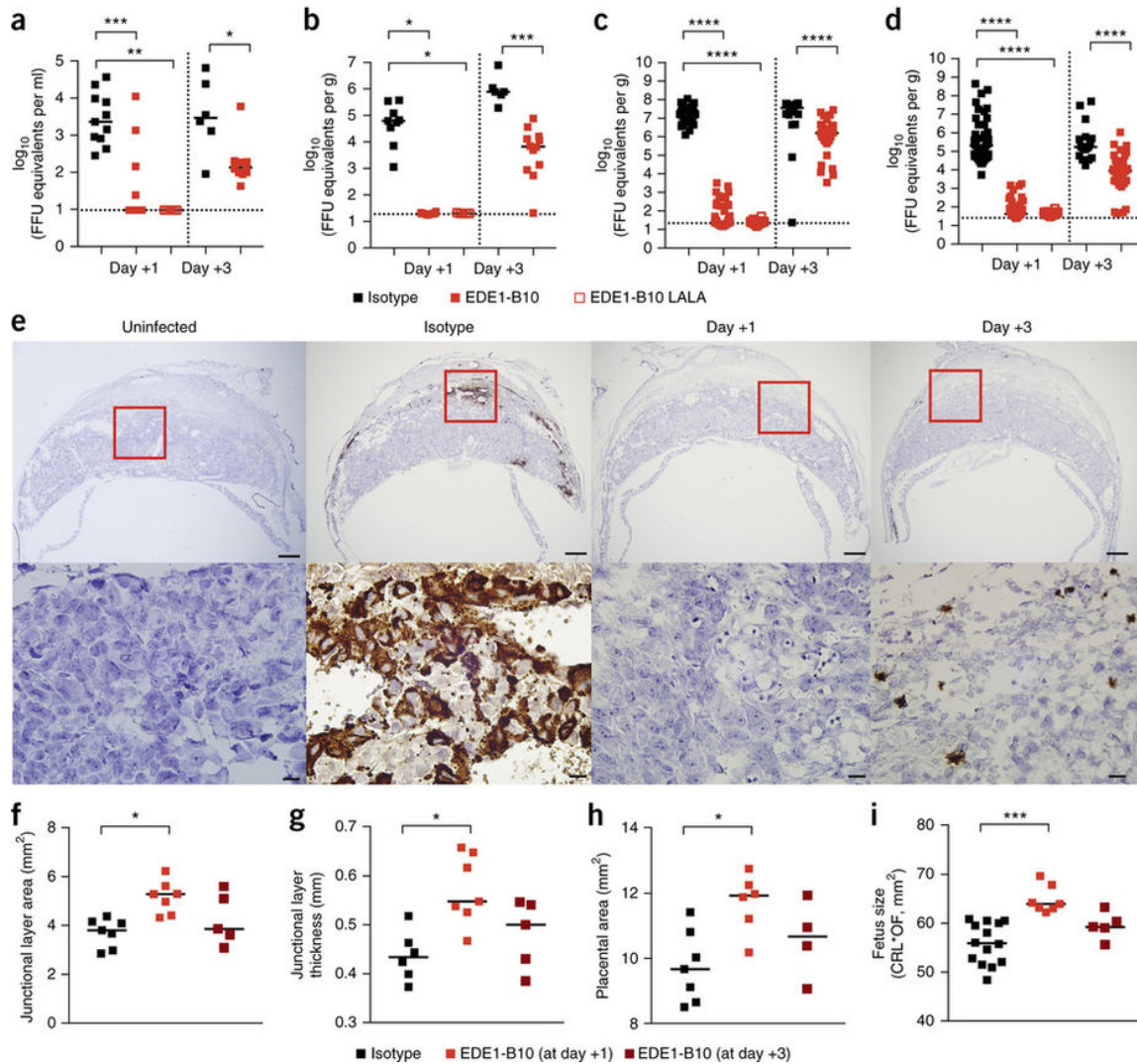
Figure 4.8: Therapeutic effect of EDE1-B10 in WT pregnant dams.

WT female mice were mated with WT sires. At E5.5, dams were treated with anti-Ifnar1. At E6.5, dams were infected subcutaneously with 10^3 FFU of mouse-adapted ZIKV-Dakar. At E7.5 (day +1 after infection) or E9.5 (day +3 after infection), dams were treated with 250 µg of either isotype control (day +1, $n = 9$ mice; day +3, $n = 6$ mice), EDE1-B10 (day +1, $n = 12$ mice; day +3, $n = 12$ mice), or EDE1-B10 LALA (day +1, $n = 5$ mice) mAbs. (**a–d**) At E13.5, viral RNA was assessed by qRT–PCR in the maternal serum (**a**), maternal brain (**b**), placenta (**c**), and fetal head (**d**). Bars indicate median values. Dashed lines indicate the limit of detection for the assay. (**e**) Low-magnification (top) and high-magnification (bottom) images after RNA ISH staining of placenta at E13.5. Scale bars, 500 µm (top) and 20 µm (bottom). (**f–i**) Measurements of the placenta (**f–h**) and fetal body size (**i**) from isotype-treated ($n = 7$ per group) or EDE1-B10-treated (day +1, $n = 7$; day +3, $n = 5$) dams. Bars indicate median values. *$P < 0.05$, **$P < 0.01$, ***$P < 0.001$, and ****$P < 0.0001$ (Kruskal–Wallis or Holm–Sidak's multiple-comparisons test (**a–d**, day +1 samples), Mann–Whitney test (**a–d**, day +3 samples), or Kruskal–Wallis test with a Dunn's multiple-comparison test (**f–h**)). Data were pooled from eight (**a–d**) or three (**f–i**) independent experiments or are representative of three (**e**) independent experiments.
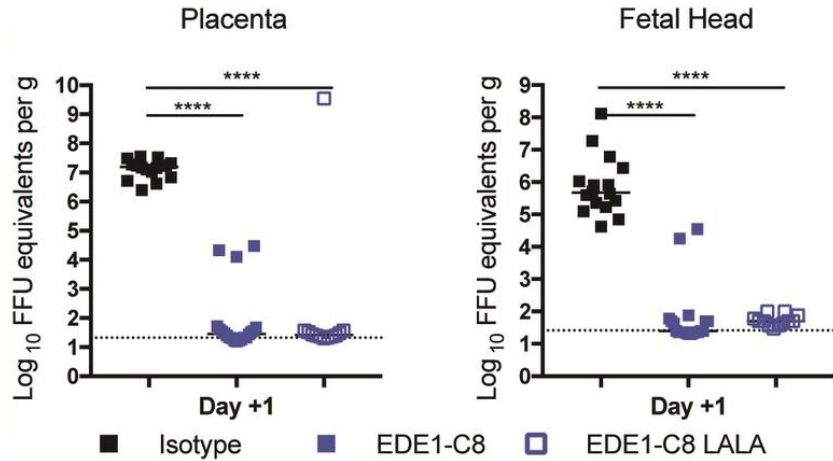
Figure 4.9: Protection of pregnant mice with WT and LALA EDE1-C8 mAbs

WT female mice were mated with WT sires. At E5.5, dams were treated with anti-Ifnar1 mAb. At E6.5, dams were infected subcutaneously with 10^3 FFU of mouse-adapted ZIKV-Dakar. At E7.5 (day +1), dams were treated with 250 μg of either isotype-control mAb or EDE1-C8 (wild-type or LALA variant). At E13.5, placentas and fetal heads were harvested, and viral RNA was assessed by qRT-PCR. Bars indicate median values. Data were pooled from two independent experiments, and symbols correspond to individual mice (isotype mAb, $n = 16$; EDE1-C8, $n = 20$; EDE1-C8 LALA, $n = 12$). Statistical significance was determined (Kruskal-Wallis test: ***, $P < 0.001$; ****, $P < 0.0001$). Dashed line indicates the limit of detection for the assay.
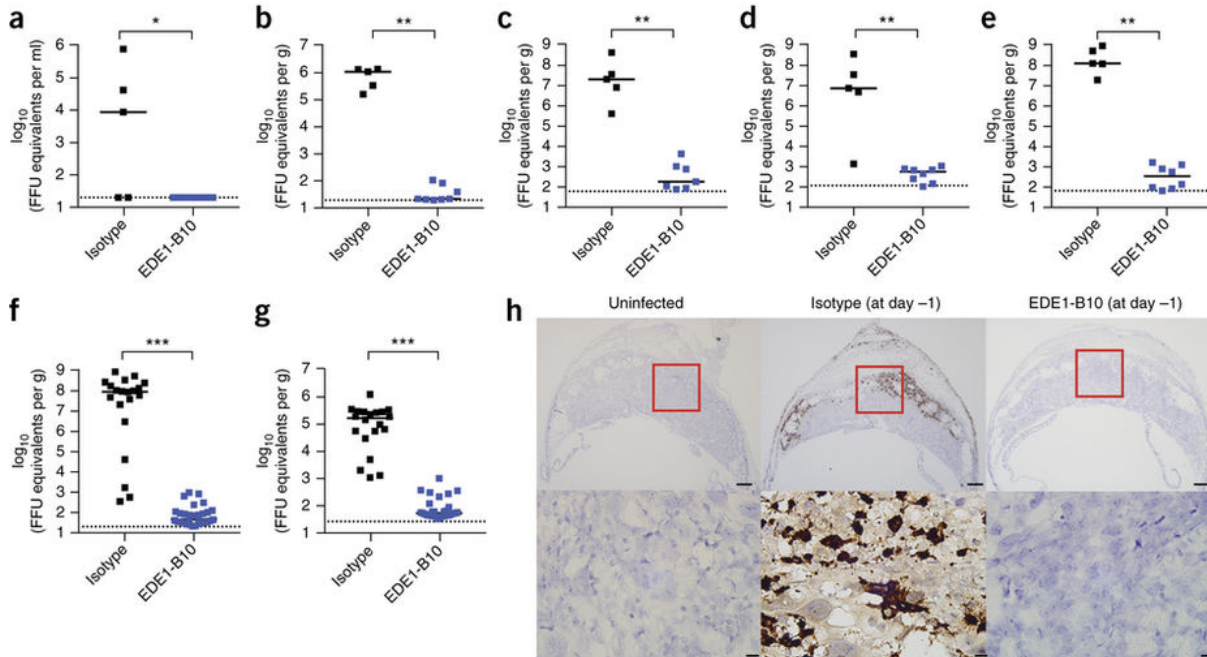
Figure 4.10: Treatment with EDE1-B10 prevents maternal and fetal ZIKV infection after intravaginal inoculation of pregnant dams

WT female mice were mated with WT sires. At E5.5 (day −1 before infection), dams were treated with anti-Ifnar1 and a single 250-μg dose of either isotype control mAb ($n = 5$) or EDE1-B10 ($n = 8$). At E6.5, dams were inoculated intravaginally with 10^5FFU of mouse-adapted ZIKV-Dakar. (**a–d**) At E13.5, viral RNA was assessed by qRT–PCR of maternal serum (**a**), maternal brain (**b**), vagina (**c**), cervix (**d**), ovary (**e**), placenta (**f**), and fetal head (**g**). Bars indicate median values. Dashed line indicates limit of detection for the assay. (**h**) Low-magnification (top) and high-magnification (bottom) images after RNA ISH staining of placenta at E13.5 from uninfected ($n = 3$) or from infected and mAb-treated ($n = 4$ per group) dams. Scale bars, 500 μm (top) and 20 μm (bottom). *$P < 0.05$, **$P < 0.01$, and ***$P < 0.0001$ (Mann–Whitney test (**a–g**)). Data were pooled from three independent experiments (**a–g**) or are representative of three (**h**) independent experiments.

Chapter 5:

Mouse and human monoclonal antibodies protect against infection of multiple genotypes of Japanese encephalitis virus

This chapter is adapted from a manuscript published in Nature Immunology:

Fernandez E, Kose N, Edeling MA, Adhikari J, Sapparapu G, Lazarte SM, Nelson CA, Govero J, Gross ML, Fremont DH, Crowe JE, Diamond MS. 2018. Mouse and human monoclonal antibodies protect against infection of multiple genotypes of Japanese encephalitis virus. *mBiol.* 2018 Feb 27; 9: e00008-18.

5.1   Summary

Japanese encephalitis virus (JEV) remains a leading cause of viral encephalitis worldwide. Although JEV-specific antibodies have been described, an assessment of their ability to neutralize multiple genotypes of JEV has been limited. Here, we describe the development of a panel of mouse and human neutralizing monoclonal antibodies (mAbs) that inhibit infection in cell culture of four different JEV genotypes tested. Mechanism-of-action studies showed that many of these mAbs inhibited infection at a postattachment step, including blockade of virus fusion. Mapping studies using site-directed mutagenesis and hydrogen-deuterium exchange with mass spectrometry revealed that the lateral ridge on domain III of the envelope protein was a primary recognition epitope for our panel of strongly neutralizing MAbs. Therapeutic studies in mice demonstrated protection against lethality caused by genotype I and III strains when mAbs were administered as a single dose even 5 days after infection. This information may inform the development of vaccines and therapeutic antibodies as emerging strains and genotypic shifts become more prevalent.

Although Japanese encephalitis virus (JEV) is a vaccine-preventable cause of viral encephalitis, the inactivated and live attenuated platforms available are derived from strains belonging to a single genotype (GIII) due to its historical prevalence in areas of JEV epidemics. Related to this, studies with vaccines and antibodies have focused on assessing the *in vitro* and *in vivo* protective responses to homologous or heterologous GIII strains. An epidemiological shift in JEV genotype distribution warrants the induction of broadly neutralizing antibody responses that inhibit infection of multiple JEV genotypes. Here, we generated a panel of mouse and human neutralizing monoclonal antibodies and evaluated

their inhibitory activity, epitope location, and capacity for protection against multiple JEV

genotypes in mice.

5.2 Introduction

Despite the existence of inactivated and live attenuated vaccine platforms, Japanese encephalitis virus (JEV) remains a primary cause of viral encephalitis. It is particularly prevalent in Asia, with approximately 68,000 clinical cases (1, 2) and an estimated 10,000 to 15,000 deaths per year (1). JEV circulation is endemic in southern tropical and subtropical areas (e.g., Australia, Indonesia, and Singapore), with epidemics occurring in northern temperate regions (e.g., Japan, Bhutan, and Nepal) (3, 4). JEV is transmitted primarily by the Culex tritaeniorhynchus mosquito and is maintained in an enzootic cycle with pigs and wading birds. In contrast, humans are infected as incidental dead-end hosts (5, 6). The high incidence of JEV in rural areas has been attributed to the presence of open water sources, the preferred breeding grounds for Culex mosquitoes (7). Approximately 5 to 15 days after mosquito inoculation of JEV, a nonspecific febrile illness develops, characterized by malaise, headache, and general discomfort (2). Symptomatic JEV infection is observed most commonly in children in areas of endemicity, children and adults in areas with JEV epidemics, and travelers to areas of endemicity and epidemics (3, 8). Severe clinical JEV disease occurs in about 1% of infected humans, with progression to encephalitis, seizures, or neurological deficits (9, 10). Beyond death, which occurs in 20 to 30% of clinical cases, severe long-term complications include paralysis, dystonia, and cognitive deficits (10–12). JEV is a flavivirus of the Flaviviridae family and is related to other viruses that cause human disease, including Zika (ZIKV), West Nile (WNV), dengue (DENV), tick-borne encephalitis (TBEV), and yellow fever (YFV) viruses. JEV is an ~50-nm enveloped, positive-stranded RNA virus with an ~11-kb genome flanked by 5 = and 3 = untranslated regions. The genome encodes a single open reading frame that is co- and

posttranslationally cleaved by viral and host proteases into three structural proteins (capsid [C], premembrane [prM], and envelope [E]) and seven nonstructural proteins. The E protein is necessary for virus binding, entry, and fusion in host cells (13) and the ectodomain is divided into three domains: domain I (E-DI) is the central -barrel domain, domain II (E-DII) is an extended dimerization domain with a distal hydrophobic fusion loop (FL), and domain III (E-DIII) is an immunoglobulin-like fold (14). Structural analysis of the JEV E protein shows a smaller dimer interface with increased contacts at the E-DI-DIII pocket compared to those of related flaviviruses (15). Although most phylogenetic analyses define four JEV genotypes based on sequence variation of the E protein, multiple strains belonging to a fifth genotype were recently identified in Malaysia and South Korea (16–18). The genotypes cluster within particular geographic distributions: for example, genotype I (GI) and GIII strains are more common in temperate regions, whereas GII and GIV strains are more common in tropical climates (19–21). GIII has been the predominant genotype historically, and as such, existing vaccines against JEV are derived from prototypical GIII strains such as JEV-Nakayama and JEV-SA14 (21). Recent reports have noted a substantial increase in GI infections in Asian countries, including China and Japan (22, 23). The humoral response to JEV, like that of other flaviviruses, is considered necessary for limiting infection, and neutralizing antibody titers often serve as a correlate of protection (24). Indeed, JEV type-specific mouse monoclonal antibodies (mAbs) with protective activity (e.g., E3.3) have been identified and were derived against GIII strains (25–28). Moreover, a humanized mAb (B2) that was derived from a chimpanzee immunized with JE-VAX also protected mice against JEV-Nakayama, a strain of the homologous JEV genotype (GIII) (29). Other neutralizing mAbs (e.g., 2H4 and 2F2) in

152

goat and monkey models of infection (30) protected against JEV strains from the homologous genotype to which they were raised. Notwithstanding these data, no study has comprehensively profiled the inhibitory activity of anti-JEV mAbs against multiple genotypes *in vitro* and *in vivo*, and no fully human anti-JEV mAbs have been described. The shift in prevalence from GIII to GI may require a different antibody repertoire for protection against infection and thus has implications for the efficacy of existing vaccines that were derived from GIII strains. Here, we generated a panel of mouse and human mAbs against JEV after immunizing mice and humans with a GIII vaccine strain (JEV-SA14-14-2) or mice with pathogenic GII and GIII strains of JEV. Six of the mouse mAbs (JEV-31, JEV-106, JEV-128, JEV-131, JEV-143, and JEV-169) neutralized infection of strains representative of the four JEV genotypes (GI, GII, GIII, and GIV) that we tested to various degrees. Site-directed mutagenesis and hydrogen-deuterium exchange mass spectrometry (HDX-MS) mapping data identified sites within E-DI (JEV-169), E-DIII (JEV-31, JEV-106, JEV-128, JEV-131, JEV-143, and hJEV-69), and additional regions of the E ectodomain (JEV-117 and hJEV-75) as key epitopes for neutralization. Passive transfer studies in lethal JEV challenge mouse models showed protective efficacy for some mouse and human mAbs even when administered up to 5 days after GI or GIII infection. These data may be relevant for the development of antibody-based therapeutics or anti-JEV vaccines with broader protective activity, which may be important as the predominant genotypes shift over time.

5.3   Results

Anti-JEV mAbs. We generated a panel of neutralizing murine mAbs against JEV to begin to address the impact of shifting genotype epidemiology on antibody-mediated protection.

We inoculated and boosted adult C57BL/6 mice deficient for interferon (IFN) regulatory factor 3 ($Irf3^{-/-}$) with 102 focus-forming units (FFU) of a vaccine strain of JEV (JEV-SA14-14-2). Additionally, we inoculated $Irf7^{-/-}$ mice with JEV-Nakayama (GIII), boosted with JEV-Bennett (GII), and administered a final intravenous boost with JEV-Nakayama before splenocyte-myeloma cell fusion. We immunized $Irf3^{-/-}$ and $Irf7^{-/-}$ rather than wild-type (WT) mice, as JEV replicated to higher titers and induced stronger neutralizing antibody responses in these animals (data not shown). We screened ~3,800 hybridoma supernatants from five independent fusions for binding to JEV-infected cells by flow cytometry and direct virus binding by enzyme-linked immunosorbent assay (ELISA) and cloned 13 JEV mAbs by limiting dilution for further characterization. Using a single-endpoint neutralization assay, we identified 8 mAbs with 95% neutralizing activity against infection of JEV-SA14-14-2 in Vero cells (data not shown). We then tested these mouse mAbs for their ability to bind recombinant JEV E ectodomain, JEV E-DI, JEV E-DIII, WNV E ectodomain, or ZIKV E ectodomain by ELISA (**Table 5.1**). JEV-169 bound E-DI, and the remaining mAbs recognized E-DIII, with the exception of JEV-117, which recognized JEV E ectodomain but not the domain fragments. JEV-31 and JEV-117 showed cross-reactivity to WNV E protein, whereas JEV-143 cross-reacted with ZIKV E protein.

To generate human mAbs against JEV, we screened neutralization profiles from donors immunized with a two-dose regimen of a commercially available inactivated JEV vaccine, IXIARO, that was based on a genotype III strain (**Figure 5.1A**). We obtained hybridoma supernatants derived from donors that bound to JEV-SA14-14-2, determined the single-endpoint neutralization titer (data not shown), and cloned 4 anti-JEV mAbs. Three of the human mAbs bound to E-DIII, whereas hJEV-75 bound to the E ectodomain

154

but not to E-DI or E-DIII (**Table 5.1**). hJEV-11 and hJEV-80 cross-reacted with WNV E protein, whereas hJEV-69 and hJEV-75 appeared specific to JEV and did not bind either WNV or ZIKV E proteins.

Breadth of neutralization of mAbs. We performed focus reduction neutralization tests (FRNTs) on Vero cells to assess the inhibitory capacity of our anti-JEV mAbs against the vaccine strain, JEV-SA14-14-2, and available prototype strains representative of multiple genotypes. We did not test a representative genotype V strain of JEV, as one was not available from the World Arbovirus Reference Collection. We determined the mAb concentration that reduced the number of foci of infection by 50% (50% effective concentration [EC_{50}]) (**Figure 5.1B and C; Table 5.1**). JEV-31 and JEV-169 had the strongest neutralization activity against the four genotypes tested (GI, GII, GIII, and GIV), with EC_{50} values between 84 and 365 ng/ml and 49 and 315 ng/ml, respectively. JEV-106, JEV-128, JEV-131, and JEV-143 had intermediate neutralizing activity, with EC_{50} values between 147 and 548 ng/ml, 102 and 1,629 ng/ml, 95 and 509 ng/ml, and 346 and 818 ng/ml, respectively, against strains of the four genotypes. As expected, the JEV-SA14-14-2 vaccine and JEV-SA14 parental strain were neutralized to similar levels by most mAbs, with the exception of JEV-117, which showed a remarkable ~1,000-fold shift in EC_{50} values. In general, JEV-27 and JEV-117 had the weakest neutralizing activity, with EC_{50} values between 1,441 and 4,830 ng/ml and 10,000 ng/ml, respectively.

We identified four human mAbs with neutralizing activity against JEV-SA14-14-2, which we characterized in greater detail. hJEV-11 and hJEV-80 exhibited relatively weak neutralizing activity (1,509 to 10,000 ng/ml and 857 to 10,000 ng/ml, respectively) against the other strains tested (**Figure 5.1C; Table 5.1**). In comparison, hJEV-69 and

hJEV-75 inhibited infection of multiple JEV strains more potently. hJEV-69 had greater activity against the GI strains (2372/79 and MAR 859; EC50, 335 to 1,102 ng/ml) than against the GIV strain (JKT 7887; EC50, 3,111 ng/ml), whereas hJEV-75 had the strongest neutralizing activity against GI, GII, and GIII strains (EC50, 9 to 457 ng/ml) but did not inhibit the GIV strain (JKT 7887; EC50, 10,000 ng/ml). Overall, the mouse-derived mAbs had greater breadth of neutralization against multiple genotypes of JEV than the human-derived mAbs. This finding could reflect the different immunogens used (live versus inactivated viruses for mice or humans, respectively), species-specific differences in the antibody repertoire, or the limited size of the panel of mAbs that we obtained.

Mechanism of neutralization. Antibody neutralization of flaviviruses can occur by inhibiting attachment, internalization, and/or fusion (31). To determine how the neutralizing mAbs inhibited infection in cell culture, we performed pre- and post-attachment neutralization assays (32–34). MAbs were incubated with JEV-SA14-14-2 before or after virus binding to cells, and infection was measured by FRNT (32–34). As expected, all mAbs efficiently neutralized infection when premixed with virus (**Figure 5.2A and 5.3** [solid lines]). All mouse mAbs also inhibited JEV infection when added after virus adsorption to the cell surface, although to a lesser extent, suggesting that at least part of their blocking activity was at a post-attachment step (**Figure 5.2A; Figure 5.3**, dashed lines). Similarly, hJEV-69 and hJEV-75 neutralized in both pre- and post-attachment assays (**Figure 5.2B**).

We next determined whether the neutralizing mouse and human mAbs could block fusion by adapting a virus fusion from without (FFWO) assay at the plasma membrane (32, 33). JEV-SA14 was adsorbed to a monolayer of Vero cells on ice and subsequently

incubated with the mAbs. Fusion at the plasma membrane was induced by brief exposure to low-pH-buffered medium at 37°C. After washing, cells were incubated overnight in the presence of 10 nM concanamycin A1 to prevent canonical endosomal fusion and allow viral replication. As described for other flaviviruses (33), in the absence of mAb treatment, ~20% of cells produced viral antigen that was measurable by flow cytometry; in contrast, minimal viral antigen (~2 to 3% of cells) was detected when fusion was induced under neutral-pH conditions (**Figure 5.2C and D**). All neutralizing mouse mAbs tested inhibited plasma membrane fusion under acidic conditions and subsequent viral antigen expression. In contrast, hJEV-69 and hJEV-75 inhibited fusion at the plasma membrane less efficiently (**Figure 5.2C and D**).

Epitope mapping. To begin to assess the basis for differential inhibition by the neutralizing mAbs, we mapped their epitopes. We defined key peptide regions and amino acid residues required for mAb binding by using both hydrogen-deuterium exchange mass spectrometry (HDX-MS) (35) and alanine-scanning site-directed mutagenesis (36) of the E protein of JEV-SA14-14-2.

(i) HDX-MS. As HDX-MS should show slower exchange at mAb binding sites (increased protection), we analyzed five mouse mAbs (JEV-31, JEV-106, JEV-128, JEV131, and JEV-143) that engaged E-DIII. The mAbs were mixed in a 1:1 ratio with E-DIII, and HDX was performed for 10, 30, 60, 120, 900, 3,600, and 14,400 s. The quenching and protein digestion conditions were optimized to obtain 32 different peptides that spanned the 11-kDa JEV E-DIII protein (**Figure 5.4A**). All five mAbs showed changes in deuterium uptake compared to unliganded E-DIII. Representative kinetic plots are shown for eight of the peptides spanning E-DIII in the presence of JEV-31 (**Figure 5.5A**). The deuterium

uptake studies showed that binding of JEV-31, JEV-106, JEV-128, JEV-131, and JEV-143 protected regions in the N-terminal region and A strand (residues 304 to 310), BC loop (residues 326 to 342), and DE loop (residues 355 to 371) of E-DIII (**Figure 5.5B; Figure 5.4B**), regions that correspond to the well-defined lateral ridge (LR) epitope (37) (E-DIII-LR).

(ii) Alanine-scanning mutagenesis. The amino acid binding sites of neutralizing mouse and human anti-JEV mAbs also were mapped by alanine-scanning mutagenesis and mammalian cell expression (36) of the JEV prM-E protein. Residues in the E protein ectodomain were replaced with alanine with two exceptions: alanine residues were mutated to serine, and cysteines were not mutated to prevent protein misfolding (data not shown). We characterized a residue as critical for mAb binding if the mutation resulted in less than 25% binding compared to the wild-type protein (**Figure 5.5C and 5.6**). We found that alanine substitution of certain amino acids (e.g., T321, D332, and I383), which correspond to sites in E-DIII-LR, caused loss of binding of most of the neutralizing murine and human mAbs tested, especially JEV-31, JEV-131, JEV-143, and hJEV-69 (**Figure 5.6A and B**). JEV-131 showed a broader binding footprint, as loss of binding was observed for alanine substitution of additional residues, including G299, L345, P376, and V384. JEV-117 and hJEV-75 demonstrated loss of binding following mutations in other regions of the E ectodomain (**Figure 5.6C**) that correspond to previously defined epitopes for related flaviviruses, including residues in the E-DI-DII-hinge region (K136 for JEV-117 and S275 for hJEV-75), E-DI-LR (L180 for hJEV-75), E-DII-hinge (E49), E-DII-LR (N82 for hJEV-75), and E-DII-central interface (W217 for hJEV-75) (15, 38). The loss of binding observed within E-DIII for alanine substitutions of residues F308 (JEV-117 and hJEV-75) and F310

(JEV-117) corresponds to sites within the previously described A-strand epitope (39) (data not shown). This pattern of mutagenesis and binding also correlates with the inability of JEV-117 and hJEV-75 to recognize isolated domains by ELISA (**Table 5.1**). JEV-169 demonstrated loss of binding with three different mutations in DI (L25, G184, and L285) and a single mutation in DII (M204), although these residues do not correspond to any published epitope. Because alanine substitutions can have only moderate structural differences compared to other residues, we also made charge substitutions in amino acids at different E-DIII epitopes, including the A strand (S309K, K312E, and H395K), DIII-LR (S331K, S364K, N367K, and K369E), C-C' loop (T349K), and FG loop (R387E and D389K). Loss of binding in the E-DIII-LR epitope (S331K and S364K) but not in other E-DIII regions was observed for the murine mAbs JEV-31, JEV-106, JEV-128, JEV-131, and JEV-143 (data not shown). Unexpectedly, we did not observe loss of binding for hJEV-69, suggesting it may recognize E-DIII somewhat differently than the neutralizing mAbs of mouse origin.

***In vivo* protection studies.** To evaluate whether neutralizing mAbs could protect against JEV infection *in vivo*, we developed challenge models of JEV-induced lethality in mice by using GIII (Nakayama) and GI (MAR 859 and 2372/79) strains. Once models were established, we treated 4- to 5-week-old male WT C57BL/6 mice on day 1 with a single 10- μg (0.5-mg/kg) prophylactic dose of seven different anti-JEV mAbs or an isotype-control mAb and then inoculated animals on day 0 with different pathogenic JEV strains.

(i) **Nakayama (GIII).** Whereas JEV-31, JEV-106, JEV-143, and JEV-169 protected all mice from lethal infection (**Figure 5.7A**), JEV-27, JEV-128, and JEV-131

conferred partial (25 to 89%) protection. We also observed protection (60 to 80%)
with similar doses of hJEV-69 and hJEV-75 (**Figure 5.7B**).

(ii) **MAR 859 (GI).** JEV-31, JEV-128, JEV-131, and JEV-169 conferred partial
protection, ranging from 40 to 55% (**Figure 5.7C**).

(iii) **2372/79 (GI).** JEV-31, JEV-131, and JEV-169 provided complete protection
against lethality, whereas JEV-106 and JEV-128 provided more limited (25 to 30%)
protection (**Figure 5.7D**).

To define the therapeutic potential of our most protective mAbs, a single 250-μg (15-mg/kg) dose was administered to mice 5 days after infection (**Figure 5.7E and F**). Whereas
JEV-31 and JEV-169 completely protected against lethality induced by JEV-Nakayama
(GIII), these mAbs showed more limited therapeutic activity against JEV-2372/79 (GI), as
they protected 50 to 60% of mice, respectively. Administration of hJEV-75 at 5 days after
infection also had significant protection against both JEV-Nakayama (GIII) and JEV-2372/79 (GI) strains. Overall, our data show that a single mAb that broadly neutralizes
multiple JEV genotypes can provide therapeutic activity *in vivo* against multiple strains.

5.4 Discussion

We sought to identify murine and human mAbs that broadly neutralize infection of
JEV strains corresponding to most genotypes. We inoculated mice with attenuated or
infectious strains of JEV to generate a panel of eight anti-JEV mAbs and characterized
them at the functional and structural levels. From our analyses, we identified three classes
of antibodies based on neutralization profile, epitope binding, and in vivo efficacy. The
two mAbs JEV-27 and JEV-117 had the weakest inhibitory profiles. Four mAbs (JEV-106,
JEV-128, JEV-131, and JEV-143) had intermediate neutralization abilities, and two mAbs

(JEV-31 and JEV-169) were strongly and broadly neutralizing. Binding analysis revealed two mouse mAbs (JEV-31 and JEV-117) that were cross-reactive with WNV. JEV-143 cross-reacted with ZIKV, and five other mouse mAbs (JEV-27, JEV-106, JEV-128, JEV-131, and JEV-169) appeared more type specific. JEV-31, which cross-reacted with WNV and was one of the most strongly neutralizing mAbs in our panel, recognized an epitope in the E-DIII-LR. A single JEV-specific neutralizing murine mAb, JEV-169, mapped to E-DI. We also generated the first human mAbs for JEV isolated from B cells of recipients of a chemically inactivated JEV vaccine; to our knowledge, this also is the first isolation of human mAbs from an individual immunized with an inactivated flavivirus vaccine. We identified two strongly neutralizing JEV-specific human mAbs: one (hJEV-69) that recognized E-DIII-LR and another (hJEV-75) that mapped to residues in the E-DI-LR, E-DI-DII-hinge, E-DII-LR, and E-DII-hinge. Future studies will need to assess the inhibitory potential of the anti-JEV humoral response against contemporary strains of JEV of all genotypes, including GV strains. Type-specific and cross-reactive neutralizing mAbs have been identified against JEV. Although others have identified E-DIII-specific anti-JEV mAbs from mice (25, 27, 28), this class of antibodies appears less immunodominant in humans, at least against some (40–44) but not all (45, 46) flaviviruses. Murine-derived E-DIII-specific mAbs (2H4, A3, and E3.3) against JEV had stronger neutralizing activity in vitro than E-DII-specific mAbs (25, 30, 47, 48). Humanization of chimpanzee-derived E-DI (A3 and B2)- and E-DIII (E3)-specific mAbs demonstrated equivalent in vitro neutralization compared to the parental mAbs, and this finding correlated with protection against JEV infection in mice by the homologous genotype (GIII) (29). We performed epitope-mapping studies on our mouse mAbs by using complementary approaches: HDX-

161

MS and alanine-scanning mutagenesis. Epitope mapping by HDX-MS identified a series of short peptides that were recognized by our strongest neutralizing E-DIII-specific mAbs (JEV-31, JEV-128, JEV-131, and JEV-143). Subsequent analysis by alanine-scanning mutagenesis confirmed and extended these findings by defining individual amino acid residues in E-DIII-LR (T321, D332, and I383) required for optimal mAb binding (JEV-31, JEV-131, JEV-143, and hJEV-69). HDX provided information on mAb reactivity with a peptide segment but lacked residue-level specificity. Reciprocally, alanine-scanning mutagenesis defined specific amino acids required for optimal binding but is of limited utility if mutation of more than one residue is required for significant loss of binding. Loss-of-binding analysis of the neutralizing hJEV-75 mAb identified residues across E-DI and E-DII, particularly within the previously defined E-DI-LR, E-DII-LR, and E-DI-DII-hinge epitopes. JEV-117, a mouse mAb that was poorly neutralizing, exhibited a similar loss-of-binding profile to hJEV-75. Although further studies are warranted, the differential functional activities of JEV-117 and hJEV-75 may be due to differences in accessibility of their epitopes or affinity of binding. Higher resolution studies, including X-ray crystallography and cryo-electron microscopy, are necessary to determine the precise geometry of binding and a complete footprint of interacting residues. We observed some variation in neutralizing activity of some mAbs against different JEV strains and genotypes. This piece of data is analogous to that observed with mAbs against different DENV-3 genotypes (49, 50). The inter-genotypic amino acid sequence divergence in the E protein among genotypes ranges from 0.6% (GII versus GIII) to 5.6% (GIII versus GIV) (51). Infection with one JEV genotype is believed to confer long-term immunity against both homologous and heterologous genotypes. We assumed it might be straightforward to

generate mouse and human mAbs that neutralized all JEV genotypes available to us. Indeed, there are limited amino acid changes in E-DIII among the JEV strains that we tested, with only 5 amino acid differences (residues 315, 327, 333, 336, and 366); accordingly, the variation in neutralization of different JEV genotypes by E-DIII-specific mAbs was limited (~10-fold). Two mAbs (JEV-117 and hJEV-75) effectively neutralized the JEV-SA14-14-2 vaccine strain but remarkably lost inhibitory activity against the parental JEV-SA14 strain. These mAbs mapped to epitopes that also contained residues outside E-DIII, in E-DI and E-DII. An alignment of the genotypic variation in JEV sequences (**Figure 5.8**) failed to show a direct correlation with the residues identified in loss-of-binding studies for JEV-117 and hJEV-75. Although the sites of genotypic variation between JEV-SA14-14-2 and JEV-SA14 are not coincident with JEV-117 or hJEV-75 epitope residues, there are several residues in close proximity. For JEV-117, the H/Q264 genotypic variation is within 5 Å of the epitope residue at position 262; M/K279 also is within 5 Å of epitope residue 49, and the K/E138 site of genotypic variation is within 10 Å of epitope residue 136. For hJEV-75, the M/K279 genotypic variation is within 5 Å of epitope residue 49 or within 10 Å of epitope residues 273 and 275. Similarly, the K/E138 site of genotypic variation is within 10 Å of epitope residue 49, and the H/Q264 site of genotypic variation is also within 10 Å of the epitope residue 262. As an alternative explanation, differences in strain and genotype residues allosterically could affect the display of JEV-117 and hJEV-75 epitopes. This idea has been described as a basis for differential neutralization of flavivirus genotypes by other antibodies (52, 53). Clearly, further studies with higher-resolution epitope mapping of the JEV-117 and hJEV-75 mAbs (e.g., atomic resolution structures of the Fab-E complexes) may resolve this question of

differential neutralization of JEV strains. Overall, our results have potential implications for assessing the breadth of the protective efficacy of existing and new JEV vaccines. It may be critical to assess whether antibody responses against the vaccine strain of a given JEV efficiently neutralize infection of heterologous genotypes that may emerge.

Mechanism-of-action studies showed that all neutralizing murine E-DIII-LR mAbs could block virus fusion, as was observed previously for E16, a WNV-specific mAb (33). Although hJEV-69 exhibited a loss-of-binding profile similar to those of E-DIII-LR-specific mouse mAbs, charge substitutions in this region (S331K and S364K) did not affect hJEV-69 binding, suggesting a somewhat unique epitope. Consistent with this observation, FFWO studies of hJEV-69 indicated that although it inhibited at a post-attachment stage, it did not efficiently block pH-dependent fusion. Although further studies are required, the neutralizing human mAbs could block at a post-entry step before fusion. Alternatively, the FFWO, which is a measure of viral fusion at the plasma membrane, may not fully recapitulate the events occurring in the late endosome. We performed protection studies *in vivo* with our mouse and human mAbs and JEV strains corresponding to the two most commonly circulating genotypes (GI and GIII). To our knowledge, the protective effect of JEV mAbs against genotype I strains *in vivo* has not been studied previously. Several of our neutralizing mAbs (JEV-31, JEV-106, JEV-131, JEV143, JEV-169, and hJEV-75) completely protected against lethal JEV-Nakayama (GIII) infection when administered as prophylaxis. A subgroup of mAbs (JEV-31, JEV-131, and JEV-169) also completely protected against JEV-2372/79, a GI strain, with all mAbs tested partially preventing lethal infection by a highly homologous second GI strain, JEV-MAR 859, with 99% amino acid identity at the E protein. Remarkably, post-exposure therapeutic administration of a single

164

dose of JEV-31 or JEV-169 at 5 days after infection also conferred complete or partial protection against GIII or GI strains, respectively. A single post-exposure dose of hJEV-75 also provided high levels of protection against GI or GIII strains. Although prior studies have reported *in vivo* efficacy of murine and humanized E-DIII mAbs against JEV (26, 29, 30), these challenge studies were performed with single, homologous JEV genotypes, and protection was limited to prophylaxis, with the exception of a single study (30). The post-exposure protection we observed is similar to that seen previously for other E-DIII-LR mAbs, including E16 and WNV (54) and E106 and DENV-1 (55). One caveat of our study is that administration of anti-JEV antibody at day 5 preceded the development of central nervous system symptoms (e.g., seizures, tremors, paralysis, or lethargy). More detailed window-of-treatment analysis is needed to determine which mAbs retain protective efficacy after the development of disease onset. In summary, we identified a panel of anti-JEV mAbs that map to epitopes in E-DI and E-DIII with broadly neutralizing activity against multiple JEV genotypes. Although both mouse and human neutralizing mAbs can block infection at a post-attachment stage, the mouse mAbs appear to have a greater capacity to block pH-dependent viral fusion. Studies using liposome-based fusion experiments (32, 33, 56) and cell entry assays (33) will be required to corroborate these findings. Overall, our combination of i*n vitro* mAb neutralization analyses with mechanism of action, epitope mapping, and *in vivo* activity provides insight into developing and refining vaccine and therapeutic countermeasures against emerging JEV strains and genotypes.

5.5   Methods

Viruses. JEV strains 2372/79 (Thailand 1979, GenBank accession no. U70401), MAR 859 (Cambodia 1967, accession no. U70410), Bennett (Korea 1951, accession no. HQ223285), Nakayama (Japan 1935, accession no. EF571853), SA14-14-2 (China 1954, accession no. JN604986), SA14 (China 1954, accession no. M55506), and JKT 7887 (Indonesia 1981; accession no. L42160) were provided by the World Reference Center for Emerging Viruses and Arboviruses (K. Plante, S. Weaver, and R. Tesh, Galveston, TX). Virus stocks were propagated in C6/36 *Aedes albopictus* cells for 5 days prior to collection, and their titers were determined by focus-forming assay (FFA) on Vero cell monolayers, as described previously (57).

MAb generation.

(i) Mouse mAbs. *Irf3*^{-/-} mice were infected and boosted with 10^2 FFU of JEV-SA14-14-2 and given a final intravenous boost with 10^6 FFU of JEV-SA14-14-2 3 days prior to fusion with P3X63.Ag.6.5.3 myeloma cells. *Irf7*^{-/-} mice were infected and boosted with 10^2 FFU of JEV-Nakayama and JEV-Bennett, respectively, and given a final boost with 10^3 FFU of JEV-Nakayama 3 days prior to fusion. Antibodies from hybridomas that bound to JEV-infected Vero cells by flow cytometry and JEV-SA14-14-2 by direct ELISA were cloned by limiting dilution. All hybridomas were screened initially with a single-endpoint neutralization assay using neat hybridoma supernatant incubated with 10^2 FFU of JEV-SA14-14-2 for 1 h at 37°C. MAb-virus complexes were added to Vero cell monolayers for 1 h at 37°C followed by 1% (wt/vol) methylcellulose in modified Eagle medium (MEM) supplemented with 4% fetal bovine serum (FBS). Plates were fixed with 2% paraformaldehyde (PFA) in phosphate-buffered saline (PBS) 30 h later and sequentially

166

stained with 500 ng/ml WNV E60 (cross-reactive mAb) (38) and horseradish peroxidase (HRP)-conjugated goat anti-mouse IgG in PBS supplemented with 0.1% saponin and 0.02% Tween 20. JEV-infected foci were visualized using TrueBlue peroxidase substrate (KPL) and quantitated on an ImmunoSpot 5.0.37 macroanalyzer (Cellular Technologies). Hybridoma supernatants with greater than 85% neutralization were purified commercially (Bio-X Cell) after adaptation for growth under serum-free conditions**.**

(ii) Human mAbs. The human donors used in this study were born in the United States and Colombia and had not experienced prior JEV infection. However, they were not tested for prior exposure to other flaviviruses (e.g., WNV or DENV). Donors were immunized voluntarily with a two-dose regimen of a commercially available inactivated JEV vaccine, IXIARO, as part of an occupational exposure program. Peripheral blood was obtained for research purposes after informed consent approximately 1 month after boosting, with prior Institutional Review Board approval from Vanderbilt University Medical Center. Peripheral blood mononuclear cells (PBMCs) from heparinized blood were isolated using Ficoll-Histopaque and density gradient centrifugation. The cells were cryopreserved in the vapor phase of liquid nitrogen until use. Ten million PBMCs were cultured in 384-well plates (Nunc) using culture medium (ClonaCell-HY medium A; StemCell Technologies) supplemented with 8 μg/ml 1 of the Toll-like receptor (TLR) agonist CpG (phosphorothioate- modified oligodeoxynucleotide ZOEZOEZZZZZOEEZOEZ ZZT; Invitrogen), 3 μg/ml of Chk2 inhibitor (Sigma), 1 μg/ml of cyclosporine (Sigma), and clarified supernatants from cultures of B95.8 cells (ATCC) containing Epstein-Barr virus. After 7 days, cells from each 384-well culture plate were expanded into four 96-well culture plates (Falcon) using ClonaCell-HY medium A containing 8 μg/ml 1 of CpG, 3

μg/ml of Chk2 inhibitor, and 10^7 irradiated heterologous human PBMCs (Nashville Red Cross) and cultured for an additional 4 days. Supernatants were screened by ELISA (described below) for reactivity with JEV-SA14-14-2. Hybridoma cell lines were cloned by single-cell flow cytometric sorting in a sterile FACSAria III cytometer (BD Biosciences).

Neutralization assays. Serial dilutions of mAbs were incubated with 10^2 FFU of different JEV strains for 1 h at 37°C as described previously (57). MAb-virus complexes were added to Vero cell monolayers for 1 h at 37°C followed by 1% (wt/vol) methylcellulose in modified Eagle medium (MEM) supplemented with 4% FBS. Plates were fixed and processed as described above. Nonlinear regression analysis was performed, and EC_{50} values were calculated after comparison to wells infected with JEV in the absence of mAb.

Flavivirus E ectodomain and JEV E-DI and JEV E-DIII expression and purification. JEV E protein (residues 1 to 399 corresponding to the E ectodomain of the JEV-SA14-14-2 strain) was prepared as previously described (15). A JEV E-DI synthetic gene was designed based on a DENV-4 DI construct (58) with modifications such that JEV E residues 1 to 50 were linked to residues 135 to 195 by a glycine dipeptide, and residues 135 to 195 were connected by a serine residue to residues 281 to 298. This fragment was cloned into the pFM1.2 mammalian expression vector (59) downstream of a pHLsec signal sequence and terminated with a C-terminal tobacco etch virus (TEV) protease and hexahistidine affinity tag. Transient expression and purification were completed using established protocols (60). JEV E-DIII (residues 299 to 399) was cloned into the NdeI and XhoI restriction enzyme sites of pET21a for expression in BL21(DE3) Codon Plus Escherichia coli cells by autoinduction (61). The protein was refolded from inclusion

168

bodies and purified by size exclusion essentially as described previously (62). WNV (63) and ZIKV (60) E ectodomain proteins were produced and purified based on established protocols.

JEV mAb domain mapping. MaxiSorp 96-well plates (Thermo, Fisher) were coated with 50 μl of 4 μg/ml of recombinant JEV E (15), JEV E-DI, JEV E-DIII, WNV E, or ZIKV E overnight at 4°C. Plates were washed three times with PBS with 0.02% Tween 20 followed by incubation with PBS and 2% bovine serum albumin (BSA) for 1 h at 37°C. MAbs were added (1 μg/ml) for 1 h at room temperature. Plates were washed again and sequentially incubated with biotin-conjugated anti-mouse IgG, streptavidin-HRP, and 3,3', 5,5'-tetramethylbenzidine (TMB) substrate. The reaction was stopped by addition of 2 M H_2SO_4, and emission (450 nm) was read using a TriStar LB 941 reader (Berthold Technologies).

Pre- and postattachment neutralization assays. For preattachment assays, serial dilutions of MAbs were prepared at 4°C in Dulbecco's modified Eagle medium (DMEM) with 2% FBS and preincubated with 10^2 FFU of JEV-SA14-14-2 for 1 h at 4°C. MAb-virus complexes were added to a monolayer of Vero cells for 1 h at 4°C. Unbound virus was removed with three washes of chilled DMEM, and adsorbed virus was allowed to internalize during a 37°C incubation for 1 h. Cells were overlaid with 1% (wt/vol) methylcellulose in MEM supplemented with 4% FBS. For postattachment assays, 10^2 FFU of JEV-SA14-14-2 was adsorbed onto a monolayer of Vero cells for 1 h at 4°C. After removal of unbound virus, serial dilutions of MAbs were added to virus-adsorbed cells for 1 h at 4°C. Virus then was allowed to internalize for 1 h at 37°C, and subsequently cells were overlaid with methylcellulose as described above. Thirty hours later, the plates were fixed with 2% PFA and analyzed for antigen-specific foci as described above.

Fusion blockade assay. The assay for plasma membrane fusion inhibition with flavivirus mAbs was described previously (32–34). Briefly, Vero cells (2 x 10^4 per well) were seeded in flat-bottom 96-well plates overnight at 37°C. The following day, cells were preincubated with 10 nM concanamycin A (Sigma catalog no. C9705), which blocks acidification of endosomes and viral fusion, for 30 min on ice and subsequently incubated with JEV-SA14 (multiplicity of infection [MOI] of 50) for 2 h. Cells were washed twice with chilled PBS followed by incubation with 100 μg/ml (murine) or 50 μg/ml (human) MAbs for 30 min on ice. Cells were pH shifted with warmed DMEM (buffered to pH 5.5 or control pH 7.5) at 37°C for ~7 min. The cells were rinsed and incubated for 24 h at 37°C in DMEM with 10 nM concanamycin A. Subsequently, cells were rinsed, fixed, permeabilized, and sequentially stained for 1 h at 4°C with JEV-13 (1 μg/ml) and goat anti-mouse Alexa Fluor 647-conjugated secondary antibody (1:2,000). Samples were processed by flow cytometry (MacsQuant), and data were analyzed using FlowJo software.

Hydrogen-deuterium exchange. Continuous HDX labeling of JEV E-DIII with or without the mAbs was performed at 25°C for 0, 10, 30, 60, 120, 900, 3,600, and 14,400 s as previously described with the following modifications (64). Briefly, stock solutions of JEV E-DIII both with and without the mAbs were prepared in PBS (pH 7.4) and incubated at 25°C for at least 1 h. Continuous labeling with deuterium was initiated by diluting the stock samples 10-fold in deuterated PBS buffer (Sigma-Aldrich). HDX control samples (nondeuterated) were prepared in the same way with H$_2$O. Quenching was performed under reducing conditions by adding a solution of 500 mM Tris (2-carboxyethyl)phosphine hydrochloride (TCEP HCl) and 4 M guanidine hydrochloride in PBS buffer (pH 7.4 [adjusted using sodium hydroxide]) to the reaction vial at a 1:1 vol/vol ratio. The sample

was mixed and incubated for a minute at 25°C before being loaded onto our custom-built HDX platform for desalting, online pepsin digestion, and reversed-phase separation and directly injected into the mass spectrometer for analysis.

The sample was passed over a custom-packed 2- by 20-mm pepsin column at 200 μl/min; immobilized pepsin was prepared according to a published protocol (65). The peptides resulting from digestion were captured by a 2.1- by 20-mm Zorbax Eclipse XDB-C 8 trap column (Agilent) and desalted at 200 μl/min 1 of H_2O containing 0.1% trifluoroacetic acid for 3 min. The peptides were separated by a 2.1 x 50 mm C_{18} column (2.5- μm XSelect CSH C18; Waters) with a 9.5-min gradient of 5 to 100% acetonitrile in 0.1% formic acid at a flow rate of 100 μl/min delivered by a LEAP 3 x Ti pump (Leap Technologies, NC). The linear part of the gradient from 0.3 min to 5.5 min raised the acetonitrile content from 15% to 50%, during which time most of the peptides eluted from the C_{18} column. The entire fluidic system was kept in an ice bath, except for the pepsin column, to minimize back exchange. Duplicate measurements were carried out for each of the time points.

HDX data analysis and epitope assignment. Acquired spectra were analyzed using HDX workbench software (66) against a peptide set generated as described below. The deuterium level was normalized to the maximum deuterium concentration (80%) contained in the reaction vial. The peptide list used to search the HDX data was identified first by a tandem-MS experiment in a data-dependent mode on a linear trap quadrupole-Fourier transform (LTQ-FT) mass spectrometer (Thermo). The six most abundant ions were submitted to collision-induced dissociation fragmentation. Product-ion spectra were then submitted to MassMatrix (version 2.4.2) for identification (67) and manually inspected, and the validated peptides were used for the HDX analysis. The epitopes were identified as

regions/sequences of amino acids (not single residues) that show a significant difference in HDX for the bound versus unbound states, as determined from the peptide-level HDX-MS data. Criteria for the selection of peptides as potential epitopes are explained further in the Immune Epitope Database (IEDB) submission mentioned below in the "Accession number(s)" section.

Site-directed mutagenesis epitope mapping. Epitope mapping was performed by alanine scanning mutagenesis as described previously (36). A JEV prM-E protein expression construct (based on JEV-SA14-14-2) was subjected to commercial alanine-scanning mutagenesis (Genewiz) to generate a mutant library. Each residue within the JEV E protein was changed to alanine, with alanine codons mutated to serine and cysteine residues left unchanged. In total, 400 mutants were generated and sequence confirmed. Each JEV E protein mutant was transfected into human 293T cells and allowed to express for 24 h and then fixed and permeabilized with Foxp3 transcription factor staining buffer (Thermo catalog no. 00-5523-00). Cells were incubated sequentially with purified MAbs at concentrations optimized for staining (range, 30 to 1,000 ng/ml) and Alexa Fluor 647-conjugated secondary antibody (Invitrogen) in permeabilization buffer. Fluorescence signal was detected by flow cytometry (MacsQuant) and analyzed using FlowJo software. Antibody reactivity against each mutant was compared to that of the WT prM-E protein after subtracting the signal from mock-transfected controls and normalizing to the signal from WT prM-E transfected controls. Mutations were identified as critical to the MAb epitope if the mutants showed less than 25% binding compared to the wild type. For charge mutants, we substituted residues in the A strand (S309K, K312E, and H395K), DIII-LR

(S331K, S364K, N367K, and K369E), C-C' loop (T349K), and FG loop (R387E and D389K) and transfected and stained as described above.

Mouse experiments. Animal studies were carried in accordance with the recommendations of the Guide for the Care and Use of Laboratory Animals of the National Institutes of Health and were approved by the Institutional Animal Care and Use Committee at the Washington University School of Medicine (assurance no. A3381-01). Mice were inoculated with JEV after induction of anesthesia using ketamine hydrochloride and xylazine, and all efforts were made to minimize pain and suffering. Antibody protection studies were performed according to the models described below.

(i) **Genotype I.** WT C57BL/6 male mice (3 weeks old; Jackson Laboratories) were inoculated with 10^3 FFU of JEV-MAR 859 or JEV-2372/79 subcutaneously in the footpad. Anti-JEV or isotype control (CHK-152) mAbs were administered intraperitoneally as a single dose on day 1 (10 μg, 0.5 mg/kg) or day 5 (250 μg, 12.5 mg/kg) after infection. Animals were monitored for lethality for 28 days.

(ii) **Genotype III.** WT C57BL/6 male mice (4 to 5 weeks old; Jackson Laboratories) were inoculated with 10^2 FFU of JEV-Nakayama subcutaneously in the footpad. Anti-JEV or isotype control (CHK-152) mAbs were administered intraperitoneally as a single dose on day 1 (10 μg, 0.5 mg/kg) or day 5 (250 μg, 12.5 mg/kg) after infection. Animals were monitored for lethality for 28 days.

Statistical analysis. Statistical significance of FFWO was determined by one-way ANOVA with Dunnett's multiple comparisons to an isotype control mAb. Statistical significance of alanine shotgun mutagenesis was determined by one-way ANOVA with Holm-Sidak's multiple comparisons of each mutant to V315 for each MAb. Kaplan-Meier

survival curves were analyzed by the log rank test for each mAb compared to an isotype control mAb.

Accession number(s). The epitopes of the five JEV-specific mAbs (E31, E106, E128, E131, and E143) have been deposited in the Immune Epitope Database (IEDB) under submission no. 1000721.

5.6   Acknowledgments

5.7 References

1. Campbell GL, Hills SL, Fischer M, Jacobson JA, Hoke CH, Hombach JM, Marfin A, Solomon T, Tsai TF, Tsu VD, Ginsburg AS. 2011. Estimated global incidence of Japanese encephalitis: a systematic review. Bull World Health Organ 89:766 –774E.
2. WHO. 2017. Japanese encephalitis. Fact sheet no. 386. WHO, Geneva, Switzerland.
3. Vaughn DW, Hoke CH. 1992. The epidemiology of Japanese encephalitis: prospects for prevention. Epidemiol Rev 14:197–221.
4. Wang H, Liang G. 2015. Epidemiology of Japanese encephalitis: past, present, and future prospects. Ther Clin Risk Manag 11:435– 448.
5. Burke DS, Tingpalapong M, Ward GS, Andre R, Leake CJ. 1985. Intense transmission of Japanese encephalitis virus to pigs in a region free of epidemic encephalitis. Southeast Asian J Trop Med Public Health 16: 199 –206.
6. Hammon WM, Tigertt WD. 1949. Isolations of Japanese B encephalitis virus from naturally infected Culex tritaeniorhynchus collected in Japan. Am J Hyg 50:51–56.
7. WHO. 2015. Japanese encephalitis vaccines: WHO position paper— February 2015. Wkly Epidemiol Rec 90:69 – 87.
8. Borah J, Dutta P, Khan SAA, Mahanta J. 2011. A comparison of clinical features of Japanese encephalitis virus infection in the adult and pediatric age group with acute encephalitis syndrome. J Clin Virol 52:45– 49.
9. Halstead SB, Solomon T. 2010. Japanese encephalitis, p 317–333. In Artenstein AW (ed), Vaccines: a biography. Springer New York, NY.
10. Solomon T, Dung NM, Kneen R, Gainsborough M, Vaughn DW, Khanh VT. 2000. Japanese encephalitis. J Neurol Neurosurg Psychiatry 68:405– 415. https://doi.org/10.1136/jnnp.68.4.405.
11. Solomon T, Kneen R, Dung NM, Khanh VC, Thuy TT, Ha DQ, Day NP, Nisalak A, Vaughn DW, White NJ. 1998. Poliomyelitis-like illness due to Japanese encephalitis virus. Lancet 351:1094 –1097.
12. Chen KM, Tsai HC, Sy CL, Lee SS, Liu YC, Wann SR, Wang YH, Mai MH, Chen JK, Wu KS, Chen YJ, Chen YS. 2009. Clinical manifestations of Japanese encephalitis in southern Taiwan. J Microbiol Immunol Infect 42:296 –302.
13. Roehrig JT, Johnson AJ, Hunt AR, Bolin RA, Chu MC. 1990. Antibodies to dengue 2 virus E-glycoprotein synthetic peptides identify antigenic conformation. Virology 177:668 – 675.
14. Rey FA, Heinz FX, Mandl C, Kunz C, Harrison SC. 1995. The envelope glycoprotein from tick-borne encephalitis virus at 2 A resolution. Nature 375:291–298.
15. Luca VC, AbiMansour J, Nelson CA, Fremont DH. 2012. Crystal structure of the Japanese encephalitis virus envelope protein. J Virol 86: 2337–2346.
16. Mohammed MA, Galbraith SE, Radford AD, Dove W, Takasaki T, Kurane I, Solomon T. 2011. Molecular phylogenetic and evolutionary analyses of Muar strain of Japanese encephalitis virus reveal it is the missing fifth genotype. Infect Genet Evol 11:855–862.
17. Uchil PD, Satchidanandam V. 2001. Phylogenetic analysis of Japanese encephalitis virus: envelope gene based analysis reveals a fifth genotype, geographic clustering, and multiple introductions of the virus into the Indian subcontinent. Am J Trop Med Hyg 65:242–251.

18.	Takhampunya R, Kim HC, Tippayachai B, Kengluecha A, Klein TA, Lee WJ, Grieco J, Evans BP. 2011. Emergence of Japanese encephalitis virus genotype V in the Republic of Korea. Virol J 8:449.
19.	Chen WR, Tesh RB, Rico-Hesse R. 1990. Genetic variation of Japanese encephalitis virus in nature. J Gen Virol 71:2915–2922.
20.	Chen WR, Rico-Hesse R, Tesh RB. 1992. A new genotype of Japanese encephalitis virus from Indonesia. Am J Trop Med Hyg 47:61– 69.
21.	Schuh AJ, Ward MJ, Brown AJ, Barrett ADT. 2013. Phylogeography of Japanese encephalitis virus: genotype is associated with climate. PLoS Negl Trop Dis 7:e2411.
22.	Wang HY, Takasaki T, Fu SH, Sun XH, Zhang HL, Wang ZX, Hao ZY, Zhang JK, Tang Q, Kotaki A, Tajima S, Liang XF, Yang WZ, Kurane I, Liang GD. 2007. Molecular epidemiological analysis of Japanese encephalitis virus in China. J Gen Virol 88:885–894.
23.	Ma SP, Yoshida Y, Makino Y, Tadano M, Ono T, Ogawa M. 2003. Short report: a major genotype of Japanese encephalitis virus currently circulating in Japan. Am J Trop Med Hyg 69:151–154.
24.	Plotkin SA. 2010. Correlates of protection induced by vaccination. Clin Vaccine Immunol 17:1055–1065.
25.	Kimura-Kuroda J, Yasui K. 1986. Antigenic comparison of envelope protein E between Japanese encephalitis virus and some other flaviviruses using monoclonal antibodies. J Gen Virol 67:2663–2672.
26.	Kimura-Kuroda J, Yasui K. 1988. Protection of mice against Japanese encephalitis virus by passive administration with monoclonal antibodies. J Immunol 141:3606 –3610.
27.	Mason PW, Dalrymple JM, Gentry MK, McCown JM, Hoke CH, Burke DS, Fournier MJ, Mason TL. 1989. Molecular characterization of a neutralizing domain of the Japanese encephalitis virus structural glycoprotein. J Gen Virol 70:2037–2049.
28.	Lin CW, Wu SC. 2003. A functional epitope determinant on domain III of the Japanese encephalitis virus envelope protein interacted with neutralizing-antibody combining sites. J Virol 77:2600 –2606.
29.	Goncalvez AP, Chien CH, Tubthong K, Gorshkova I, Roll C, Donau O, Schuck P, Yoksan S, Wang SD, Purcell RH, Lai CJ. 2008. Humanized monoclonal antibodies derived from chimpanzee Fabs protect against Japanese encephalitis virus in vitro and in vivo. J Virol 82:7009 –7021.
30.	Zhang MJ, Wang MJ, Jiang SZ, Ma WY. 1989. Passive protection of mice, goats, and monkeys against Japanese encephalitis with monoclonal antibodies. J Med Virol 29:133–138.
31.	Pierson TC, Diamond MS. 2008. Molecular mechanisms of antibodymediated neutralisation of flavivirus infection. Expert Rev Mol Med 10:e12.
32.	Pal P, Dowd KA, Brien JD, Edeling MA, Gorlatov S, Johnson S, Lee I, Akahata W, Nabel GJ, Richter MKS, Smit JM, Fremont DH, Pierson TC, Heise MT, Diamond MS. 2013. Development of a highly protective combination monoclonal antibody therapy against Chikungunya virus. PLoS Pathog 9:e1003312.
33.	Thompson BS, Moesker B, Smit JM, Wilschut J, Diamond MS, Fremont DH. 2009. A therapeutic antibody against West Nile virus neutralizes infection by blocking fusion within endosomes. PLoS Pathog 5:e1000453.

34. Liao M, Kielian M. 2005. Domain III from class II fusion proteins functions as a dominant negative inhibitor of virus membrane fusion. J Cell Biol 171:111–120.

35. Chen E, Salinas ND, Huang Y, Ntumngia F, Plasencia MD, Gross ML, Adams JH, Tolia NH. 2016. Broadly neutralizing epitopes in the Plasmodium vivax vaccine candidate Duffy binding protein. Proc Natl Acad Sci U S A 113:6277– 6282.

36. Davidson E, Doranz BJ. 2014. A high-throughput shotgun mutagenesis approach to mapping B-cell antibody epitopes. Immunology 143:13–20.

37. Nybakken GE, Oliphant T, Johnson S, Burke S, Diamond MS, Fremont DH. 2005. Structural basis of West Nile virus neutralization by a therapeutic antibody. Nature 437:764 –769.

38. Oliphant T, Nybakken GE, Engle M, Xu Q, Nelson CA, Sukupolvi-Petty S, Marri A, Lachmi BE, Olshevsky U, Fremont DH, Pierson TC, Diamond MS. 2006. Antibody recognition and neutralization determinants on domains I and II of West Nile virus envelope protein. J Virol 80:12149 –12159.

39. Sukupolvi-Petty S, Austin SK, Purtha WE, Oliphant T, Nybakken GE, Schlesinger JJ, Roehrig JT, Gromowski GD, Barrett AD, Fremont DH, Diamond MS. 2007. Type- and subcomplex-specific neutralizing antibodies against domain III of dengue virus type 2 envelope protein recognize adjacent epitopes. J Virol 81:12816 –12826.

40. Beltramello M, Williams KL, Simmons CP, Macagno A, Simonelli L, Quyen NT, Sukupolvi-Petty S, Navarro-Sanchez E, Young PR, de Silva AM, Rey FA, Varani L, Whitehead SS, Diamond MS, Harris E, Lanzavecchia A, Sallusto F. 2010. The human immune response to dengue virus is dominated by highly cross-reactive antibodies endowed with neutralizing and enhancing activity. Cell Host Microbe 8:271–283.

41. Jarmer J, Zlatkovic J, Tsouchnikas G, Vratskikh O, Strauß J, Aberle JH, Chmelik V, Kundi M, Stiasny K, Heinz FX. 2014. Variation of the specificity of the human antibody responses after tick-borne encephalitis virus infection and vaccination. J Virol 88:13845–

42. Smith SA, de Alwis AR, Kose N, Harris E, Ibarra KD, Kahle KM, Pfaff JM, Xiang X, Doranz BJ, de Silva AM, Austin SK, Sukupolvi-Petty S, Diamond MS, Crowe JE. 2013. The potent and broadly neutralizing human dengue virus-specific monoclonal antibody 1C19 reveals a unique cross-reactive epitope on the bc loop of domain II of the envelope protein. mBio 4:e00873-13.

43. Robbiani DF, Bozzacco L, Keeffe JR, Khouri R, Olsen PC, Gazumyan A, Schaefer-Babajew D, Avila-Rios S, Nogueira L, Patel R, Azzopardi SA, Uhl LFK, Saeed M, Sevilla-Reyes EE, Agudelo M, Yao KH, Golijanin J, Gristick HB, Lee YE, Hurley A, Caskey M, Pai J, Oliveira T, Wunder EA, Sacramento G, Nery N, Orge C, Costa F, Reis MG, Thomas NM, Eisenreich T, Weinberger DM, de Almeida ARP, West AP, Rice CM, Bjorkman PJ, Reyes-Teran G, Ko AI, MacDonald MR, Nussenzweig MC. 2017. Recurrent potent human neutralizing antibodies to Zika virus in Brazil and Mexico. Cell 169:597– 609.e11.

44. Throsby M, Geuijen C, Goudsmit J, Bakker AQ, Korimbocus J, Kramer RA, Clijsters-van der Horst M, de Jong M, Jongeneelen M, Thijsse S, Smit R, Visser TJ, Bijl N, Marissen WE, Loeb M, Kelvin DJ, Preiser W, ter Meulen J, de Kruif J. 2006. Isolation and characterization of human monoclonal antibodies from individuals infected with West Nile virus. J Virol 80: 6982– 6992.

45. Vratskikh O, Stiasny K, Zlatkovic J, Tsouchnikas G, Jarmer J, Karrer U, Roggendorf M, Roggendorf H, Allwinn R, Heinz FX. 2013. Dissection of antibody specificities induced by yellow fever vaccination. PLoS Pathog 9:e1003458.

46. Wahala WM, Kraus AA, Haymore LB, Accavitti-Loper MA, de Silva AM. 2009. Dengue virus neutralization by human immune serums: role of envelope protein domain III-reactive antibody. Virology 392:103–113. https://doi.org/10.1016/j.virol.2009.06.037.

47. Kimura-Kuroda J, Yasui K. 1983. Topographical analysis of antigenic determinants on envelope glycoprotein V3 (E) of Japanese encephalitis virus, using monoclonal antibodies. J Virol 45:124 –132.

48. Shimoda H, Mahmoud HY, Noguchi K, Terada Y, Takasaki T, Shimojima M, Maeda K. 2013. Production and characterization of monoclonal antibodies to Japanese encephalitis virus. J Vet Med Sci 75:1077–1080.

49. Brien JD, Austin SK, Sukupolvi-Petty S, O'Brien KM, Johnson S, Fremont DH, Diamond MS. 2010. Genotype-specific neutralization and protection by antibodies against dengue virus type 3. J Virol 84:10630 –10643.

50. Wahala WM, Donaldson EF, de Alwis R, Accavitti-Loper MA, Baric RS, de Silva AM. 2010. Natural strain variation and antibody neutralization of dengue serotype 3 viruses. PLoS Pathog 6:e1000821.

51. Schuh AJ, Li L, Tesh RB, Innis BL, Barrett ADT. 2010. Genetic characterization of early isolates of Japanese encephalitis virus: genotype II has been circulating since at least 1951. J Gen Virol 91:95–102.

52. Austin SK, Dowd KA, Shrestha B, Nelson CA, Edeling MA, Johnson S, Pierson TC, Diamond MS, Fremont DH. 2012. Structural basis of differential neutralization of DENV-1 genotypes by an antibody that recognizes a cryptic epitope. PLoS Pathog 8:e1002930.

53. Goo L, VanBlargan LA, Dowd KA, Diamond MS, Pierson TC. 2017. A single mutation in the envelope protein modulates flavivirus antigenicity, stability, and pathogenesis. PLoS Pathog 13:e1006178.

54. Oliphant T, Engle M, Nybakken GE, Doane C, Johnson S, Huang L, Gorlatov S, Mehlhop E, Marri A, Chung KM, Ebel GD, Kramer LD, Fremont DH, Diamond MS. 2005. Development of a humanized monoclonal antibody with therapeutic potential against West Nile virus. Nat Med 11:522–530.

55. Shrestha B, Brien JD, Sukupolvi-Petty S, Austin SK, Edeling MA, Kim T, O'Brien KM, Nelson CA, Johnson S, Fremont DH, Diamond MS. 2010. The development of therapeutic antibodies that neutralize homologous and heterologous genotypes of dengue virus type 1. PLoS Pathog 6:e1000823.

56. Stiasny K, Brandler S, Kössl C, Heinz FX. 2007. Probing the flavivirus membrane fusion mechanism by using monoclonal antibodies. J Virol 81:11526 –11531.

57. Brien JD, Lazear HM, Diamond MS. 2013. Propagation, quantification, detection, and storage of West Nile virus. Curr Protoc Microbiol 31: 15D.3.1–15D.3.18.

58. Cockburn JJ, Navarro Sanchez ME, Goncalvez AP, Zaitseva E, Stura EA, Kikuti CM, Duquerroy S, Dussart P, Chernomordik LV, Lai CJ, Rey FA. 2012. Structural insights into the neutralization mechanism of a higher primate antibody against dengue virus. EMBO J 31:767–779.

59. Mancia F, Patel SD, Rajala MW, Scherer PE, Nemes A, Schieren I, Hendrickson WA, Shapiro L. 2004. Optimization of protein production in mammalian cells with a coexpressed fluorescent marker. Structure 12: 1355–1360.

60.   Zhao H, Fernandez E, Dowd KA, Speer SD, Platt DJ, Gorman MJ, Govero J, Nelson CA, Pierson TC, Diamond MS, Fremont DH. 2016. Structural basis of Zika virus-specific antibody protection. Cell 166:1016 –1027.
61.   Studier FW. 2005. Protein production by auto-induction in high density shaking cultures. Protein Expr Purif 41:207–234.
62.   Edeling MA, Austin SK, Shrestha B, Dowd KA, Mukherjee S, Nelson CA, Johnson S, Mabila MN, Christian EA, Rucker J, Pierson TC, Diamond MS, Fremont DH. 2014. Potent dengue virus neutralization by a therapeutic antibody with low monovalent affinity requires bivalent engagement. PLoS Pathog 10:e1004072.
63.   Nybakken GE, Nelson CA, Chen BR, Diamond MS, Fremont DH. 2006. Crystal structure of the West Nile virus envelope glycoprotein. J Virol 80:11467–11474.
64.   Yan Y, Grant GA, Gross ML. 2015. Hydrogen-deuterium exchange mass spectrometry reveals unique conformational and chemical transformations occurring upon [4Fe-4S] cluster binding in the type 2 L-serine dehydratase from Legionella pneumophila. Biochemistry 54:5322–5328.
65.   Busby SA, Chalmers MJ, Griffin PR. 2007. Improving digestion efficiency under H/D exchange conditions with activated pepsinogen coupled columns. Int J Mass Spectrom 259:130 –139.
66.   Pascal BD, Willis S, Lauer JL, Landgraf RR, West GM, Marciano D, Novick S, Goswami D, Chalmers MJ, Griffin PR. 2012. HDXWorkbench: software for the analysis of H/D exchange MS data. J Am Soc Mass Spectrom 23:1512–1521.
67.   Xu H, Freitas MA. 2009. MassMatrix: a database search program for rapid characterization of proteins and peptides from tandem mass spectrometry data. Proteomics 9:1548 –1555.

Table 5.1: Binding and neutralization of inhibitory anti-JEV mAbs

Mab	Isotype[a]	Domain[a]	Cross-reactivity[a]	FRNT$_{50}$ (ng/ml)[b]						
				GI			**GIII**			
				2372/79	**MAR 859**	**GII, Bennett**	**Nakayama**	**SA14**	**SA14-14-2**	**GIV, JKT 7887**
Mouse										
JEV-27	IgG2c	DIII	N	4,830	4,053	3,846	2,332	1,441	1,779	2,433
JEV-31	IgG2c	DIII	W	365	272	241	223	94	84	211
JEV-106	IgG2c	DIII	N	449	500	548	334	147	199	270
JEV-117	IgG2c	N	W	>10,000	>10,000	>10,000	>10,000	>10,000	11	>10,000
JEV-128	IgG2c	DIII	N	1,629	561	276	267	189	102	555
JEV-131	IgG2c	DIII	N	509	336	263	409	207	95	815
JEV-143	IgG2c	DIII	Z	435	405	358	346	368	379	818
JEV-169	IgG2c	DI	N	69	80	88	112	148	49	315
Human										
hJEV-11	hIgG1, κ	DIII	W	5,445	1,509	4,116	>10,000	4,528	2,226	>10,000
hJEV-69	hIgG1, κ	DIII	N	1,102	335	524	2,444	475	211	3,111
hJEV-75	hIgG1, λ	N	N	457	228	388	294	414	9	>10,000
hJEV-80	hIgG1, λ	DIII	W	3,371	1,117	1,036	>10,000	857	1,007	7,733

[a]Immunoglobulin isotype, domain specificity, and cross-reactivity to WNV (W) and ZIKV (Z) were determined by ELISA. "N" indicates no binding to either WNV (W) or ZIKV (Z) recombinant E protein or JEV E protein domains.
[b]Purified MAb was incubated with 10² FFU of the indicated JEV strain of genotypes GI to GIV for 1 h at 37°C. Fifty percent FRNT (FRNT$_{50}$) values were determined by nonlinear regression. Results are the average from three independent experiments performed in triplicate.
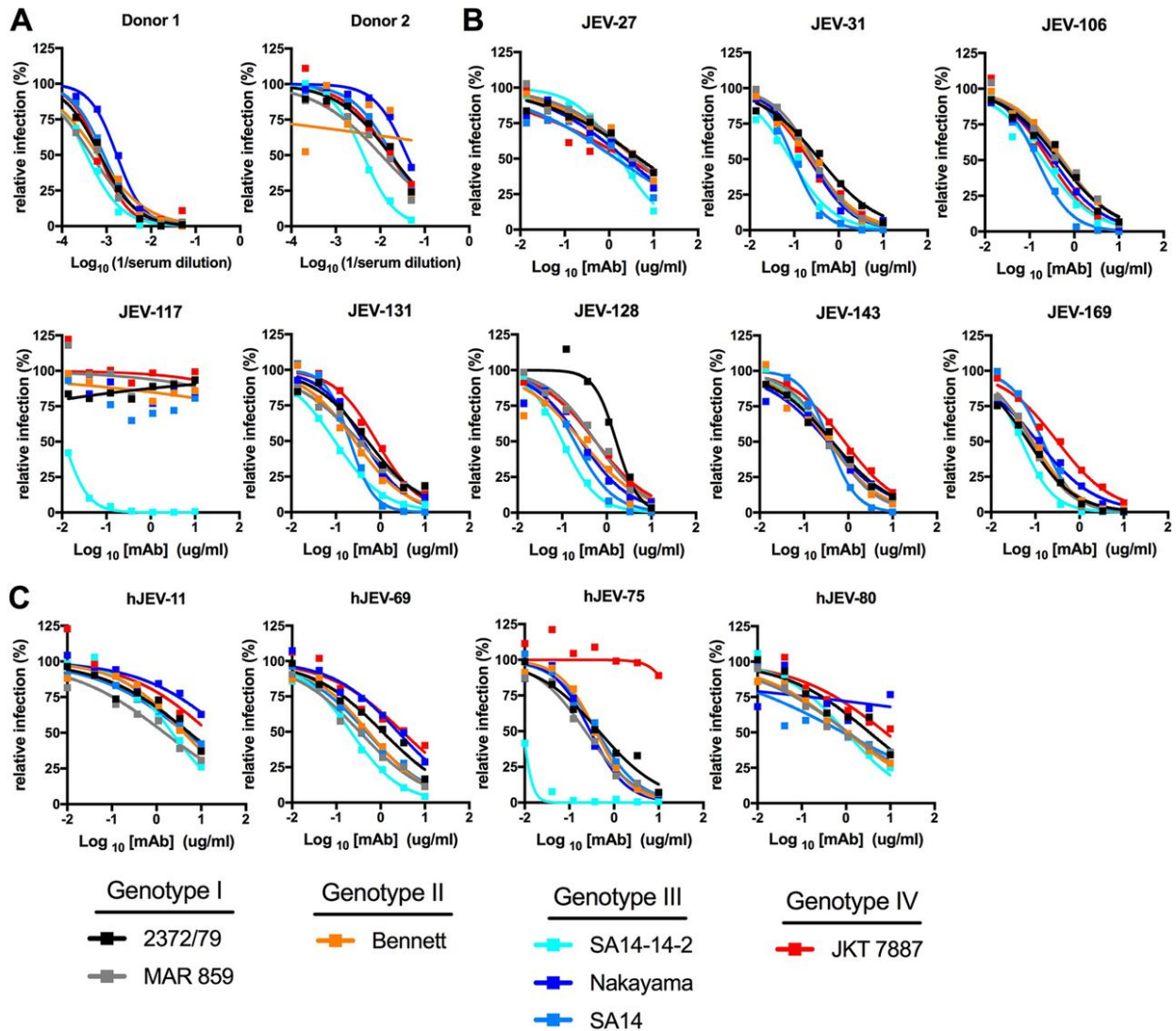
Figure 5.1: Neutralization activity of anti-JEV mAbs.

(A) Serum samples from humans previously immunized against JEV with an inactivated virion vaccine were tested against a panel of JEV strains (2372/79 [GI], MAR 859 [GI], Bennett [GII], SA14 [GIII], SA14-14-2 [GIII], Nakayama [GIII], and JKT 7887 [GIV]) by focus-forming assay (FFA) for neutralization activity. Serial serum dilutions were incubated with 10^2 FFU for 1 h at 37°C, and Vero cells were subsequently infected and stained. **(B)** Neutralization curves of eight mouse anti-JEV mAbs (JEV-27, JEV-31, JEV-106, JEV-117, JEV-131, JEV-128, JEV-143, and JEV-169) against the indicated strains. **(C)** Neutralization curves of human-derived anti-JEV mAbs (hJEV-11, hJEV-69, hJEV-75, and hJEV-80) against the indicated strains. All data are representative of three independent experiments performed in triplicate.
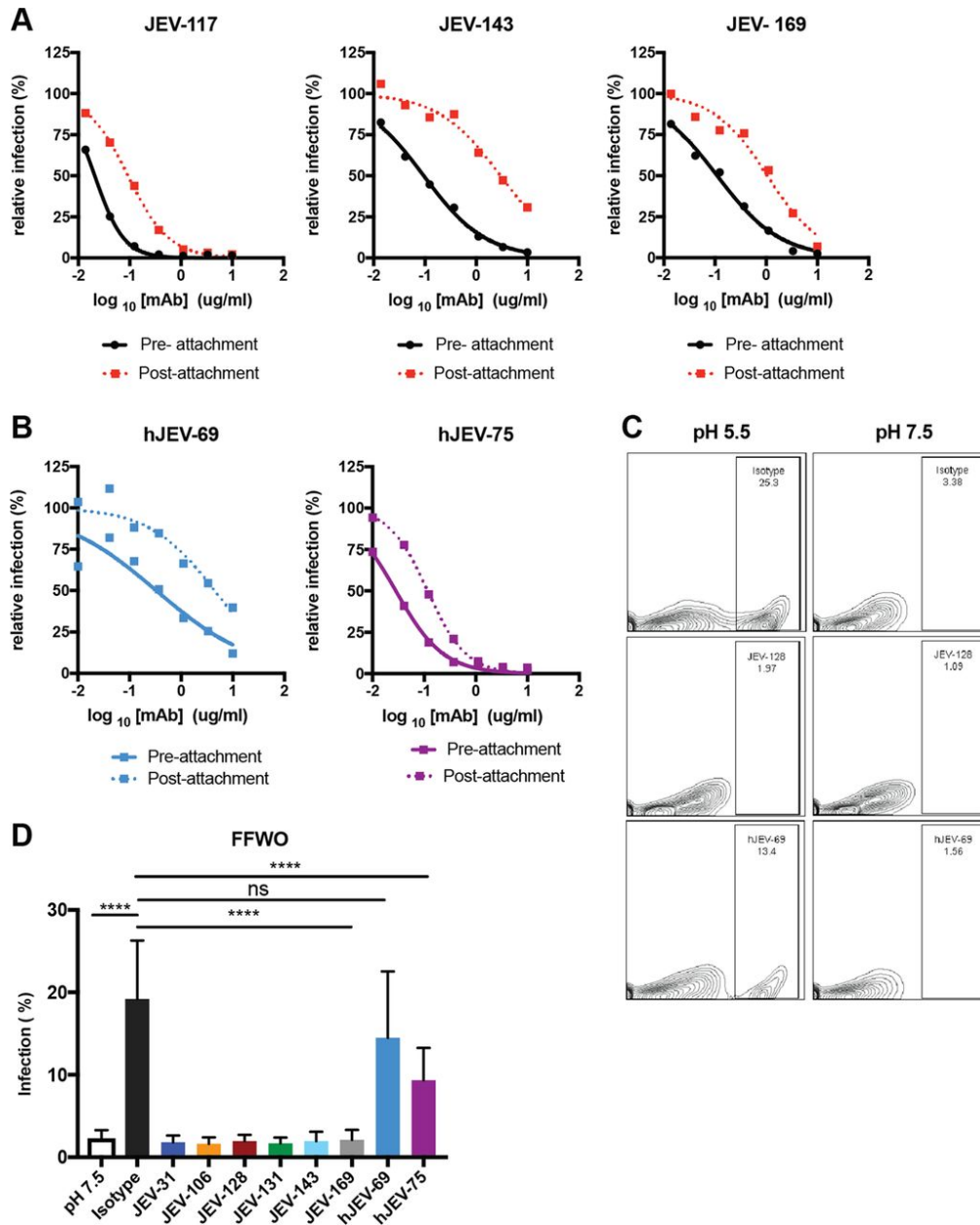
Figure 5.2: Mechanism of neutralization by anti-JEV mAbs.

(A and B) The preattachment inhibition assay (solid lines) was performed by incubating 10^2 FFU of JEV-SA14-14-2 with serial dilutions of mAbs starting at 10 µg/ml for 1 h at 4°C before addition to prechilled Vero cells at 4°C and subsequently following the FFA protocol. The postattachment assay (dashed lines) was performed by adding 10^2 FFU of JEV-SA14-14-2 to cells for 1 h at 4°C. After extensive washing to remove unbound virus, serial dilutions of mAbs were added, starting at 10 µg/ml, and incubated for 1 h at 4°C, and the FFA then was completed at 37°C. Data are representative of three experiments performed in triplicate. **(C)** The fusion-from-without (FFWO) assay was performed after incubating Vero cells at 4°C with JEV-SA14 (MOI of 50) for 2 h. For these experiments, we used JEV-SA14 instead of JEV-SA14-14-

2 because it could be grown to a higher titer. Cells were washed extensively, and the indicated mAbs were added for 30 min. Plasma membrane fusion was induced by exposing the cells briefly (~7 min) to an acidic pH buffer. After pH normalization, cells were incubated with 10 nM concanamycin for 24 h to inhibit infection via the endosomal pathway and collected, fixed, permeabilized, and stained for E protein expression. The treatment and percentage of positive cells are shown. **(D)** The data are pooled from three independent experiments, each performed in triplicate, with error bars (standard deviation) and were analyzed using one-way ANOVA with Dunnett's multiple comparisons to the isotype control condition. ****, $P < 0.0001$; ns, not significant.
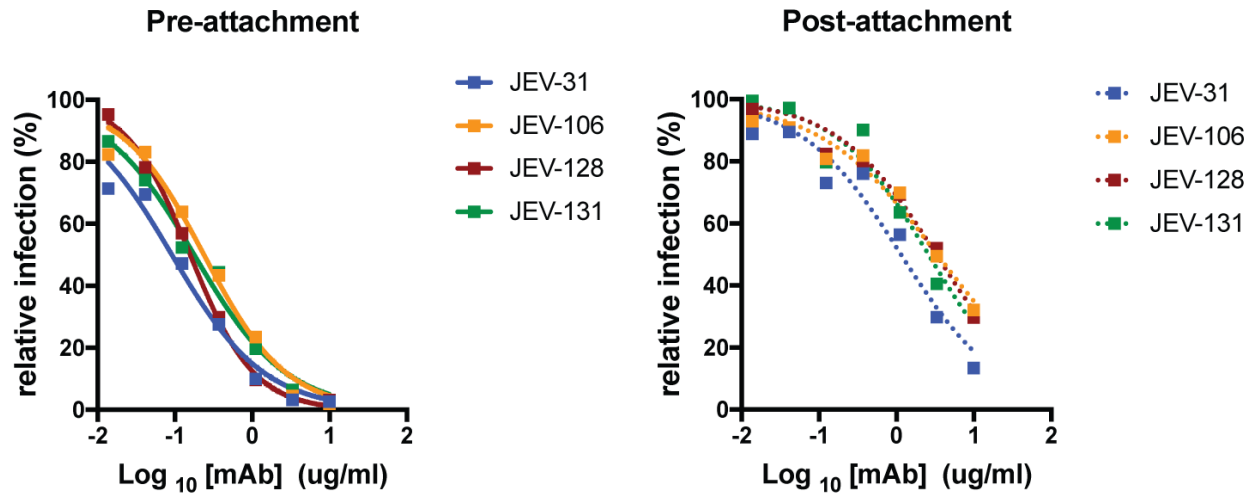
Figure 5.3: Mechanism of neutralization by JEV neutralizing mAbs.

Shown are the pre- and postattachment assays for mouse MAbs (JEV-31, JEV-106, JEV-128, and JEV-131) against JEV-SA14-14-2, as described in **Figure 2.** Data are representative of three experiments, each performed in triplicate.
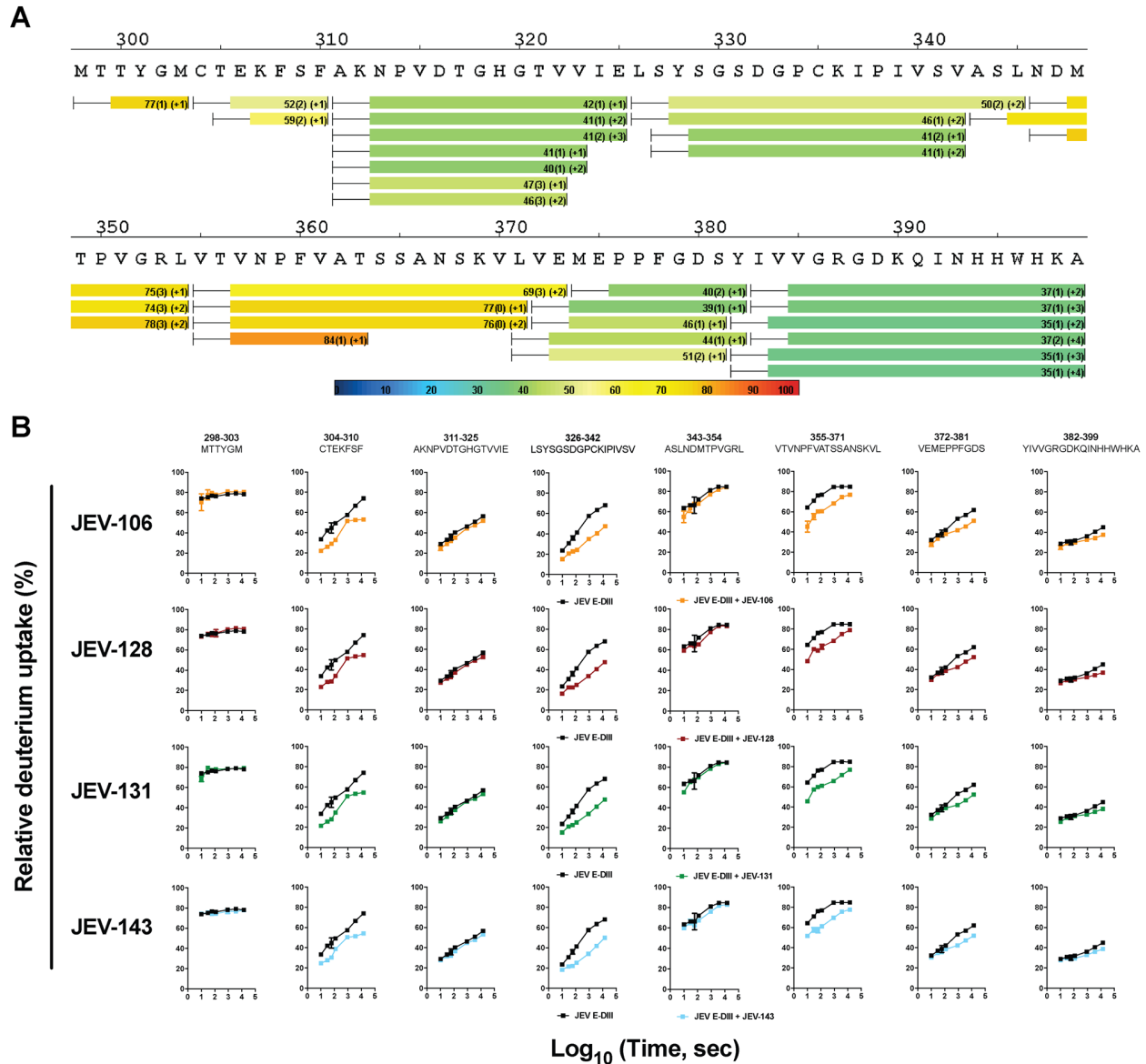
Figure 5.4: Sequence coverage map of peptic digestion of JEV E-DIII.

(A) A total of 32 peptides were identified with complete sequence coverage for JEV E-DIII. Each bar indicates a peptide identified by mass spectrometry. The colored bars represent the average deuterium uptake percentage (D%) for the duplicate analysis of seven exchange time points. (The warmer the color, the higher the deuterium uptake is.) The deuterium uptake percentages for the duplicate analyses are indicated inside the bars, along with the standard deviation and the charge states of the peptide in parentheses. **(B)** Comparison of the kinetics of HDX for eight different peptides covering the entire E-DIII in the absence (E-DIII alone, black lines) or presence (E-DIII plus mAbs) of various mAbs (colored lines). Each region (column) is represented by a peptic peptide, as measured by mass spectrometry. Each row represents a state bound with a mAb (JEV-106, orange; JEV-128, maroon; JEV-131, green; JEV-143, light blue); the antibody is listed on the left. Regions showing reduced rates of exchange for the sample of E-DIII with MAbs (non-black lines) are considered to contain the epitopes. Regions with no difference are examples of regions that do not contain the epitopes and can be viewed as controls.

185
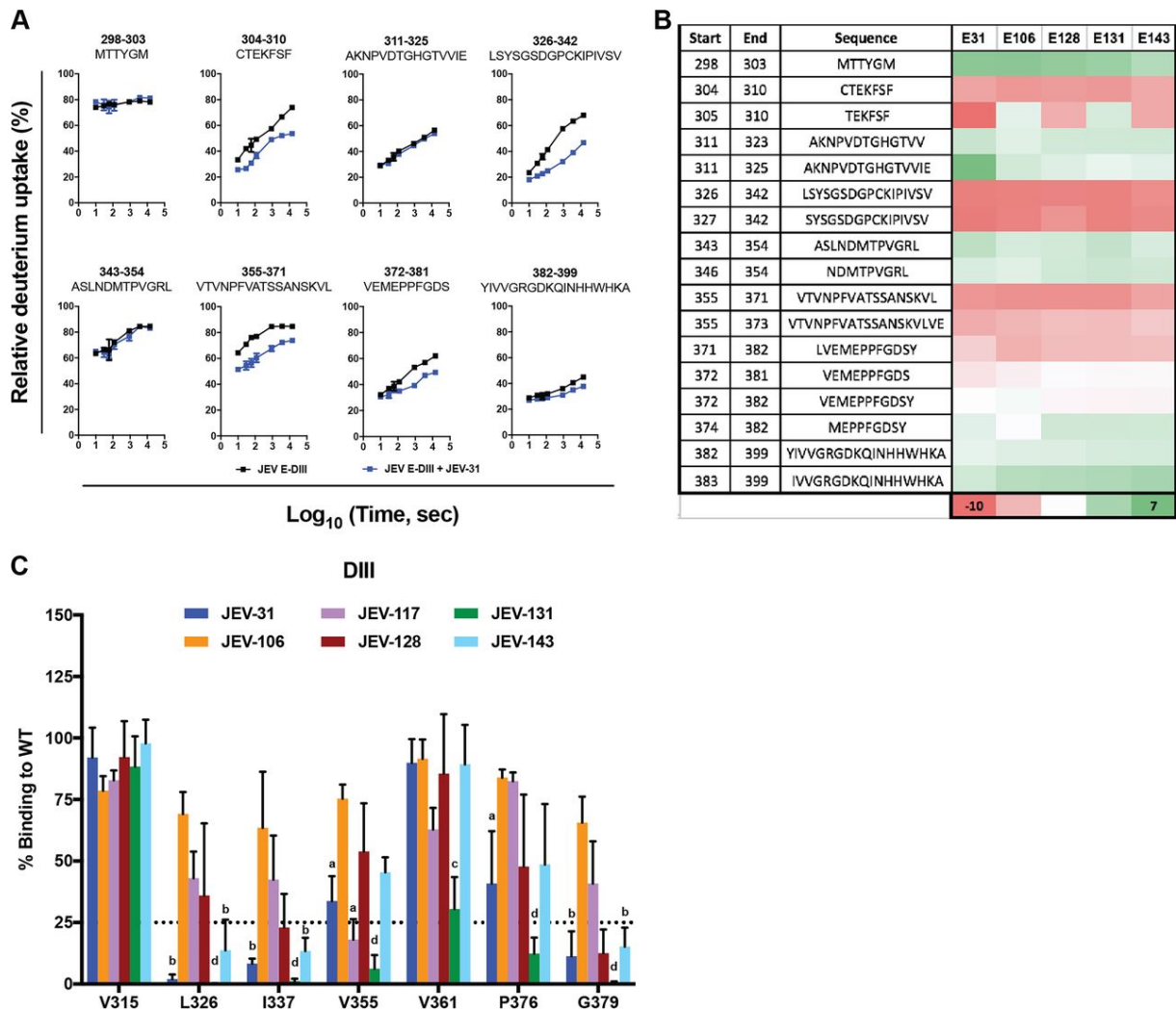
Figure 5.5: Epitope mapping by hydrogen-deuterium exchange and alanine-scanning mutagenesis.

(A) Representative HDX kinetic plots for eight different peptides spanning JEV E-DIII in the presence (blue lines) or absence (black lines) of JEV-31. Regions showing reduced rates or extents of exchange are considered to contain the binding epitopes. All experiments were performed in duplicate, and data are representative of two independent experiments. **(B)** Heat map depicting the average difference of deuterium incorporation between E-DIII alone and the corresponding E-DIII-mAb complex states across all seven time points (ΔD%). Negative values of ΔD% indicate less deuterium incorporation in the DIII-mAb state. The regions with significant protection are shown in red. Peptides with no or little change in deuterium uptake are indicated by white and green. **(C)** Representative alanine-scanning mutagenesis. 293T cells were transfected with 1 μg of the indicated plasmid and incubated overnight prior to fixation, permeabilization, and staining with JEV-31, JEV-106, JEV-117, JEV-128, JEV-131, and JEV-143. Loss of binding was detected by flow cytometry. Data are representative of three independent experiments, with error bars (standard error of the mean [SEM]) and were analyzed by one-way ANOVA with Holm-Sidak's multiple comparisons of each mutant compared to V315 for each mAb. Superscript letters indicate significance: a, $P < 0.05$; b, $P < 0.01$; c, $P < 0.001$; d, $P < 0.0001$.
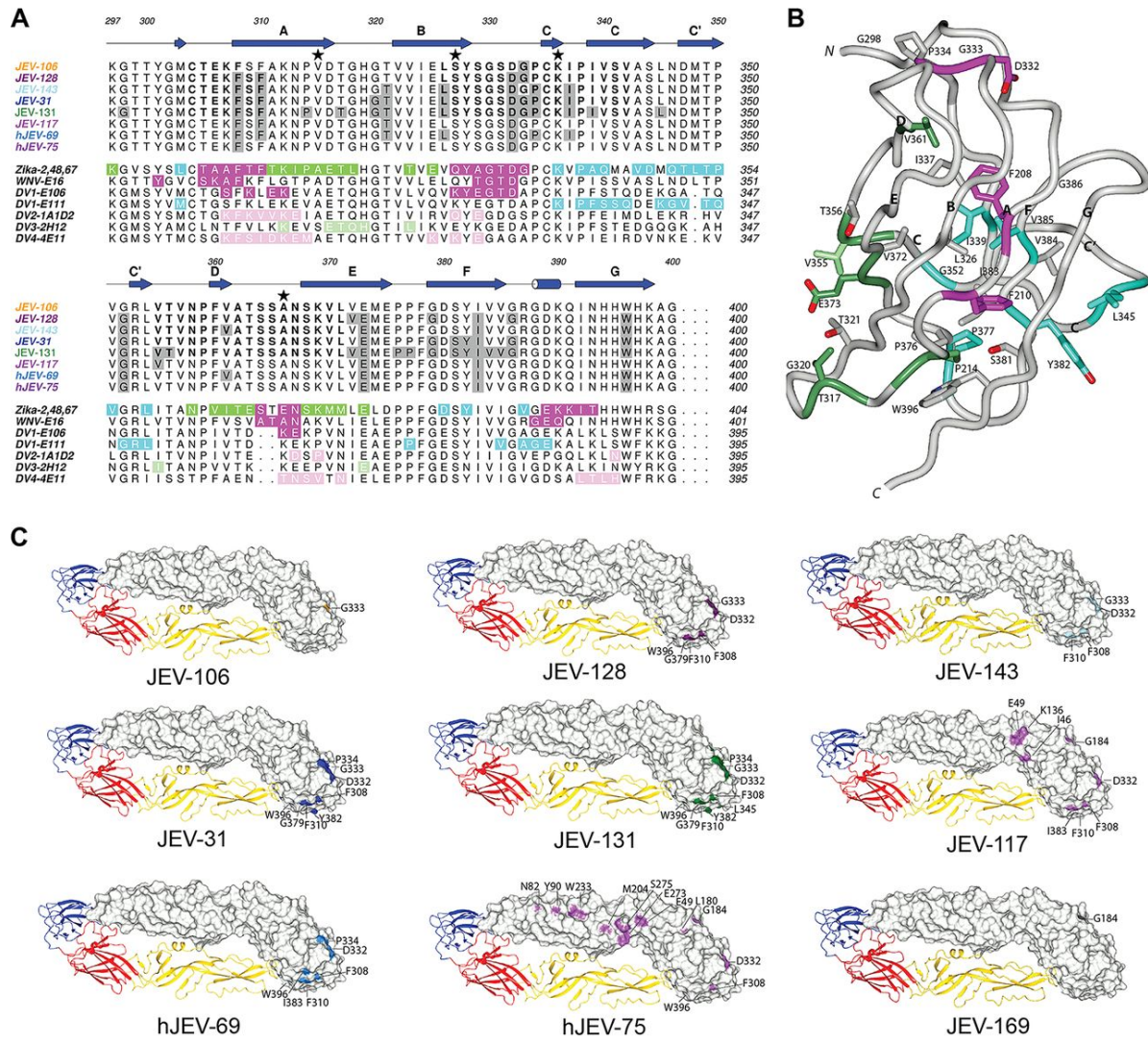
Figure 5.6: Structural representation of JEV E epitopes defined by alanine-scanning mutagenesis and HDX.

(A) JEV E-DIII epitopes for each of the eight mouse and human JEV mAbs were defined by alanine-scanning mutagenesis (shaded gray boxes) and HDX (boldface letters). Genotypic differences from the JEV-SA14-14-2 strain (GIII) are highlighted by a star: V315 is A in the JEV-2372/79 (GI), JEV-MAR 859 (GI), JEV-Bennett (GII), and JEV-Nakayama (GIII) strains; S327 is T in the JEV-2372/79 (GI), JEV-MAR 859 (GI), and JEV-Bennett (GIII) strains; K336 is N in the JEV-2372/79 (GI) and JEV-MAR 859 (GI) strains; and A366 is S in the JEV-2372/79 (GI), JEV-MAR 859 (GI), and JEV-Bennett (GIII) strains. For comparison to the JEV E-DIII epitopes, immediately below we show the structurally defined E-DIII epitopes of ZIKV in complex with ZV-2 (green, ABDE epitope), ZV-48 (cyan, C-C') and ZV-67 (magenta, lateral ridge [LR]), WNV E16 (magenta, LR), DV1-E106 (magenta, LR), DV1-E111 (cyan, C-C′ loop), DV2-1A1D-2 (pink, A strand), DV3-2H12 (light green, AB loop), and DV4-4E11 (pink, A strand). **(B)** JEV E-DIII epitopes defined by alanine-scanning mutagenesis are depicted on the JEV E-DIII structure (based on the full-length JEV E structure, PDB accession no. 3P54). **(C)** JEV epitopes defined by alanine-scanning mutagenesis, HDX mapping, and surface exposure are shown in the context of the full-length JEV E structure.

187
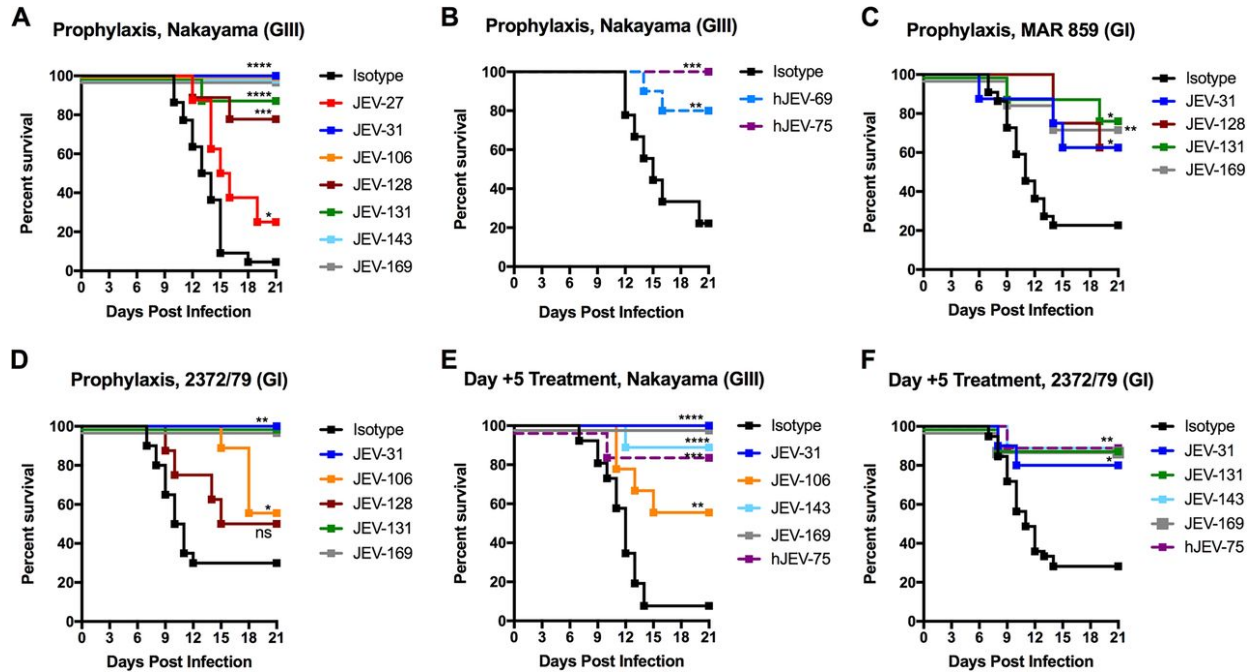
Figure 5.7: Protective efficacy of anti-JEV mAbs in mice.

(A and B) Four- to 5-week-old male C57BL/6 mice were passively administered 10 µg of the indicated (A) mouse or (B) human MAb via intraperitoneal injection 1 day prior to inoculation with 10^2 FFU of JEV-Nakayama via the subcutaneous route. JEV-31 ($n = 9$), JEV-106 ($n = 8$), JEV-143 ($n = 8$), and JEV-169 ($n = 10$) provided complete protection against lethality. JEV-27 ($n = 8$), JEV-128 ($n = 9$), and JEV-131 ($n = 9$) provided partial protection compared to the isotype control mAbs**. (C and D)** Three-week-old male C57BL/6 mice were passively administered 10 µg of the indicated mAb as described above 1 day prior to inoculation with 10^3 FFU of (C) JEV-MAR 859 (JEV-31, $n = 8$; JEV-131, $n = 9$; JEV-169, $n = 8$) or (D) JEV-2372/79 (JEV-31, $n = 9$; JEV-106, $n = 9$; JEV-131, $n = 9$; JEV-169, $n = 9$). **(E and F)** Two hundred fifty micrograms of the indicated mAb was administered 5 days postinfection to (E) 4- to 5-week-old mice infected with 10^2 FFU of JEV-Nakayama (JEV-31, $n = 9$; JEV-106, $n = 9$; JEV-143, $n = 9$; JEV-169, $n= 9$; hJEV-75, $n = 8$) or (F) 3-week-old mice infected with 10^3 FFU of JEV-2372/79 (JEV-31, $n = 10$; JEV-131, $n = 9$; JEV-143, $n = 9$; JEV-169, $n = 10$; hJEV-75, $n = 9$). Data are pooled from at least two independent experiments. Survival was analyzed for each MAb compared to the isotype control mAb by the log rank test. *, $P < 0.05$; **, $P < 0.01$; ***, $P < 0.001$; ****, $P < 0.0001$; ns, not significant.

SA_14_14_2 F N C L G M G N R D F I E G A S G A T W V D L V L E G D S C L T I M A N D K P T L D V R M I N I E A S Q L 53
SA_14 F N C L G M G N R D F I E G A S G A T W V D L V L E G D S C L T I M A N D K P T L D V R M I N I E A S Q L 53
Nakayama F N C L G M G N R D F I E G A S G A T W V D L V L E G D S C L T I M A N D K P T L D V R M I N I E A V Q L 53
Bennett F N C L G M G N R D F I E G A S G A T W V D L V L E G D S C L T I M A N S D K P T L D V R M I N I E A S Q L 53
2372_79 F N C L G M G N R D F I E G A S G A T W V D L V L E G D S C L T I M A S D K P T L D V R M I N I E A S Q L 53
MAR_859 F N C L G M G N R D F I E G A S G A T W V D L V L E G D S C L T L M V D D K P T L D V R M I N I E A S Q L 53

SA_14_14_2 A E V R S Y C Y H A S V T D I S T V A R C P T T G E A H N E K R A D S S Y V C K Q G F T D R G W G N G C G 106
SA_14 A E V R S Y C Y H A S V T D I S T V A R C P T T G E A H N E K R A D S S Y V C K Q G F T D R G W G N G C G 106
Nakayama A E V R S Y C Y H A S V T D I S T V A R C P T T G E A H N K K R A D S S Y V C K Q G F T D R G W G N G C G 106
Bennett A E V R S Y C Y H A S V T D I S T V A R C P T T G E A H N E K R A D S S Y V C K Q G F T D R G W G N G C G 106
2372_79 A E V R S Y C Y H A S V T D I S T V A R C P T T G E A H N E K R A D S S Y V C K Q G F T D R G W G N G C G 106
MAR_859 A E V R S Y C Y H A S V T D I S T V A R C P T T G E A H N E K R A D S S Y V C K Q G F T D R G W G N G C G 106

SA_14_14_2 F F G K G S I D T C A K F S C T S K A I G R T I Q P E N I K Y K V G I F V H G T T T S E N H G N Y S A Q V 159
SA_14 L F G K G S I D T C A K F S C T S K A I G R T I Q P E N I K Y E V G I F V H G T T T S E N H G N Y S A Q V 159
Nakayama L F G K G S I D T C A K F S C T S K A I G R T I Q P E N I K Y E V G I F V H G T T T S E N H G N Y S A Q V 159
Bennett L F G K G S I D T C A K F S C T S K A I G R T I Q P E N I K Y E V G I F V H G T T T S E N H G N Y S A Q V 159
2372_79 L F G K G S I D T C A K F S C T S K A I G R T I Q P E N I K Y K V G I F V H G A T T S E N H G N Y S A Q V 159
MAR_859 L F G K G S I D T C A K F S C T S K A I G R T I Q P E N I K Y K V G I F V H G A T T S E N H G N Y S A Q V 159

SA_14_14_2 G A S Q A A K F T V T P N A P S V A L K L G D Y G E V T L D C E P R S G L N T E A F Y V M T V G S K S F L 212
SA_14 G A S Q A A K F T V T P N A P S I T L K L G D Y G E V T L D C E P R S G L N T E A F Y V M T V G S K S F L 212
Nakayama G A S Q A A K F T V T P N A P S T T L K L G D Y G E V T L D C E P R S G L N T E A F Y V M T V G S X S F L 212
Bennett G A S Q A A K F T V T P N A P S I T L K L G D Y G E V T L D C E P R S G L N T E A F Y V M T V G S K S F L 212
2372_79 G A S Q A A K F T V T P N A P S I T L K L G D Y G E V T L D C E P R S G L N T E A F Y V M T V G S K S F L 212
MAR_859 G A S Q A A K F T V T P N A P S I T L K L G D Y G E V T L D C E P R S G L N T E A F Y V M T V G S K S F L 212

SA_14_14_2 V H R E W F H D L A L P W T S P S S T A W R N R E L L M E F E G A H A T K Q S V V A L G S Q E G G L H H A 265
SA_14 V H R E W F H D L A L P W T S P S S T A W R N R E L L M E F E G A H A T K Q S V V A L G S Q E G G L H Q A 265
Nakayama V H R E W F H D L A L P W T P P S S T A W R N R E L L M E F E E A H A T K Q S V V A L G S Q E G G L H Q A 265
Bennett V H R E W F H D L S L P W T S P S S T A W R N R E L L M E F E E A H A T K Q S V V A L G S Q E G G L H Q A 265
2372_79 V H R E W F H D L S L P W T S P S S T A W R N R E L L M E F E E A H A T K Q S V V A L G S Q E G G L H Q A 265
MAR_859 V H R E W F H D L S L P W T S P S S T A W R N R E L L M E F E E A H A T K Q S V V A L G S Q E G G L H Q A 265

SA_14_14_2 L A G A I V V E Y S S S V M L T S G H L K C R L K M D K L A L K G T T Y G M C T E K F S F A K N P V D T G 318
SA_14 L A G A I V V E Y S S S V K L T S G H L K C R L K M D K L A L K G T T Y G M C T E K F S F A K N P V D T G 318
Nakayama L A G A I V V E Y S N S V K L T S G H L K C R L R M D K L A L K G T T Y G M C T E K F S F A K N P A D T G 318
Bennett L A G A I V V E Y S S S V K L T S G H L K C R L K M D K L A L K G T T Y G M C T E K F S F A K N P A D T G 318
2372_79 L A G A I V V E Y S S S V K L T S G H L K C R L K M D K L A L K G T T Y G M C T E K F S F A K N P A D T G 318
MAR_859 L A G A I V V E Y S S S V K L T S G H L K C R L K M D K L A L K G T T Y G M C T E K F S F A K N P A D T G 318

SA_14_14_2 H G T V V I E L S Y S G S D G P C K I P I V S V A S L N D M T P V G R L V T V N P F V A T S S A N S K V L 371
SA_14 H G T V V I E L S Y S G S D G P C K I P I V S V A S L N D M T P V G R L V T V N P F V A T S S A N S K V L 371
Nakayama H G T V V I E L S Y S G S D G P C K I P I V S V A S L N D M T P V G R L V T V N P F V A T S S A N S K V L 371
Bennett H G T V V I E L T Y S G S D G P C K I P I V S V A S L N D M T P V G R L V T V N P F V A T S S S N S K V L 371
2372_79 H G T V V I E L T Y S G S D S P C N I P I V S V A S L N D M T P V G R L V T V N P F V A T S S S N S K V L 371
MAR_859 H G T V V I E L T Y S G S D G P C N I P I V S V A S L N D M T P V G R L V T V N P F V A T S S S N S K V L 371

SA_14_14_2 V E M E P P F G D S Y I V V G R G D K Q I N H H W H K A G S T L G 404
SA_14 V E M E P P F G D S Y I V V G R G D K Q I N H H W H K A G S T L G 404
Nakayama V E M E P P F G D S Y I V V G R G D K Q I N H H W H K A G S T L G 404
Bennett V E M E P P F G D S Y I V V G R G D K Q I N H H W H K A G S T L G 404
2372_79 V E M E P P F G D S Y I V V G R G D K Q I N H H W H K A G S T L G 404
MAR_859 V E M E P P F G D S Y I V V G R G D K Q I N H H W H K A G S T L G 404

Figure 5.8: Alignment of sequences of different JEV strains.

Genotypic differences from the JEV-SA14-14-2 strain (GIII) are highlighted as shaded black residues. The secondary structure elements above the alignment are derived from the structure of JEV E protein (PDB accession no. 3P54). The GenBank identification numbers for each viral sequence are described in Materials and Methods. The JEV-Nakayama strain includes an unknown amino acid at position 209 (denoted by an X).

189

Chapter 6:

Conclusions and Future Directions

6.1   Summary and Future Directions: mAb-defined ZIKV epitopes

We initially mapped a panel of human- and murine-derived ZIKV neutralizing and non-neutralizing mAbs[1]. These studies identified two epitopes bound by non-neutralizing mAbs and multiple epitopes bound by mAbs that neutralize with variable efficacy.

Cross-reactive mAbs to flavivirus infections have been largely mapped to the fusion loop epitope of DII (DII-FL)[2–4]. The DII-FL is highly conserved across flaviviruses and although bound by type-specific mAbs, these tend to be weakly neutralizing[5]. We isolated one murine (ZV-13) and two human (ZIKV-12 and ZIKV-15) mAbs that recognize the DII-FL. Binding studies with ZV-13 identified cross-reactivity with flaviviruses, including all DENV serotypes that share 54-59% homology by alignment of the E protein amino acid sequence[6] and the more distantly related JEV, with 53% homology by E protein. Previous studies have shown variable *in vitro* neutralization efficacy of DII-FL specific mAbs. For example, DV2-30[5] and WNV-E53[4] neutralized their respective viruses while DV2-36 and WNV-E28 were unable to neutralize their indicated flaviviruses. Neutralization studies with ZV-13 demonstrate an inability to inhibit infection against any of the ZIKV strains tested. Conversely, DENV-derived cross-reactive 2A10G6[2] neutralized ZIKV *in vitro* and provided complete protection against ZIKV in a murine lethality model[7]. A consequence of DII-FL specific mAbs is the potential for antibody-dependent enhancement (ADE), where previous cross-reactive mAbs are present but fail to neutralize a secondary infection and instead augment infection in FcR-bearing myeloid cells[8]. This phenomenon has been observed *in vitro* and *in vivo* in the context of sequential DENV infection of differing serotypes. We described the ability of ZV-13 to enhance secondary DENV and ZIKV

191

infection *in vitro.* Recently, convalescent plasma from DENV- or WNV-infected patients was shown to enhance secondary ZIKV infection *in vitro* and *in vivo* as shown by increased lethality and disease score, particularly for those receiving the plasma from DENV-infected patients[9]. An important consideration is the predominance of the human immune response to the cross-reactive epitopes instead of the type-specific immune response[10]. Future studies should focus on identifying features of the cross-reactive mAbs that are promote protection in order to skew the humoral immune response toward a broadly-neutralizing response. Vaccine design will need to take this into consideration in order to avoid sensitizing recipients to subsequent augmented disease, especially if vaccines will be implemented in regions where DENV and ZIKV co-circulate.

The antibodies that bound E-DIII were specific to ZIKV and were the most strongly neutralizing. Within DIII, the lateral ridge (DIII-LR) specific mAbs (ZV-54 and ZV-67) reduced *in vitro* infection of four strains of ZIKV representative of the two current lineages. Similarly, ZIKV-116, a human mAb isolated from an infected patient was also a potent neutralizer of ZIKV *in vitro*, with reduced inhibitory activity against the historical strain MR 766. Administration of ZV-54 or ZV-67 one day prior to infection was able to confer complete protection in a murine lethal model of infection. Previous studies on related flaviviruses have shown a similar protective *in vivo* effect of DIII-LR specific mAbs against lethality by WNV[11], DENV-1[12], and DENV-2[5]. The mechanism of neutralization of the human and murine mAbs is undertermined but studies with a comparable mAb (E16) against WNV[13] indicates inhibition at a post-attachment step, potentially by inhibiting fusion at the plasma membrane. The ability of DIII-LR mAbs against ZIKV to bind and neutralize may be potentiated by the accessibility of the epitope on the mature virion, as

was observed by docking ZV-67 onto a previously published cryo-EM structure of a mature ZIKV virion[14,15].

A second E-DIII epitope bound by neutralizing ZIKV mAbs (ZV-48 and ZV-64) is the C-C' loop, a cryptic epitope found to also be important in related flaviviruses[16]. Previous studies conducted with DV1-E111 found the C-C' loop residues bound by mAb to be important for E-dimer associations on the mature virion indicating that exposure of this epitope may require structural reorganization. The variability in neutralization of DV1-E111 against different DV1 strains also highlights potential structural organization variation that impacts mAb binding and therefore neutralization. This group of mAbs were unable to neutralize heterologous strains of ZIKV *in vitro* and compared with ZV-54 and ZV-67 had higher EC_{50} values against the ZIKV strains against which they were derived (H/PF/2013). The last E-DIII epitope bound by ZIKV-specific mAb (ZV-2) was the ABDE sheet, a site exposed on the mature virion, conserved between ZIKV strains, but is highly divergent across flaviviruses and is therefore not cross-reactive. An analogous mAb against DENV, 2H12, was found to bind six of the same residue positions[17]. However, 2H12 does neutralize multiple serotypes of DENV and may only bind in the context of extensive conformational changes implying that it may only exist as a cryptic epitope. Future studies may interrogate whether there are variations in E-dimer associations between flaviviruses that may permit the same site to be exposed in one virus (as in ZIKV) but cryptic in another (DENV). Differential binding analysis by biolayer interferometry further confirmed the neutralization profiles as the most potent, DIII-LR specific, neutralizing mAbs (ZV-54 and ZV-67) had greater binding affinity and slower dissociation rates compared to the C-C' loop (ZV-48 and ZV-64) and ABDE (ZV-2) mAbs.

Lastly, mAbs against structural epitopes in ZIKV were found to be potently neutralizing *in vitro* and protective in adult and pregnant models of infection. ZIKV-117 was isolated from a ZIKV-infected patient and potently neutralized all five strains of ZIKV against which it was tested *in vitro*. Therapeutic administration of ZIKV-117 one or five days post-infection conferred complete protection against ZIKV lethality in adult male mice. Administration of ZIKV-117 in three models of infection early in pregnancy (E6.5) demonstrated 1) *Ifnar*^{+/-} pups had 90% protection against ZIKV induced lethality when ZIKV-117 was administered one day prior to infection 2) wild-type (WT) dams and the pups had reduced viral load in the placenta and fetal when ZIKV-117 was administered one day prior to infection and 3) WT dams and pups had reduced viral load in the placenta and fetal heads when ZIKV-117 was administered one day after infection. Dams and pups were assessed seven days post-infection including maternal tissues to determine viral distribution and we observed that prophylactic administration prevented virus from entering maternal brain while therapeutic administration only decreased the viral load present in the brain. Epitope mapping by alanine scanning mutagenesis identified residues within E-DII but not those comprising the DII-FL. Subsequent cryo-EM studies demonstrated that ZIKV-117 cross-links the E monomers within a dimer also identified a novel binding pattern in which ZIKV-117 can also cross-link the E monomers across the E dimer[18]. This pattern of binding may sterically impede mAb binding and thus saturation can be achieved at lower concentration.

The E-dimer epitope (EDE) was introduced in Chapter 1 as eliciting protective mAbs against DENV and ZIKV[19,20]. The EDE epitope is made up of residues present in all three domains within the E protein and as such, can only be found in the whole virion. *In vitro*

studies with a panel of EDE1 and EDE2 mAbs found the ability to neutralize multiple strains of ZIKV representative of the Asian and American lineages. EDE1-B10 was able to bind and neutralize multiple strains of ZIKV *in vitro*. We first determined the kinetics of viral seeding of immune privileged sites in an adult murine model following infection and found that by two days post-infection, the brain, testis, epididymis, and eye had become infected with ZIKV. We next assessed the ability of EDE1-B10 to protect immune privileged sites from viral seeding when administered at different time points following infection in the acute and long-term stages. When administered one day post infection, EDE1-B10 was able to reduce viral seeding significantly suggesting that it was preventing viral entrance into the immune privileged sites. Administration of EDE1-B10 at three days post infection showed limited protection in the acute phase of infection (day +5) but more marked reduction when assessed long-term (day +21) indicating that while it may reduce viral burden in immune privileged sites, it was not completely able to prevent seeding. Follow up studies demonstrated that EDE1-B10 was able to reach immune privileged sites. Treatment with EDE1-B10 five days post infection was unable to reduce infection indicating that viral seeding had occurred and viral replication had exceeded the potential for mAb neutralization. Two additional important findings from the study in male mice were 1) the eye was negative for viral RNA by 21 days post-infection for the isotype- and EDE1-B10 treated mice indicating that it is naturally cleared and 2) EDE1-B10 administration up to three days post-infection was able to rescue testicular damage and sperm motility. In the pregnancy model of infection, systemic prophylactic EDE1-B10 administration was able to reduce viral RNA burden in maternal tissues (brain and female reproductive tract) and fetal tissues following intravaginal infection.

The potential for immune enhancement following secondary infection has been previously discussed. Briefly, sub-neutralizing levels of mAb from a primary infection may bind virus and allow for viral internalization by Fc-receptor mediated pathways. The internalization of virus can subsequently permit viral replication for release on infection progeny. In order to address this concern, studies using the structural mAbs (ZIKV-117 and EDE1-B10) modified at the Fc-receptor binding region (LALA) were completed. *In vitro* studies demonstrated equivalent neutralization against multiple strains of ZIKV by ZIKV-117 LALA and EDE1-B10 LALA as well as an inability to cause antibody-dependent enhancement (ADE) in myeloid cells. Administration of ZIKV-117 LALA prophylactically or EDE1-B10 LALA one day following infection showed equivalent reduction in viral RNA burden following subcutaneous infection. This result indicates that LALA variants of strongly neutralizing mAbs ZIKV-117 and EDE1-B10 may be considered as prophylactic or for acute administration following infection without risk of severe disease resulting from enhancement.

Our studies have focused on single mAb therapy administration for reduction of viral burden which may limit the window at which protection can be observed. Future studies should look into combination mAb therapy at later time points post-infection. Furthermore, our studies in wild-type mice were completed with a mouse-adapted strain of ZIKV that may vary from contemporary, circulating strains. *In vitro* assays indicate that *in vivo* protective efficacy will be observed but our mAbs will need to be evaluated in other models of infection as they continue to arise. It will be important to test our panel of mAbs, particularly the human-derived mAbs, in non-human primate models of infection.

6.2   Summary and Future Directions: mAb inhibition of JEV

We generated a panel of eight anti-JEV mAbs from mice immunized with the vaccine (JEV-SA 14-14-2) or virulent strains (JEV-Nakayama and JEV-Bennett) of JEV. We identified six mAbs to be directed at DIII, one mAb against DI (JEV-169), and one mAb (JEV-117) to unable to bind either domain by ELISA but able to bind the full-length E protein. *In vitro* neutralization studies against a panel of JEV strains representative of the four lineages indicates a wide breadth of neutralization efficacy against the different genotypes and between strains of the same genotype. We tested individuals mAbs *in vivo* against JEV-2372/79 (GI) or JEV-Nakayana (GIII) in a murine lethal model of infection and noted that the strongest neutralizing mAb *in vitro,* JEV-169, was not consistently the most protective mAb. Future studies should identify residue-level mapping of JEV-169 to determine if the site is variably exposed during viral maturation which may explain discrepancy observed *in vitro* and *in vivo* data.

We also identified two human-derived mAbs from vaccinated individuals that are able to neutralize the panel of JEV representative of the four genotypes. hJEV-69 bound E-DIII by ELISA and alanine scan mutagenesis indicated loss of binding at various residues, however, a pattern consistent with an epitope is yet to be determined. hJEV-75 was strongly neutralizing against JEV-SA 14-14-2 and significantly decreased neutralization potential against JEV-JKT 7884 (GIV). Domain mapping by ELISA was unable to identify binding of hJEV-75 to a specific domain and alanine scan mutagenesis of E-DIII indicated a single residue, E373, for loss of binding. *In vivo* studies with prophylactic administration of human-derived JEV mAbs indicated 80% and 100% protection by hJEV-69 and hJEV-75, respectively.

The time course to lethality varies across flaviviruses and while the kinetics of viral dissemination has been extensively studied in realted viruses, such as DENV, WNV, and ZIKV, similar studies have been limited in JEV. Future studies should aim to understand the kinetics of viral entry to the central nervous system as that usually precipitates lethality. Particularly, it should be determined whether there are differences in viral dissemination kinetics between strains of JEV that may alter the window of therapy between strains of JEV. Lastly, the emergence of a GV strain raises the concern of efficacy of current vaccination on emerging strains, therefore currently available panels of mAbs should be tested *in vitro* and *in vivo* against JEV-Muar (GV) to determine further breadth of humoral response.

6.3 Conclusions

The rapid rise of ZIKV infections and the associated clinical manifestations that occurred in 2014 suggests that there is potential for emerging arboviruses to cause sudden distress. Similarly, the emergence of new genotypes of existing flaviviruses, such as JEV, suggests that current flaviviruses have the potential to alter their current infectious capability by further altering their genome. The work presented in this dissertation provides insight into how current vaccination strategies may be optimized to improve breadth of protection by epitope analysis and the potential for acute management of emerging flaviviruses.

6.4   References

1. Zhao, H. *et al.* Structural Basis of Zika Virus-Specific Antibody Protection. *Cell* **166,** 1016–1027 (2016).
2. Deng, Y.-Q. Q. *et al.* A broadly flavivirus cross-neutralizing monoclonal antibody that recognizes a novel epitope within the fusion loop of e protein. *PLoS One* **6,** (2011).
3. Smith, S. A. *et al.* The Potent and Broadly Neutralizing Human Dengue Virus-Specific Monoclonal Antibody 1C19 Reveals a Unique Cross-Reactive Epitope on the bc Loop of Domain II of the Envelope Protein. *MBio* **4,** e00873-13-e00873-13 (2013).
4. Vogt, M. R. *et al.* Poorly Neutralizing Cross-Reactive Antibodies against the Fusion Loop of West Nile Virus Envelope Protein Protect In Vivo via Fc Receptor and Complement-Dependent Effector Mechanisms. *J. Virol.* **85,** 11567–11580 (2011).
5. Sukupolvi-Petty, S. *et al.* Structure and function analysis of therapeutic monoclonal antibodies against dengue virus type 2. *J. Virol.* **84,** 9227–9239 (2010).
6. Dejnirattisai, W. *et al.* Dengue virus sero-cross-reactivity drives antibody-dependent enhancement of infection with zika virus. *Nat. Immunol.* **17,** 1102–1108 (2016).
7. Dai, L. *et al.* Structures of the Zika Virus Envelope Protein and Its Complex with a Flavivirus Broadly Protective Antibody. *Cell Host Microbe* **19,** 696–704 (2016).
8. Halstead, S. B., Mahalingam, S., Marovich, M. A., Ubol, S. & Mosser, D. M. Intrinsic antibody-dependent enhancement of microbial infection in macrophages: disease regulation by immune complexes. *Lancet Infect. Dis.* **10,** 712–722 (2010).
9. Bardina, S. V. *et al.* Enhancement of Zika virus pathogenesis by preexisting antiflavivirus immunity. *Science (80-.).* **356,** 175–180 (2017).
10. Beltramello, M. *et al.* The Human Immune Response to Dengue Virus is Dominated by Highly Cross- Reactive Antibodies Endowed with Neutralizing and Enhancing Activity. *Cell Host Microbe* **8,** (2010).
11. Oliphant, T. *et al.* Development of a humanized monoclonal antibody with therapeutic potential against West Nile Virus. *Nat. Med.* **11,** 522–530 (2005).
12. Shrestha, B. *et al.* The development of therapeutic antibodies that neutralize homologous and heterologous genotypes of dengue virus type 1. *PLoS Pathog.* **6,** e1000823 (2010).
13. Thompson, B. S. *et al.* A Therapeutic Antibody against West Nile Virus Neutralizes Infection by Blocking Fusion within Endosomes. *PLoS Pathog.* **5,** e1000453 (2009).
14. Sirohi, D. *et al.* The 3.8 A resolution cryo-EM structure of Zika virus. *Science (80-.).* **352,** 467–470 (2016).
15. Kostyuchenko, V. A. *et al.* Structure of the thermally stable Zika virus. *Nature* (2016).
16. Austin, S. K. *et al.* Structural Basis of Differential Neutralization of DENV-1 Genotypes by an Antibody that Recognizes a Cryptic Epitope. *PLoS Pathog.* **8,** (2012).
17. Midgley, C. M. *et al.* Structural Analysis of a Dengue Cross-Reactive Antibody Complexed with Envelope Domain III Reveals the Molecular Basis of Cross-Reactivity. *J. Immunol.* **188,** 4971–4979 (2012).
18. Hasan, S. S. *et al.* A human antibody against Zika virus crosslinks the E protein to prevent infection. *Nat. Commun.* **8,** 14722 (2017).
19. Barba-Spaeth, G. *et al.* Structural basis of potent Zika–dengue virus antibody cross-neutralization. *Nature* **536,** 48–53 (2016).
20. Dejnirattisai, W. *et al.* A new class of highly potent, broadly neutralizing antibodies isolated from viremic patients infected with dengue virus. *Nat. Immunol.* **16,** 170–177 (2014).

Estefania Fernandez

estefania.fernandez1@gmail.com

EDUCATION

Washington University School of Medicine   **Expected May 2019**
Medical Scientist Training Program
Department of Immunology

The University of Texas at Austin G.P.A 3.84/4.00   **May 2011**
Bachelor of Science in Biochemistry
Magna Cum Laude

CAREER DEVELOPMENT

Research:

2011- 2012   **National Institute of Health Academy**
                    NIAID Office of Training and Diversity Program
- Characterize potential targets of mTOR in the decapping complex and detail how the candidate protein reacts during inhibition of mTOR as a part of Dr. Peter Williamson's laboratory
- Assess the onset of autophagy following *Cryptococcus neoformans* infection

2007- 2011   **Freshmen Research Initiative**
- Carried out research ranging from botany to biology alongside professionals in the field and composed research papers and target proposals on the proteins involved

2010- 2011   **Dr. Katherine Willets – University of Texas- Austin**
- Utilize stochastic optical reconstruction microscopy (STORM) to predict the shape of nanoparticles
- See Koen KA *et al.* below

Summer 2010 **HHMI Exceptional Research Opportunities – University of Washington**
- Develop a protocol to study the effects of lipids on cell membrane protein function as part of Dr. Tamir Gonen's laboratory

Summer 2009 **Research Experience for Undergraduates – UCSF**
- Determine the effects of autophagy gene mutation on mitochondria
- See Radoshevich L *et al*. below

Publications:

Fernandez E, Kose N, Edeling MA, Adhikari J, Sapparapu G, Lazarte SM, Nelson CA, Govero J, Gross ML, Fremont DH, Crowe JE, Diamond MS. 2018. Mouse and human monoclonal antibodies protect against infection by multiple genotypes of Japanese encephalitis virus. *mBio.* 2018 Feb 27; 9(1): 8-18. PMID: 29487230.

Fernandez E, Dejnirattisai W, Cao B, Scheaffer SM, Supasa P, Wongwiwat W, Esakky P, Drury A, Mongkolsapaya J, Moley KH, Mysorekar IU, Screaton GR, Diamond MS. 2017. Human antibodies to the dengue virus E-dimer epitope have therapeutic activity against Zika virus infection. *Nat Immnol.* 2017 Nov; 18(11): 1261-1269. PMID: 28945244

Fernandez E and Diamond MS. 2017. Vaccination strategies against Zika virus. *Curr. Opin. Virol.* 2017 Apr 19; 23: 59-67. PMID: 28432975.

Sapparapu G*, **Fernandez E*,** Kose N, Cao B, Fox JM, Bombardi RG, Zhao H, Nelson CA, Bryan AL, Barnes T, Davidson E, Mysorekar IU, Fremont DH, Doranz BJ, Diamond MS, Crowe JE. 2016. Neutralizing human antibodies prevent Zika virus replication and fetal disease in mice. *Nature.* 2016 Nov 7; 540(7633): 443-447. PMID: 27819683.

Zhao H*, **Fernandez E*,** Dowd KA, Speer SD, Platt DJ, Gorman MJ, Govero J, Nelson CA, Pierson TC, Diamond MS, Fremont DH. 2016. Structural basis of Zika virus- specific antibody protection. *Cell.* 2016 Aug 11; 166(4): 1016- 27. PMID: 27475895.

Salazar V, Jagger BW, Mongkolsapaya J, Burgomaster KE, Dejnirattisai W, Winkler ES, **Fernandez E**, Nelson CA, Fremont DH, Pierson TC, Crowe JE, Screaton GR, Diamond MS. 2019. Dengue and Zika virus cross-reactive human monoclonal antibodies protect against Spondweni virus infection and pathogenesis in mice. *Cell Reports.* 2019 Feb 5; 26(6): 1585-1597.e4. PMID: 30716740.

Long F, Doyle M, **Fernandez E**, Miller AS, Klose T, Sevvana M, Bryan A, Davidson E, Doranz BJ, Kuhn RJ, Diamond MS, Crowe JE, Rossman MG. 2018. Structural basis of a potent human monoclonal antibody against Zika virus targeting a quaternary epitope. *PNAS.* 2018 Jan 14; Epub. PMID: 30642974.

Scott JM, Lebratti TJ, Richner JM, Jiang X, Zhao H, **Fernandez E,** Fremont DH, Diamond MS, Shin H. 2018. Cellular and humoral immunity protect against vaginal Zika virus infection in mice. *Journal of Virology.* 2018 Jan 17. PMID: 29343577.

Zhe Z, Gorman MJ, McKenzie LD, Chai JN, Hubert CG, Prager BC, **Fernandez E**, Richner JM, Zhang R, Shan C, Wang X, Shi P, Diamond MS, Rich JN, Chheda MG. 2017. Zika virus has oncolytic activity against glioblastoma stem cells. *J. Exp. Med.* 2017 Sep 6; 214(10): 2843-2857. PMID: 28874392.

Hasan SS, Miller A, Sapparapu G, **Fernandez E,** Klose T, Long F, Fokine A, Porta JC, Jiang W, Diamond MS, Crowe JE, Kuhn RJ, Rossman MG. 2017. A human antibody against Zika virus crosslinks the E protein to prevent infection. *Nature Communications.* 2017 Mar 16; 8:14722. PMID: 28300075

Govero J*, Esakky P*, Scheaffer SM, **Fernandez E**, Drury A, Platt DJ, Gorman MJ, Richner JM, Caine EA, Salazar V, Moley KH, Diamond MS. 2016. Zika virus infection damages the testes in mice. *Nature.* 2016 Dec 15; 540(7633): 438-442. PMID: 27798603.

Acharya D, Bastola P, Le L, Paul AM, **Fernandez E**, Diamond MS, Miao W, Bai F. 2016. An ultrasensitive electrogenerated chemiluminescence- based immunoassay for specific detection of Zika virus. *Scientific Reports.* 2016 Aug 24; 6: 32227. PMID: 27554037.

Zhang R, Miner JJ, Forman MJ, Rausch K, Ramage H, White JP, Zuiani A, Zhang P, **Fernandez E**, Zhang Q, Dowd KA, Pierson TC, Cherry S, Diamond MS. 2016. A CRISPR screen defines a signal peptide processing pathway required by flaviviruses. *Nature.* 2016 Jul 7; 535(7610): 164- 8. PMID: 27383988.

Miner JJ*, Cao B*, Govero J*, Smith AM, **Fernandez E**, Cabrera OH, Garber C, Noll M, Klein RS, Noguchi KK, Mysorekar IU, Diamond MS. 2016. Zika virus infection during pregnancy in mice causes placental damage and fetal demise. *Cell.* 2016 May 19; 165(5): 1081-91. PMID: 27180225.

Lazear HM, Govero J, Smith AM, Platt DJ, **Fernandez E**, Miner JJ, Diamond MS. 2016. A mouse model of Zika virus pathogenesis. *Cell Host & Microbe.* 2016 May 11; 19(5): 720-30. PMID: 27066744

Koen KA, Weber ML, Mayer KM, **Fernandez E,** Willets KA. 2012. Spectrally, resolved polarization anisotropy of single plasmonic nanoparticles excited by total internal reflection. *J. Phys. Chem. C*. 2012 Jul 13; *116* (30): 16198–206. DOI: 10.1021/jp301878e.

Radoshevich L, Murrow L, Chen N, **Fernandez E**, Roy S, Fung C and Debnath J. 2010. ATG12 Conjugation to ATG3 Regulates Mitochondrial Homeostasis and Cell Death. *Cell.* 2010 Aug 20; 142(4): 590-600. PMID: 20723759.

* equal contributions

Experience:

2009- 2011   **Freshmen Research Initiative (FRI) Research Mentor**
               University of Texas- Austin, Austin TX

Summer 2008 **Summer Medical and Dental Educational Program (SMDEP)**
Yale University, New Haven, CT

Summer 2008 **Louis Stokes Alliance for Minority Participation (LSAMP)**
University of Texas- Austin, Austin TX

2008 **Freshmen Research Initiative (FRI) Undergraduate Research Teaching Assistant**
University of Texas- Austin, Austin TX

HONORS /AWARDS

2018	**Robert Silverman M.D., Ph.D. and Randi Leavitt M.D., Ph.D. Fellow**
2017	**David M. Kipnis Award in Biomedical Sciences**
2014	**Frank O. Richards Medical Student Scholarship Prize**
2010- 2011	**Aspire Research Excellence Award**
2010- 2011	**Aspire Academic Excellence Award**
2009- 2011	**Annual Department of Chemistry and Biochemistry Scholarship**
2007- 2011	**University Honors**

ACTIVITIES

2013- 2017	**Latino Medical Student Association**
2014	**Camp Cardio**
2013- 2015	**Casa de Salud**